Regulation of the Actin Cytoskeleton and Polarized Growth in *Schizosaccharomyces pombe.*

A thesis submitted to the University of Kent for the degree of PhD in the Faculty of Sciences.

2014

Matthew Johnson

Abstract

The fission yeast, *Schizosaccharomyces pombe* grows only in length in a highly polarized manner in a process tightly regulated by both the microtubule and actin cytoskeletons, which play key roles in the establishment of cell polarity and growth of the cell respectively. Previous studies have shown that within the microtubule cytoskeleton a large group of proteins accumulate at the cell poles, where they are believed to form a "polarisome" which coordinates the cell's polarity. Whilst the main functions and key interactions between these proteins are known, many of the finer details remain unclear. The actin cytoskeleton is a highly dynamic network of different actin structures, with multiple changes occurring that are regulated by actin binding proteins (ABPs). One of the most important actin binding proteins is tropomyosin, which is responsible for stabilising interphase actin cables and the cytokinetic actomyosin ring (CAR). Within fission yeast tropomyosin is present in both acetylated and unacetylated forms which each localise to distinct actin structures.

Interphase actin cables and the CAR are nucleated by two different formins; For3 and Cdc12 respectively. Within this study it has been shown that it is these formins that determine which tropomyosin isoform associates with specific actin structures. Exchanging the localisation of these formins results in a corresponding exchange of tropomyosin present on actin filaments. This exchange also has a subsequent effect on actin dynamics and the interaction of other ABPs. In addition, when investigating the regulation of cell polarity, it was shown that this is a very complex process. Proteins from both the actin and microtubule cytoskeletons playing key roles in the transport, recruitment, tethering and turnover of each other as shown by deletions of one polarity protein often having a significant effect on the localisation and abundance of others.

Table of Contents

Figures

Figure.1.13. The role of the inverter domain. In (c) the power-stroke of a conventional barbed (+) end directed myosin is shown. (d) Shows how the inverter domain (red) between the converter region (blue) and the lever arm (green) reverses the direction of the power stroke and resulting in a pointed (-) end directed myosin (Tsiavaliaris, Fujita-Becker & Manstein 2004).

Figure.1.14. (Left) A model of the tropomyosin molecule. The dimeric form of the protein is shown, demonstrating 2 tropomyosin α-helices coiled around each other to form the coiled coil dimer. The slight curvature which allows tropomyosin to coil around actin filaments is also visible. The molecular ends of the Tm molecule were determined relative to the cysteine residue at position 190 (Cys 190) (Whitby & Phillips 2000). (Right) A 3 dimensional reconstruction of the thin filament. (A) shows the F-actin control with no tropomyosin present, in B the tropomyosin polymer coiling around the actin filament is clearly visible (Skoumpla et al. 2007).

Figure.1.16. A representation of the coiled coil structure and its heptad repeat. The heptad repeat is shown by the letters a-g and a'-g' with a/a' and d/d' being the core residues. The solid black arrows linking residues a/a' and d/d' represent the hydrophobic interactions between the core residues, which bring about the majority of the stability of the coiled coil. The black outlined arrows between e/g' and g/e' represent the ionic interactions between acidic and basic amino acids which can interact by way of ionic bonds and contribute to the stability of the structure. Residues labelled X play no role in stabilising the coiled coil structure. From (Perry 2001).

Figure.1.17. A solution structure of α-tropomyosin showing the splaying of the C-terminus of a tropomyosin molecule, creating a cleft for the N-terminus of another tropomyosin molecule to slot into. This results in an 11 amino acid overlap between the two molecules and allows tropomyosin molecules to polymerize along the actin filament. From (Hitchcock-DeGregori & Singh 2010).

Figure.1.18. α-Carbon drawings illustrating differences at the N-terminus of unacetylated (left) and acetylated (right) tropomyosin. In the case of the unacetylated tropomyosin, the alpha helical structure is lost, with residues 1 and 2 extending sideways away from the adjacent molecule, resulting in the loss of coiled coil structure at the extreme N-terminus of the dimer. From (Brown et al. 2001).

Figure 1.19. Microtubule dynamics Microtubules grow at the + end via the addition of GTP bound tubulin. The GTP-tubulin at the + end is stable and the microtubule continues to grow until free tubulin concentration becomes too low and there is no longer enough GTP-tubulin to cap the + end. The GTP is hydrolysed to GDP and catastrophe occurs, with the rapid depolymerisation of the microtubule by the removal of GDP-tubulin. This continues until the microtubule is completely depolymerised, or a rescue event resulting in the formation of a new GTP-tubulin cap occurs (Cheeseman & Desai 2008).

Figure.1.20. The two proposed mechanisms of CAR formation, (b) shows the search, capture, pull, release (SPCR) model, whilst (c) shows the leading cable model. Adapted from (Kovar, Sirotkin & Lord 2011).

Figure.1.21. The fission yeast microtubule cytoskeleton. Over time interphase microtubules (green) disappear and the mitotic spindle (red) is formed. The spindle elongates and the chromosomes (blue) are segregated to opposite poles of the cell. The post anaphase array (PAA) is then formed and cell division takes place, resulting in the formation of two daughter cells and the normal interphase microtubule cytoskeleton is observed in both cells (Hagan 1998).

Figure.1.22. A schematic to show the regulation of Cdc42 and its targets, as well as its localisation to the cell poles when in its active GTP bound form (Chang & Martin 2009)**.**

Figure.1.23. Anchoring of Tea1 at the cell poles. (A) Tea1 is delivered to the cell cortex on microtubule plus ends. (B) Tea1 interacts with Mod5p at both cell tips. (C) At non-growing cell tips, Tea1 interacts with Tea3, which is anchored at the cortex via its interaction with Mod5 (D). (E) At growing cell tips, Tea1 interacts with Tea4, which has a function similar to that of Tea3 at non-growing tips, playing a role in the initiation of NETO. (F) A partially functional interaction between Tea1 and Tea3 can occur without Mod5, but Tea1 and Tea3 are

poorly anchored at the cell cortex. (G) when all of these interactions occur proper Tea1 anchoring at both cell tips occurs (Snaith, Samejima & Sawin 2005).

Figure.1.24. The localisation of Mid1, Cdr1, Cdr2 and Wee1 to the medial cortex is promoted by nuclear signals, whilst Pom1 inhibits the localisation of these proteins and subsequently septum formation at areas other than the medial cortex. A gradient of Pom1 is also formed with Pom1 levels highest the cell poles, decreasing towards the middle of the cell (shown in orange). Once cells reach a critical length and Pom1 levels are sufficiently low at the middle of the cell, mitotic entry occurs (Chang & Martin 2009).

Figure.1.25. The arrangement of polarity proteins at the growing and non-growing ends of cells. A double headed arrow represents a physical interaction between two proteins while association with the cortex at the cell poles is represented by a dashed arrow when a direct interaction has not been identified (La Carbona, Le Goff & Le Goff 2006).

Figure.3.1. A cartoon representing fusion proteins used to localise formins to the cell poles. Tea1 was fused to the N-terminus of the formin, either For3 or Cdc12 with a $(Gly\text{-}Ala)_5$ linker and a fluorophore tag was located at the C-terminus of the fusion protein.

Figure.3.2. Maximum projection images (31 Z slices) of a *for3Δ s*train expressing the fluorescent tagged formin fusion proteins. Tea1-GFP and For3-mCherry localise to the cell poles as expected, Cdc12-GFP localises to the CAR, whilst fusing Tea1 to the N-terminus of both and Cdc12 and For3 results in them localising to the cell poles. Scale bars 5 µm.

Figure 3.3. Maximum projection images (31 Z slices) of wild-type, *tea1Δ* and *tea4Δ s*trains expressing the GFP tagged formin fusion proteins. As seen in a *for3Δ* strain, Tea1--GFP localises to the cell poles as expected, whilst Tea1-Cdc12-GFP and Tea1-For3-GFP also localise the cell poles. Scale bars 5 µm.

Figure.3.4. *for3Δ cdc10-v50 myo52-mCherry* cells expressing Tea1-GFP, For3-GFP, Tea1-Cdc12-GFP and Tea1-For3-GFP were incubated at 36 °C for 4 hours and the localisation of the formin proteins was then observed. Both Tea1-GFP and Tea1-For3-GFP had almost completely bi-polar localisation, whilst Tea1-Cdc12-GFP and For3-GFP had a mix of monopolar and bipolar localisation. The localisation of Myo52-mCherry is also shown, and in the case of For3-GFP was used to count For3 localisation due to the low levels of For3-GFP. Images are a maximum projection of 31 Z slices. Scale bars 5 µm.

Figure 3.5. Growth curve of *for3Δ* cells expressing formin proteins at 25 °C. Expression of Cdc12-GFP alone lead to slower growth, whilst expression of Tea1-GFP, For3-GFP and Tea1-Cdc12-GFP all grew at similar rates. Expression of Tea1-For3-GFP resulted in a faster rate of growth and the cells also reached a higher optical density.

Figure.3.6. Maximum projection images (31 Z slices) of *for3 gfp-CHD* cells expressing mCherry tagged formin proteins. GFP-CHD is shown in green and formin proteins are shown in magenta. As expected expression of For3-mCherry results in a restoration of actin cables, (shown here by GFP-CHD), whilst expression of Cdc12-mCherry failed to restore the presence of actin cables. Expression of both formin fusions, Tea1-For3-mCherry and Tea1-Cdc12-mCherry resulted in nucleation of actin cables. Scale bars 5 µm.

Figure 3.7. Immunofluorescence images of *for3Δ* cells expressing either Tea1-GFP, Tea1-Cdc12-GFP or Tea1-For3-GFP. Cells were probed with an antibody that binds to all Tm in the cell (upper row) or an acetylation specific antibody that only binds to acetylated Tm (lower row). Expression of either formin fusion resulted in the presence of actin filaments with Tm bound to them however acetylated Tm was only seen on interphase actin cables nucleated by Tea1-Cdc12. Scale bars 5 µm.

Figure 3.8. Maximum projection images (31 Z slices) of *for3Δ* cells expressing Tea1-Cdc12-mCherry and either Rng2YFP or Adf1-GFP and a Rng2-YFP strain alone. Tea1-Cdc12-mCherry is shown in magenta and Adf1-GFP or Rng2YFP is shown in green. Expression of Tea1-Cdc12-mCherry results in the localisation of Rng2-YFP being affected, with foci seen at the cell poles colocalising with Tea1-Cdc12-mCherry. Usually Rng2-YFP is only seen at the contractile ring of dividing cells. Scale bars 5 µm.

Tables

Abbreviations

α	Alpha
β	Beta
γ	Gamma
Δ	delta, deletion of a gene
µL	Microlitre
µM	Micromolar
ABPs	Actin Binding Proteins
bp	Base Pairs
CAR	Cytokinetic Actomyosin Ring
D. melanogaster	*Drosophila melanogaster*
DNA	Deoxyribonucleic Acid
E. coli	*Escherichia coli*
EMM2	Edinburgh Minimal Media
EPP	Epithelial Polarity Programme
F-actin	Filamentous-actin
FH1	Formin Homology domain 1
FH2	Formin Homology domain 2
G-actin	Globular-actin
GAP	GTPase Activating Protein
GDP	Guanosine Diphosphate
GEF	Guanosine exchange factor
GFP	Green Fluorescent Protein
GTP	Guanosine Triphosphate
IF	Intermediate Filaments
kb	Kilobase
kDa	Kilodalton
LB	Luria Bertani Broth
MDa	Megadalton
mg	Milligrams
ml	Millilitre
mM	Millimolar
MT	Microtubules
MTOC	Microtubule Organising Centre
NETO	New End Take Off
nM	Nanomolar
PCR	Polymerase Chain Reaction
PEG-4000	Polyethylene glycol - 4000
Pi	Inorganic phosphate
RNA	Ribonucleic Acid
RPM	Revolutions Per Minute
S. cerevisiae	*Saccharomyces cerevisiae*
S. pombe	*Schizosaccharomyces pombe*
SPB	Spindle Pole Body
Tm	Tropomyosin

TnC, TnI, TnT	Troponin C, I, T
TRIS	Tris(hydroxymethyl)aminomethane
YES	Yeast Extract with Supplements
YFP	Yellow Fluorescent Protein

Acknowledgements

Throughout my PhD I have received help, support and guidance from many people, to whom I am very grateful.

Firstly I would like to thank my supervisor, Dan Mulvihill for giving me the opportunity to do this PhD. In addition I thank members of both the Geeves and Mulvihill groups, for their assistance in the lab, as well as useful discussions and advice.

I would also like to thank all of my friends and family, who have always been there when needed to offer advice and support, as well as providing a much needed escape from work life at times.

Finally my biggest thanks go to my partner Sarah, without whom I would not be the person I am today. Over the last 3 and a half years, Sarah has always been there for me, through the good and bad times. Whenever I've been down she's always been there to pick me up again and when I've needed help or advice she's always been there for me in any way she could. She has been my rock throughout my PhD, and for this I am eternally grateful.

Chapter 1: Introduction

1.1. Overview

Cells are the basic biological unit of all living organisms, often referred to as the building blocks of life. The overall objective of all cells, whether as unicellular organisms or as part of a larger multicellular organism is to grow and divide, passing genetic material onto newly generated cells, ensuring the continued presence of that cell type or species. The order of processes by which a cell grows and divides into 2 new cells is known as the cell cycle (Hunt & Murray 1993). At a most basic level the cell cycle can be divided into 3 events, chromosome replication, chromosome segregation and cell division, however years of research has provided us with a much more in depth understanding of the cell cycle than this. The cell cycle is divided into two fundamental stages, interphase and mitosis.

Interphase accounts for the majority of the cell cycle and during this stage growth of the cell occurs, with the synthesis of ribosomes, membranes, mitochondria and cellular proteins occurring. Chromosome replication also occurs during a specific portion of interphase referred to as S phase (DNA synthesis) which occurs between two gap phases referred to as G1 and G2. Once the chromosomes have been replicated the two daughter chromosomes are attached to one another and are referred to as sister chromatids. During interphase DNA is diffusely distributed in the nucleus and individual chromosomes cannot be observed (Hunt & Murray 1993). Once chromomsome replication has occurred and the cell has completed the G2 phase, the cell enters M phase (Mitosis).

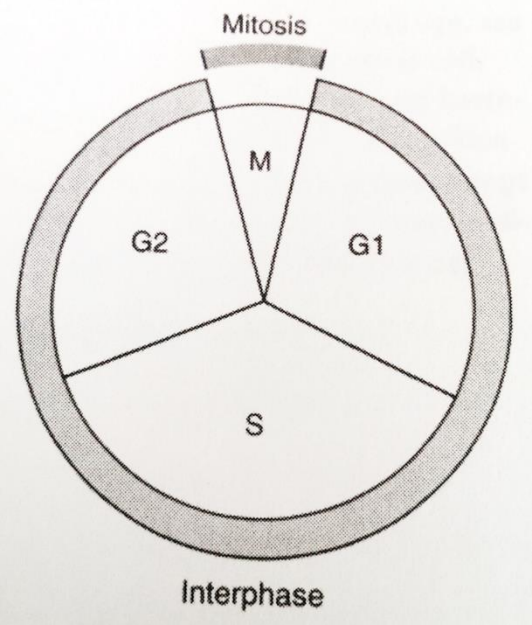

Figure 1.1. The stages of the cell cycle. The DNA synthesis (S phase) during interphase occurs between the gap phases G1 and G2. Mitosis (M Phase) occurs after the G2 phase of interphase (Hunt & Murray 1993).

During M phase there is a large reorganisation within the cell which results in the segregation of replicated chromosomes and cell division (cytokinesis) is initiated. Mitosis is divided into several stages, the first of which is prophase. During this stage the chromosomes condense and become distinct from one another with individual sister chromatids visible. Microtubule organising centres known as centrosomes or spindle pole bodies also move to opposite ends of the nucleus and there is a reorganisation of microtubule structures to form the mitotic spindle (see section 1.3.6). During the next stage; prometaphase, a protein complex known as the kinetochore is formed on the sister chromatids and microtubules from opposite poles then attach to each one of the sister chromatids via these kinetochores. This attachment is often preceded by the breakdown of the nuclear envelope (referred to as open mitosis) however in certain cells such as yeast and other fungi the nuclear envelope remains intact and the spindle is formed inside the nucleus and the nucleus subsequently is split into 2. Opposing forces from these

microtubules then work to align the sister chromatids midway between the 2 spindle poles in an area referred to as the metaphase plate. Once aligned the cells enter the anaphase stage during which the link between the 2 sister chromatids is dissolved and they separate, moving to opposite poles of the cell. As the chromosomes approach the cell poles cytokinesis is initiated and the cell divides into two daughter cells, with the process facilitated by a contractile ring formed by the actin cytoskeleton (see section 1.3.1). As cytokinesis occurs the chromosomes decondense and a new nuclear envelope is formed (in cells that have undergone open mitosis) and the microtubules re-form their interphase array (Hunt & Murray 1993).

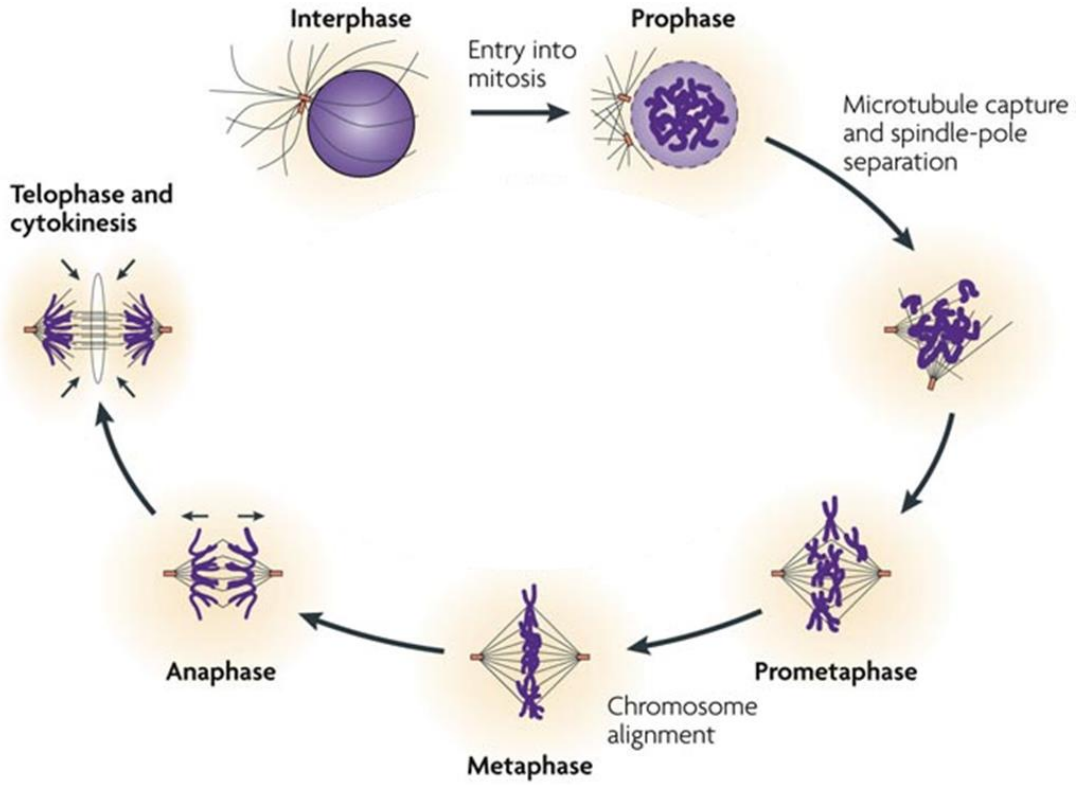

Figure 1.2. The stages of mitosis. During prophase the chromosomes condense and the centrosomes move to opposite poles. The nuclear envelope then breaks down and microtubules attach to the kinetochores on sister chromatids. The sister chromatids then align on the metaphase plate before the linkage between them is dissolved and they are segregated to separate poles by forces applied by microtubules. Cytokinesis then occurs, chromosomes decondense and a new nuclear envelope is formed. Adapted from (Jackson et al. 2007).

1.2. Cell Polarity

Cell polarity is a fundamental property of almost all cells, defining the shape of a cell. At a molecular level it is the spatial arrangement and composition of proteins to form functionally specialized domains in the cytoplasm and the cell membrane (Drubin & Nelson 1996). Cell polarity is incredibly important for the function of cells, and in higher eukaryotes such as metazoans, it is important for the development of a whole organism (Martin & Chang 2003). The correct organisation of proteins at the cell membrane and in the cytoplasm facilitates an incredibly diverse variety of cellular processes such as differentiation, membrane growth, cell migration, activation of the immune response and transport of vesicles across cellular layers (Drubin & Nelson 1996). The regulation of cell polarity is coordinated by interactions between components of both the actin and microtubule cytoskeletons, as well as other networks of polarity factors.

1.2.1 The Regulation of Cell Polarity in Higher Eukaryotes

Within higher eukaryotes, cell polarity has been heavily studied in mammalian epithelial cells. Epithelial cells are crucial to Metazoa as they are able to segregate their inner medium from their external environment; a key Metazoan requirement for tissue structures (Cereijido, Contreras & Shoshani 2004). Epithelial cells form sheets of polarised cells to form the epithelium, the first tissue to emerge during ontogenesis, where epithelial cells play fundamental roles in embryo morphogenesis and organ development (Bryant & Mostov 2008). Epithelial cells have asymmetric apical and basal membranes and the development of cell polarity and the apical-basal axis is regulated by an epithelial polarity

programme (EPP) which is regulated by a number of proteins and lipids (Rodriguez-Boulan & Macara 2014). The typical morphology of epithelial cells is shown in figure 1.3 below.

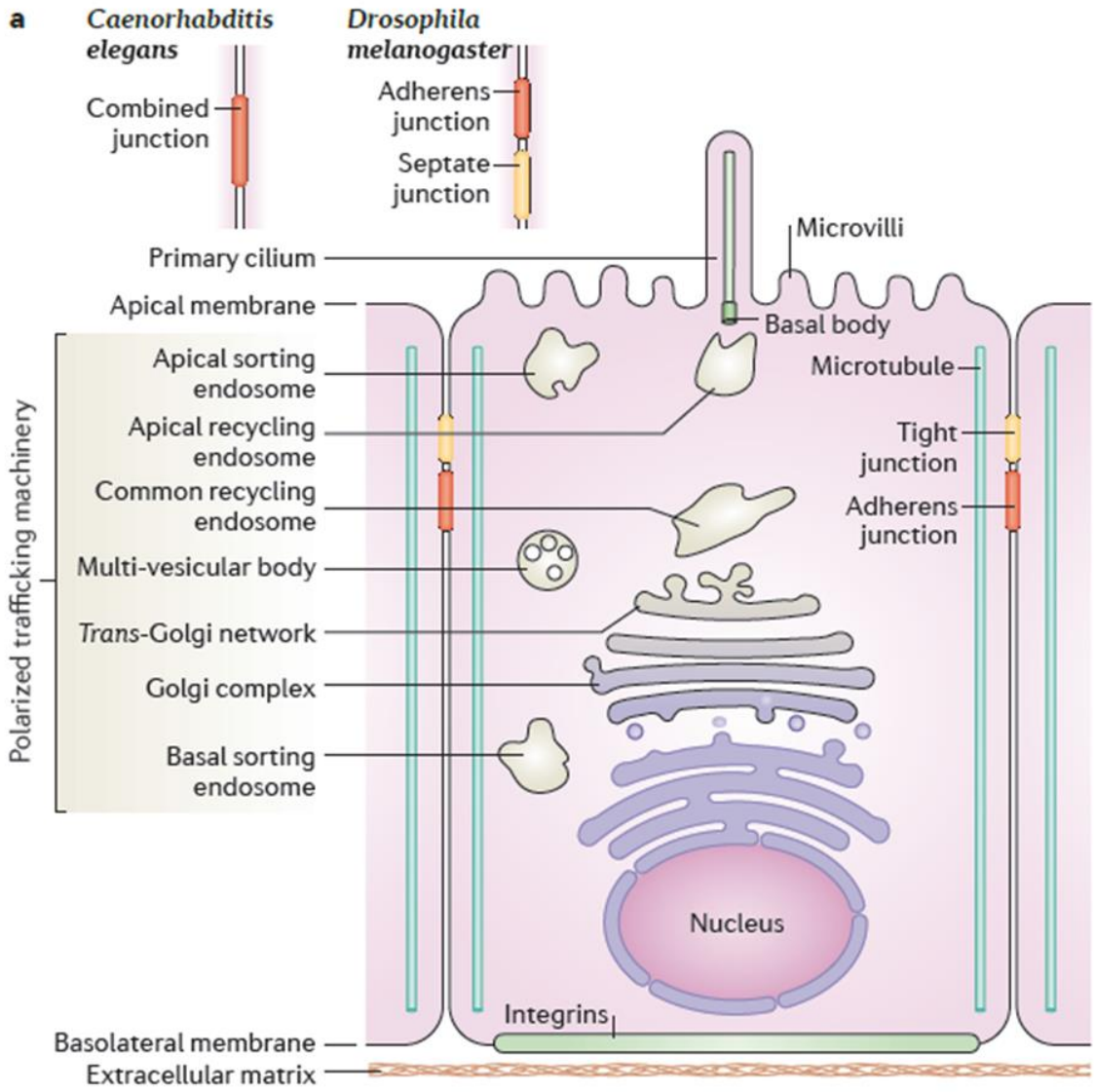

Figure.1.3. The morphology of epithelial cells. Epithelial cells possess a highly polarized morphology with asymmetrical apical and basolateral membranes at opposite poles of the cell (Rodriguez-Boulan & Macara 2014)

1.2.1.1 Proteins Involved in the Regulation of the EPP

The EPP is composed of a number of protein families that are all interlinked, playing key roles in coordinating the polarity of the cell, including the partitioning defective (PAR), Crumbs (CRB), Scribble (SCRIB), Coracle and Rho GTPase groups (Rodriguez-Boulan & Macara 2014).

The PAR group of proteins are ubiquitously expressed and play roles in cell polarity, cell proliferation and differentiation (Rodriguez-Boulan & Macara 2014). They were first discovered in a *C. elegans* screen to identify proteins required for the arrangement of cytoplasm components at the anterior and posterior cells in the early embryo (Kemphues et al. 1988). Homologues have since been identified in *D. melanogaster* (Goldstein & Macara 2007). The PAR group consists of PAR1 and PAR4 (known as LKB1 and STK11 in mammals) which are both serine threonine kinases, PAR5 a member of the 14-3-3 group of proteins which are recruited to phosphorylated serines and threonines and PAR3 and PAR6, two scaffolding/adapter proteins containing PDZ domains (Goldstein & Macara 2007). Atypical protein kinase C (aPKC) is also considered to be a part of the PAR group (Rodriguez-Boulan & Macara 2014).

The CRB and SCRIB groups, unlike the PAR group are specific to epithelial cells however they do interact with PAR proteins (Rodriguez-Boulan & Macara 2014). The CRB complex consists of CRB, a transmembrane protein (Tepass 1996), Stardust (Sdt- known as PALS1 in vertebrates) a membrane associated guanylate kinase (MAGUK) (Tepass & Knust 1993) and PALS1-associated tight junction homologue (PATJ), a protein that interacts with Stardust (Assémat et al. 2008). The SCRIB complex consists of SCRIB and discs-large homologue

(DLG), both of which have several PDZ domains and are believed to associate with transmembrane proteins (Bilder, Li & Perrimon 2000) and lethal giant larvae (LGL) which is involved in targeted secretion of membrane components at the exocyst via an interaction with t-SNARE proteins (Bilder, Li & Perrimon 2000). An additional group of proteins called the Coracle group has been identified in *D. melanogaster* which also plays a role in the EPP, and includes the FERM proteins Moesin and Yurt, Coracle , Neurexin IV and Na^+, K^+ ATPase.

The final group of proteins to play a role in the EPP is the RHO family of GTPases, which has over 20 members, including CDC42, RAC1 and RHOA (Etienne-Manneville & Hall 2002; Jaffe & Hall 2005). RHO GTPases cycle between an active (GTP-bound) and inactive (GDP-bound) state in a process controlled by guanidine exchange factors (GEFs) and GTPase activating proteins (GAPs), which are also involved in their localisation (Jaffe & Hall 2005). The most extensively studied role of RHO GTPases is their function in the organisation of the actin cytoskeleton. RHOA regulates the assembly of actin-myosin filaments which controls the generation of contractile forces, whilst RAC1 and CDC42 are responsible for organising actin structures at the cell periphery, regulating the generation of lamellipodia and filopodia (Nobes & Hall 1995). The generation of contractile forces via RHOA antagonises adhesive forces generate by RAC1, however other roles of RHO GTPases in the EPP are independent of their actin organising roles (Iden & Collard 2008).

1.2.1.2 The Role of Lipids in the EPP

Phosphoinositides comprise 1% of the total lipids within a cell however they play key roles as precursors of lipid messengers and act as membrane docking sites for signalling cascades (Di Paolo & De Camilli 2006). Phosphoinositides are spatiotemporally regulated by phosphoinositide kinases and phosphatases and have been shown, along with other lipids to play a role in epithelial polarity (Gassama-Diagne & Payrastre 2009). Phosphatidylinositol-3,4,5-triphosphate (PtdIns(3,4,5)P_3) and Phosphatidylinositol-,4,5-bisphosphate (PtdIns(4,5)P_2) are involved in basolateral (Gassama-Diagne et al. 2006) and apical membrane (Martin-Belmonte et al. 2007) identity respectively. PtdIns(3,4,5)P_3 is converted to PtdIns(4,5)P_2 by the phosphatase PTEN at the apical membrane, after which Annexin2 (Anx2) binds to the newly generated PtdIns(4,5)P_2 at the apical membrane. Anx2 then binds Cdc42, followed by the recruitment of aPKC by Cdc42 to the apical membrane.

1.2.1.3. Organisation of the EPP

The EPP is organised through a large number of interactions between the different protein families and lipids involved. The apical polarity protein CRB recruits proteins associated with PALS1 via its PDZ-binding domain (Bilder, Schober & Perrimon 2003), which then subsequently recruits the scaffolding protein PAR6 to mediate the phosphorylation of another scaffold protein; PAR3 by the kinase PAR1 and the phosphorylation of LGL by aPKC (Yamanaka et al. 2001). This process is mediated by the activation of PAR6 by CDC42, which itself is activated by the GEF, Tuba (Qin et al. 2010). This phosphorylation results in the exclusion of these proteins and members of the SCRIB complex, DLG and SCRIB from the apical domain. Conversely, PAR1/PAR5-mediated phosphorylation events prevent basal

invasion by the apical polarity determinants, such as PAR3. In this case PAR1 is responsible for the phosphorylation of PAR3 on the lateral membrane, excluding PAR3 from this domain (Benton & St Johnston 2003). PAR5 then binds to phosphorylated PAR3 which is present on the lateral membrane and this triggers the dissociation of the PAR3-PAR5 complex into the cytoplasm, and PAR3 is subsequently dephosphorylated (Benton & St Johnston 2003). Polarity lipids also play a role in generating membrane asymmetries, specifically PTEN which is recruited to the junctional area via an interaction with PAR3 (Martin-Belmonte et al. 2007). PTEN then generates PtdIns(4,5)P_2, which recruits CDC42 via Anx2 (Martin-Belmonte et al. 2007). CDC42 participates in the activation of atypical protein kinase C (aPKC) through PAR6 (Martin-Belmonte et al. 2007). Basolateral phosphoinositide kinase PI3K associates with epithelial cadherin (E-cadherin) and β-catenin at adherens junctions (Pece et al. 1999). PI3K recruits DLG whilst also generating PtdIns(3,4,5)P_3 and this contributes to basal membrane identity via the recruitment of SCRIB (Rodriguez-Boulan & Macara 2014). The actin and microtubule cytoskeletons (described in section 1.3) also contribute to the initiation of cell polarity. The arrangement of the components of the EPP and their interactions are shown in figure 1.4.

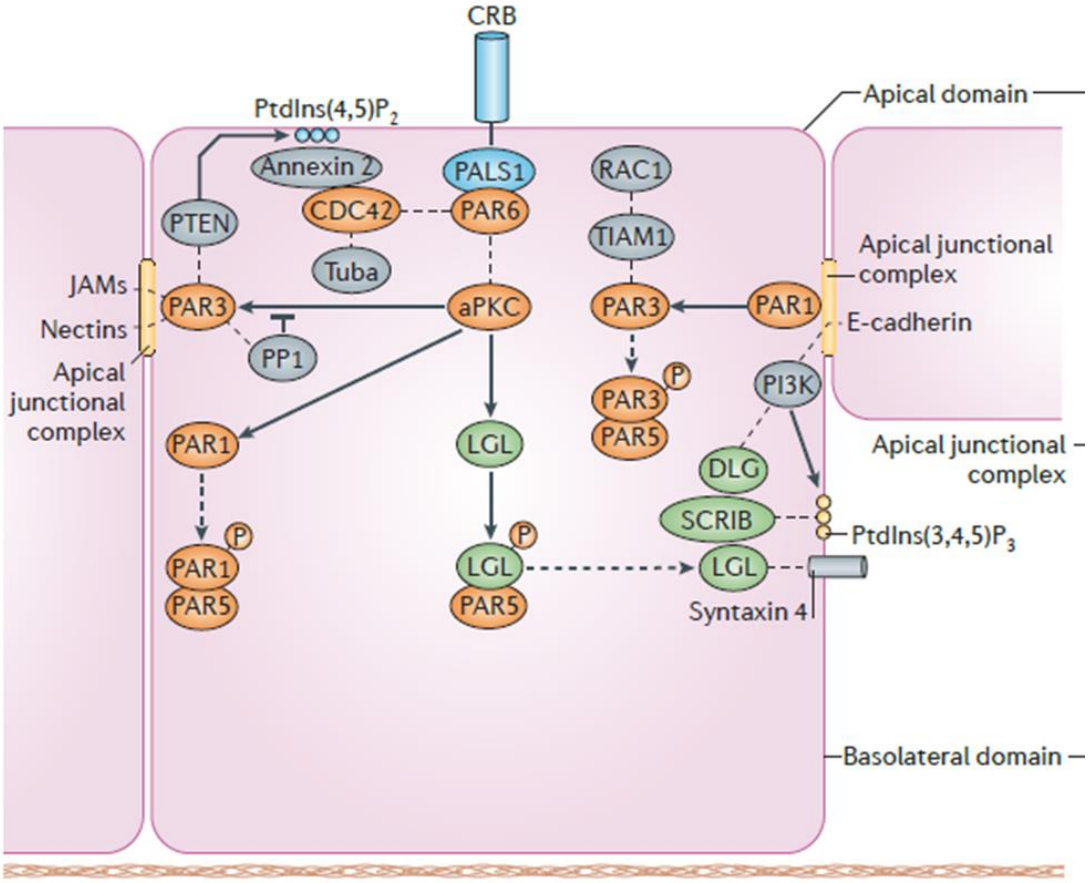

Figure 1.4. The localisation and interactions of components of the EPP. Solid arrows indicate a phosphorylation event, dashed arrows indicate a change to or from a phosphorylated state. The dashed lines indicate binding interactions (Rodriguez-Boulan & Macara 2014).

In this study, the fission yeast *Schizosaccharomyces pombe* was used to examine the regulation of cell polarity, and current knowledge of cell polarity regulation within *S. pombe* is described further in section 1.4.5.

1.3. The Cytoskeleton

The cytoskeleton is a network of filamentous structures within the cytoplasm of a cell, which forms a scaffold to support the cell. The term cytoskeleton was first used in 1903 by Nikolai K Koltsov when he proposed that the shape of a cell was determined by a network of tubules which he called the cytoskeleton, however little was known about the actual structure. It is now known that eukaryotic cells possess up to 3 different types of filaments which make up the cytoskeleton: actin containing microfilaments, intermediate filaments and tubulin containing microtubules (Wickstead & Gull 2011). It was long thought that the cytoskeleton was exclusive to eukaryotic cells, however in approximately the last 20 years homologues of both tubulin (de Boer, Crossley & Rothfield 1992; Erickson 1995) and actin (Bork, Sander & Valencia 1992) have been identified in prokaryotes.

1.3.1. The Actin Cytoskeleton

Actin is a highly conserved protein found in all eukaryotes with a homologue MreB found in prokaryotes (Bork, Sander & Valencia 1992). It is a globular ATP binding protein that polymerises to form double stranded filaments, with two populations of actin found within all cells. It is either present as a monomer referred to a globular actin (G-actin) or as part of a microfilament, referred to as filamentous actin (F-actin). In addition three main isoforms of actin have been identified in vertebrates, α, β and γ-actin, each of which have specific functions (Perrin & Ervasti 2010).

Actin is one of the most abundant proteins in eukaryotes, being present throughout the cytoplasm in many different structures where it plays a wide variety of roles,

corresponding to the cell type ranging from acting as a scaffold on which myosin generates force in muscle cells (Huxley & Niedergerke 1954; Huxley & Hanson 1954), providing mechanical support to cells, assisting in cell migration, generating the cytokinetic actomyosin ring (CAR) for cell division and providing tracks for myosins to transport cargoes around the cell (Pollard & Cooper 2009).

In the cell, monomeric G-actin can polymerise to form polar filaments, with this nucleation of actin filaments carried out by the Arp2/3 complex or formins (described in section 1.3.2) (Mullins, Heuser & Pollard 1998; Evangelista et al. 1997). These filaments are polar with a barbed (+ end) and a pointed (- end) with filament polymerisation occurring primarily at the barbed end and depolymerisation occurring primarily at the pointed end. This polymerisation is an ATP dependent process, during which ATP binds to a monomeric G-actin molecule in the cytoplasm and this G-actin is then added to the barbed end of the actin filament in a process mediated by profilin (Carlsson et al. 1977). At the same time as additional G-actin monomers are added to the barbed end of the filament, G-actin moves towards the pointed end of the filament. During this movement the G-actin hydrolyses ATP to ADP + Pi and the phosphate is subsequently released. At the same time as this is happeneing, G-actin monomers are removed from the pointed end of the filament in a process mediated by cofilin. Once in the cytosol the ADP bound to the G-actin monomer is exchanged for ATP and the G-actin monomer is then able to re-bind at the barbed end of the filament (Pollard 2007). This rate of polymerisation and depolymerisation is dependent upon the concentration of monomeric G-actin and in optimum conditions the rate of polymerisation and depolymerisation are the same, with the process referred to as actin treadmilling (Wegner 1976).

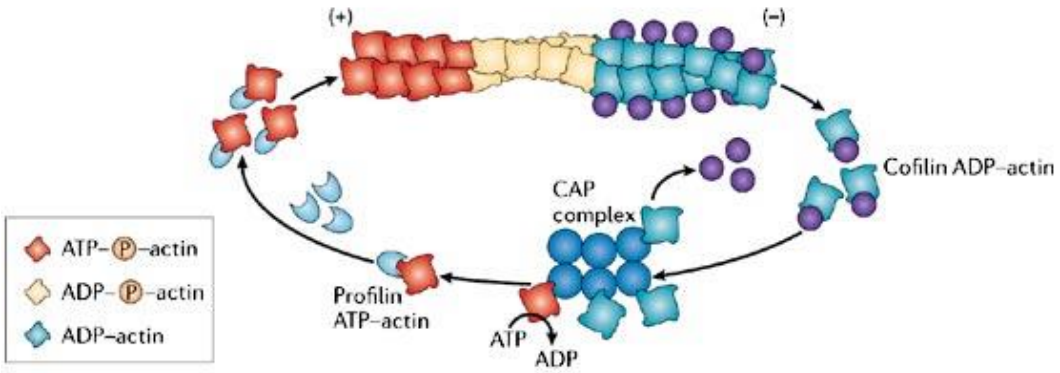

Figure 1.5. A schematic to show actin treadmilling, highlighting growth of filaments by the addition of ATP-actin monomers to the "barbed" end with profilin mediating the process. ATP is then hydrolysed and phosphate is released. ADP-actin is then removed from the pointed end of the filament by cofilin (Baum et al. 2006).

1.3.2. Actin Nucleators: Formins and the Arp2/3 complex

Although actin dynamics are driven by the concentration of free G-actin monomer (Pollard 1986), they require an initial nucleation event to stimulate polymerization which is carried out by either the Arp2/3 complex (Mullins, Heuser & Pollard 1998) or a family of proteins called Formins (Woychik et al. 1990; Castrillon & Wasserman 1994; Evangelista et al. 1997; Petersen et al. 1998; Chang, Drubin & Nurse 1997; Feierbach & Chang 2001). Similarly in order to prevent excessive filament polymerization, mechanisms exist to control this, either through the binding of profilin to the barbed end of the filament, which allows monomer addition but prevents subsequent nucleation (Pring, Weber & Bubb 1992) or the binding of capping proteins to the barbed end which prevent monomer addition (Casella, Maack & Lin 1986; Schafer, Jennings & Cooper 1996). The Arp2/3 complex and formins are responsible for nucleating different actin structures and do so via different mechanisms, with the Arp2/3 complex responsible for nucleating branched actin networks in structures such as actin patches (Pollard & Borisy 2003) whilst formins nucleate unbranched actin

filaments for incorporation into structures such as contractile rings required for cell division (Wallar & Alberts 2003).

The Arp2/3 complex consists of seven subunits including 2 actin-related proteins (Arp2 and Arp3) and all of these subunits are found in metazoans, fungi, plants and amoebae (Muller et al. 2005). Actin nucleation occurs when the Arp2/3 complex nucleates new filaments branching off the side of existing filaments from the point at which Arp2/3 is bound (Mullins, Heuser & Pollard 1998). The pointed end of the newly nucleated filament is anchored to the pre-existing filament by the Arp2/3 complex whilst actin polymerisation occurs at the newly created barbed end of the filament (Mullins, Heuser & Pollard 1998). The Arp2/3 complex is intrinsically inactive and is stimulated to create this new branch by a combination of actin filaments, an actin monomer and nucleation-promoting factors (NPFs) such as Wiskott-Aldrich syndrome protein (WASp) (Derry, Ochs & Francke 1994) and Scar (Bear, Rawls & Iii 1998; Machesky & Insall 1999) This process is demonstrated in figure 1.6.

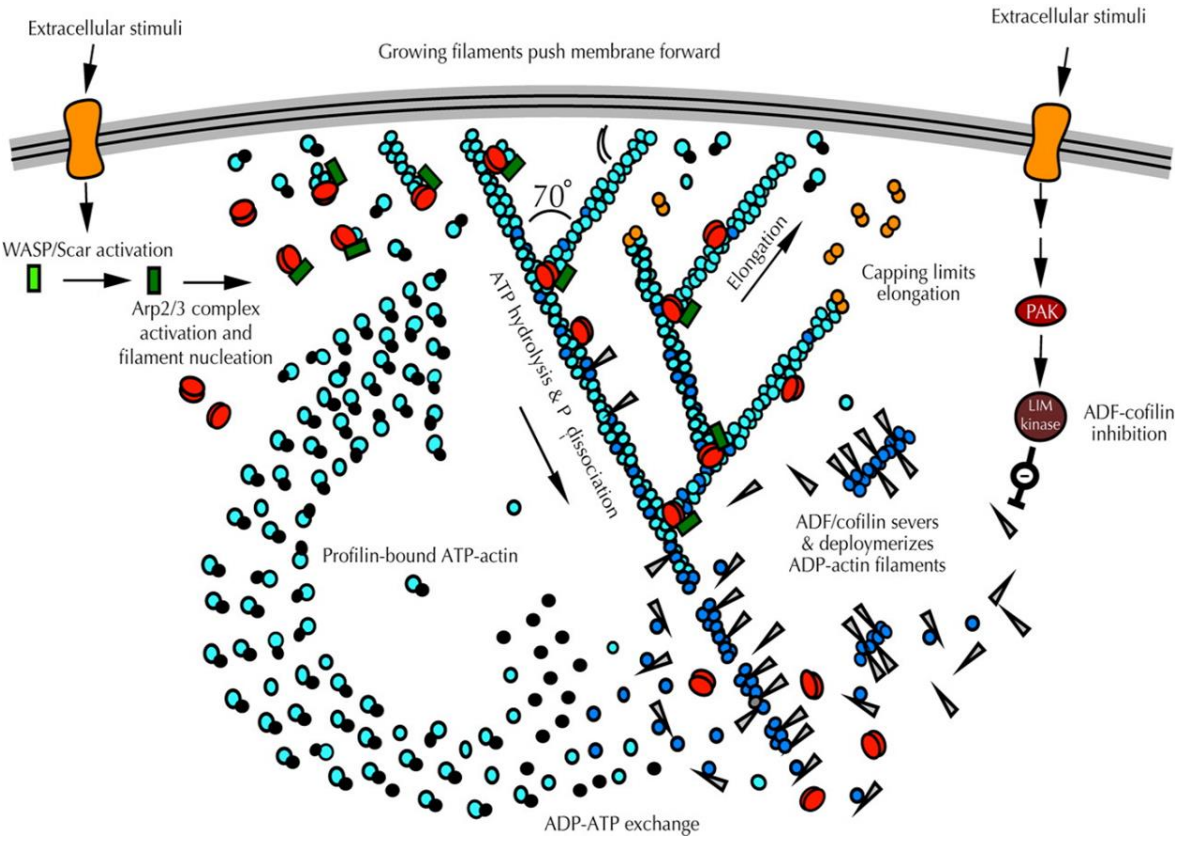

Figure 1.6. Arp2/3 complex activation and actin branching. The Arp2/3 complex is branching off of the side of existing filaments. The pointed end of the newly nucleated filament is anchored to the pre-existing filament by the Arp2/3 complex whilst actin polymerisation occurs at the newly created barbed end of the filament. Actin filament polymerization and depolymerisation occur as previously discussed (Pollard, Blanchoin & Mullins 2001).

Formins are present within all eukaryotic cells, with the first formin, Formin-1 identified in mice (Woychik et al. 1990) and was followed by the identification of homologues in *Drosophila* (Castrillon & Wasserman 1994) , *Saccharomyces cerevisiae* (Evangelista et al. 1997) and *Schizosaccharomyces pombe* (Chang, Drubin & Nurse 1997; Petersen et al. 1998; Feierbach & Chang 2001). Between these formin isoforms three regions of homology have been identified, named FH (formin homology domain) 1,2 and 3 (Castrillon & Wasserman 1994; Petersen et al. 1998). The formins are key regulators of cellular processes such as cytokinesis, cell polarity, cell adhesion and migration, cell morphogenesis and endocytosis (Kovar et al. 2003; Evangelista et al. 1997; Feierbach & Chang 2001)(Goode & Eck 2007). They play a key role in actin nucleation, however they do this in a way different from the

previously described actin nucleator, the Arp2/3 complex (Pruyne et al. 2002). Formins differ greatly from the Arp2/3 complex, both in their structure as they do not contain any actin-like domains and in their function as they are able to nucleate linear actin filaments, with an absence of any branching (Evangelista et al. 1997), whilst also being able to remain associated with the growing end of the actin filament(Evangelista, Zigmond & Boone 2003).

Formins are homodimers with the FH2 domain forming a circular shape with a central hole, believed to be where actin is located when formins are bound to the barbed end of the filament, essentially with the FH2 domains forming a sleeve around actin (Otomo et al. 2005). The binding of the formins to the barbed end of the actin filament has varying effects on filament polymerisation between different formins Fission yeast Cdc12 is able to nucleate filament growth however filament polymerisation only occurs at the pointed end. The addition of profilin allows growth at both ends in a similar fashion to actin filaments with no formin bound (Kovar et al. 2003). Conversely, binding of the mouse formin, mDia1 to the barbed end results in only a 10% reduction in polymerisation rate at the barbed end, whilst the presence of profilin greatly increases polymerisation rate 4 to 5 times (Kovar et al. 2006; Romero et al. 2004). This increase in polymerisation brought about by the presence of profilin is due to the FH1 domain of formins, which contains several polyproline sequences that bind to profilin, allowing profilin bound actin to interact with the FH1 domain and be tethered to the barbed end of the polymerising actin filament (Chang, Drubin & Nurse 1997). This interaction with profilin bound actin via the FH1 domains accelerates the rate of filament polymerisation significantly as the concentration of profilin bound actin near the FH2 domain allows for rapid transfer of actin monomers onto the growing filament. One theory for the inhibition of filament polymerisation when the FH2

domain is bound to the barbed end is that it can occupy one of at least 2 states on the end of the filament; an open state which allows actin subunits to bind and a capped state in which it does not, essentially functioning like a capping protein and models have been proposed for both states (Otomo et al. 2005). One way in which the formin may maintain its position on the end of the filament is by occupying this closed state after the addition of each actin subunit, preventing addition of subunits that would be too quick to allow the formin to stay at the end (Pollard 2007).

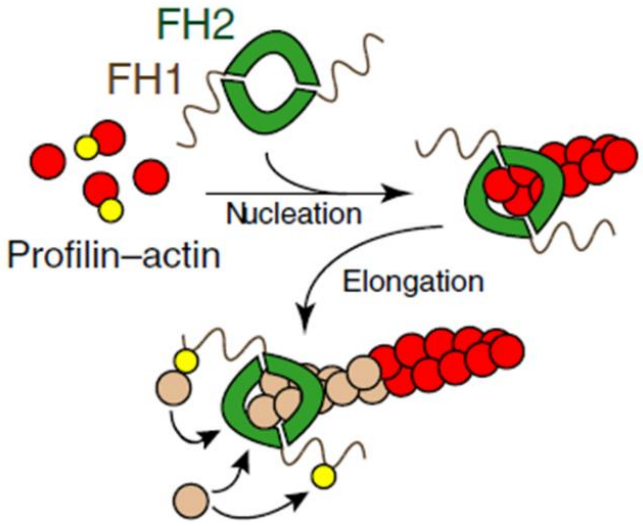

Figure 1.7. Formins nucleate actin filaments via FH1 and FH2 domains. Profilin actin is added to the barbed end of the actin filament whilst the formin remains associated with the barbed end (Kovar 2006).

1.3.3. Actin Associated Motor Proteins: Myosins

Myosins are a family of ATP-dependent motor proteins that associate with actin and carry out a wide variety of roles in processes including muscle contraction, cell motility, cytokinesis and intracellular transport. This variation in function is accompanied by structural differences in different classes of myosins which allows them to carry out these specific functions, with 35 classes of myosins currently identified (Odronitz & Kollmar 2007; MA & Spudich 2012). All of these classes share similar properties in that they bind to actin and hydrolyse ATP to generate force. It was originally thought that myosin was restricted to muscle cells, however the discovery of a myosin-like enzyme in *Acanthamoeba castellanii* in 1973 was the catalyst for the discovery of a large number of myosin genes in various organisms (Pollard & Korn 1973) and myosins are now believed to be expressed almost ubiquitously within eukaryotes (Odronitz & Kollmar 2007). This separation between muscle myosin and subsequently identified myosins has resulted in myosins being separated into 2 groups, conventional myosins which are class II myosins (including muscle myosin) and unconventional myosins which encompasses all other myosin classes (MA & Spudich 2012).

Most myosins are similar in their structure with the protein divided into 3 main regions. The first is an amino terminal head or motor domain which is responsible for binding to actin and the binding and hydrolysis of ATP. The amino acid sequence of the head domain is highly conserved across eukaryotes, and it is this head domain that is used to phylogenetically classify myosins. The neck domain is an alpha-helical region which can vary in length and contains varying numbers of IQ motifs for the binding of light chains such

as calmodulins. The binding of these light chains is responsible for regulation of the myosin. Finally the carboxyl terminal tail domain is the most variable part of the myosin in terms of sequence, structure and function between different classes and it plays roles in cargo binding and dimerization of myosin heavy chains (Krendel & Mooseker 2005).

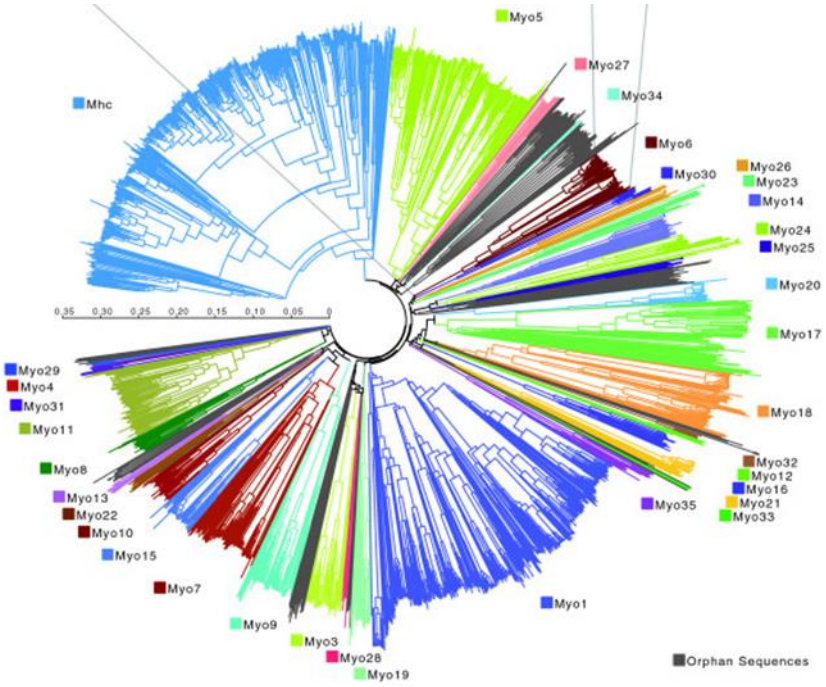

Figure 1.8. A schematic representation of division of the myosin superfamily into 35 classes (Odronitz & Kollmar 2007).

1.3.3.1. Conventional and Unconventional Myosins

It is the variation in tail domain which can affect whether myosins are observed as single headed monomers or two headed dimers. The dimerization of two myosins is facilitated by a heptad repeat within the tail region allowing the formation of alpha-helical coiled coils and thus dimerization (Krendel & Mooseker 2005). However not all myosins that have a predicted coiled coil motif dimerise, an example being Myo6 (Lister et al. 2004). The conventional myosins (class II) are always dimeric, two headed myosins (Trotta, Dreizen &

Stracher 1968), however there is variation between the unconventional myosins with some observed as monomers such as class I myosins (Stafford et al. 2005) whilst some such as class V myosins are dimeric (Mehta et al. 1999), with this monomeric or dimeric formation being specifically tailored to their function. A small number of unconventional myosins are observed as either monomeric or dimeric proteins, with their dimerisation being regulated by other mechanisms in addition to the presence of a predicted coiled-coil motif such as class VI myosins. This variation in monomeric or dimeric myosins is shown in figure 1.9 below.

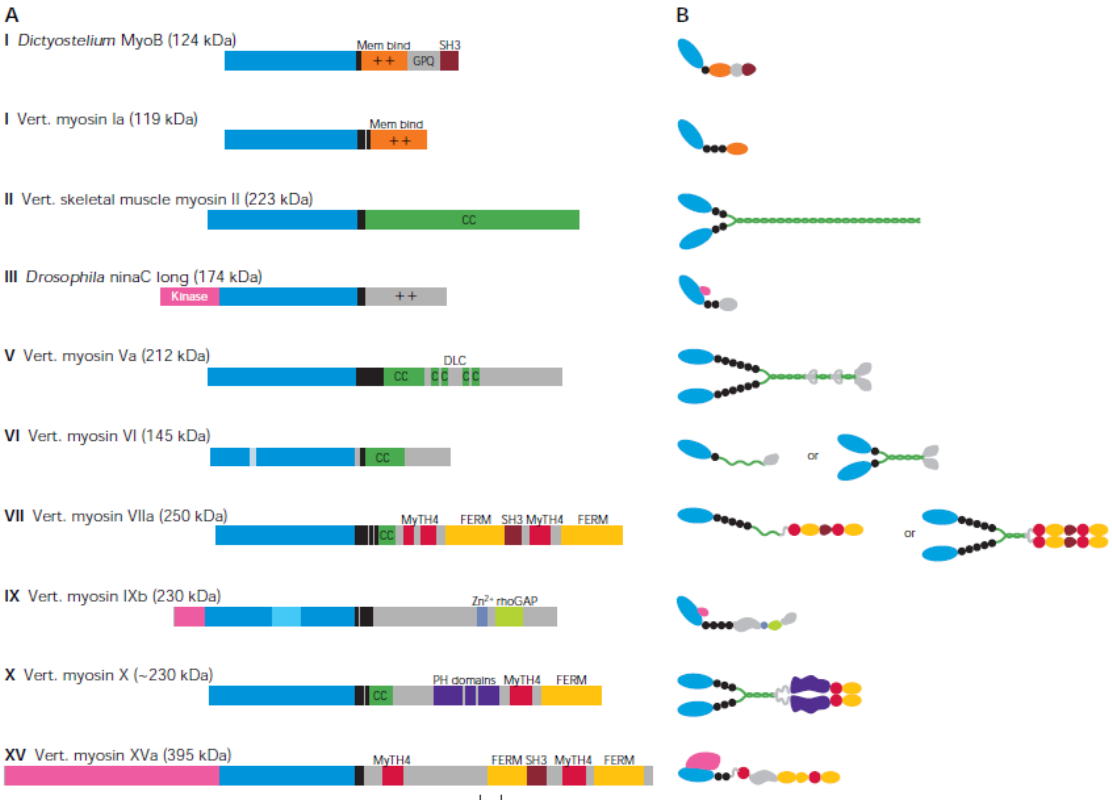

Figure 1.9. A schematic showing the structure of myosin heavy chains (left) and how different myosins exist as monomers, dimers or both (right). Taken from (Krendel & Mooseker 2005).

1.3.3.2. The Cross Bridge Cycle

In order for myosins to carry out their function they require binding to actin and the hydrolysis of ATP in order to produce a mechanical force. This occurs in a cyclic manner, beginning with the binding of myosin to actin. ATP then binds to the myosin which causes a decrease in its affinity for actin resulting in myosin dissociation from actin. The ATP is then hydrolysed to ADP + Pi which remain bound to the myosin and causes its affinity for actin to increase resulting in re-binding. After this re-binding of myosin to actin there is a conformational change in the myosin, resulting in the release of Pi which is accompanied by the powerstroke, this being the movement of the myosin relative to the actin. Once the powerstroke has occurred ADP is released from the myosin and the nucleotide binding pocket is ready for the binding of ATP which restarts the cycle (Smith & Geeves 1995). The modulation of myosin affinity for actin results in two myosin binding states for actin being adopted within the cross bridge cycle, these being the strong and weak binding states. The weak binding state is observed when myosin is bound to either ATP or ADP + Pi and during these states myosin can attach and detach from actin at submicrosecond rates and has a low affinity for actin (micromolar range). These states are also referred to as the “pre-force generating” states (Geeves & Holmes 1999; De La Cruz & Ostap 2004). The strong binding state is observed when myosin is bound to actin alone, or in the presence of just ADP, and has submicromolar affinities for actin. These states are also referred to as “force-bearing” states (De La Cruz & Ostap 2004; Geeves & Holmes 1999).

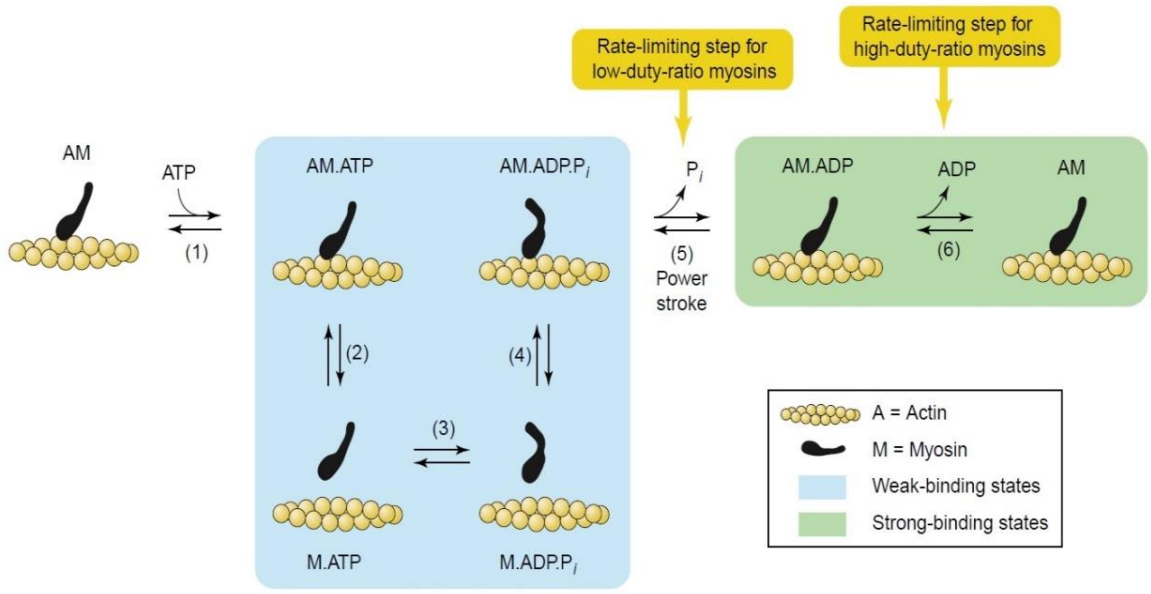

Figure.1.10. The cross bridge cycle, also showing the weak and strong binding states of myosin. In the absence of ATP myosin binds tightly to actin. The binding of ATP (1) induces a conformational change in the myosin that reduces its actin affinity and the myosin detaches from actin (2). ATP is then hydrolysed to ADP and inorganic phosphate (Pi) (3) and these both remain bound to myosin. The myosin then rebinds to the actin (4) and phosphate is released, accompanied by the powerstroke (5). ADP is then released (6) and the cycle can restart when ATP binds to myosin (De La Cruz & Ostap 2004).

1.3.3.3. Processivity and Duty Ratio

The diversity in myosin function is reflected by significant changes in certain motor properties between different isoforms, with two of the largest factors being processivity and duty ratio. Some myosins are referred to as processive motors, which means that they are able to take multiple steps along an actin track without dissociating (Mehta et al. 1999). These myosins, including class V myosins are dimeric thus having two head domains, one of which always remains bound to the actin filament as they move along in a hand-over-hand motion (Mehta et al. 1999; Tyska & Mooseker 2003; Warshaw et al. 2005). This hand-over-hand movement is shown in figure 1.11.

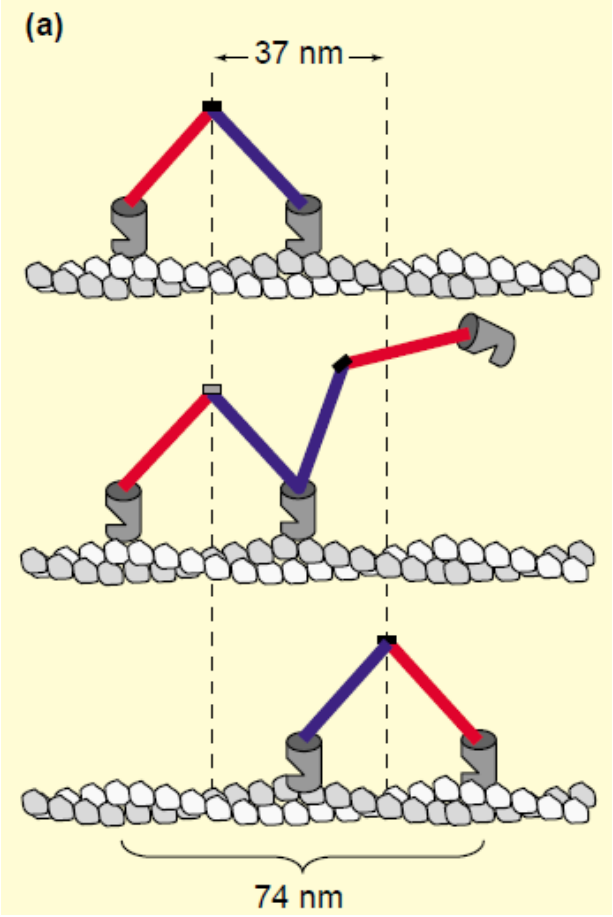

Figure.1.11. A simple schematic to show to hand-over-hand movement of processive myosins. A flipping motion occurs and the trailing head (red) moves to the next actin binding site in front of the leading head (blue) resulting in the myosin taking 37 nm steps (Tyska & Mooseker 2003).

Duty ratio refers to the proportion of time during the cross bridge cycle that a myosin remains bound to actin (Krendel & Mooseker 2005). High duty ratio myosins spend a large proportion of their time bound to actin, an example being processive myosins such as Myosin V which almost always have at least one of the 2 myosin heads bound to the actin filament at any given time (Mehta et al. 1999; Tyska & Mooseker 2003; Warshaw et al. 2005). In contrast low duty ratio myosins spend very little time bound to actin, an example of this being class II myosins (Marston & Taylor 1980; Kovács et al. 2003). It is this duty ratio that determines whether a myosin is classed as a fast or slow myosin, with high duty ratio myosins referred to as slow myosins and low duty ratio myosins referred to as fast myosins.

1.3.3.4. Role of actomyosin in muscle contraction

Myosin function has been most extensively studied in muscle cells and the role it plays in muscle contraction. Conventional type II myosins are present in muscle cells, with two myosin heavy chains dimerised via the coiled-coil domain within the tail region. Muscle cells are arranged into fibres consisting of many sarcomeres (Huxley & Hanson 1954; Huxley & Niedergerke 1954). Within these sarcomeres are a thin and thick filament which are arranged in an anti-parallel manner. The thick filament is comprised of a long chain of type II myosin dimers, whilst the thin filament is comprised of actin and other regulatory proteins such as tropomyosin (Tm) (Bailey 1946) and the troponin complex (Ohtsuki et al. 1967). The sarcomere is contained between two Z disks and the thin filament is attached to these Z disks directly whilst the thick filament is attached via Titin (Fürst et al. 1988). When muscles contract there is an interaction between the thick and thin filaments. ATP hydrolysis by the myosin within the thick filament results in the sliding of the thin filament and the Z disks moving closer together. This is referred to as the sliding filament theory and was first described in 1954 (Huxley & Niedergerke 1954; Huxley & Hanson 1954). The arrangement of the sarcomere is shown in figure 1.12.

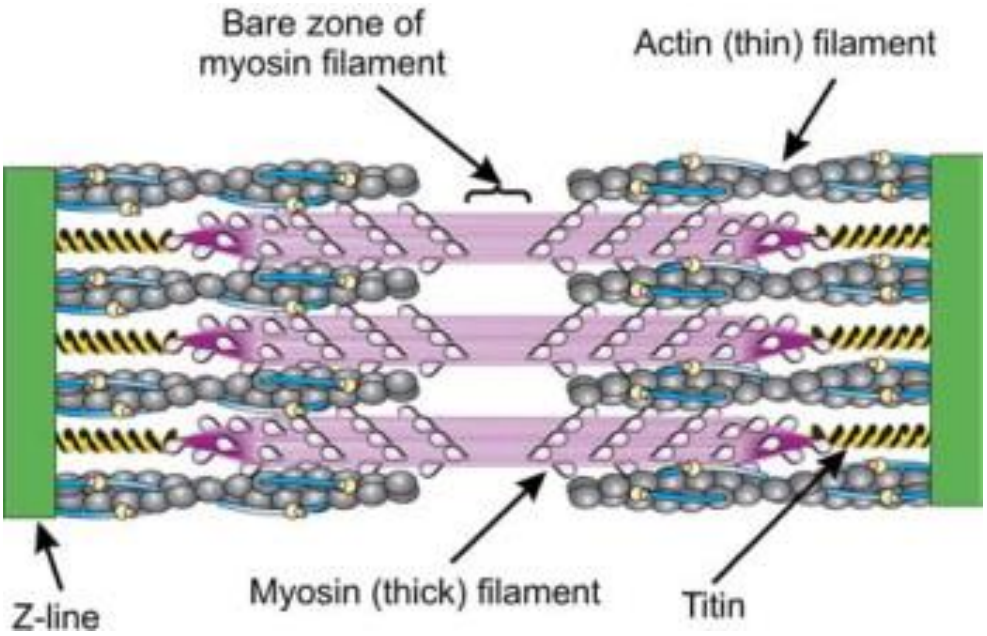

Figure.1.12. A schematic representation of the sarcomere. The sarcomere is housed between 2 Z disks which the actin thin filament is attached to. The myosin containing thick filament runs anti parallel to the thin filament and is attached to the Z disks via Titin (Plotnikov et al. 2006).

1.3.3.5. Myosin V and VI

In this study, particular attention is paid to the unconventional, processive class V and VI myosins. Myosin V is a two headed motor protein formed by the dimerization of two myosin heavy chains via the coiled-coil in the tail region (Cheney et al. 1993). Myosin V binds cargoes through the cargo binding domain within the tail region and is responsible for the transport of a wide variety of intracellular cargoes along actin cables (Reck-Peterson et al. 2000; Vale 2003; Hammer & Sellers 2011). Myosin V cargoes have been identified in a wide variety of organisms. In budding yeast mRNA, secretory vesicles and vacuoles are transported by two class V myosins (Kwon & Schnapp 2001; Ishikawa et al. 2003). In mammalian cells melanosomes are transported by Myosin V via an interaction between the adaptor protein melanophilin and GTP bound Rab27 on the melanosome membrane (Langford 2002). Finally in the fission yeast *Schizosaccharomyces pombe* class V myosins have roles in the delivery of an α-glucan synthase involved in cell wall synthesis, (Win, et

al. 2001), a β-1-3-glucan synthase during cytokinesis (Mulvihill, Edwards and Hyams 2006) whilst it has also been implicated to play roles in vacuole organisation and maintenance (Motegi, Arai & Mabuchi 2001; Mulvihill, Edwards & Hyams 2006) and transporting the SNARE protein, synaptobrevin, to its proper cellular location (Edamatsu and Toyoshima 2003).

The double headed Myosin V dimer moves along actin filaments in a highly processive manner, taking multiple steps along the actin filament towards the barbed end whilst one head always remains bound to actin in a hand over hand manner (as described in section 1.3.3.3) (Mehta et al. 1999; Tyska & Mooseker 2003; Warshaw et al. 2005). These steps span a 37 nm distance (Mehta et al. 1999), which corresponds to the pseudorepeat distance within the actin filament. From this it was suggested that Myosin V "walks" along the top of the actin filament rather than following the spiral of the filament, which was later shown to be true by EM studies (Walker et al. 2000). This large 37 nm step is facilitated by its long lever arm, an α-helical region containing six IQ motifs to which calmodulin light chains can bind (Burgess et al. 2002).

Myosin VI is observed as either a monomeric motor protein with a large 18 nm working stroke (Lister et al. 2004) or as a double headed dimer that moves processively along actin in a similar manner to Myosin V (Rock et al. 2001). Myosin VI has been shown to play roles in clathrin mediated endocytosis (Buss et al. 2001; Buss, Luzio & Kendrick-Jones 2001; Aschenbrenner, Lee & Hasson 2003) and in stabilising tension in stereocillia (Avraham et al. 1995; Cramer 2000).

Myosin VI and it's mechanism of movement is of particular interest as there are several clear differences from typical processive myosins such as myosin V. Firstly, Myosin VI moves in the opposite direction to all myosins except class IX myosins, in that it moves "backwards" towards the pointed (-) end of the actin filament (Wells et al. 1999). This backward movement is facilitated by a 53 amino acid insert within the neck region, named the inverter domain (Wells et al. 1999). This insert results in the lever arm being rotated by 180° which then alters the direction that the motor moves in (Tsiavaliaris, Fujita-Becker & Manstein 2004; Ménétrey et al. 2005). This is shown in figure 1.13 below. The second intriguing property of Myosin VI is that whilst moving processively in a hand over hand manner it is able to take large steps of 30 ± 12 nm (Rock et al. 2001) despite having a short lever arm containing only 2 calmodulin binding IQ motifs (Bahloul et al. 2004). This ability to make large steps has been attributed to a flexible domain within the tail region of Myosin VI, with the working stroke of the motor first occurring which provides directionality of movement and is followed by a diffusive search for subsequent actin binding sites by the leading head (Rock et al. 2001; Okten et al. 2004).

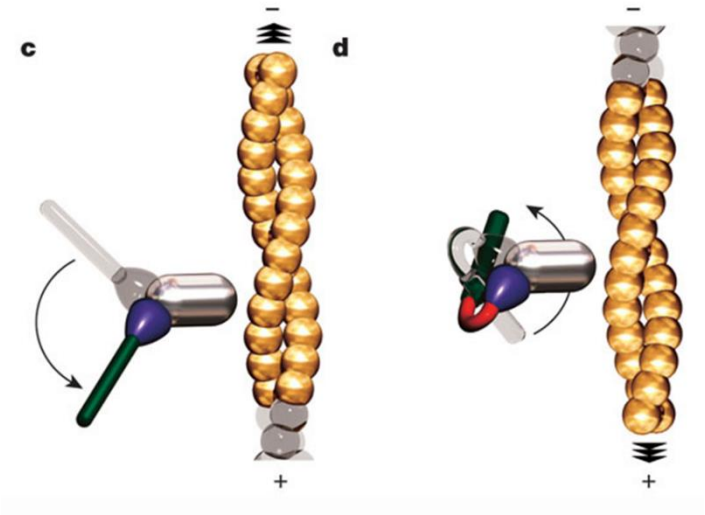

Figure.1.13. The role of the inverter domain. In (c) the power-stroke of a conventional barbed (+) end directed myosin is shown. (d) Shows how the inverter domain (red) between the converter region (blue) and the lever arm (green) reverses the direction of the power stroke and resulting in a pointed (-) end directed myosin (Tsiavaliaris, Fujita-Becker & Manstein 2004).

1.3.4. Tropomyosin

Tropomyosin (Tm) is an evolutionarily conserved dimeric α-helical coiled coil protein as shown in figure 1.14 which polymerises to form strands that coil around and associate with actin. This results in structural stabilisation and maintenance of the actin filaments within eukaryotic cells (Perry 2001). Tm is present in many different types of cells and different isoforms have different functions depending on the type of cell they are present in. In addition the length of the Tm dimer varies greatly spanning from up to 284 amino acids in verterbrates down to 161 amino acids in yeasts. These different length tropomyosins span different numbers of actin biding sites (7-4) on the actin filament respectively.

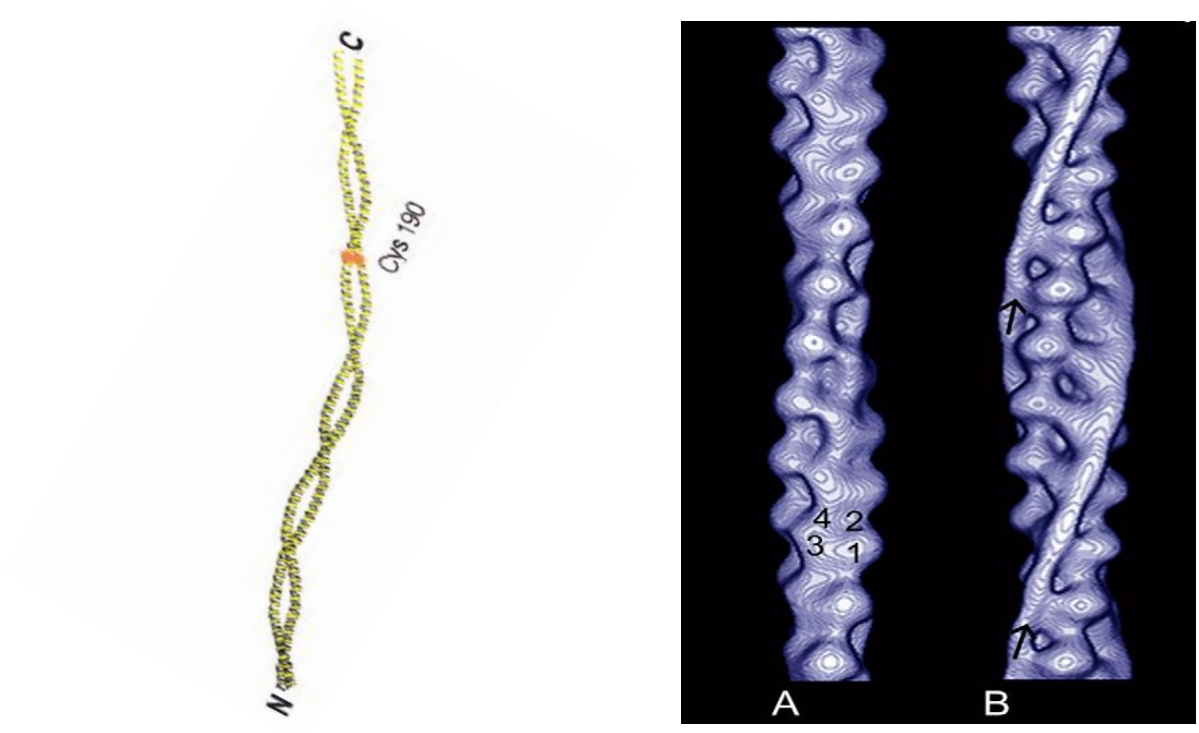

Figure.1.14. (Left) A model of the tropomyosin molecule. The dimeric form of the protein is shown, demonstrating 2 tropomyosin α-helices coiled around each other to form the coiled coil dimer. The slight curvature which allows tropomyosin to coil around actin filaments is also visible. The molecular ends of the Tm molecule were determined relative to the cysteine residue at position 190 (Cys 190) (Whitby & Phillips 2000). (Right) A 3 dimensional reconstruction of the thin filament. (A) shows the F-actin control with no tropomyosin present, in B the tropomyosin polymer coiling around the actin filament is clearly visible (Skoumpla et al. 2007).

The most extensive research on tropomyosin has been carried out in muscle, where it is a 284 amino acid protein and plays a key role in regulating muscle contraction. Muscular tropomyosin along with the troponin complex is associated with actin fibres and then modulates the binding of myosin to actin (Smith, Maytum & Geeves 2003). Both a two state and three state model have been proposed to explain how tropomyosin regulates myosin binding to actin in muscle (Huxley 1973; McKillop & Geeves 1993). The two state model proposes that tropomyosin binds to actin filaments in muscle and can occupy one of two states. In a resting muscle tropomyosin covers myosin binding sites and is locked in position by tropomyosin binding troponin (Troponin T) and inhibitory troponin (Troponin I). When calcium is released from the sarcoplasmic reticulum it binds to calcium-binding troponin (Troponin C) which induces a conformational change in tropomyosin causing it to move on the actin filament and expose myosin binding sites, allowing myosin to bind and cause muscle contraction (Huxley 1973). The later proposed 3 state model suggests a slightly different system but starts in the same way, when in a resting muscle the tropomyosin covers the myosin binding sites and is locked in position by Troponin T and Troponin I. This is known as the “blocked” position. When calcium is released from the sarcoplasmic reticulum it again binds to Troponin C, which in turn unlocks tropomyosin from the actin filament. However in contrast to the two state model the tropomyosin does not shift and fully expose myosin binding sites, instead the tropomyosin moves slightly, partially unblocking the myosin binding sites, occupying what is known as the “closed” position. Occasionally a myosin molecule is able to slot past the tropomyosin and bind weakly, resulting in steric hindrance which then prevents the tropomyosin from blocking this and adjacent myosin binding sites, causing it to occupy the “open” position. This eventually leads to full myosin binding, resulting in muscle contraction (McKillop & Geeves 1993)

(Vibert, Craig & Lehman 1997). This binding is referred to as cooperative binding, as the initial binding of myosin to the actin filament leads to a further increase in myosin affinity for actin due to the exposure of more binding sites. Once muscle contraction is completed, both models propose that calcium is then actively pumped out of the cytoplasm of muscle cells and this drop in calcium levels causes tropomyosin to move back into the "blocked" position and prevent myosin binding once again. The three positions that tropomyosin can occupy on the actin filament are shown in figure 1.15 below.

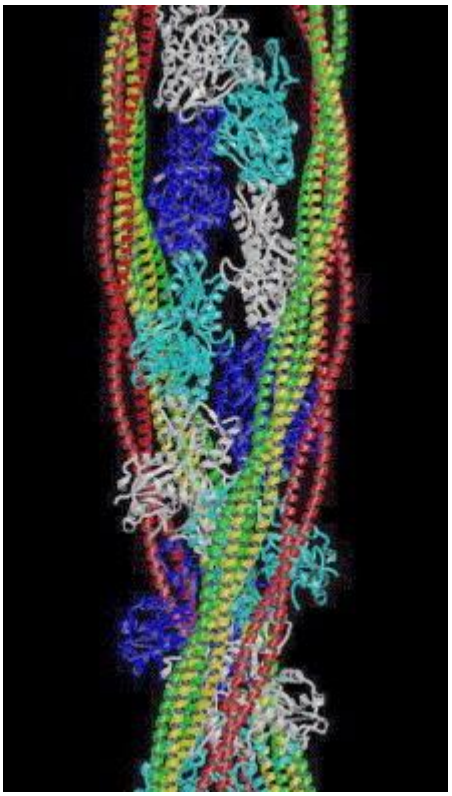

Figure.1.15. A model showing the 3 states of tropomyosin. The actin filament is shown in white, blue and sky blue. The blocked position of tropomyosin is shown in red, in this state all of the myosin binding sites are covered. The closed position is shown in yellow, tropomyosin adopts this position when calcium binds to troponin C. This binding of calcium causes the tropomyosin filament to shift 25° from the blocked to the closed position. The open position is shown in green, this is a further 10° shift from the closed position, brought about by a small amount of myosin binding to the actin filament. In this state all myosin binding sites are exposed (Poole et al. 2006).

The functions of actin, myosin and tropomyosin are very different in simple unicellular eukaryotes, where they form a complex cytoskeleton involved in many processes such as

transport of intracellular organelles and cargoes, cell fusion and cytokinesis. The role of tropomyosin within this environment is to stabilise and maintain the actin filaments, whilst also playing a key role in the formation of the cytokinetic actomyosin ring (CAR).

1.3.4.1. Yeast Tropomyosins

Yeasts are a very popular model for studying the function of tropomyosin in simple unicellular eukaryotes. The two most commonly used yeasts are the budding yeast *Saccharomoyces cerevisiae* and the fission yeast *Schizosaccharomyces pombe* (discussed later, section 1.4.3). The *S. cerevisiae* genome contains 2 genes encoding for tropomyosins: *TPM1*, for a tropomyosin with a molecular weight of 23.5 kDa and consisting of 199 amino acids; and *TPM2,* for a tropomyosin with a molecular weight of 19.0 kDa and consisting of 161 amino acids. When aligned the two tropomyosins have 64.5% homology (Drees et al. 1995) however they carry out different functions within the cell. Tpm1 binds to all actin, stabilising the filaments whereas Tpm2 is shown to regulate the interaction between F-actin and myosins, in particular inhibiting retrograde actin cable flow (Drees et al. 1995). Type II myosin is shown to promote retrograde actin cable flow when bound to actin in budding yeast, and Tpm2 binding to the F-actin prevents the binding of myosin and thus inhibits retrograde cable flow (Huckaba, Lipkin & Pon 2006). Tpm1 has been shown to be more important to the cells than Tpm2, with deletion of *TPM1* resulting in disappearance of actin cables from the cytoskeleton and actin patches being randomly spread throughout the cells (Drees et al. 1995). Defects in growth are observed, together with defects in mating projection formation and cell fusion during mating. Chitin is also found randomly distributed throughout the cell wall, rather than being limited to just the septum during

budding (Drees et al. 1995). These defects are believed to be a result of the partial defect in the transportation of cellular components to the cell surface (Drees et al. 1995; Liu & Bretscher 1992). *TPM2* deletion cells show no phenotypical consequence, being indistinguishable from wild type cells in their morphology, budding patterns, cytoskeleton organisation, osmotic sensitivity or mating efficiency (Drees et al. 1995). Furthermore it has been shown that over-expression of *TPM2* in *TPM1* deletion cells is not able to restore wild type morphology, providing more evidence that the two isoforms of tropomyosin within *S. cerevisiae* have distinct functions (Drees et al. 1995). The presence of the two tropomyosins also have different effects on the other's ability to bind to actin, which has been demonstrated using co-sedimentation assays. Addition of Tpm1 has been shown to have no effect on Tpm2's ability to bind to actin, however addition of Tpm2 has a negative effect on Tpm1 actin binding, suggesting that Tpm2 has a higher actin affinity than Tpm1 (Drees et al. 1995). The fact that Tpm1 binds to actin with a weaker affinity, although it plays a more major role is most likely due to the fact that the actin cytoskeleton is a very dyamic structure, and the weaker binding of Tpm1 means that the dynamics of the actin filament are not affected.

1.3.4.2. Tropomyosin Structure

Tropomyosin has a coiled-coil structure, whereby two alpha-helical tropomyosin molecules coil around each other to form the dimeric coiled coil protein (Perry 2001; Brown et al. 2001). The interaction between these two tropomyosin molecules, and the subsequent stability of the coiled coil structure is a consequence of the amino acid sequence of the tropomyosin molecule. Tropomyosin exhibits a heptad repeat with the seven amino acid

residues within the repeat named *a*-*g*. This heptad repeat structure of coiled coil proteins was first suggested by Crick in 1953 (Crick 1953) and was confirmed when the amino acid sequence of tropomyosin was published in 1978 (Stone & Smillie 1978). Amino acids within these positions usually possess similar properties such as polarity and hydrophobicity. Residues at positions *a* and *d* are referred to as the "core" residues and are responsible for much of the stability of the coiled coil structure (Perry 2001). Residues at these positions in the heptad repeat often contain hydrophobic side-chains, which can lead to hydrophobic interactions with hydrophobic side-chains on the adjacent tropomyosin molecule, as shown in figure 1.16. Residues in positions *e* and *g* also contribute to the stability of the coiled coil structure by way of ionic interactions (Perry 2001).

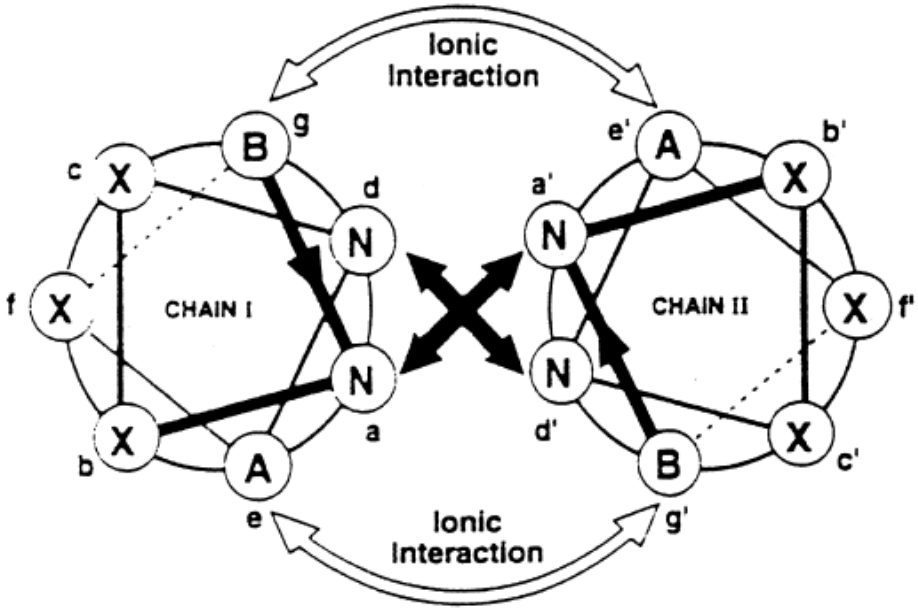

Figure.1.16. A representation of the coiled coil structure and its heptad repeat. The heptad repeat is shown by the letters a-g and a'-g' with a/a' and d/d' being the core residues. The solid black arrows linking residues a/a' and d/d' represent the hydrophobic interactions between the core residues, which bring about the majority of the stability of the coiled coil. The black outlined arrows between e/g' and g/e' represent the ionic interactions between acidic and basic amino acids which can interact by way of ionic bonds and contribute to the stability of the structure. Residues labelled X play no role in stabilising the coiled coil structure. From (Perry 2001).

In order for tropomyosin to stabilise actin filaments, tropomyosin dimers have to polymerise by head-to-tail interactions, with the polymerisation occurring along the actin filament, not prior to tropomyosin binding to actin (Greenfield 1994; Bharadwaj et al. 2004). This head-to-tail interaction between molecules is highly dependent upon the N and C termini of tropomyosin molecules and requires an 11 amino acid overlap between the N and C termini. This overlap is formed when the C terminus of one tropomyosin dimer splays apart to from a cleft in which the N-terminus of a subsequent tropomyosin molecule can bind and overlap the 11 amino acids of the C-terminus (figure 1.17) (Hitchcock-DeGregori & Singh 2010).

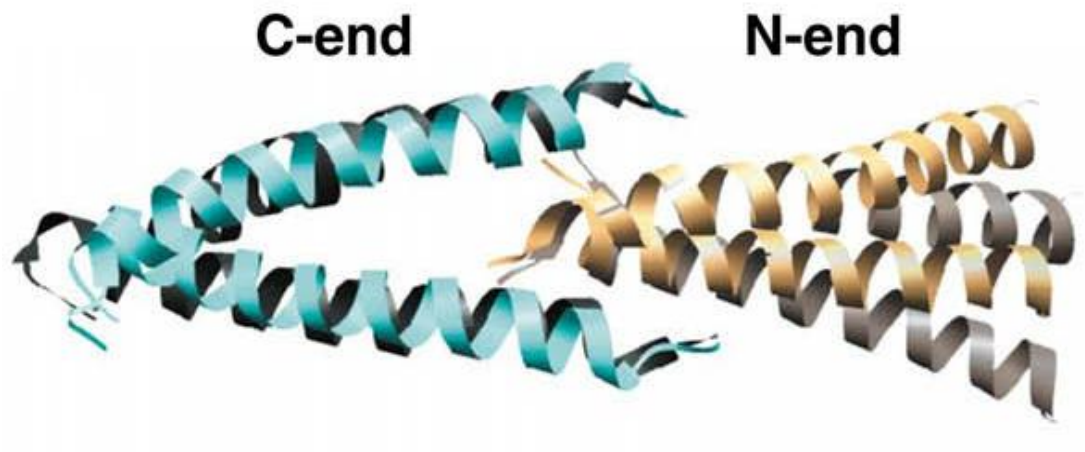

Figure.1.17. A solution structure of α-tropomyosin showing the splaying of the C-terminus of a tropomyosin molecule, creating a cleft for the N-terminus of another tropomyosin molecule to slot into. This results in an 11 amino acid overlap between the two molecules and allows tropomyosin molecules to polymerise along the actin filament. From (Hitchcock-DeGregori & Singh 2010).

Many tropomyosins require acetylation at the N-terminus, which helps to stabilise the coiled coil structure and ensures that the N-terminus remains as a coiled coil, unlike the C-terminus which must splay apart (Brown et al. 2001; Greenfield 1994). The N-terminal acetylation has also been shown to be crucial for the head-to-tail polymerization of

tropomyosin filaments. It is believed that the acetyl group is essential as it shields the charge of the initiation methionine in the *a* position within the heptad repeat whilst also stabilising ionic interactions within the coiled coil. If acetylation does not occur the charge on the methionine may lead to repulsion between *a* residues which could lead to destabilization of the coiled coil (figure 1.18) and reduce the ability of tropomyosin molecules to polymerise (Greenfield 1994; Monteiro, Lataros & Ferro 1994; Brown et al. 2001).

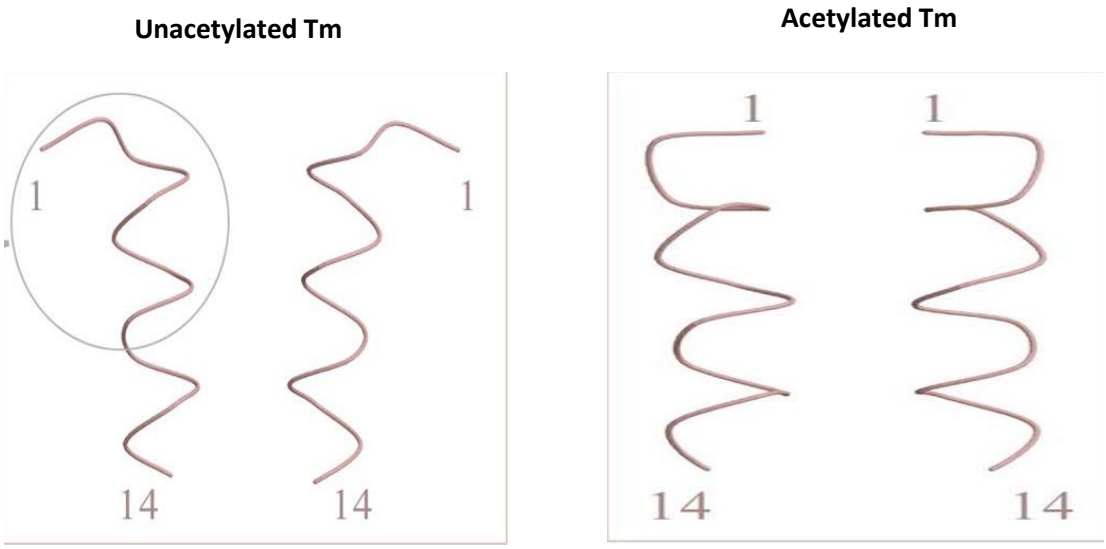

Figure.1.18. α-Carbon drawings illustrating differences at the N-terminus of unacetylated (left) and acetylated (right) tropomyosin. In the case of the unacetylated tropomyosin, the alpha helical structure is lost, with residues 1 and 2 extending sideways away from the adjacent molecule, resulting in the loss of coiled coil structure at the extreme N-terminus of the dimer (Brown et al. 2001).

1.3.5. N-terminal Acetylation of Proteins

Acetylation is a ubiquitous co-translational protein modification occurring in as many as 84% of eukaryote proteins (Arnesen et al. 2009) and has been shown to be crucial for the stability and function of many proteins and in some cases has been shown to actively regulate protein function. Acetylation can occur either at the amino terminus of proteins or at specific residues within the polypeptide chain. N-terminal acetylation is one of the most common post-translational modifications of proteins in eukaryotes, which involves the transfer of an acetyl group from acetyl coenzyme A to the amino-terminal amino acid of a protein (Polevoda & Sherman 2000). The addition of the acetyl group to the N-terminal residue neutralizes positive charges which may affect the function and stability of the protein, as well as regulating interactions with other proteins/molecules or further modifications such as phosphorylation and ubiquitination (Polevoda & Sherman 2003). N-terminal acetylation occurs in approximately 84% of cytosolic mammalian proteins, 57% of yeast proteins, but is rarely observed in prokaryotic or archaeal proteins (Polevoda & Sherman 2003b; Arnesen et al. 2009). Evidence from *in vitro* studies suggests that in eukaryotes acetylation occurs when between 25 and 50 amino acid residues have been translated and are protruding from the exit region of the ribosome (Polevoda & Sherman 2003).

1.3.5.1. N-α-terminal Acetyltransferases

The acetylation of amino terminal amino acids is catalyzed by a group of enzymes known as N-α-terminal acetyltransferases (NATs) (Polevoda & Sherman 2000). The NATs have been extensively studied in the budding yeast *Saccharomyces cerevisiae*, in which three

major classes of NAT were first identified; NatA, NatB and NatC, which have since been shown to be conserved in humans (Arnesen et al. 2009). The NATs usually consist of two subunits; a catalytic subunit and an auxiliary subunit, however some NATs have 3 subunits (Polevoda, Arnesen & Sherman 2009). As well as being comprised of different subunits the different NATs also have distinct substrate amino acid sequence specificity (Polevoda & Sherman 2003).

1.3.5.2. NatB

It has previously been shown that Tpm1 in *S. cerevisiae* is acetylated at its N-terminus by the NatB complex, consisting of Nat3 and Mdm20 subunits, due to its N-terminal amino acid sequence being Met-Asp-Lys-Ile-Arg, a predicted NatB substrate (Polevoda et al. 2003). NatB consists of two subunits: a 23 kDa catalytic subunit Nat3; and a 92 kDa auxiliary subunit Mdm20 (Polevoda and Sherman 2003). NatB target proteins always have an N-terminal methionine residue, which is followed by an acidic or arginine residue. Two major targets for NatB have been identified in yeast, these are the essential cytoskeletal proteins tropomyosin (Tm) as previously mentioned and actin (Singer & Shaw 2003; Polevoda et al. 2003). Whilst tropomyosin can be observed in cells in both acetylated and unacetylated forms (Skoumpla et al. 2007; Coulton & East 2010), actin is always acetylated at its N-terminus (Martin & Rubenstein 1987)Previous studies have shown that deletion of either *NAT3* or *MDM20* has detrimental effects on the cell, the majority of which are attributed to a lack of acetylation of tropomyosin and actin (Singer & Shaw 2003; Polevoda et al. 2003). These defects include slow growth, temperature and osmotic sensitivity, deficiency in utilization of non-fermentable carbon sources, reduced mating efficiency, inability to

form functional actin cables, defects in mitochondrial and vacuolar inheritance, random polarity in budding, sensitivity to antimitotic drugs, and susceptibility to a number of DNA damaging agents (Singer & Shaw 2003; Polevoda et al. 2003).

1.3.6. The Microtubule Cytoskeleton

Similar to actin, the microtubule cytoskeleton is an important cytoskeletal component found in all eukaryotic cells which plays key roles in maintaining cell structure, transport of cellular cargo and chromosome segregation. Microtubules are formed by the assembly of α and β tubulin heterodimers which polymerise in an end to end fashion to form a protofilament. 13 parallel protofilaments are then bundled together to form a hollow cylindrical microtubule filament which is an imperfect helix. Like actin, these microtubules are polar and polymerisation occurs 3 times faster at the positive end than at the negative end (Summers & Kirschner 1979).

Similar to actin which hydrolyses ATP during filament polymerisation, nucleotide hydrolysis is also important during microtubule polymerisation however GTP is hydrolysed by tubulin rather than ATP. The tubulin heterodimer has two nucleotide binding sites, one on the α-tubulin and one on the β-tubulin (Weisenberg 1972). GTP binds to α-tubulin and is stable in this form and is not hydrolysed, however GTP bound to β-tubulin can be hydrolysed to GDP. (Weisenberg, Deery & Dickinson 1976). Microtubules are highly dynamic filaments undergoing constant polymerisation and depolymerisation and these dynamics are regulated by the concentration of tubulin and the two states of microtubules that are present, these being distinguished by the presence or absence of a GTP bound tubulin cap at the microtubule tip (Mitchison & Kirschner 1984). Microtubule tips without a GTP cap

are unstable and depolymerise very rapidly as the rate of depolymerisation far exceeds that of GTP bound subunit addition. However in the presence of GTP bound tubulin at the tip microtubules are highly stable, with the depolymerisation rate of GTP bound tubulin 2-3 orders of magnitude slower than that of GDP bound tubulin (Mitchison & Kirschner 1984). The existence of this GTP tubulin cap is due to the fact that the rate of GTP hydrolysis lags very slightly behind that of polymerisation. The hydrolysis of GTP is a first-order reaction, with there being a fixed probability of GTP hydrolysis occurring once a GTP tubulin monomer has been incorporated into a microtubule. However microtubule polymerisation is a second order reaction with the rate dependent on free tubulin concentration. At high tubulin concentrations there is a large amount of GTP tubulin available to form a stable cap on the microtubule tip, resulting in almost all microtubules within a cell growing. However as the free tubulin concentration decreases there is a lower chance of a GTP tubulin cap on the microtubule tip, and so GDP bound tubulin is exposed at the tip. This results in rapid depolymerisation of the microtubule due to the continuous exposure of GDP bound tubulin at the tip. Depolymerisation continues until the microtubule is completely dispersed or a rare re-capping with GTP tubulin occurs (Mitchison & Kirschner 1984). The switch between microtubule growth and shrinkage is referred to as catastrophe.

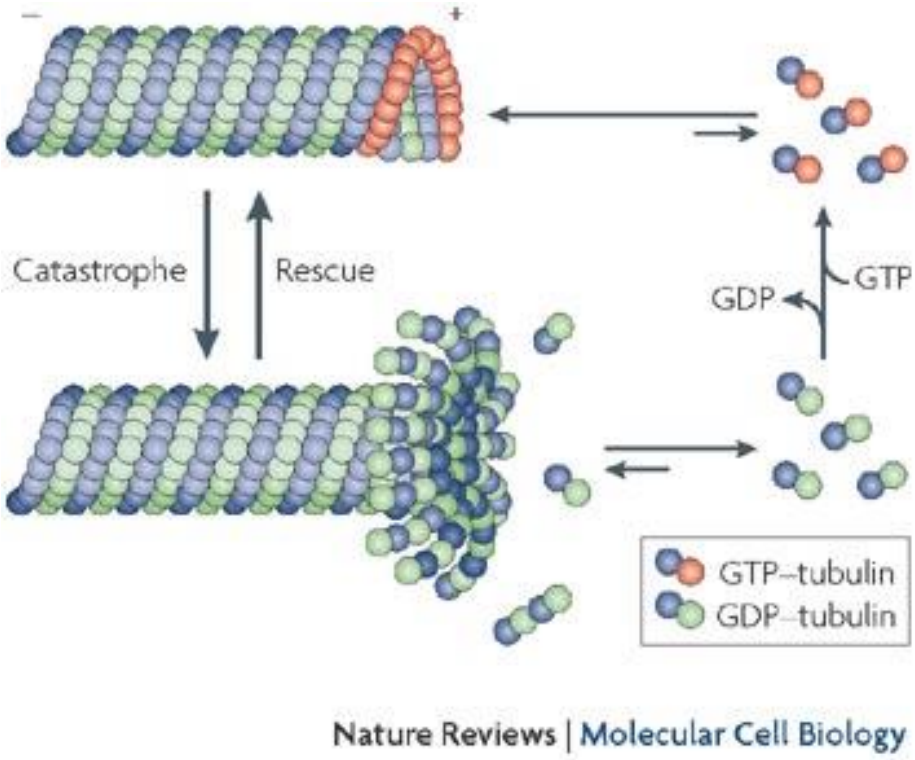

Figure 1.19. Microtubule dynamics: Microtubules grow at the + end via the addition of GTP bound tubulin. The GTP-tubulin at the + end is stable and the microtubule continues to grow until free tubulin concentration becomes too low and there is no longer enough GTP-tubulin to cap the + end. The GTP is hydrolysed to GDP and catastrophe occurs, with the rapid depolymerisation of the microtubule by the removal of GDP-tubulin. This continues until the microtubule is completely depolymerised, or a rescue event resulting in the formation of a new GTP-tubulin cap occurs (Cheeseman & Desai 2008).

1.3.6.1. Microtubule Organising Centres (MTOCs)

Microtubule organising centres are the starting point for microtubule nucleation, playing a key role in the formation and orientation of the mitotic spindle required for chromosome segregation and other microtubule structures. MTOCs vary in name depending on which organism they are present in. In animal cells MTOCs include centrosomes and basal bodies and are found in the cytoplasm whilst in yeasts they are found as spindle pole bodies. The

key component of MTOCs is γ-tubulin, another member of the tubulin family of proteins. γ-tubulin is imperative to the nucleation of new microtubules and is also responsible for maintaining the polarity of microtubules via interactions with the negative end of the microtubule (Bornens 2002).

After cell division a cell only possesses one MTOC, however during S phase of the cell cycle this MTOC is duplicated. Upon maturation the MTOCs then migrate to opposite poles of the cell during prophase. During mitosis microtubules are nucleated from the MTOC and then bind to chromosomes where they are responsible for chromosome segregation. The cell then undergoes cytokinesis and each daughter cell inherits one of the two MTOCs.

1.3.6.2. Microtubule Motor Proteins

Similar to actin, microtubule filaments are associated with motor proteins; with the two most important classes of microtubule associated motor proteins being kinesins and dyneins.

Kinesins were first discovered in 1985 and are microtubule dependent ATPase motor proteins which usually move towards the positive end of the microtubules in a processive hand-over-hand manner similar to that of certain myosins (Vale, Reese & Sheetz 1985)(Yildiz et al. 2004). They are classified according to the position of their motor domain, which can be either N-terminal, central or C-terminal (Hirokawa 1998). Kinesins are involved in vesicle and organelle transport and cell division (Hirokawa 1998) and the movement towards the positive end of the microtubule corresponds to moving cargoes from the central part of a cell towards the cell periphery. Kinesins involved in cell division

are usually different to most kinesins in that they move towards the negative ends of microtubules (Hirokawa 1998).

Cytoplasmic dynein is another microtubule associated motor protein first discovered in 1987 (Paschal, Shpetner & Vallee 1987). It is a large protein complex of approximately 1.2 MDa consisting of 2 heavy chains containing AAA-type ATPase, 3 intermediate chains of approximately 74 kDa, 4 light intermediate chains of approximately 55 kDa and several light chains (Hirokawa 1998; Höök & Vallee 2006). Like kinesins, dyneins produce their force via the hydrolysis of ATP, however unlike most kinesins, dyneins move towards the negative end of microtubules in a processive manner towards the centre of the cell (Hirokawa 1998; Höök & Vallee 2006). Dyneins move along microtubules processively via interactions between the microtubule and a coiled-coil projection from the dynein head referred to as the stalk (Gee & Vallee 1998). Dyneins are involved in several biological processes including moving cargoes such as organelles along microtubules (Hirokawa 1998; Höök & Vallee 2006) , the formation and orientation of the spindle and nuclear migration (Steuer, Wordeman & Schroer 1990; Vaisberg & Koonce 1993; Carminati & Stearns 1997).

1.3.7. Intermediate Filaments

Intermediate filaments are components of the cytoskeleton found in metazoans and are referred to as intermediate filaments as their diameter is between that of the thin and thick filaments found in muscle cells (Ishikawa, Bischoff & Holtzer 1968) . They are composed of intermediate filament proteins that contain an α-helical rod section with globular C and N-terminal domains, all of which were predicted from similarities in secondary structure to the first intermediate filament protein identified, human epidermal keratin (Hanukoglu &

Fuchs 1982). Intermediate filament proteins form a parallel coiled-coil dimer via the α-helical rod section, which then associates with another dimer to form an anti-parallel tetramer. Tetramers then bind end to end forming 2-3 nm thick protofilaments which then pair together into protofibrils. The 10 nm thick intermediate filament is formed when four protofibrils coil together to form the intermediate filament (Lodish et al. 2000). Unlike actin and microtubules, intermediate filaments are non-polar and do not bind nucleotides and whilst not undergoing treadmilling they are dynamic. Intermediate filaments form networks in both the cytoplasm and nucleus where their main function is to reinforce cell and nuclear structure (Lodish et al. 2000).

1.4. The Fission Yeast Scizosaccharmoyces pombe

The fission yeast, *Schizosaccharomyces pombe* is a popular model organism, that was first isolated from African Millet beer in the late 19th century. However it did not rise to prominence as a model organism until the 1950's when it was used by Urs Leupold for genetic studies (Leupold 1958) and Murdoch Mitchison for cell cycle studies (Mitchison 1957). Today it is used as a model system to study a wide variety of cellular processes including DNA damage and repair, the cell cycle, cytoskeleton studies and DNA replication and segregation. In 2001 Sir Paul Nurse was awarded the Nobel Prize in Physiology or Medicine in conjunction with Sir Tim Hunt and Leland Hartwell for his work on cell cycle regulation using *S. pombe.*

The fission yeast is a simple unicellular organism which grows in a highly polarised manner. Cells grow in length, with the width remaining constant at approximately 4μm and the cell length correlates directly to the cells stage within the cell cycle (Mitchison & Nurse 1985). Fission yeast follows a typical cell cycle, however unlike budding yeast which remains in the G1 phase of the cell cycle for an extended period of time, fission yeast has an extended G2 phase.

S. pombe is a popular research tool for many reasons. It's genome was fully sequenced in 2002, during which 50 genes that coded for proteins or mutations linked to human disease states were identified, 23 of which were cancer related (Wood et al. 2002). Also homologues for a number of genes responsible for cell growth, division and cell cycle regulation in fission yeast are also found in humans (Wood et al. 2002). This means that

research carried out using fission yeast is very relevant and can be applied to higher eukaryotes such as animals and humans.

In addition fission yeast possesses many attributes that make it a popular model organism. It is cheaply and easily grown, and is readily amenable to genetic manipulation and the generation of mutants. It has a short generation time of 2.4 to 4 hours depending on growth conditions and can be grown in either a diploid or haploid state, although it is usually seen as a haploid. A wide variety of microscopic techniques including immunofluorescence, fluorescent tagging of proteins, FRET and FRAP can also be applied.

Despite these strengths as a model organism there are limitations to using fission yeast. One of the biggest is its multidrug resistance. Fission yeast is resistant to a large range of drugs due to the expression of a large number of drug efflux pumps (Kawashima et al. 2012). This has prevented fission yeast form being a suitable model organism for chemical drug research studies. In addition although several of the key molecular mechanisms are conserved from humans to yeasts, they way in which the cell uses these mechanisms may vary between the two, in particular due to the difference in their environment. Finally the other main drawback is that fission yeast is a unicellular organism, meaning that lacks a level of complexity including cell-cell interactions observed in multicellular organisms.

1.4.1. The Fission Yeast Cytoskeleton

1.4.1.1 The Fission Yeast Actin Cytoskeleton

In all eukaryotic cells the actin cytoskeleton plays major roles in the processes of cell growth and division. Within *S. pombe* there is a single actin gene, *act1* (Mertins and Gallwitz 1987) and this gene is 90% identical to that of mammalian actin and budding yeast actin and forms filaments in a similar way (Takaine and Mabuchi 2007). Within *S. pombe* there are 3 main types of actin structures observed, these are patches, cables and the cytokinetic actomyosin ring (CAR) (Marks and Hyams 1985). However, despite these very specific structures, the actin cytoskeleton is highly dynamic with multiple changes occurring, all regulated by different proteins.

Actin patches are found at the growing tips of the cell and are have roles in actin polymerisation (Pelham and Chang 2001) and deposition of cell wall materials (Kobori, et al. 1989). After *S.pombe* divides growth occurs only at the "old" cell end until the cell reaches a critical size, when the cell passes early G2 growth begins at the new end, an event known as new end take off (NETO) (Mitchison and Nurse 1985). Actin patch localisation directly corresponds with these specific areas of growth during the cell cycle (Marks, Hagan and Hyams 1986).

In all eukaryotic cells actin cables play roles in a variety of cellular processes including polarization, nuclear segregation, cytokinesis and vesicle trafficking. These filaments are polar consisting of the "barbed" fast growing end and the "pointed" slow growing end. Elongation of actin filaments occurs almost exclusively at the barbed end of the filament.

In *S.pombe* actin cables are seen in cells during interphase and are sometimes attached to the actin patches at the tips of the cells usually orientated with their barbed ends towards the cell tips (Kamasaki, et al. 2005).

When the cell enters mitosis the actin patches disappear from the cell ends, an aster like structure branches from actin filaments at the cell equator (Arai and Mabuchi 2002) and actin filaments accumulate at the medial cortex. As the aster extends to form the primary ring accumulated actin filaments are bundled together (Pelham and Chang 2002) to form a ring consisting of two semi-circular populations of parallel filaments of opposite directionality (Kamasaki, Osumi and Mabuchi 2007). Longitudinal actin filaments, orientated with barbed ends towards the cell equator are also seen attached to the growing ring (Kamasaki, et al. 2005).

These observations have led to two models for the formation of the CAR in fission yeast being proposed, however this process is still not fully understood. The first model is the Search-Capture-Pull-Release model (SPCR), in which the anilin like protein Mid1 plays a key role. Approximately one hour before the onset of mitosis ~65 nodes of Mid1 appear around the nucleus at the medial cortex of the cell (Vavylonis et al. 2008). Immediately before mitosis additional Mid1 is recruited from the nucleus to these nodes, followed by the IQGAP Rng2, the F-BAR protein Cdc15 which then recruits the type II myosin Myo2 and the formin Cdc12, and finally α-actinin Ain1 (Coffman et al. 2009; Vavylonis et al. 2008). After the cell enters mitosis Cdc12 nucleates the growth of actin filaments which elongate at a high rate. As these filaments are nucleated from one node towards another they are captured by the Myo2 motor at the subsequent node and are pulled towards it. This is

followed by the release step, mediated by the cofilin Adf1 severing actin filaments (Nakano & Mabuchi 2006; Vavylonis et al. 2008; Stark et al. 2010). The continued repetition of this process results in the compaction of the nodes into a tight ring structure, in which Ain1 is responsible for cross-linking the actin filaments into anti-parallel bundles (Kamasaki, Osumi & Mabuchi 2007; Wu, Bähler & Pringle 2001).

The second model focusses upon the re-organisation of existing cables into the CAR, and is sometimes referred to as the "leading cable" model. This model was first proposed after observation of actomyosin cables arranging into rings from a single spot at the cell cortex (Arai & Mabuchi 2002; Kamasaki, Osumi & Mabuchi 2007). It has subsequently been shown that as well as its association with node structures Cdc12 is also present as faint non-medial cytoplasmic speckles, and that non-medial cables nucleated by the Cdc12 are also incorporated into the CAR (Huang et al. 2012). This model is dependent on the septation initiation network (SIN), however Mid1 is not required, and it has been shown that CAR formation can still occur in a *mid1Δ* strain, providing evidence for this model (Hachet & Simanis 2008; Huang, Yan & Balasubramanian 2008). Both of these mechanisms for CAR formation are shown in figure 1.20 below.

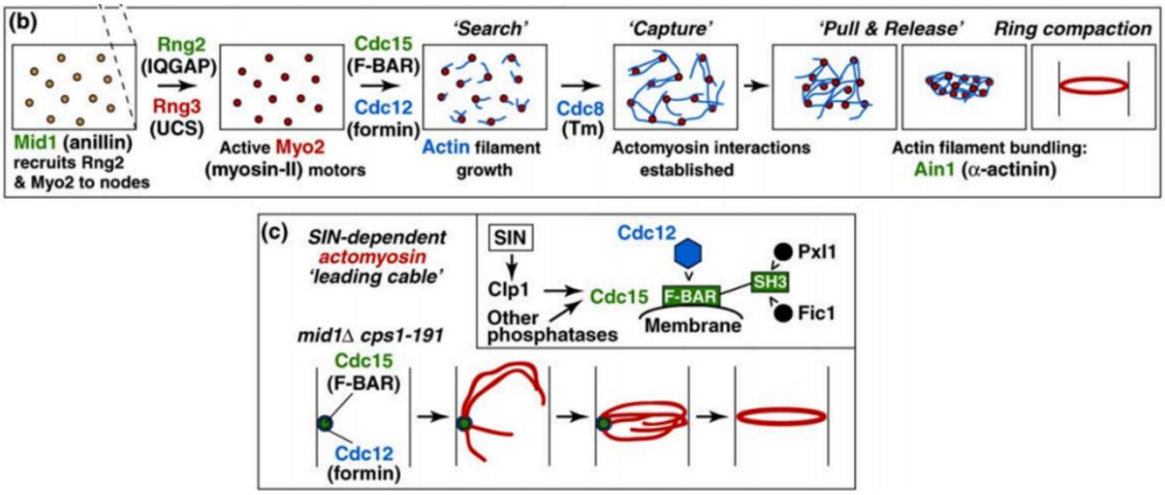

Figure.1.20. The two proposed mechanisms of CAR formation, (b) shows the search, capture, pull, release (SPCR) model, whilst (c) shows the leading cable model. Adapted from (Kovar, Sirotkin & Lord 2011).

The identification of these different actin structures and the way in which actin reorganises from one structure to another shows that the actin cytoskeleton is a highly dynamic structure, which is regulated by a number of other actin binding proteins (ABP's).

1.4.1.2. The Role of Formins in Actin Nucleation in Fission Yeast

3 formins have been identified within *S.pombe*, Fus1, Cdc12 and For3, each having discrete localization and function. Fus1 was the formin in which the third FH domain, FH3 was identified and plays a key role in cell mating (Petersen, et al. 1998). Fus1 is a cytoplasmic protein that strongly localises to the projection tip when mating occurs, where it is responsible for actin localization, with loss of Fus1 function resulting in disrupted actin localization to the projection tip (Petersen, et al. 1998). The second formin, Cdc12 was originally shown to be one of 6 genes required for actin ring formation to allow cell division (Nurse and Thuriaux 1976). The Cdc12 protein has since been shown to be a component of the CAR that interacts with profilin (Chang, Drubin and Nurse 1997). During interphase a single Cdc12 spot is observed at the approximate site of ring formation and the protein plays a key role in ring formation during mitosis (Chang, Drubin and Nurse 1997). Much work has been done to examine the way in which Cdc12 functions, which has showed that it's interaction with profilin is extremely important (Kovar, et al. 2003). When profilin is not bound to Cdc12, Cdc12 adopts a "capped state" in which it acts as a capping protein, preventing actin subunit loss and addition at the barbed end of the filament with all of the actin assembly occurring exclusively at the pointed end (Kovar, et al. 2003). The binding of profilin to Cdc12 causes a shift in polarity of actin filament assembly, resulting in Cdc12 now adopting an "open" state at the barbed end and the actin filament grows exclusively at the barbed end (Kovar, et al. 2003). The final formin, For3 is involved in the organization of the actin cytoskeleton during interphase, promoting proper cell polarity, symmetric cell division and is required for the formation of actin cables observed along the length of the cell during interphase (Feierbach and Chang 2001). During interphase For3 localises to both tips of the cell, where it is associated with the actin patches. When the cell is in early mitosis

For3 is seen as a medial spot in a similar fashion to Cdc12, which then progresses to a double ring in late mitosis however it does not associate with the CAR (Feierbach & Chang 2001). When septation occurs all of the For3 is localized to the new ends of the daughter cells before also re-localizing to the old end, giving the interphase localization at both tips of the cell (Feierbach and Chang 2001).

1.4.2. Myosins in Fission Yeast

Myosins are a family of motor proteins that associate with actin and carry out a wide variety of roles in different organisms and tissue types. This variation in function is accompanied by structural differences in different classes of myosins, which allows them to carry out these specific functions. Currently 35 classes of myosins have been identified (Odronitz and Kollmar 2007) of which classes I, II and V are present in *S. pombe.* Currently one class I myosin (Myo1) two class II myosins (Myo2 and Myp2) and two class V myosins (Myo51 and Myo52) have been identified in *S. pombe* with each having distinct function.

Myo1 was the final myosin to be identified in *S. pombe,* using data from the genome sequencing project (Lee, Bezanilla and Pollard 2000). Myo1 is a monomeric protein which plays a key role in the activation of the Arp2/3 complex (Lee, Bezanilla and Pollard 2000) which in turn stimulates actin polymerization. As well as promoting this actin polymerization Myo1 localises to actin patches where it is believed to play roles in membrane remodelling and endocytosis (Takeda & Chang 2005; Attanapola, Alexander & Mulvihill 2009)

Class II myosins produce the contractile force in muscle, and this force generating function is carried over to *S. pombe,* where the class II myosins are involved in the formation of the CAR, and provide the contractile force at the CAR for cell division. Of the 2 class II myosins in *S. pombe* only Myo2 is essential with cells remaining viable when Myp2 is absent. (May et al. 1997; Bezanilla, Wilson & Pollard 2000; Lord, Laves & Pollard 2005; Mulvihill & Hyams 2003).

The class V myosins are dimeric proteins which walk along actin filaments within the cell whilst carrying cargoes to discrete cellular locations. The 2 class V myosins within *S. pombe* have discrete localisation patterns, with Myo51 found at the CAR, and is not observed moving around the cells as Myo52 does, which is highly motile within the cell and accumulates at areas of cell growth and cell wall deposition (Motegi, Arai and Mabuchi 2001, Win, et al. 2001). A small number of specific roles of Myo52 have been identified, including the delivery of the α-glucan synthase Mok1 to promote the proper synthesis of the cell wall (Win, et al. 2001) and delivery of the β-1-3-glucan synthase Cps1 during cytokinesis (Mulvihill, Edwards and Hyams 2006). It has also been shown to play roles in vacuole organisation and maintenance (Motegi, Arai and Mabuchi 2001 (Mulvihill, Pollard, et al. 2001)) and transporting the SNARE protein, synaptobrevin, to its proper cellular location (Edamatsu and Toyoshima 2003). The function of Myo51 is less clear, however a function during the sexual life cycle was identified by monitoring the expression of the *myo51 gene* (Mata, et al. 2002). Like Myo52, Myo51 localises to the tip of mating cells promoting cell fusion (Doyle, et al. 2009) and later playing a role in chromosome segregation.

1.4.3. Fission Yeast Contains a Single Tropomyosin

S. pombe has only one tropomyosin gene in its genome, *cdc8*$^{+}$ (Balasubramanian, Helfman & Hemmingsen 1992); encoding a tropomyosin made up of 161 amino acids with a molecular weight of 18.9 kDa. Cdc8 plays a crucial role in the formation, stabilisation and maintenance of actin filaments and plays a crucial role during cytokinesis, assisting the

formation and function of the CAR (Balasubramanian, Helfman & Hemmingsen 1992; Skoumpla et al. 2007). The role of Cdc8 in cytokinesis and cell fusion has been investigated and it was found to have an important roles in both. Mutants lacking functional Cdc8 exhibited major defects in both processes, however cell fusion was shown to be less reliant on Cdc8 than cytokinesis, where it is vital (Kurahashi, Imai & Yamamoto 2002). It has also been shown that Cdc8 regulates the binding of myosin to actin in a two state fashion (Skoumpla et al. 2007). Like Tpm1 within S*. cerevisiae* Cdc8 is acetylated at its N-terminus by a homologue of the NatB complex, consisting of Naa20 and Naa25 subunits. However within *S.pombe* there are populations of both acetylated and unacetylated Cdc8, with approximately 80% of Cdc8 being acetylated. Unlike other isoforms of tropomyosin which cannot bind to actin in an unacetylated state, unacetlyated Cdc8 is able to bind to actin, however this interaction is much weaker (approximately 5 times weaker than acetylated Cdc8) (Skoumpla et al. 2007). It has more recently been shown that these 2 populations of Cdc8 have discrete localisation patterns, with acetylated Cdc8 found to be associated with actin filaments incorporated into the CAR and unacetlyated Cdc8 associated with actin cables extending through the cell during interphase (Coulton & East 2010).

1.4.4. Microtubules

Within *S. pombe* four tubulin genes have been identified; two α (*nda2*+, *atb2*+), one β (*nda3*+) and one γ (*gtb1*+/*tug1*+) (Yanagida 1987; Horio et al. 1991; Stearns, Evans & Kirschner 1991). As with all eukaryotes, fission yeast microtubules are polymers of α and β tubulin, whilst γ tubulin is found at microtubule organising centres where it acts as a nucleating template for the polymerisation of microtubules (Pereira & Schiebel 1997). As

is the case with the *S.pombe* actin cytoskeleton, there are distinct microtubule structures when the cell is at different stages of the cell cycle. During interphase microtubules span along the axis of the cell, playing important roles in the correct distribution of nuclei and mitochondria, the maintenance of cell polarity and the integrity of the Golgi stacks (Ayscough et al. 1993; Yaffe et al. 1996; Hagan & Yanagida 1997; Hagan 1998). Once the cell becomes committed to mitosis a small dot of tubulin associates with the nucleus whilst the rest of the cytoskeleton remains intact. This dot is between two microtubule organising centres (MTOCs) called spindle pole bodies (SPBs), and is soon replaced by a short bar which extends to produce the prophase spindle, whilst at the same time cytoplasmic microtubules disappear (Hagan & Yanagida 1995). As this spindle elongates to span the nucleus the chromosomes line up on the metaphase plate and it is at this point that microtubules associate with the chromosomes via kinetochores. Additionally during metaphase astral microtubules extend tangentially from the cytoplasmic faces of the SPBs (Hagan & Hyams 1996) and it is believed that these astral microtubules provide the force required for segregation of the chromosomes. Two models have been proposed for this force generation, the first suggests that astral microtubules provide a track for the SPB to slide along (Hagan & Hyams 1996) whilst the second suggests that they may interact with motor proteins lining the cortex in a manner similar to that observed in budding yeast (Shaw et al. 1997; Carminati & Stearns 1997). Once the nuclei have separated and are localised towards the cell ends the spindle breaks down and microtubules accumulate in the middle of the cell in what is called the post-anaphase array (PAA) (Hagan & Hyams 1988). These microtubules then extend to form a ring of tubulin that colocalises with the CAR (Hagan 1998). The PAA is required to maintain the CAR and it's components in the middle of the cell, preventing asymmetric cell divisions which could lead to genome

instability (Hagan & Yanagida 1997; Pardo & Nurse 2003). The re-organisation of the microtubule cytoskeleton is shown in figure 1.21.

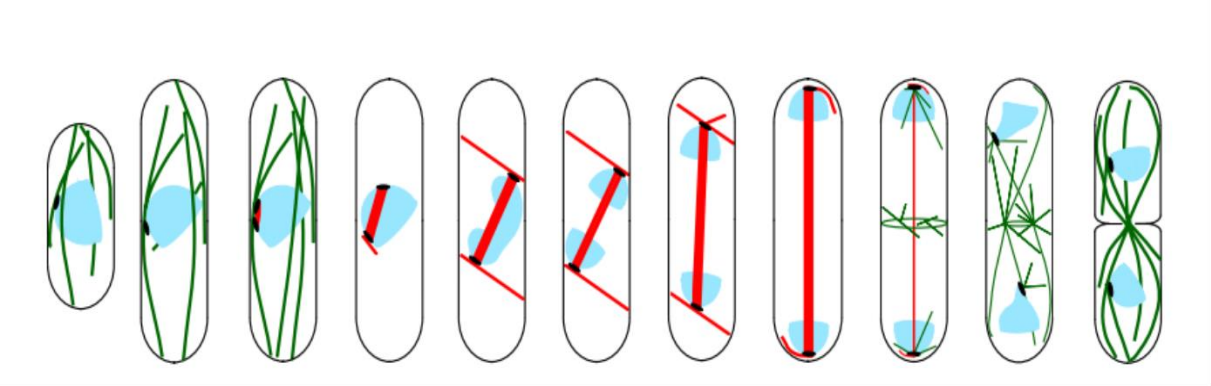

Figure.1.21. The fission yeast microtubule cytoskeleton. Over time interphase microtubules (green) disappear and the mitotic spindle (red) is formed. The spindle elongates and the chromosomes (blue) are segregated to opposite poles of the cell. The post anaphase array (PAA) is then formed and cell division takes place, resulting in the formation of two daughter cells and the normal interphase microtubule cytoskeleton is observed in both cells (Hagan 1998).

1.4.5. Regulation of Cell Polarity in Fission Yeast

The fission yeast cell grows only in length in a highly polarized manner, growing first at one end before a critical point in G2 when growth becomes bipolar in a process referred to as New End Take Off (NETO) (Mitchison & Nurse 1985). Polarized growth in fission yeast is a highly regulated process with proteins from a wide variety of families playing a role. Mutant strains with polarity defects can be classified into two groups, the first contains cells which lack polarity and are short, rounded cells, whilst some are completely spherical. The second group contains cells which whilst retaining some polarity become bent or have a branched morphology. These phenotypes correspond directly to which cell polarity pathway is affected by the mutation.

1.4.5.1. The Cdc42 GTPase and the Orb kinase family.

One of the key regulators of cell polarity, conserved throughout many organisms is the small Rho family GTPase Cdc42. *cdc42* is an essential gene and it's deletion results in small round cells, whilst overexpression of a constitutively active form results in large rounded cells (Miller & Johnson 1994). Cdc42 is activated by 2 guanidine exchange factors, Scd1 and Gef1 (Coll et al. 2003; Hirota & Tanaka 2003), deletions of which have shown that Scd1 is necessary for polarized growth while Gef1 is required for NETO. Scd1 is activated by a Ras homolog, Ras1 (Chang et al. 1994), with this Ras1-Scd1-Cdc42 pathway being homologous to the Bud1-Cdc24-Cdc42 pathway for polarity identified in budding yeast (Park et al. 1997). It has also been shown that Cdc42 can be activated independently of Ras1. The Bar domain protein Hob3 can activate Cdc42 via Gef1 (Coll et al. 2007). As well as these activating factors, there is a negative regulator of Cdc42, Rga4 belonging to the Cdc42 GTPase

activating protein family (GAPs) (Nakano, Mutoh & Mabuchi 2001). While Cdc42 and its GEFS are localized to the plasma membrane at areas of growth, i.e. the cell tips and the septum Rga4 is localized to non-growing regions in the cell such as the cell sides to restrict Cdc42 activity to areas of growth (Das et al. 2007). One of the best characterized targets of Cdc42 is the formin For3 (see section 1.4.1.2). For3 adopts an auto-inhibited state which is relieved through the binding of Cdc42 and the formin binding protein Bud6 (described later). This activation allows For3 to localize to the cell poles and nucleate actin cables (Martin, Rincon & Basu 2007).

As well as its clear role in For3 activation, Cdc42 also interacts with a much larger group of proteins from the Orb kinase family, all of which encode for kinases or kinase regulators. Similar to Cdc42, mutants of any of the orb family of proteins result in rounded cells (Verde, Mata & Nurse 1995). These proteins include Orb2, Orb3, Orb4, Orb5 and Orb6, of which Orb2 is a key target for Cdc42 (Chang et al. 1994).

Orb2 is a Ste20-like kinase which forms a complex with the GEF Scd1 and Cdc42 via association with a scaffolding protein, Scd2 (Chang et al. 1994). Potential phosphorylation substrates of Orb2 include Tea1, a microtubule associated protein which plays a key role in cell polarity (described later) (Kim et al. 2003) and the Rho GAP Rga8, a protein of unknown function (Yang et al. 2003). As well as its role in polarity, Orb2 also plays a role in regulating cytokinesis, where it has been shown to localise to the CAR and phosphorylate the myosin regulatory light chain Rlc1 which inhibits cytokinesis until Rlc1 becomes subsequently dephosphorylated (Loo & Balasubramanian 2008).

The kinase Orb6 forms a complex with Mob2 and Mor2 (Verde, Wiley & Nurse 1998; Hirata et al. 2002; Hou et al. 2003) which subsequently interacts with Orb3 and its cofactor Mo25 (Kanai et al. 2005; Mendoza, Redemann & Brunner 2005). It has been shown that Orb6 plays a key role in regulating Cdc42, with Orb6 required for the proper localization and activation of Cdc42 and its GEF Gef1 at the cell tips, with loss of Orb6 activity resulting in Cdc42 localising to the cell sides (Das et al. 2009). Orb3 has been shown to be responsible for the correct polarisation of the actin cytoskeleton at cell tips and during cell division (Leonhard & Nurse 2005). The regulation of Cdc42 and its subsequent targets are shown in figure 1.22 below.

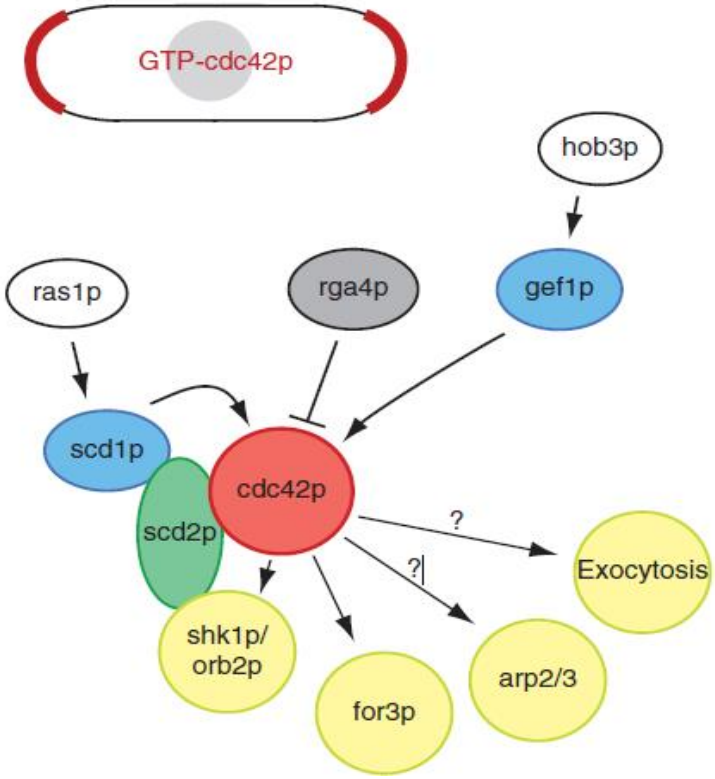

Figure.1.22. A schematic to show the regulation of Cdc42 and its targets, as well as its localisation to the cell poles when in its active GTP bound form (Chang & Martin 2009).

1.4.5.2. The role of the microtubule and actin cytoskeletons in cell polarity

As well as regulation by Cdc42 and the Orb kinase family, the microtubule and actin cytoskeletons also play a key role in polarized growth of fission yeast. Microtubules play the key role, by delivering specific proteins, which come together to form the "polarisome" to the sites of cell growth. Once these proteins have been delivered and form the appropriate complexes, cell growth is then activated. The actin cytoskeleton is required once growth has been activated (La Carbona, Le Goff & Le Goff 2006).

The microtubule cytoskeleton plays a key role in shaping the cell, with cells that have an abnormal cytoskeleton having a disrupted morphology. Unlike mutants of Cdc42 and the Orb family, cells with abnormal microtubule cytoskeletons still grow in a polarized manner, however the cells are curved or branched, forming T shaped cells (Umesono et al. 1983; Toda et al. 1983; Sawin & Nurse 1998). The major way in which microtubules regulate cell polarity is through the "Tea" system. This consists of a number of proteins, mutants of which result in curved or T shaped cells, similar to those with microtubule defects. The first "Tea" protein, Tea1 was originally identified in a screen for morphology mutants (Verde, Mata & Nurse 1995) with cells found to be monopolar, with a failure to activate growth at the new end. At higher temperatures the cells become curved or T shaped (Mata & Nurse 1997). Deletion of *tea1* has an effect on microtubules, with microtubule catastrophe inhibited. When MT's reach the poles of a *tea1Δ* strain they curve around the cell ends rather than depolymerising as they would in a wild type cell (Mata & Nurse 1997). Tea1 localises at both cell poles throughout the cell cycle and is also seen on growing microtubule plus ends. Its localisation to the cell poles is microtubule dependent, with Tea1 carried from the middle of the cell to the poles on microtubules, where it is then deposited

and microtubules undergo catastrophe (Mata & Nurse 1997; Behrens & Nurse 2002a; Browning, Hackney & Nurse 2003). The retention of Tea1 at the cell poles is mediated by a coiled-coil region at the C-terminus of the protein which interacts with the cell membrane (Behrens & Nurse 2002a).

The localisation of Tea1 to the cell tips is also regulated by Mod5, a plasma membrane protein (Snaith & Sawin 2003). Mod5 localises to the poles of the cell where it is involved in the anchoring of Tea1. Mod5 interacts with the cell membrane via a CaaX domain at it's C-terminus (Snaith & Sawin 2003). When *mod5* is deleted there is a slight effect on cell polarity, with cells appearing bent and occasionally "T" shaped, as with a *tea1Δ.* The localisation of Tea1 is affected in the absence of Mod5, Tea1 is still transported along microtubules to the cell ends however it fails to anchor and accumulate to appropriate levels (Snaith & Sawin 2003). Interestingly, as well as Mod5 being required for correct Tea1 localisation, the opposite is also observed with Tea1 being required for proper Mod5 localisation, suggesting the presence of a positive feedback loop (Snaith & Sawin 2003; Chang & Martin 2009). When Tea1 is deleted Mod5 is still associated with the plasma membrane but is not restricted to just the tips of the cells, it is diffused around the entire membrane (Snaith & Sawin 2003).

In addition to Mod5 playing a role in the anchoring of Tea1, another "Tea" protein Tea3, is also involved in the anchoring of Tea1 at the non-growing cell pole (Snaith & Sawin 2005). Tea3 shares 21% identity with Tea1 and plays a key role in the stimulation of NETO, however *tea3Δ* cells do not display the stereotypically "Tea" phenotype of curved and T shaped cells (Arellano, Niccoli & Nurse 2002). Tea3 localises to both cell poles in a

microtubule and Tea1 dependent manner, however it is slightly enriched at the non-growing end (Arellano, Niccoli & Nurse 2002). It also localises to the septum of dividing cells as a late event of cytokinesis, and is required for the correct positioning of the septum (Arellano, Niccoli & Nurse 2002).

Once anchored at the cell tip Tea1 interacts with another "Tea" protein, Tea4 which is key for its function (Martin et al. 2005). Tea4 co-localises with Tea1 at the cell tips and at microtubule plus ends, with this microtubule association dependent upon Tea1 and its localisation to the cell poles dependent on Tea1, Tip1 and Tea 2 (both described later). Its stabilisation at the cell poles is also dependent on Mod5 (Martin et al. 2005). Tea4 acts as the link between Tea1 and the formin For3, ensuring that For3 becomes localised to the new cell pole during NETO, allowing bipolar growth of the cell (Martin et al. 2005). Tea1 establishes growth at cell poles by the recruitment of For3 and Bud6 to the cell poles, via physical interactions with both in different complexes (Glynn et al. 2001; Feierbach, Verde & Chang 2004; Martin et al. 2005; Tatebe et al. 2005). The function of For3 has been previously described in section 1.4.1.2, whilst Bud6 is an actin binding protein which plays a role in the initiation of NETO and is required for the correct localisation of For3 to the cell poles (Glynn et al. 2001). Bud6 localizes to the cell tips in an actin dependent manner and also to the CAR. The localization of Bud6 is also dependent upon the microtubule associated factor Tea1, but is not dependent upon microtubules. The localisation of Bud6 throughout the cell is also depedent upon secretory pathway mediated transport (Jin & Amberg 2001). Cell morphology is not affected by the deletion of *bud6*, with the only affect being a failure of ~50% of the cells to initiate NETO, consequently only growing at the old end until cell division occurs (Glynn et al. 2001). When *bud6* deletion is combined with a temperature sensitive mutant that fails to septate at the restrictive temperature bent and "T" shaped

cells are observed, indicating that Bud6 plays a role in cell polarity (Glynn et al. 2001). These polarity phenotypes are very similar to those of *tea1* deletion and Bud6 and Tea1 have been shown to physically interact by co-immunoprecipitation in large complexes, demonstrating the clear link between the actin cytoskeleton (Bud6) and the microtubule cytoskeleton and how a pathway is established in which microtubule plus end factors interact with actin associated polarity factors to polarize the actin cytoskeleton (Glynn et al. 2001). The subsequent link is Bud6's interaction with For3 via a physical interaction similar to their budding yeast homologues Bud6 and Bni1 (Evangelista et al. 1997), where Bud6 has been shown to be a key activator of Bni1 actin nucleation (Moseley & Goode 2005). It appears Bud6 plays a similar role in fission yeast, with *bud6Δ* cells possessing fewer actin cables (Feierbach & Chang 2001).

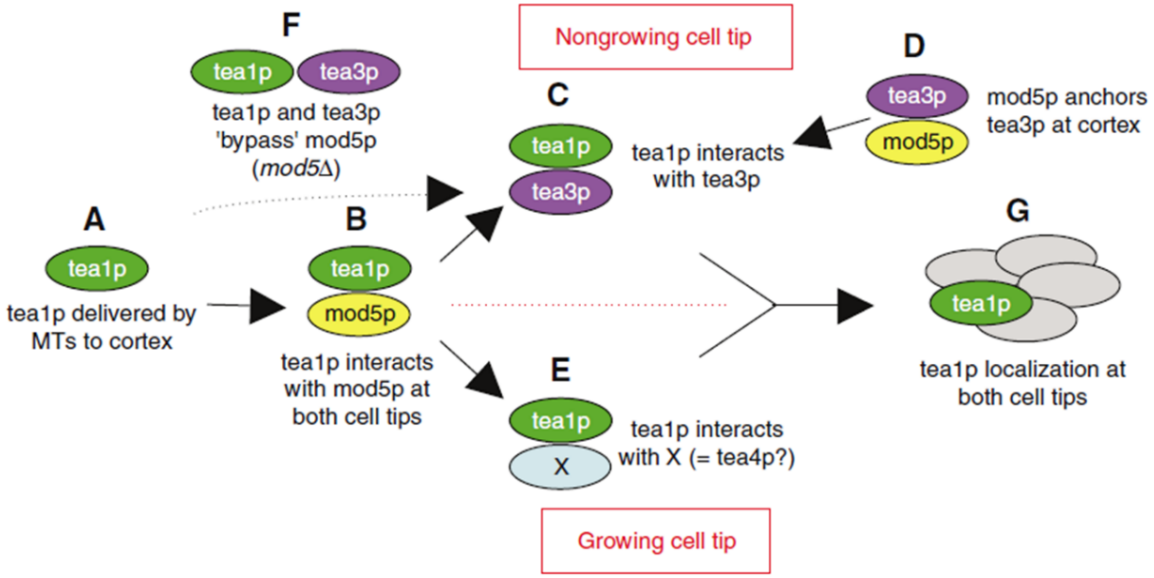

Figure.1.23. Anchoring of Tea1 at the cell poles. (A) Tea1 is delivered to the cell cortex on microtubule plus ends. (B) Tea1 interacts with Mod5p at both cell tips. (C) At non-growing cell tips, Tea1 interacts with Tea3, which is anchored at the cortex via its interaction with Mod5 (D). (E) At growing cell tips, Tea1 interacts with Tea4, which has a function similar to that of Tea3 at non-growing tips, playing a role in the initiation of NETO. (F) A partially functional interaction between Tea1 and Tea3 can occur without Mod5, but Tea1 and Tea3 are poorly anchored at the cell cortex. (G) when all of these interactions occur proper Tea1 anchoring at both cell tips occurs (Snaith et al. 2005).

In addition to linking Tea1 to For3 and Bud6, Tea4 also plays a role in the bipolar localisation of another protein involved in cell polarity, Pom1 (Tatebe et al. 2005). Pom1 was originally identified in a morphological screen, with mutant cells being curved or branched and also having mis-positioned septa (Bähler & Pringle 1998). Pom1 has been identified as a member of the DYRK (Dual-specificity Yak-related Kinase) family and members of this kinase family have been shown to play roles in cell polarity and division. *pom1* mutant cells grow in a monopolar fashion and once cell division has occurred growth is initiated at either the old or new end, suggesting that Pom1 plays roles in both selecting which pole the cell will grow at, and in initiating bipolar growth via NETO (Bähler & Pringle 1998). Pom1 localises to both cell tips, being more concentrated at the new end in a microtubule and Tea1 dependent manner. At these cell poles its kinase activity is regulated by the cell cycle, with Pom1 active during bipolar growth and inactive during monopolar growth (Bähler & Pringle 1998; Bähler & Nurse 2001). More recently Pom1 has been shown to play a key role in linking cell length and mitotic entry, whilst also defining septa position (Martin & Berthelot-Grosjean 2009; Moseley et al. 2009). A Pom1 gradient is formed with levels highest at the cell tip and decreasing towards the middle of the cell. As a cell elongates, the concentration of Pom1 at the medial cortex decreases until a critical low concentration is reached and cells enter mitosis. This regulation occurs via a regulatory network localised to cortical nodes in the middle of the cell consisting of Wee1 (an inhibitor of Cdk1), Cdr1 and Cdr2 (inhibitory kinases of Wee1) and the anilin-like protein Mid1 (Moseley et al. 2009; Martin & Berthelot-Grosjean 2009). This regulation of mitotic entry and septa positioning via the Pom1 gradient is shown in figure 1.24.

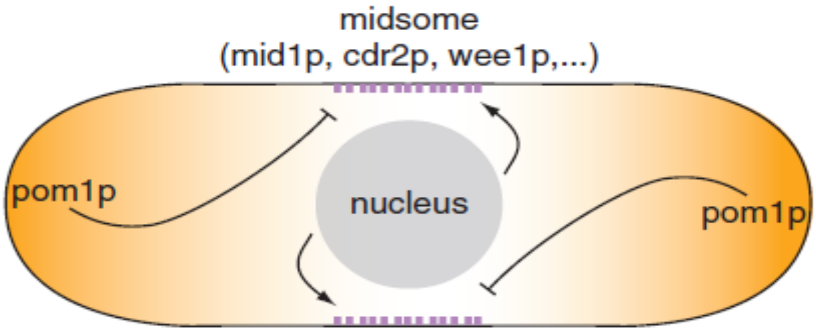

Figure.1.24. The localisation of Mid1, Cdr1, Cdr2 and Wee1 to the medial cortex is promoted by nuclear signals, whilst Pom1 inhibits the localisation of these proteins and subsequently septum formation at areas other than the medial cortex. A gradient of Pom1 is also formed with Pom1 levels highest the cell poles, decreasing towards the middle of the cell (shown in orange). Once cells reach a critical length and Pom1 levels are sufficiently low at the middle of the cell, mitotic entry occurs (Chang & Martin 2009).

The localisation of the "Tea" proteins and their subsequent interaction with the actin cytoskeleton is dependent upon an intact microtubule cytoskeleton. Three proteins, Tip1, Tea2 and Mal3 play a key role in regulating microtubules and delivering other "Tea" proteins to the cell poles. *tip1Δ, mal3Δ and tea2Δ* cells all display typical "Tea" phenotypes with cells being curved and branched (Brunner & Nurse 2000; J.D. Beinhauer et al. 1997; Browning et al. 2000a). All 3 deletion also possess abnormal microtubule cytoskeletons, with only short microtubules around the nucleus present (J.D. Beinhauer et al. 1997; Browning et al. 2000a; Brunner & Nurse 2000).

Tip1 is a member of the CLIP-170 family, a group of proteins heavily involved in microtubule dynamics. Human CLIP-170 was initially identified as a link between microtubules and endosomes, whilst also associating with desmosomal plaques which are a target for microtubules in polarized epithelial cells (Pierre et al. 1992; Wacker et al. 1992). Tip1, like other CLIP-170 proteins localises to microtubule plus ends and the cell poles and prevents microtubules undergoing catastrophe until they reach the cell poles (Brunner & Nurse

2000), however the localisation of Tip1 to the cell poles is not microtubule dependent. Tip1 prevents catastrophe when growing microtubule tips reach other regions of the membrane, indicating that Tip1 can distinguish between the cell tips and other regions of the cell membrane (Brunner & Nurse 2000). The deletion of *tip1* results in microtubules undergoing catastrophe when they reach the cell membrane at any point in the cell, and the rate of catastrophe is also twice as fast as in wild-type cells, resulting in microtubules being 30-60% shorter than wild type (Brunner & Nurse 2000). The levels of Tip1 at the cell poles are regulated by Myo52 through interaction with the ubiquitin receptor protein Dph1, promoting Dph1 dependent turnover of Tip1 (Martín-García & Mulvihill 2009).

Tea2 is a plus-end directed kinesin-like motor protein which travels on microtubule plus ends to the cell poles. It has been shown to promote microtubule growth, with cells lacking Tea2 having a severely reduced microtubule cytoskeleton (Browning et al. 2000a). It is also believed to travel along microtubules, carrying Tea1 as a cargo to the cell ends, as loss of Tea2 leads to Tea1 only being found on short cytoplasmic microtubule structures (Browning et al. 2000a).

Mal3 is a microtubule plus-end tracking protein, homologous to human EB-1 (J.D. Beinhauer et al. 1997). EB-1, was identified by its ability to interact with the carboxyl terminus of the tumour-suppressor protein adenomatous polyposis coli (APC) at the ends of microtubules (Su et al., 1995). Mal3 localises to both cytoplasmic microtubules and the mitotic spindle, whilst faint localization to a central ring structure during anaphase is also observed (J.D. Beinhauer et al. 1997). Mal3 acts as a regulator of microtubule dynamics,

promoting the initiation of microtubule growth and inhibiting catastrophe at cellular locations other than the cell poles (Busch & Brunner 2004).

These three proteins all interact with one another whereby they regulate the localisation of each other, the localisation of other "Tea" proteins and the organisation of the microtubule cytoskeleton. Whilst all localise to the growing plus ends of microtubules, Tea2 and Tip1 have a higher affinity for these ends than Mal3 (Browning, Hackney & Nurse 2003). Similarly whilst Tea2 and Tip1 are deposited at the cell pole once microtubules reach the poles, Mal3 disappears at cell ends immediately before microtubule catastrophe occurs (Browning, Hackney & Nurse 2003; Busch & Brunner 2004). The localisation of Tip1 and Tea2 at the cell tips is required for Tea1 and Tea4 localisation to these areas, however Tea1 is also required for the deposition of Tea2 and Tip1 (Brunner & Nurse 2000; Browning, Hackney & Nurse 2003; Feierbach, Verde & Chang 2004; Browning et al. 2000a; Martin et al. 2005). All 3 associate in complexes, and the binding to, and movement on microtubules of Tea2 and Tip1 are dependent on Mal3. In addition Tea2 is required for the localisation and movement of Tip1 on microtubules (Busch & Brunner 2004). Mal3 and Tip1 have an unstable interaction, where Mal3 is required for Tip1 to associate with the growing ends of microtubules but Tip1 can interact elsewhere on microtubules independent of Mal3. Conversely Mal3 dissociation from microtubule plus ends is promoted by Tip1 (Busch & Brunner 2004). The association between Tip1 and Mal3 is via a CAP-Gly (cytoskeletal associated protein glycine-rich) domain, which is speculated to also allow Tip1 to bind microtubules *in vitro* (Brunner & Nurse 2000; Busch & Brunner 2004). Mal3 and Tea2 also interact with each other and this interaction results in both being recruited to microtubules (Browning & Hackney 2005a). Mal3 stimulates the ATPase activity of Tea2 by recruiting it

to microtubules, however when motor activity is blocked in Tea2 rigor mutants Tea2 can still associate with microtubules even in the absence of Mal3 (Browning, Hackney & Nurse 2003; Browning & Hackney 2005a). Similarly, whilst Tea2 stimulates the binding of Mal3 to microtubules, the binding of Mal3 to microtubules is independent of Tea2 (Busch et al. 2004; Browning & Hackney 2005a). An overall view of the assembly of the polarisome is shown in figure 1.25 below.

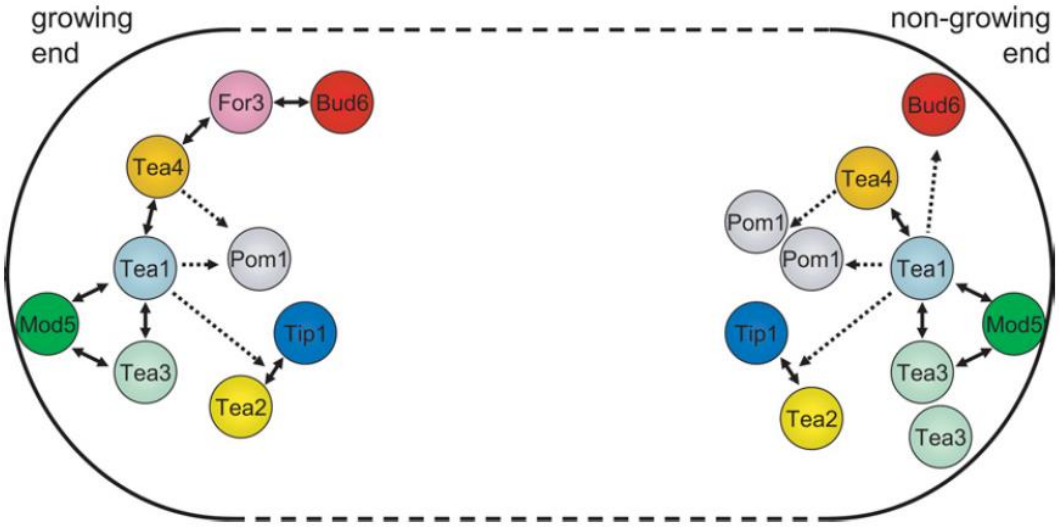

Figure.1.25. The arrangement of polarity proteins at the growing and non-growing ends of cells. A double headed arrow represents a physical interaction between two proteins while association with the cortex at the cell poles is represented by a dashed arrow when a direct interaction has not been identified (La Carbona, Le Goff & Le Goff 2006).

1.5. Aim of this study

This study aims to further our understanding of how the actin cytoskeleton and polarised growth are regulated in fission yeast. In order to do this the study has been separated into 3 distinct parts, each looking at a different aspect of the actin cytoskeleton or polarised growth. The first section focuses on the contribution of formins to the regulation of the actin cytoskeleton, which is achieved by altering the localisation of formins through use of chimeric proteins. The effect of these chimeras on actin organisation, dynamics and the interaction of actin structures with other actin binding proteins is investigated. The second section focuses on the regulation of polarised growth, and how a number of proteins from both the actin and microtubule cytoskeletons which play roles in cell polarity interact with one another. The localisation and abundance of each polarity protein is investigated when the genes encoding for other polarity proteins have been deleted, with the overall aim to build a more complete picture of how the polarisome is formed and contributes to polarised growth. The final section focuses specifically on one of these polarity proteins, the class V myosin Myo52 and how it functions within the cell. Novel chimeras are used in order to fuse the cargo binding tail domain of Myo52 with head domains of other type V myosins from fission yeast and *Drosophila melanogaster* as well as the class VI myosins from *Drosophila melanogaster*, with the ability of these chimeras to complement Myo52 function examined.

Chapter 2: Materials and Methods

2.1. Reagents

Table 2.1- List of Fission Yeast Strains Used

Stock Code	Strain Name	Genotype	Source
DMY237	*wild type (ura-,leu-)*	*ura4-d18 leu1-32 ade6-M210*	This Lab
DMY244	*wild Type (ura-,leu-)*	*ura4-d18 leu1-32 his2-*	This Lab
DMY336	*for3Δ*	*for3::kanMX6 leu1.32 ura4.d18 ade6-M210*	(Feierbach & Chang 2001)
DMY338	*bud6Δ*	*bud6::kanMX6*	(Glynn et al. 2001)
DMY211	*myo52Δ*	*myo52::ura4 ura4-d18 leu1-32 ade6-M210*	(T Z Win et al. 2001)
DMY212	*myo52Δ*	*myo52::ura4 ura4-d18 leu1-32 ade6-M210*	(T Z Win et al. 2001)
DMY341	*mal3Δ*	*mal3::ura4 ura4-d18 leu1-32 ade6-M210*	(J D Beinhauer et al. 1997)
DMY422	*tip1Δ*	*tip1::kanMX6 ura4-d18*	(Brunner & Nurse 2000)
DMY423	*tip1Δ*	*tip1::kanMX6 ura4-d18 his2-leu1.32*	(Brunner & Nurse 2000)
DMY1658	*gef1Δ*	*gef1::ura4 ura4-d18*	(Coll et al. 2003)
DMY1659	*gef1Δ*	*gef1::ura4 ura4-d18*	(Coll et al. 2003)
DMY511	*mod5Δ*	*mod5::kanMX6 ura4-d18 leu1-32 ade6-M216*	(Snaith & Sawin 2003)
DMY417	*tea1Δ*	*tea1::ura4 ura4-d18*	(Mata & Nurse 1997)
DMY2068	*tea2Δ*	*tea2::hphMX6*	This Study

DMY1814	*tea3Δ*	*tea3::kanMX6*	This Study
DMY1067	*tea4Δ*	*tea4::natMX6*	(Martin et al. 2005)
DMY335	*for3-gfp*	*for3-gfp:kanMX6 leu1-32 ura4-d18*	(Feierbach & Chang 2001)
DMY1739	*for3-gfp*	*for3-gfp:kanMX6 ura4-d18*	This Study
DMY337	*bud6-gfp*	*bud6-gfp:kanMX6 leu1-32 ura4-d18*	(Glynn et al. 2001)
DMY1678	*bud6-gfp*	*bud6-gfp:kanMX6 ura4-d18*	This Study
DMY347	*myo52-gfp*	*myo52-gfp:kanMX6 ade6-M210 ura4-d18 leu1-32*	(T Z Win et al. 2001)
DMY1764	*myo52-gfp*	*myo52-gfp:kanMX6 ura4-d18*	This study
DMY1210	*mal3-gfp*	*mal3-gfp:ura4 ura4-d18 leu1-32 ade6-M210*	(J D Beinhauer et al. 1997)
DMY1681	*mal3-gfp*	*mal3-gfp:ura4 ura4-d18*	This Study
DMY421	*tip1-gfp*	*tip1-gfp:kanMX6 leu1-32 ura4-d18*	(Brunner & Nurse 2000)
DMY422	*tip1-gfp*	*tip1-gfp:kanMX6 leu1-32 ura4-d18*	(Brunner & Nurse 2000)
DMY512	*mod5-gfp*	*nmt81mod5-gfp:kanMX6 ura4.d18 leu-32 ade6-M210*	(Snaith & Sawin 2003)
DMY1680	*mod5-gfp*	*nmt81mod5-gfp:kanMX6 ura4.d18 leu-32*	This Study
DMY419	*tea1-gfp*	*tea1-gfp:ura4 ura4-d18 leu1-32*	(Mata & Nurse 1997)
DMY1825	*tea1-gfp*	*tea1-gfp:ura4 ura4-d18 leu1-32*	This Study

DMY450	*tea2-gfp*	*tea2-gfp:kanMX6 ura4.d18 leu1-32 his3-d1*	(Browning et al. 2000)
DMY1701	*tea2-gfp*	*tea2-gfp:kanMX6 ura4.d18 leu1-32 his3-d1*	This Study
DMY1657	*tea3-gfp*	*tea3-gfp:kanMX6*	(Arellano, Niccoli & Nurse 2002)
DMY1779	*tea3-gfp*	*tea3-gfp:kanMX6*	This Study
DMY1074	*tea4-gfp*	*tea4-gfp:ura4 ura4-d18 lue1-32*	(Martin et al. 2005)
DMY1679	*tea4-gfp*	*tea4-gfp:ura4 ura4-d18*	This Study
DMY1835	*for3Δ bud6-gfp*	*for3::kanMX6 bud6-gfp:kanMX6*	This Study
DMY1813	*for3Δ myo52-gfp*	*for3:: kanMX6 myo52-gfp:kanMX6*	This Study
DMY1804	*for3Δ mal3-gfp*	*for3:: kanMX6 mal3-gfp:ura4 ura4-d18*	This Study
DMY1826	*for3Δ tip1-gfp*	*for3:: kanMX6 tip1-gfp:kanMX6*	This Study
DMY1810	*for3Δ mod5-gfp*	*for3:: kanMX6 nmt81mod5-gfp:kanMX6*	This Study
DMY1805	*for3Δ tea1-gfp*	*for3:: kanMX6 tea1-gfp:ura4 ura4-d18*	This Study
DMY1811	*for3Δ tea2-gfp*	*for3:: kanMX6 tea2-gfp:kanMX6*	This Study
DMY1827	*for3Δ tea3-gfp*	*for3:: kanMX6 tea3-gfp:kanMX6*	This Study
DMY1806	*for3Δ tea4-gfp*	*for3:: kanMX6 tea4-gfp:ura4 ura4-d18*	This Study
DMY2327	*bud6Δ for3-gfp*	*bud6::kanMX6 for3-gfp:kanMX6*	This Study
DMY1809	*bud6Δ myo52-gfp*	*bud6::kanMX6 myo52-gfp:kanMX6*	This Study
DMY1808	*bud6Δ mal3-gfp*	*bud6::kanMX6 mal3-gfp:ura4 ura4-d18*	This Study

DMY1812	*bud6Δ tip1-gfp*	*bud6::kanMX6 tip1-gfp:kanMX6*	This Study
DMY2027	*bud6Δ mod5-gfp*	*bud6::kanMX6 nmt81mod5-gfp:kanMX6*	This Study
DMY1803	*bud6Δ tea1-gfp*	*bud6::kanMX6 tea1-gfp:ura4 ura4-d18*	This Study
DMY1770	*bud6Δ tea2-gfp*	*bud6::kanMX6 tea2-gfp:kanMX6*	This Study
DMY2338	*bud6Δ tea3-gfp*	*bud6::kanMX6 tea3-gfp:kanMX6*	This Study
DMY2350	*bud6Δ tea4-gfp*	*bud6::kanMX6 tea4-gfp:ura4 ura4-d18*	This Study
DMY348	*myo52Δ for3-gfp*	*myo52::ura4 for3-gfp:kanMX6 ura4-d18*	This Lab
DMY1708	*myo52Δ bud6-gfp*	*myo52::ura4 bud6-gfp:kanMX6 ura4-d18*	This Study
DMY630	*myo52Δ mal3-gfp*	*myo52::ura4 mal3-gfp:ura4 ura4-d18*	This Lab
DMY531	*myo52Δ tip1-gfp*	*myo52::ura4 tip1-gfp:kanMX6 ura4-d18*	This Lab
DMY536	*myo52Δ mod5-gfp*	*myo52::ura4 nmt81mod5-gfp:kanMX6 ura4-d18*	This Lab
DMY628	*myo52Δ tea1-gfp*	*myo52::ura4 tea1-gfp: ura4-d18*	This Lab
DMY470	*myo52Δ tea2-gfp*	*myo52::ura4 tea2-gfp:kanMX6 ura4-d18*	This Lab
DMY1707	*myo52Δ tea3-gfp*	*myo52::ura4 tea3-gfp:kanMX6 ura4-d18*	This Study
DMY1847	*myo52Δ tea4-gfp*	*myo52::ura4 tea4-gfp:ura4 ura4-d18*	This Study
DMY1750	*mal3Δ for3-gfp*	*mal3::ura4 for3-gfp:kanMX6 ura4-d18*	This Study
DMY1752	*mal3Δ bud6-gfp*	*mal3::ura4 bud6-gfp:kanMX6 ura4-d18*	This Study
DMY610	*mal3Δ myo52-gfp*	*mal3::ura4 myo52-gfp:kanMX6 ura4-d18*	This Lab

DMY1753	*mal3Δ tip1-gfp*	*mal3::ura4 tip1-gfp:kanMX6 ura4-d18*	This Study
DMY1751	*mal3Δ mod5-gfp*	*mal3::ura4 nmt81mod5-gfp:kanMX6 ura4-d18*	This Study
DMY1737	*mal3Δ tea1-gfp*	*mal3::ura4 tea1-gfp:ura4 ura4-d18*	This Study
DMY1829	*mal3Δ tea2-gfp*	*mal3::ura4 tea2-gfp:kanMX6 ura4-d18*	This Study
DMY1830	*mal3Δ tea3-gfp*	*mal3::ura4 tea3-gfp:kanMX6 ura4-d18*	This Study
DMY1738	*mal3Δ tea4-gfp*	*mal3::ura4 tea4-gfp:ura4 ura4-d18*	This Study
DMY1726	*tip1Δ for3-gfp*	*tip1::kanMX6 for3-gfp:kanMX6*	This Study
DMY1763	*tip1Δ bud6-gfp*	*tip1::kanMX6 bud6-gfp:kanMX6*	This Study
DMY552	*tip1Δ myo52-gfp*	*tip1::kanMX6 myo52-gfp:kanMX6*	This Lab
DMY1709	*tip1Δ mal3-gfp*	*tip1::kanMX6 mal3-gfp:ura4 ura4-d18*	This Study
DMY1729	*tip1Δ mod5-gfp*	*tip1::kanMX6 nmt81mod5-gfp:kanMX6*	This Study
DMY1710	*tip1Δ tea1-gfp*	*tip1::kanMX6 tea1-gfp:ura4 ura4-d18*	This Study
DMY1727	*tip1Δ tea2-gfp*	*tip1::kanMX6 tea2-gfp:kanMX6*	This Study
DMY1730	*tip1Δ tea3-gfp*	*tip1::kanMX6 tea3-gfp:kanMX6*	This Study
DMY1716	*tip1Δ tea4-gfp*	*tip1::kanMX6 tea4-gfp:ura4 ura4-d18*	This Study
DMY1734	*gef1Δ for3-gfp*	*gef1::ura4 for3-gfp: kanMX6 ura4-d18*	This Study
DMY1732	*gef1Δ bud6-gfp*	*gef1::ura4 bud5-gfp:kanMX6 ura4-d18*	This Study

DMY1733	*gef1Δ myo52-gfp*	*gef1::ura4 myo52-gfp:kanMX6 ura4-d18*	This Study
DMY1822	*gef1Δ mal3-gfp*	*gef1::ura4 mal4-gfp:ura4 ura4-d18*	This Study
DMY1749	*gef1Δ tip1-gfp*	*gef1::ura4 tip1-gfp:kanMX6 ura4-d18*	This Study
DMY1731	*gef1Δ mod5-gfp*	*gef1::ura4 nmt81mod5-gfp:kanMX6 ura4-d18*	This Study
DMY1735	*gef1Δ tea1-gfp*	*gef1::ura4 tea1-gfp:ura4 ura4-d18*	This Study
DMY1742	*gef1Δ tea2-gfp*	*gef1::ura4 tea2-gfp:kanMX6 ura4-d18*	This Study
DMY1743	*gef1Δ tea3-gfp*	*gef1::ura4 tea3-gfp:kanMX6 ura4-d18*	This Study
DMY1736	*gef1Δ tea4-gfp*	*gef1::ura4 tea4-gfp:ura4 ura4-d18*	This Study
DMY2231	*mod5Δ for3-gfp*	*mod5::kanMX6 for3-gfp:kanMX6*	This Study
DMY1828	*mod5Δ bud6-gfp*	*mod5::kanMX6 bud6-gfp:kanMX6*	This Study
DMY1917	*mod5Δ myo52-gfp*	*mod5::kanMX6 myo52-gfp:kanMX6*	This Study
DMY1801	*mod5Δ mal3-gfp*	*mod5::kanMX6 mal3-gfp:ura4 ura4-d18*	This Study
DMY1769	*mod5Δ tip1-gfp*	*mod5::kanMX6 tip1-gfp:kanMX6*	This Study
DMY1834	*mod5Δ tea1-gfp*	*mod5::kanMX6 tea1-gfp:ura4 ura4-d18*	This Study
DMY1867	*mod5Δ tea2-gfp*	*mod5::kanMX6 tea2-gfp:kanMX6*	This Study

DMY1768	*mod5Δ tea3-gfp*	*mod5::kanMX6 tea3-gfp:kanMX6*	This Study
DMY1781	*mod5Δ tea4-gfp*	*mod5::kanMX6 tea4-gfp:ura4 ura4-d18*	This Study
DMY1776	*tea1Δ for3-gfp*	*tea1::ura4 for3-gfp:kanMX6 ura4-d18*	This Study
DMY1773	*tea1Δ bud6-gfp*	*tea1::ura4 bud6-gfp:kanMX6 ura4-d18*	This Study
DMY1772	*tea1Δ myo52-gfp*	*tea1::ura4 myo52-gfp:kanMX6 ura4-d18*	This Study
DMY1823	*tea1Δ mal3-gfp*	*tea1::ura4 mal3-gfp:ura4 ura4-d18*	This Study
DMY1748	*tea1Δ tip1-gfp*	*tea1::ura4 tip1-gfp:kanMX6 ura4-d18*	This Study
DMY1775	*tea1Δ mod5-gfp*	*tea1::ura4 nmt81mod5-gfp:kanMX6 ura4-d18*	This Study
DMY1771	*tea1Δ tea2-gfp*	*tea1::ura4 tea2-gfp:kanMX6 ura4-d18*	This Study
DMY1774	*tea1Δ tea3-gfp*	*tea1::ura4 tea3-gfp:kanMX6 ura4-d18*	This Study
DMY1777	*tea1Δ tea4-gfp*	*tea1::ura4 tea4-gfp:ura4 ura4-d18*	This Study
DMY2238	*tea2Δ for3-gfp*	*tea2::hphMX6 for3-gfp:kanMX6*	This Study
DMY2239	*tea2Δ bud6-gfp*	*tea2::hphMX6 bud6-gfp:kanMX6*	This Study
DMY2240	*tea2Δ myo52-gfp*	*tea2::hphMX6 bud6-gfp:kanMX6*	This Study
DMY2235	*tea2Δ mal3-gfp*	*tea2::hphMX6 mal3-gfp:ura4 ura4-d18*	This Study
DMY2237	*tea2Δ tip1-gfp*	*tea2::hphMX6 tip1-gfp:kanMX6*	This Study

DMY2236	*tea2Δ mod5-gfp*	*tea2::hphMX6 nmt81mod5-gfp:kanMX6*	This Study
DMY2232	*tea2Δ tea1-gfp*	*tea2::hphMX6 tea1-gfp:ura4 ura4-d18*	This Study
DMY2233	*tea2Δ tea3-gfp*	*tea2::hphMX6 tea3-gfp:kanMX6*	This Study
DMY2234	*tea2Δ tea4-gfp*	*tea2::hphMX6 tea4-gfp:ura4 ura4-d18*	This Study
DMY2230	*tea3Δ for3-gfp*	*tea3::kanMX6 for3-gfp:kanMX6*	This Study
DMY2025	*tea3Δ bud6-gfp*	*tea3::kanMX6 bud6-gfp:kanMX6*	This Study
DMY2004	*tea3Δ myo52-gfp*	*tea3::kanMX6*	This Study
DMY1849	*tea3Δ mal3-gfp*	*tea3::kanMX6*	This Study
DMY2229	*tea3Δ tip1-gfp*	*tea3::kanMX6*	This Study
DMY2038	*tea3Δ mod5-gfp*	*tea3::kanMX6*	This Study
DMY1848	*tea3Δ tea1-gfp*	*tea3::kanMX6*	This Study
DMY2228	*tea3Δ tea2-gfp*	*tea3::kanMX6*	This Study
DMY1850	*tea3Δ tea4-gfp*	*tea3::kanMX6*	This Study
DMY1757	*tea4Δ for3-gfp*	*tea4::natMX6 for3-gfp:kanMX6*	This Study
DMY1761	*tea4Δ bud6-gfp*	*tea4::natMX6 bud6-gfp:kanMX6*	This Study
DMY1754	*tea4Δ myo52-gfp*	*tea4::natMX6 myo52-gfp:kanMX6*	This Study
DMY1780	*tea4Δ mal3-gfp*	*tea4::natMX6 mal3-gfp:ura4 ura4-d18*	This Study
DMY1758	*tea4Δ tip1-gfp*	*tea4::natMX6 tip1-gfp:kanMX6*	This Study
DMY1756	*tea4Δ mod5-gfp*	*tea4::natMX6 nmt81mod5-gfp:kanMX6*	This Study
DMY1760	*tea4Δ tea1-gfp*	*tea4::natMX6 tea1-gfp:ura4 ura4-d18*	This Study

DMY1759	*tea4Δ tea2-gfp*	*tea4::natMX6 tea2-gfp:kanMX6*	This Study
DMY1755	*tea4Δ tea3-gfp*	*tea4::natMX6 tea3-gfp:kanMX6*	This Study
DMY843	*sid4-tomato myo51-gfp*	*sid4-tomato:hphMX6 myo51-gfp:kanMX6*	This Lab
DMY840	*sid4-tomato myo51Δ*	*sid4-tomato:hphMX6 myo51::ura4*	This Lab
DMY1666	*for3-gfp sid4-tomato*	*for3-gfp:kanMX6 sid4-tomato:hphMX6*	This Study
DMY1664	*bud6-gfp sid4-tomato*	*bud6-gfp:kanMX6 sid4-tomato:hphMX6*	This Study
DMY1665	*myo52-gfp sid4-tomato*	*myo52-gfp:kanMX6 sid4-tomato:hphMX6*	This Study
DMY1673	*mal3-gfp sid4-tomato*	*mal3-gfp:ura4 sid4-tomato:hphMX6 ura4-d18*	This Study
DMY1741	*tip1-gfp sid4-tomato*	*tip1-gfp:kanMX6 sid4-tomato:hphMX6*	This Study
DMY1671	*mod5-gfp sid4-tomato*	*nmt81mod5-gfp:kanMX6 sid4-tomato:hphMX6*	This Study
DMY1711	*tea1-gfp sid4-tomato*	*tea1-gfp:ura4 sid4-tomato:hphMX6 ura4-d18*	This Study
DMY1724	*tea2-gfp sid4-tomato*	*tea2-gfp:kanMX6 sid4-tomato:hphMX6*	This Study
DMY1740	*tea3-gfp sid4-tomato*	*tea3-gfp:kanMX6 sid4-tomato:hphMX6*	This Study
DMY1704	*tea4-gfp sid4-tomato*	*tea4-gfp:ura4 sid4-tomato:hphMX6 ura4-d18*	This Study
DMY761	*Wildtype ura-, leu+*	*ura4-d18*	This Lab
DMY1623	*cdc12-112*	*cdc12-112 leu1-32*	This Study
DMY1543	*cdc12-112 myo2-mCherry*	*cdc12-112 myo2-mCherry:hphMX6 leu1-32*	This Lab
DMY1832	*cdc12Δ diploid*	*cdc12::ura4 leu1- ade6-m216 ura4- h+ X wt cdc12 leu1-ade6-m210 ura4- h-*	(Chang, Drubin &

			Nurse 1997)

DMY1820	*cdc12-112 mts3-1*	*Cdc12-112 mts3-1 leu1-32*	This Study
DMY1530	*for3D myo52-mCherry*	*for3::kanMX6 myo52-mCherry:hphMX6 ura4-d18 leu1-32*	This Lab
DMY416	*cdc10-v50*	*cdc10-v50 leu1-32 ura4-d18*	This Lab
DMY1625	*for3D cdc10-v50 myo52-mCherry*	*for3::kanMX6 cdc10-v50 myo52-mCherry:hphMX6*	This Study
DMY1356	*-gfp-CHD*	*nmt41-gfpCHDRng2:LEU2 leu1-32 ura4-d18 ade6-M216*	(Huang, Yan & Balasubramanian 2008)
DMY1714	*for3Δ -gfp-CHD*	*for3::kanMX6 nmt41-gfpCHDRng2:LEU2 leu1-32 ura4-d18*	This Study
DMY1873	*pINT41for3-mCherry*	*leu1:nmt41for3-mCherry:ura4 ura4-d18*	This Study
DMY1871	*pINT41cdc12-mCherry*	*leu1:nmt41cdc12-mCherry:ura4 ura4-d18*	This Study
	pINT41tea1-for3-mCherry	*leu1:nmt41tea1-for3-mCherry:ura4 ura4-d18*	This Study
DMY1872	*pINT41tea1-cdc12-mCherry*	*leu1:nmt41tea1-cdc12-mCherry:ura4 ura4-d18*	This Study
DMY1833	*pINT41myo2T-for3-mCherry*	*leu1:nmt41myo2T-for3-mCherry:ura4 ura4-d18*	This Study
DMY1909	*for3Δ pINT41for3-mCherry*	*leu1:nmt41for3-mCherry:ura4* *ura4-d18*	This Study
DMY1908	*for3Δ pINT41cdc12-mCherry*	*leu1:nmt41cdc12-mCherry:ura4* *ura4-d18*	This Study
DMY1912	*for3Δ pINT41tea1-for3-mCherry*	*leu1:nmt41tea1-for3-mCherry:ura4 ura4-d18*	This Study

DMY1910	*for3Δ pINT41tea1-cdc12-mCherry*	*leu1:nmt41tea1-cdc12-mCherry:ura4 ura4-d18*	This Study
DMY1915	*for3Δ pINT41myo2T-for3-mCherry*	*leu1:nmt41myo2T-for3-mCherry:ura4 ura4-d18*	This Study
DMY1919	*for3Δ gfp-CHD pINT41for3-mCherry*	*for3::kanMX6 nmt41-gfpCHDRng2:LEU2 leu1:nmt41for3-mCherry:ura4 leu1-32 ura4-d18*	This Study
DMY1920	*for3Δ gfp-CHD pINT41cdc12-mCherry*	*for3::kanMX6 nmt41-gfpCHDRng2:LEU2 leu1:nmt41cdc12-mCherry:ura4 leu1-32 ura4-d18*	This Study
DMY2342	*for3Δ gfp-CHD pINT41tea1-for3-mCherry*	*for3::kanMX6 nmt41-gfpCHDRng2:LEU2 leu1:nmt41tea1-for3-mCherry:ura4 leu1-32 ura4-d18*	This Study
DMY1921	*for3Δ gfp-CHD pINT41tea1-cdc12-mCherry*	*for3::kanMX6 nmt41-gfpCHDRng2:LEU2 leu1:nmt41tea1-cdc12-mCherry:ura4 leu1-32 ura4-d18*	This Study
DMY1874	*for3Δ gfp-CHD pINT41myo2T-for3-mCherry*	*for3::kanMX6 nmt41-gfpCHDRng2:LEU2 leu1:nmt41myo2T-for3-mCherry:ura4 leu1-32 ura4-d18*	This Study
DMY2334	*for3Δ gfp-CHD cdc12-112 pINT41for3-mCherry*	*for3::kanMX6 nmt41-gfpCHDRng2:LEU2 cdc12-112 leu1:nmt41for3-mCherry:ura4 leu1-32 ura4-d18*	This Study

DMY2335	*for3Δ gfp-CHD cdc12-112 pINT41cdc12-mCherry*	*for3::kanMX6 nmt41-gfpCHDRng2:LEU2 cdc12-112 leu1:nmt41cdc12-mCherry:ura4 leu1-32 ura4-d18*	This Study
	for3Δ gfp-CHD cdc12-112 pINT41tea1-for3-mCherry	*for3::kanMX6 nmt41-gfpCHDRng2:LEU2 cdc12-112 leu1:nmt41tea1-for3-mCherry:ura4 leu1-32 ura4-d18*	This Study
DMY2336	*for3Δ gfp-CHD cdc12-112 pINT41tea1-cdc12-mCherry*	*for3::kanMX6 nmt41-gfpCHDRng2:LEU2 cdc12-112 leu1:nmt41tea1-cdc12-mCherry:ura4 leu1-32 ura4-d18*	This Study
DMY2337	*for3Δ gfp-CHD cdc12-112 pINT41myo2T-for3-mCherry*	*for3::kanMX6 nmt41-gfpCHDRng2:LEU2 cdc12-112 leu1:nmt41myo2T-for3-mCherry:ura4 leu1-32 ura4-d18*	This Study
DMY1639	*for3D +pREP41for3-gfp*	*for3::kanMX6+ pREP41for3-gfp leu1-32 ura4-d18*	This Study
DMY1636	*for3D + pREP41tea1-gfp*	*for3::kanMX6 + pREP41tea1-gfp leu1-32 ura4-d18*	This Study
DMY1635	*for3D + pREP41tea1-for3-gfp*	*for3::kanMX6 + pREP41tea1-for3-gfp leu1-32 ura4-d18*	This Study
DMY1637	*for3D + pREP41tea1-cdc12-gfp*	*for3::kanMX6 + pREP41tea1-cdc12-gfp leu1-32 ura4-d18*	This Study
DMY1638	*for3D + pREP41cdc12-gfp*	*for3::kanMX6 + pREP41cdc12--gfp leu1-32 ura4-d18*	This Study
DMY1558	*cdc12-112 myo2-mCherry + pREP41myo2T-gfp*	*cdc12-112 myo2-mCherry:hphMX6 + pREP41myo2T-gfp leu1-32*	This Study
DMY1559	*cdc12-112 myo2-mCherry + pREPmyo2T-for3-gfp*	*cdc12-112 myo2-mCherry:hphMX6 + pREPmyo2T-for3-gfp leu1-*	This Study
DMY1578	*cdc12-112 myo2-mCherry + pREP41cdc12-gfp*	*cdc12-112 myo2-mCherry:hphMX6 + pREP41cdc12-gfp leu1-32*	This Study

DMY1574	*cdc12-112 myo2-mCherry + pREP41tea1-cdc12-gfp*	*cdc12-112 myo2-mCherry:hphMX6 + pREP41tea1-cdc12-gfp leu1-32*	This Study
DMY1858	*cdc12-112 mts3-1 + pREP41myo2T-gfp*	*cdc12-112 mts3-1 + pREP41myo2T-gfp leu1-32*	This Study
DMY1844	*cdc12-112 mts3-1 + pREPmyo2T-for3-gfp*	*cdc12-112 mts3-1 + pREPmyo2T-for3-gfp leu1-*	This Study
DMY1861	*cdc12-112 mts3-1 + pREP41cdc12-gfp*	*cdc12-112 mts3-1 + pREP41cdc12-gfp leu1-32*	This Study
DMY1859	*cdc12-112 mts3-1 + pREP41tea1-cdc12-gfp*	*cdc12-112 mts3-1 + pREP41tea1-cdc12-gfp leu1-32*	This Study
DMY 2344	*cdc12-112 + pREP41myo2T-cdc12-gfp*	*cdc12-112 + pREP41myo2T-cdc12-gfp leu1-32*	This Study
DMY2140	*2yfp-rng2*	*ura4-Prng2-mYFPx2-rng2 ade6-M210 leu1-32 ura4-D18*	(Takaine, Numata & Nakano 2009)
DMY2139	*gfp-adf1*	*adf1::[adh--GFP-adf1-ura4+] ade6-M216 leu1-32 ura4-D18*	(Nakano & Mabuchi 2006)
DMY2215	*for3ΔpINT41tea1-cdc12-mCherry 2yfp-rng2*	*leu1:nmt41tea1-cdc12-mCherry:ura4 ura4-Prng2-mYFPx2-rng2 ade6-M210 leu1-32 ura4-D18*	This Study
DMY2227	*for3ΔpINT41tea1-cdc12-mCherry gfp-adf1*	*leu1:nmt41tea1-cdc12-mCherry:ura4 adf1::[adh--GFP-adf1-ura4+] ade6-M216 leu1-32 ura4-D18*	This Study
DMY2281	*myo52Δ + pREP41myo52H+myo52T-gfp*	*myo52::ura4 + pREP41myo52H+myo52T-gfp ura4-d18*	This Study
DMY2302	*myo52Δ + pREP41myo51H+myo52T-gfp*	*myo52::ura4 + pREP41myo51H+myo52T-gfp*	This Study

		ura4-d18	
DMY2280	*myo52Δ + pREP41Dm.myoVH+myo52T-gfp*	*myo52::ura4 + pREP41Dm.myoVH+myo52T-gfp ura4-d18*	This Study
DMY2303	*myo52Δ + pREP41Dm.myoVIH+myo52T-gfp*	*myo52:: ura4+ pREP41Dm.myoVIH+myo52T-gfp ura4-d18*	This Study
DMY2064	*myo52Δ + pREP41Dm.myoVIH(+converter) + myo52T-gfp*	*myo52::ura4 + pREP41Dm.myoVIH(+converter)+ myo52T-gfp ura4-d18*	This Study
DMY2313	*myo52-tomato + pREP41myo52H+myo52T-gfp*	*myo52-tomato:hphMX6 + pREP41myo52H+myo52T-gfp*	This Study
DMY2315	*myo52-tomato + pREP41myo51H+myo52T-gfp*	*myo52-tomato:hphMX6 + pREP41myo51H+myo52T-gfp*	This Study
DMY2312	*myo52-tomato + pREP41Dm.myoVH+myo52T-gfp*	*myo52-tomato:hphMX6 + pREP41Dm.myoVH+myo52T-gfp*	This Study
DMY2316	*myo52-tomato + pREP41Dm.myoVIH+myo52T-gfp*	*myo52-tomato:hphMX6 + pREP41Dm.myoVIH+myo52T-gfp*	This Study
DMY2314	*myo52-tomato + pREP41Dm.myoVIH(+converter) + myo52T-gfp*	*myo52-tomato:hphMX6 + pREP41Dm.myoVIH(+converter)+ myo52T-gfp*	This Study

*A single colon (:) denotes a gene marker, for example a fluorescent tag selected for by an antibiotic, where as two colong (::) denotes a gene deletion, for example where a gene has been replaced by an antibiotic resistance gene to allow for selection of the deletion mutant

Table 2.2 List of Plasmids Used

Stock Code	Plasmid	Source
DMV9	pREP41-gfp	(Craven et al. 1998)
DMV474	pREP41tea1-for3-gfp	This Study
DMV478	pREP41tea1-gfp	This Study
DMV479	pREP41myo2T-gfp	This Study
DMV491	pREP41tea1-cdc12-gfp	This Study
DMV492	pREP41myo2T-for3-gfp	This Study
DMV639	pREP41myo2T-cdc12-gfp	This Study
DMV536	pREP41cdc12-gfp	This Study
DMV537	pREP41for3-gfp	This Study
DMV636	pGEM-T-Easy myo2T-cdc12	This Study
DMV480	pGEM-T-Easy cdc12	This Study
DMV466	pGEM-T-Easy for3	This Study
DMV461	pGEM-T-Easy tea1	This Study
DMV470	pGEM-T-Easy tea1-for3	This Study
DMV483	pGEM-T-Easy myo2T-for3	This Study
DMV580	pINT41for3-mCherry	This Study
DMV577	pINT41tea1-cdc12-mCherry	This Study
DMV576	pINT41myo2T-for3-mCherry	This Study
DMV578	pINT41cdc12-mCherry	This Study
DMV579	pINT41tea1-for3-mCherry	This Study
DMM159	pREP41myo52T-gfp	This Study
DMM146	pGEM-T-Easy myo52T	This Study
DMM182	pGEM-T-Easy myo52H	This Study
DMM140	pGEM-T-Easy myo51H	This Study
DMM171	pGEM-T-Easy Dm.myoVH	This Study
DMM156	pGEM-T-Easy Dm.myoVIH	This Study
DMM157	pGEM-T-Easy Dm.myoVIH(+converter)	This Study
DMM174	pREP41myo52H+myo52T-gfp	This Study

DMM178	pREP41myo51H+myo52T-gfp	This Study
DMM173	pREP41Dm.myoVH+myo52T-gfp	This Study
DMM179	pREP41Dm.myoVIH+myo52T-gfp	This Study
DMM175	pREP41Dm.myoVIH(+converter)+ myo52T-gfp	This Study

Table 2.3: List of Oligonucleotides Used

Stock Code	Oligonucleotide Name	Restriction site	Sequence
DMO471	myo52H F	NdeI	CAT ATG ATG ACA TCG GGG ATT TAT TAC
DMO319	myo52H R	SalI	GTC GAC TCT CGC ACT CTC TAA AAG GGG
DMO322	myo51H F		GTC GAC AAT GAG TCA TGC AAG ATT ATC
DMO323	myo51H R	SalI	
DMO469	Dm. myoVH F		CAT ATG ATG TCT AGC GAG GAG ATG CTA
DM331	Dm. myoVH R	SalI	GTC GAC CCG AAC CTG TTC AAG GAA GGC
DMO468	Dm. myoVIH F		AAT ATT ATG TTG GAG GAC ACC CAA CTG
DM333	Dm. myoVIH R	XhoI	CTC GAG CAT GAT GCG ATC GAA CTC CAC
DM334	Dm. myoVI(+converter)HR	XhoI	CTC GAG ATT ACG CAG CTT GAT CAC GC
DMO400	for3 F	NdeI	CAT ATG GCA TCT AAA ATG CCT GAA GGG
DMO367	for3 R	BamHI	GGA TCC TTG TTT TTG GCG GTG ATT TTC AAC
DMO399	cdc12 F	NdeI	CAT ATG CGA AAT TCG TCA AAG GG
DMO369	cdc12 R	BamHI	GGA TCC TTT CTC ATT CTC CTT AGG CGC C

2.2. Yeast cell culture

S. pombe culture and maintenance were carried out as described in (Moreno, Klar & Nurse 1991) Cells were grown in Edinburgh minimal medium (EMM2) or Yeast Extract (YES) medium supplemented with the appropriate amino acids. Genetic crosses were undertaken on sporulating medium (MSA).

The following recipes were used for media preparation and media was prepared using Molecular Biology Grade Water (Fisher, UK):

EMM2

- Potassium Hydrogen Phthalate 3 g/l
- Na_2HPO_4 2.2 g/l
- NH_4Cl 5 g/l
- Glucose 20 g/l
- 50x Salts 20 ml/l
- 1000x Vitamins 1 ml/l
- 10000x Minerals 100 µl/l

YES

- Glucose 30 g/l
- Yeast Extract 5 g/l

MSA

- NaCl 0.1 g/l
- KH2PO4 1 g/l
- Arginine 2 g/l
- MgSO4.7H2O 0.2 g/l
- CaSO4.2H2O 0.1 g/l
- 1000x Vitamins 1 ml/l
- 10000x Minerals 100 µl/l

Salt, vitamin and mineral supplements for EMM2 and MSA medium were prepared as follows:

50x Salts

- $MgCl_2.6H_20$ 52.5 g/l
- $CaCl_2.2H_20$ 0.735 g/l
- KCl 50 g/l
- Na_2SO_4 2 g/l

1000x Vitamins

- Pantothenic acid 1 g/l
- Nicotinic acid 10 g/l
- Inositol 10 g/l
- Biotin 10 mg/l

10000x Minerals

- Boric acid 5 g/l
- $MnSO_4$ 4 g/l
- $ZnSO_4.7H_20$ 4 g/l
- $FeCl_2.6H_20$ 2 g/l
- Molybdic acid 0.4 g/l
- KI 1 g/l
- $CuSO_4.5H_20$ 0.4 g/l
- Citric acid 10 g/l

Amino acids supplements (adenine, histidine, leucine, uracil) were added to media at a final concentration of 225 mg/l. If gene expression was under the control of the *nmt41* promoter media was supplemented with either 15 µM or 4 pM Thiamine Hydrochloride (Fisher). When solid media was required 20 g/l agar was added.

2.2.1. Tetrad Dissection

When tetrad dissection was required cells were streaked onto YES plates and tetrads then dissected using a Singer Instruments MSM400 Dissection Microscope.

2.3. Microscopy

2.3.1. Visualisation of fluorescently tagged proteins

Samples were visualised using an Olympus IX71 microscope with PlanApo 100x OTIRFM-SP 1.45 NA lens mounted on a PIFOC *z*-axis focus drive (PhysikInstrumente, Karlsruhe, Germany), and illuminated using LED light sources (Cairn Research Ltd, Faversham, UK) with appropriate filters (Chroma, Bellows Falls, VT). An Optisplit device (Cairn Research Ltd) was used to allow simultaneous acquisition of multiple wavelengths. Samples were visualised using either a QuantEM CCD (Photometrics) or Orca Flash (Hamamatsu) camera, and the system was controlled with Metamorph software (Molecular Devices). Each 3D-maximum projection of volume data was calculated from 31 *z*-plane images, each 0.2 µm apart, using Metamorph or Autoquant X software. During live-cell imaging, cells were mounted onto coverslips with lectin (Sigma L2380; 1 mg/ml) in a Bioptechs FCS2 (Bioptechs, Butler, PA), fitted onto an ASI motorised stage (ASI, Eugene, OR) on the above system, with the sample holder, objective lens and environmental chamber held at the required temperature. All live-cell imaging was undertaken using EMM2 media supplemented with appropriate amino acids.

2.3.2. Microscopic Mix Experiments

For each experiment wild-type cells expressing the GFP tagged polarity protein to be tested as well as a red labelled spindle pole body component (Sid4) were mixed and mounted together on a coverslip with a deletion strain expressing the GFP tagged polarity protein alone. In this way it was possible to confidently conclude that any difference in GFP

fluorescence between the two strains is due to the gene deletion alone and not external factors such as media, or fluctuations in temperature or light source intensity.

2.3.3. Analysis of Polarity Protein Intensity

The intensity of GFP tagged polarity proteins was measured in Metamorph software using maximum projections of 31 Z slice images unless otherwise stated. A 3 μm diameter circle was drawn in the software and the signal intensity inside the circle was measured and recorded at both ends of the cell and in the cytoplasm. Measurements were taken of the image background, both ends of the cell with End 1 being the end with brighter GFP signal and of the cytoplasm. These intensity measurements within the cell were background corrected by subtracting the background intensity measurement. Both the average intensity and the maximum intensity within the circle were recorded, and the difference between wild type and deletions were calculated.

The average signal intensity within the entire circle was useful for seeing large changes in intensity, for example if the entire cytoplasm was much brighter, however it was not as useful at the cell poles as even if there was an increase in brightness at cell poles, this could be counteracted by the majority of the circle measuring the cytoplasm, which may not have reflected the large change. This was shown better by the maximum signal intensity, which recorded the brightest signal within the circle, and was a lot more useful for recording increases or decreases in protein levels at the cell poles.

A difference in intensity between wildtype and mutant cells of over 10% was regarded as significant, however differences between 12% and 8% were T-tested to confirm significance.

2.3.4. Analysis of Actin Cable Dynamics

Growth and shrinkage of actin filaments was measured using Metamorph software. Timelapse movies of 13 0.2 µm Z slice time frames (0.667 sec / time point; 200 time points,) were acquired and analysed in a frame-by-frame manner, looking for actin filament growth from the cell poles. Care was taken to ensure that only growth events from a single point at the cell poles were measure, to ensure that movement/flow of existing cables was not measured. The difference in filament length and time taken were recorded, and the rate of filament growth or shrinkage was then calculated. At least 10 growth events were measured for each strain.

2.3.5. Immunofluorescence

Immunofluorescence experiments were carried out following the method described in (Hagan & Hyams 1988), omitting glutaraldehyde. A 30% solution of paraformaldehyde (Sigma) was prepared in PEM buffer (100 mM PIPES, 1 mM EGTA, 1 mM $MgSO_4$ pH 6.9) and cells were fixed in a final concentration of 3% paraformaldehyde for whilst shaking at room temperature for 30 minutes. The cells were then pelleted by centrifugation at 3000 RPM for 5 minutes at room temperature. The sample was then washed 3 times in 1 ml of PEM. The cells were then incubated in PEMSZ buffer (PEM + 1.2 M Sorbitol and 1 mg/ml 20T Zymolyase) for 30 minutes at 37°c. The cells were then pelleted by centrifugation at 13000 RPM for 1 minute at room temperature and subsequently incubated in PEMST (PEM + 1.2M Sorbitol +1% triton) for 30 seconds. 3 PEM washes were then carried out before incubation in PEMBAL (PEM + 1% IgG Free BSA, 0.1% Sodium Azide, 100 mM Lysine Hydrochloride pH 6.9). Cells were then incubated in 100 µl of PEMBAL + primary antibody on a rotating wheel

overnight at room temperature. Concentrations of primary antibody used were as follows: anti-cdc8: 1:100, anti-acetylated cdc8 1:50, anti-unacetylated cdc8 1:5. Cells were then washed 3 times in PEM and incubated in 100 µl PEMBAL + secondary antibody (1:5000 TRITC conjugated anti-rabbit IgG, Sigma) on a rotating wheel overnight at room temperature. Cells were then washed once in PEM and once in PBC, before being resuspended in 10-20 µl PBS.

2.4. Molecular Biology

2.4.1 Polymerase Chain Reaction (PCR)

The polymerase chain reaction was used to amplify genes of interest such as formins or myosin heads for cloning into *S. pombe* expression vectors. A typical PCR reaction mixture consisted of:

- Template DNA (15 ng/ µl) 1 µl
- Oligonucloetides (10 µM) 1 ul
- Water 41.5 µl
- 10x Reaction Buffer 5 µl
- dNTPs (10 µM) 1 µl
- Expand High Fidelity Polymerase (Roche) 0.5 µl

A typical PCR reaction programme was as follows, with variations in annealing temperature and elongation time depending on the gene to be amplified. The denaturation, annealing and elongation steps were cycled up to 30 times;

- Initial denaturation step- 92 °C 2 minutes
- Denaturation step- 92 °C 30 seconds
- Annealing step 50 °C 1 minute
- Elongation step 72 °C or 68 °C 30 seconds/ kb
- Final elongation step 72 °C 10-30 minutes

2.4.2. Gel purification of DNA

PCR product or DNA fragments from restriction digests were run on 1% agarose gels containing Ethidium Bromide (10 ng/ml) in 0.5x TAE buffer (0.4 mM Tris base, 0.4 mM

glacial acetic acid, 0.01 mM EDTA). DNA bands were visualized by exposure to UV light and excised using a razor blade. The DNA was then purified using the Bioline Gene Clean 3 kit using the manufacturer's reagents and protocol.

2.4.3 Cloning Genes of Interest into the *S. pombe* expression system

Gel purified PCR products were ligated into the pGEM-T-Easy vector and correct clones were identified by restriction digests and sequencing. pGEM-T-Easy ligation reactions were carried out at 4 °C and the typical reaction mixture was as follows:

- pGEM-T-Easy 1 µl
- Purified PCR product 3 µl
- Water 4 µl
- Ligase Buffer (10x) 1 µl
- T4 Ligase (Roche) 1 µl

Genes of interest were then removed from pGEM-T-Easy by restriction digest and cloned into a vector which had also been cut with compatible restriction enzymes.

S. pombe for3 and *cc12* were cloned as an NdeI/BamHI fragment into NdeI/BamHI cut *pREP41-gfp*. *mCherry* was cloned as an NdeI/BglII into NdeI/BamHI cut *pINT41. Myo2T-for3, cdc12, for3, tea1-cdc12 and tea1-for3* were subsequently cloned in as NdeI/BamHI fragments into NdeI/BamHI cut *pINT41-mCherry.* The *pINT41psy1-for3-mCherry* construct was generated by cutting *pINT41tea1-for3-mCherry* with NdeI and SalI to excise the *tea1* fragment, *and psy1* was subcloned in as an AseI/SalI fragment.

Base pairs 767 to 4918 of the *S.pombe myo52* gene encoding for the converter, IQ, coiled coil and globular tail domains were cloned as a SalI/SmaI fragment into SalI/SmaI cut *pREP41-gfp* to generate *pREP41-myo52T-gfp*. The following myosin heads were subsequently cloned into this plasmid as follows:

- *S. pombe myo52H* (base pairs 1-766) was cloned as an NdeI/SalI fragment into NdeI/SalI cut *pREP41myo52T-gfp*
- *S. pombe myo51H* (base pairs 1-749) was cloned as a SalI fragment into SalI cut *pREP41myo52T-gfp*
- *D. melanogaster myoVH* (base pairs 1-779) was cloned as an NdeI/SalI fragment into NdeI/SalI cut *pREP41myo52T-gfp*
- *D. melanogaster myoVIH* (-converter) (base pairs 1-766) and *myoVIH* (+inverter) (base pairs 1-804) were cloned as an AseI/XhoI fragment into NdeI/SalI cut *pREP41myo52T-gfp*

Ligation reactions typically consisted of:

- Vector DNA 4 µl
- Insert DNA 4 µl
- Ligase Buffer 1 µl
- T4 DNA Ligase 1 µl

Small scale digests were carried out in order to check constructs whilst large scale digests were carried out for cloning of genes into *pREP41-GFP*. Typical reaction mixtures were as follows:

Small scale digest

- DNA 2 µl
- Buffer 2 µl
- Water 14/15 µl
- Restriction enzyme 1 µl /enzyme

Large scale digest

- DNA 10 µl
- Buffer 10 µl
- Water 76/78 µl
- Restriction enzyme 2 µl /enzyme

2.4.5 Preparation of competent cells

DH5α or DH10β *E. coli*, were streaked out onto Luria Broth (LB) agar plates and incubated at 37 ºC overnight. From this a single colony was inoculated into 5 ml of LB medium and grown shaking at 37 ºC at 220 RPM overnight. 0.5 ml of this pre culture was then inoculated into 50 ml of fresh LB medium and grown at 37 ºC shaking at 180 RPM until the optical density at 600 nm of the culture was between 0.6-0.8. The cells were then cooled on ice for 10 minutes, before being centrifuged at 2700 RPM at 4 ºC for 10 minutes. The pelleted cells were then resuspended in 10 ml of 0.1 M $CaCl_2$/10% glycerol solution and kept on ice for 15 minutes. The cells were then centrifuged again at 2700 RPM at 4 ºC for 10 minutes. The pelleted cells were then resuspended in 1 ml of 0.1M $CaCl_2$/10% glycerol solution and dispensed into 50 ml aliquots and stored at -80ºC.

2.4.6. Bacterial Transformation

50 µl of competent bacterial cells were defrosted on ice, inoculated with an appropriate volume of DNA (1-10 µl), and were then incubated on ice for 20 minutes. The cells were heat shocked at 42 ºC for 60 seconds, and transferred back onto ice for 2 minutes. 200 µl of LB media was then added to the cells and then grown at 37 ºC shaking at 220 RPM for 1

hour. 200 µl of cells were then plated out on LB agar plates supplemented with appropriate antibiotics.

2.4.7. *S. pombe* transformation

50 ml of a mid-log (1-4 x 10^6 cells/ml) *S. pombe* culture was centrifuged at 4000 RPM for 5 minutes at room temperature. The cell pellet was resuspended in 1 ml of 0.1 M Lithium Acetate pH 4.8 and was transferred to a 1.5 ml microfuge tube. The cells were then centrifuged at 4000 RPM for 1 minute at room temperature and the cell pellet was then resuspended in 1 ml 0.1 M Lithium Acetate pH 4.8 and incubated at 25 °C for 1 hour. 5 µl of DNA and 100 µl of 70% PEG-4000 was then added to a 100 µl aliquot of cells (1x10^7 cells), vortexed and then incubated at 25 °C for 1 hour. The cells were then heat shocked in a water bath at 42 °C for 10 minutes before being centrifuged at 4000 RPM for 1 minute at room temperature. The cells were then washed with 100 µl of sterile water and centrifuged again at 4000 RPM for 1 minute at room temperature. The cells were then resuspended in 50 µl sterile water and plated onto EMM2 or YES solid agar and incubated at 25 °C for up to 1 week.

2.4.8. Small scale preparation of plasmid DNA from bacteria

5 ml of LB media with appropriate antibiotics was inoculated with a single colony from a transformation plate and grown shaking at 37 °C at 220 RPM overnight. 2ml of this culture was then centrifuged at 4000 RPM for 5 minutes and DNA preparation was then carried

out using a Qiagen Qiaprep Spin Miniprep Kit using the manufacturer's reagents and protocol, based on an alkaline lysis method.

2.4.9. Preparation of *S .pombe* genomic DNA

1 ml of a mid-log culture was centrifuged at 4000 RPM for 2 minutes at room temperature. The cell pellet was then resuspended in 300 µl of lysis buffer (50 mM Tris pH 7.5, 50 mM EDTA, 1% SDS) and transferred to a 2 ml screw top tube. 0.5 ml of cold, acid washed glass beads was then added to the cells and the cells were lysed by performing 2x 30 second runs at maximum speed in a FastPrep 3000 instrument (Bio101). The base of the screw top tube was then pierced and the tube was placed inside a 15 ml falcon tube. This was then centrifuged at 3000 RPM for 3 minutes in order to pellet the glass beads in the 2 ml screw top tubes whilst the cell lysate span through into the 15 ml falcon tube. 300 µl of phenol-chloroform was then added to the cell lysate and was mixed by vortexing. This was then centrifuged at 13000 RPM for 10 minutes at 4 °C and the aqueous layer was removed. 3x volumes of ice-cold ethanol and 1/10 volume of 3 M sodium acetate was then added and this was incubated at -20 °C for at least 30 minutes. This was then centrifuged at 13000 RPM for 10 minutes at 4 °C in order to pellet the precipitated DNA. The pelleted DNA was washed with 200 µl of ice-cold 70% ethanol and then dried by incubation at 65 °C for 10 minutes. The pellet was then resuspended in 50 µl of sterile water and 1 µl of RNAase (1 mg/ml stock).

Chapter 3: Formin Mediated Recruitment of Tropomyosin to Distinct Actin Structures.

3.1. Fusing Formins to the Cell End Marker Tea1 Recruits Them to the Cell Poles.

As there is a clear correlation between the localization of For3 and unacetlyated tropomyosin (unacetylated Cdc8 is present on For3 nucleated cables) and Cdc12 and acetylated Cdc8 (acetylated Cdc8 is present at the Cdc12 nucleated CAR) it was hypothesized that formins may play a role in this tropomyosin organization. A series of formin fusions which altered the localisation of the formins, whilst also tagging the protein at the C-terminus were generated in order to investigate this.

To investigate the regulation of interphase actin cables, For3 and Cdc12 were fused to the carboxyl terminus of Tea1, a polarity factor that localises to the cell poles. It was anticipated that this would anchor both formins at the cell poles. Both a multi-copy plasmid (*pREP41*) with a C-terminal GFP tag and a construct allowing the integration of the gene with a C-terminal mCherry tag into the *leu1* locus of the *S. pombe* chromosome 1 (*pINT41)* were generated. A cartoon of these constructs is shown in 3.1.

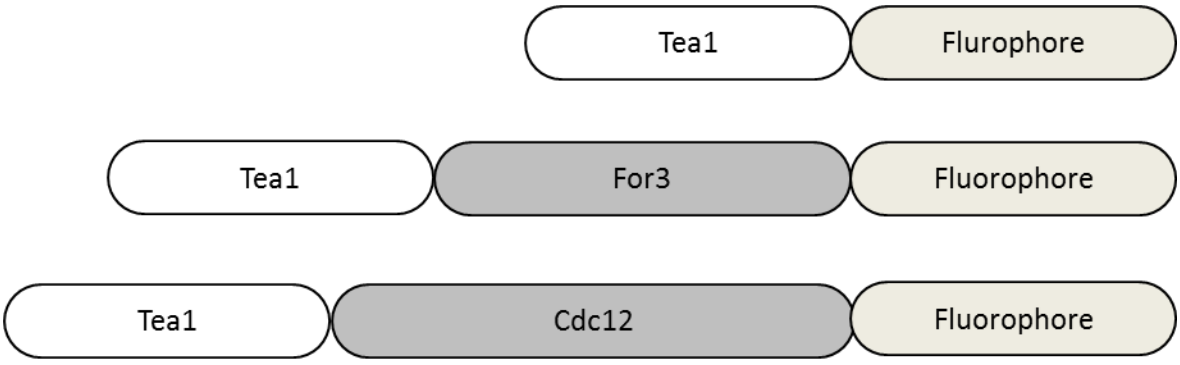

Figure.3.1. A cartoon representing fusion proteins used to localise formins to the cell poles. Tea1 was fused to the N-terminus of the formin, either For3 or Cdc12 with a $(Gly\text{-}Ala)_5$ linker and a fluorophore tag was located at the C-terminus of the fusion protein.

The localisation of these fusion proteins (hereon referred to as Tea1-For3 and Tea1-Cdc12) was investigated in a *for3Δ* strain in order to examine their localisation without the possible interaction with For3. As can be seen in figure 3.2 Tea1-For3 and Tea1-Cdc12 localised to the cell poles when expressed on a multi-copy plasmid, and this result was also seen when the fusion proteins were integrated into the *S. pombe* genome (shown later in figure 3.5). The Tea1-Cdc12 fusion was seen on occasions in large foci towards the centre of the cell, presumably a result of Cdc12 recruiting this fusion to the centre of the cell. The localisation of Tea1, For3 and Cdc12 was also examined, with Cdc12 localising to the CAR and Tea1 localising to the cell poles as expected. It was only possible to see For3 localising to the cell poles when using the integrated For3-mCherry, but was seen at the medial cortex of the cells using both the multi-copy plasmid and integrant version of the construct.

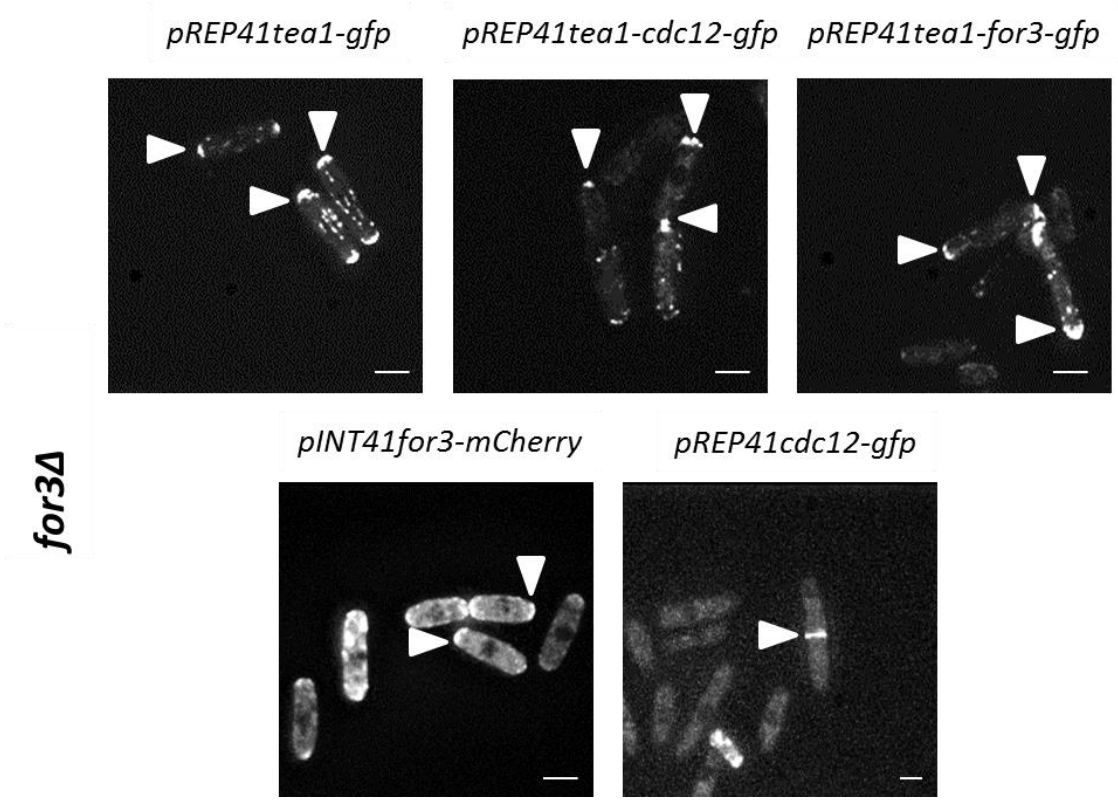

Figure.3.2. Maximum projection images (31 Z slices) of a *for3Δ* strain expressing the fluorescent tagged formin fusion proteins. Tea1-GFP and For3-mCherry localise to the cell poles as expected, Cdc12-GFP localises to the CAR, whilst fusing Tea1 to the N-terminus of both and Cdc12 and For3 results in them localising to the cell poles. Scale bars 5 µm.

The localisation of Tea1-GFP, Tea1-For3-GFP and Tea1-Cdc12-GFP was also examined in Wild-Type, *tea1Δ* and *tea4Δ* strains, with figure 3.3 showing all of the constructs localising to the cell poles in each of these strains, however the localisation of Tea1-For3-GFP and Tea1-Cdc12-GFP was less bipolar in a *tea4Δ* strain (figure 3.3). The localisation of these constructs in each strain is quantified in table 3.1.

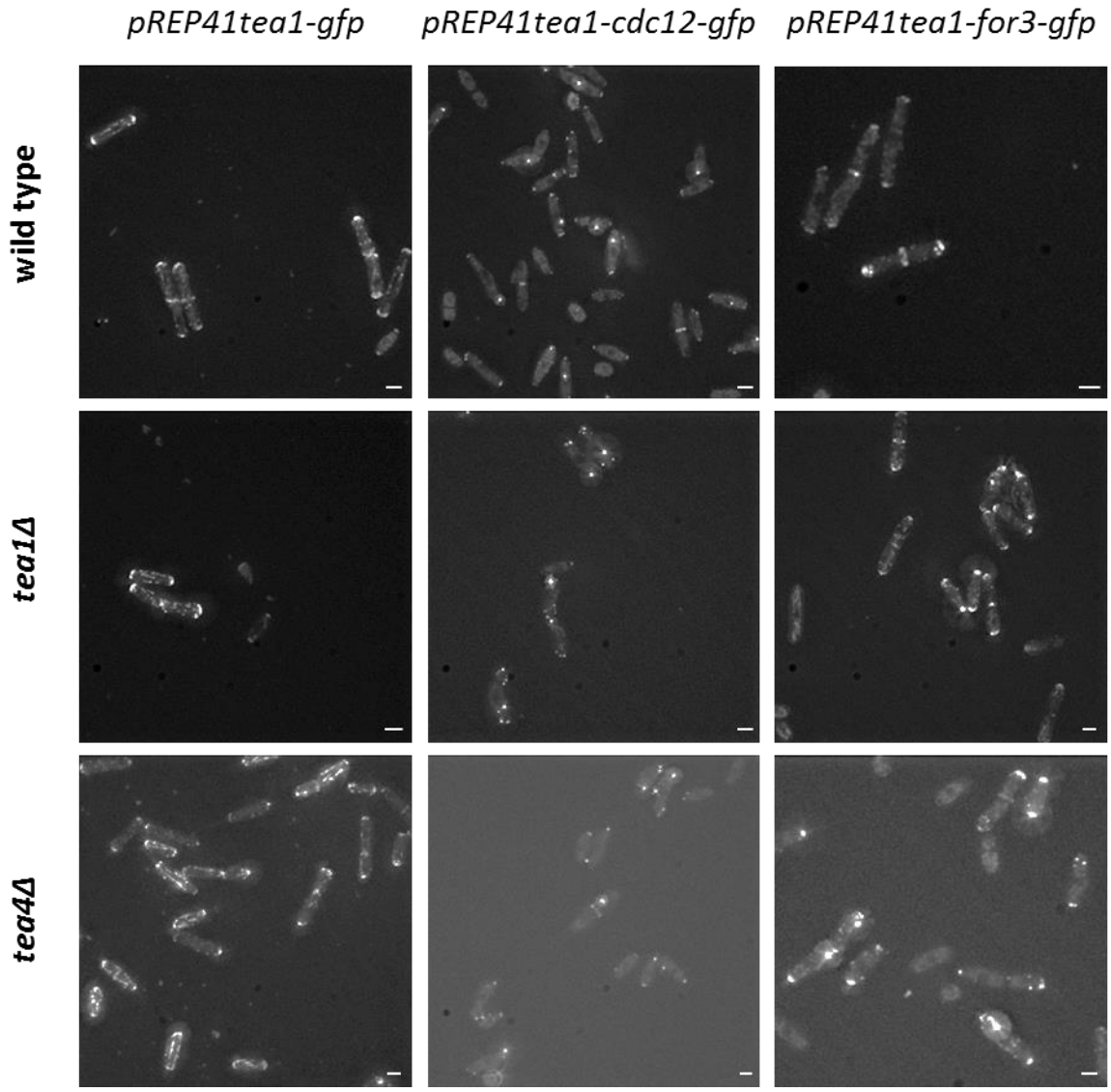

Figure 3.3. Maximum projection images (31 Z slices) of wild-type, *tea1Δ* and *tea4Δ* strains expressing the GFP tagged formin fusion proteins. As seen in a *for3Δ* strain, Tea1--GFP localises to the cell poles as expected, whilst Tea1-Cdc12-GFP and Tea1-For3-GFP also localise the cell poles. Scale bars 5 µm.

A *for3Δ* strain typically exhibits a mild morphological phenotype in which cells are shorter and/or wider, as can be seen in figure 3.2 (Feierbach & Chang 2001). Expression of the Tea1-Cdc12 fusion but not Cdc12 alone resulted in the cells being morphologically more similar to of wild-type cells, suggesting that Cdc12 is able to complement For3 function when localised to the cell poles.

Tea1-GFP		Wild Type	*tea1Δ*	*for3Δ*	*tea4Δ*
(v478)	Concentrated at one cell pole	0 %	0 %	0 %	0 %
	Concentrated at two cell poles	99 %	98.5 %	100 %	99.5 %
	Concentrated to cytoplasmic dot(s)	0 %	0 %	0 %	0 %
	Medial ring	1 %	1.5 %	0 %	0.5 %
	No discrete localisation	0 %	0 %	0 %	0 %
Tea1-For3-GFP	Concentrated at one cell pole	2.5 %	2 %	1 %	28.5 %
(v474)	Concentrated at two cell poles	94.5 %	94.5 %	94 %	71.5 %
	Concentrated at cytoplasmic dot(s)	0 %	1 %	0 %	0 %
	Medial ring	3 %	2.5 %	5 %	0 %
	No discrete localisation	0 %	0 %	0 %	0 %
Tea1-Cdc12-GFP	Concentrated at one cell pole	15 %	26 %	35 %	19 %
(v491)	Concentrated at two cell poles	30.5 %	45 %	50 %	47 %
	Concentrated at cytoplasmic dot(s)	31.5 %	28 %	10 %	28 %
	Medial ring	11 %	11 %	5 %	6 %
	No discrete localisation	12 %	n.d.	n.d.	17 %

Table.3.1. Quantification of the localisation of formin fusion proteins in wild-type, *for3Δ, tea4Δ* and *tea1Δ* cells. n=200 cells.

3.2. Expression of the Formin Fusions Allows Cells to Bypass NETO

As table 3.1 shows, by fusing either For3 or Cdc12 to Tea1, their localisation in wild-type, *for3Δ, tea1Δ and tea4Δ* is largely bipolar at all stages of the cell cycle, although there is a reduction in bipolar localisation in a *tea4Δ* strain. This is unlike the normal localisation of For3, which typically has a monopolar localisation in early G1 phase before becoming bipolar after NETO has occurred. In order to confirm that this bipolar localisation of the formin fusions occurs before NETO takes place, and that growth is occurring at both ends of the cells when these formins have bipolar localisation (in a mechanisms independent of NETO) Tea1-For3-GFP, Tea1-Cdc12-GFP and For3-GFP were expressed in a *for3Δ cdc10-v50 myo52-mCherry* strain in order to arrest the cells before NETO occurs, as the temperature sensitive *cdc10-v50* allele arrests cells in the G1 stage of the cell cycle.

The localisation of the formins was then examined after cells had been arrested at the restrictive temperature for 4 hours. In the case of For3-GFP, due to low levels of signal the localisation of Myo52-mCherry was examined, which only concentrates to cell poles when there is a formin present to nucleate actin cables. Figure 3.4 shows that the localisation of Tea1-For3-GFP was almost completely bipolar, (98%). The localisation of Myo52-mCherry was also seen to mirror that of the Tea1-For3-GFP. The localisation of Tea1-Cdc12-GFP was more varied, with 35% of cells exhibiting monopolar localisation, 41% of cells exhibiting bipolar localisation and 24% of cells exhibiting localisation at a single bright dot in the centre of the cell, presumably as a result of Cdc12 dragging Tea1 to the centre of the cell.

It was again seen that Myo52-mCherry localisation corresponded with that of Tea1-Cdc12-GFP. Despite the localisation of Tea1-Cdc12-GFP not being completely bipolar as is the case with Tea1-For3-GFP, it was in contrast to the localisation of Myo52-mCherry (and presumably For3-GFP) in the strain expressing For3-GFP, in which the majority of the cells (58%) exhibited monopolar localisation whilst 42% exhibited bipolar localisation. It was expected that in this strain the localisation of Myo52-mCherry (and For3-GFP) would be completely monopolar, however when repeated on multiple occasions the same mixture of monopolar and bipolar localisation was observed. Possible explanations for this finding are discussed later (see chapter 6).

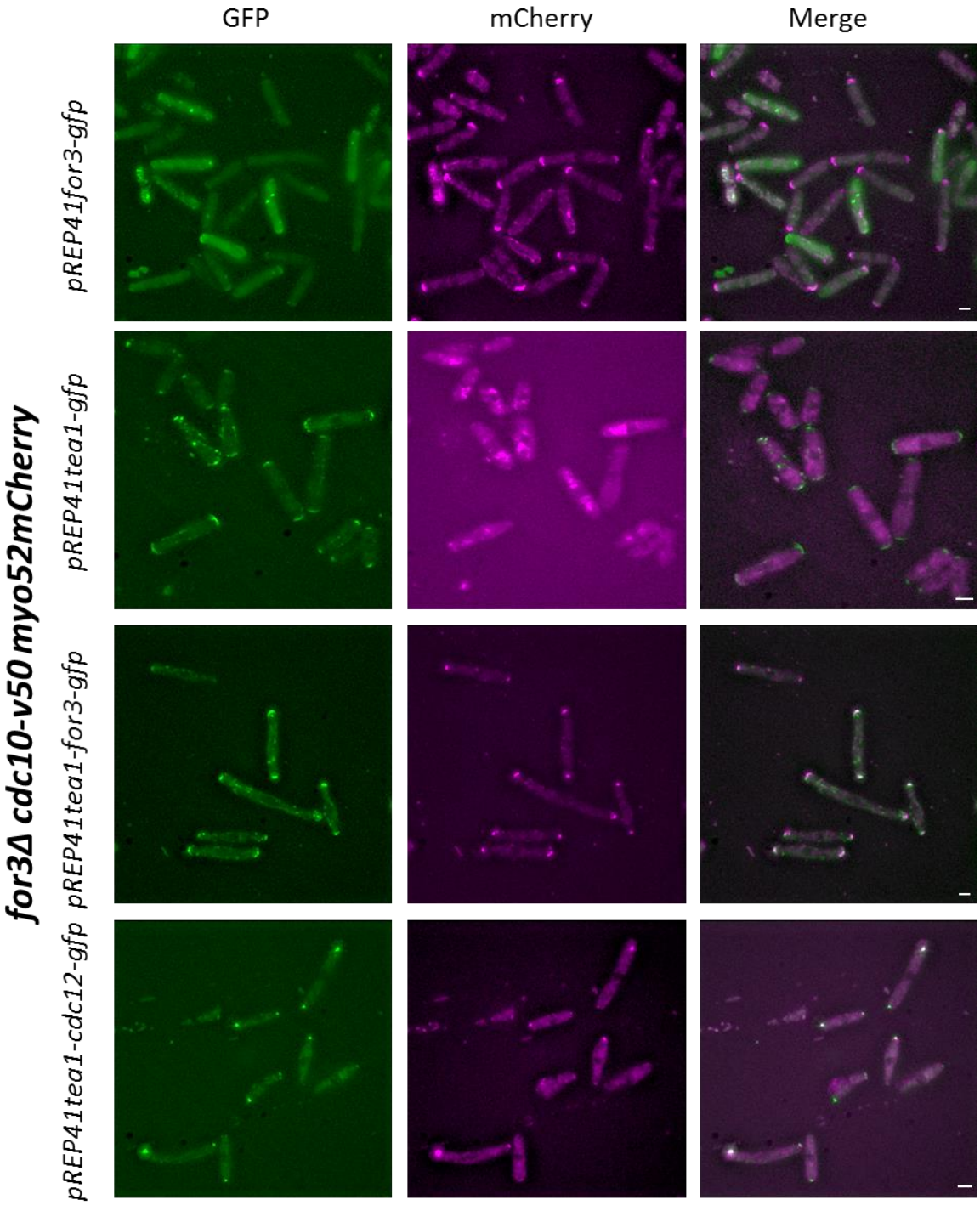

Figure.3.4. *for3Δ cdc10-v50 myo52-mCherry* cells expressing Tea1-GFP, For3-GFP, Tea1-Cdc12-GFP and Tea1-For3-GFP were incubated at 36 °C for 4 hours and the localisation of the formin proteins was then observed. Both Tea1-GFP and Tea1-For3-GFP had almost completely bi-polar localisation, whilst Tea1-Cdc12-GFP and For3-GFP had a mix of monopolar and bipolar localisation. The localisation of Myo52-mCherry is also shown, and in the case of For3-GFP was used to count For3 localisation due to the low levels of For3-GFP. Images are a maximum projection of 31 Z slices. Scale bars 5 µm.

Having seen that the fusion of formins to Tea1 allowed cells to bypass NETO and maintain bipolar growth at all times, the effect of this on cell growth rate and cell length was examined. As can be seen in figure 3.5, *for3Δ* cells expressing Tea1-For3-GFP exhibited a quicker growth rate than cells expressing Tea1-Cdc12-GFP or For3-GFP, which had very similar growth rates. These findings correspond with a difference in cell length, with cells expressing Tea1-For3-GFP having a longer average cell length than cells expressing For3-GFP or Tea1-Cdc12-GFP,both of which had very similar average lengths (table 3.2).

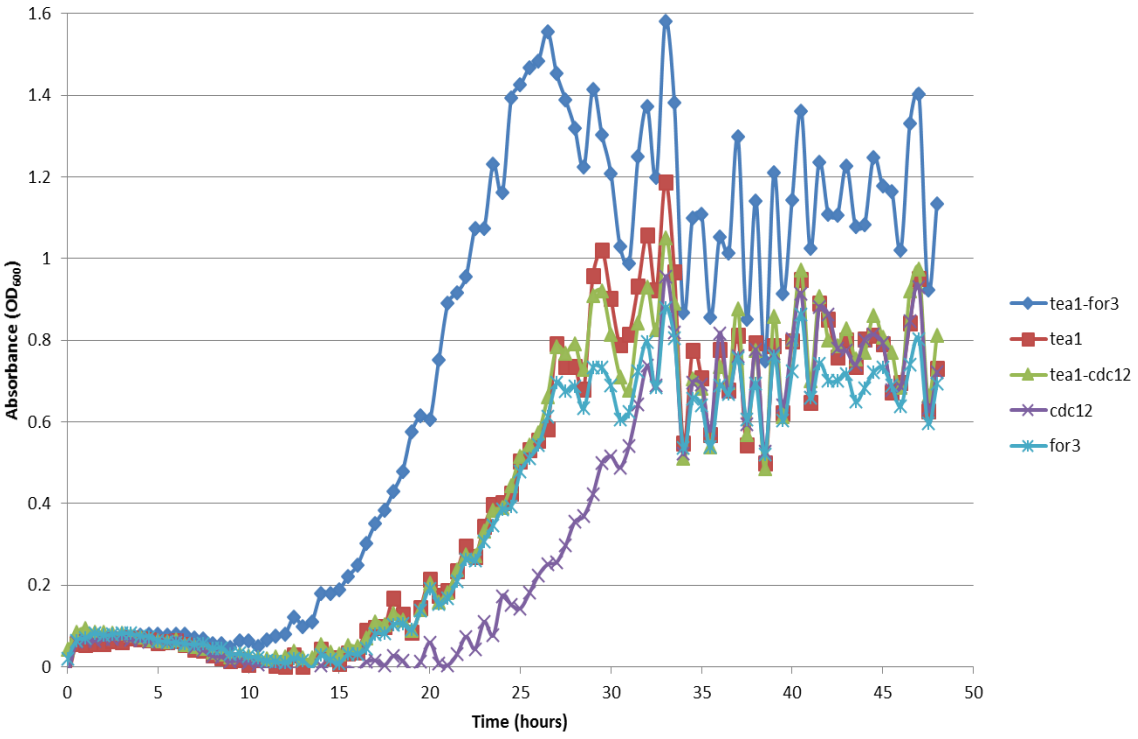

Figure 3.5. Growth curve of *for3Δ* cells expressing formin proteins at 25 °C. Expression of Cdc12-GFP alone lead to slower growth, whilst expression of Tea1-GFP, For3-GFP and Tea1-Cdc12-GFP all grew at similar rates. Expression of Tea1-For3-GFP resulted in a faster rate of growth and the cells also reached a higher optical density.

Strain	Average Cell length (µm)	Standard Deviation
for3Δ	11.87	2.21
for3Δ + pREP41for3-gfp	13.6	2.73
for3Δ + pREP41tea1-gfp	13.9	2.75
for3Δ + pREP41tea1-for3-gfp	15.41	3.02
for3Δ + pREP41tea1-cdc12-gfp	14.08	2.85

Table.3.2. Average cell lengths of *for3Δ* cells expressing different formin proteins. Cells expressing For3-GFP, Tea1-GFP and Tea1-Cdc12-GFP all had very similar lengths, comparable to that of wild type cells whilst expression of Tea1-For3-GFP resulted in a slight elongation of the cells. n=200 cells.

3.3. Formin Fusions Are Able to Nucleate Interphase Actin Cables with Distinct Physical Properties

After observing that both Tea1-For3 and Tea1-Cdc12 localise to the cell polls, the function of these formin fusions was investigated by looking for the presence of actin cables in *for3Δ* cells. *for3Δ* cells do not possess any interphase actin cables, with only actin patches and the CAR present (Feierbach & Chang 2001). In order to investigate whether the Tea1-For3 and Tea1-Cdc12 were able to nucleate actin cables, a GFP fused calponin homology domain (GFP-CHD) (Karagiannis & Bimbó 2005) of the fission yeast protein Rng2, which binds to all actin structures within the cell, was used in conjunction with a *for3Δ* strain. As can be seen in figure 3.6 interphase actin cables were present in *for3Δ gfp-CHD* cells expressing Tea1-For3-mCherry, Tea1-Cdc12-mCherry and For3-mCherry. To show that the presence of actin cables in the strain expressing Tea1-Cdc12-mCherry was as a result of Cdc12 being localised to the cell poles, a *for3Δ gfp-CHD* strain expressing Cdc12-mCherry was examined, in which no actin cables were seen, thus showing that switching the localisation of Cdc12 to the cell poles enables it to nucleate interphase actin cables. In order to ensure that the presence of these cables was not due to the Tea1-Cdc12 dimerising with endogenous Cdc12, the experiment was repeated in the presence of the *cdc12-112* temperature sensitive allele at the restrictive temperature, in which cables were again observed when expressing Tea1-Cdc12 (not shown).

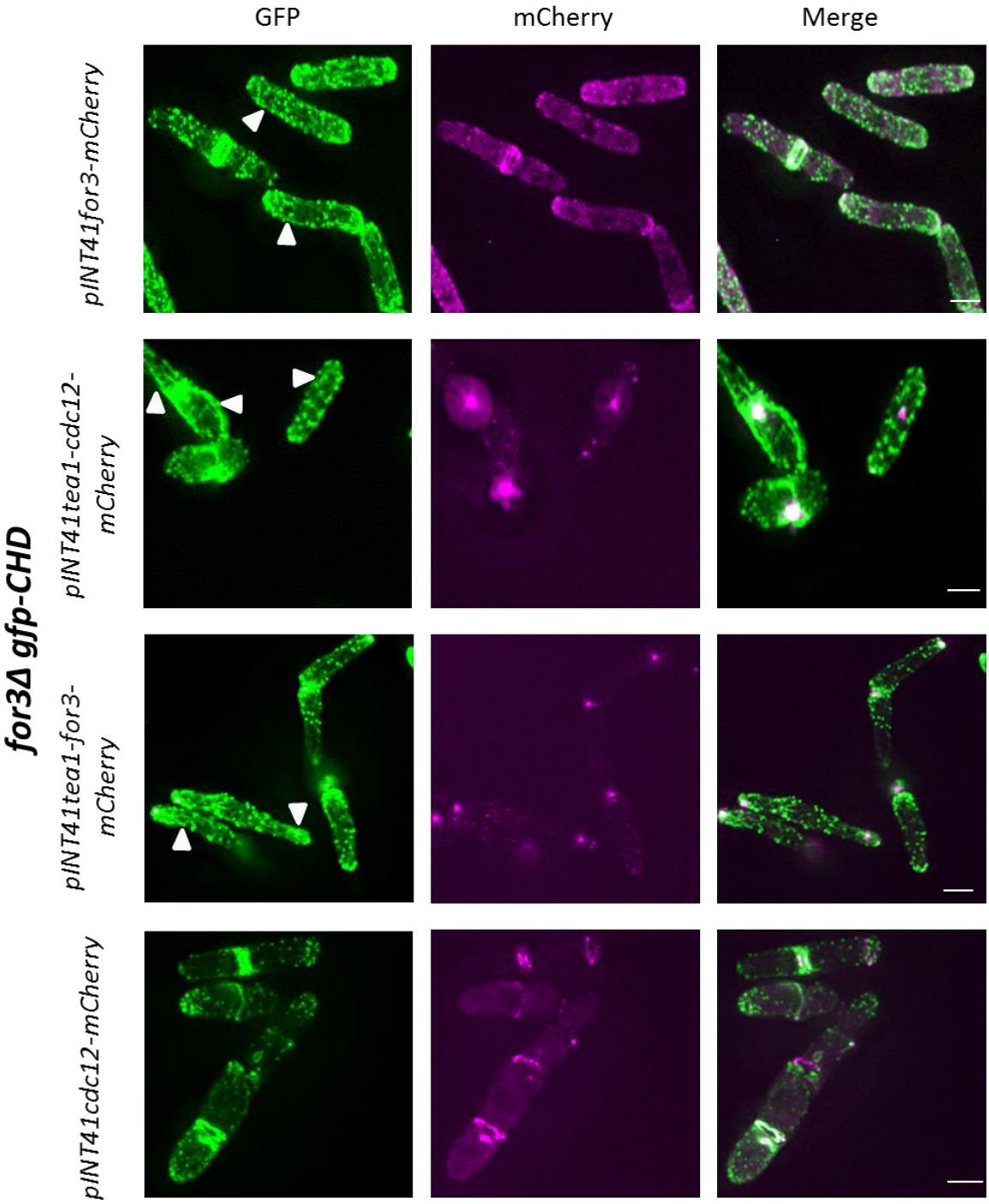

Figure.3.6. Maximum projection images (31 Z slices) of *for3 gfp-CHD* cells expressing mCherry tagged formin proteins. GFP-CHD is shown in green and formin proteins are shown in magenta. As expected expression of For3-mCherry results in a restoration of actin cables, (shown here by GFP-CHD), whilst expression of Cdc12-mCherry failed to restore the presence of actin cables. Expression of both formin fusions, Tea1-For3-mCherry and Tea1-Cdc12-mCherry resulted in nucleation of actin cables. Scale bars 5 µm.

Having seen that Tea1-Cdc12 was able to complement For3's function and nucleate interphase actin cables, the properties of these actin cables was investigated. The growth and shrinkage rates of actin cables as well as the average GFP signal intensity were measured in *for3Δ gfp-CHD* cells expressing Tea1-Cdc12-mCherry and For3-mCherry. They were also measured in wild type cells expressing GFP-CHD. As can be seen in table 3.4, the growth rate of actin cables was quicker when nucleated by Tea1-Cdc12 than by For3 (either in wildtype cells or *for3Δ* cells expressing For3-mCherry), increasing from 0.57-0.59 $\mu msec^{-1}$ to 0.79 $\mu msec^{-1}$. In contrast, the shrinkage rate of actin cables remained approximately the same, in the region of 0.8 $\mu msec^{-1}$, whether the cables were nucleated by Tea1-Cdc12 or For3. Finally, GFP-CHD intensity of actin cables was lower when cables were nucleated by Tea1-Cdc12 than by For3, with the intensity falling from 141 AU/μm^2 to 107 AU/μm^2.

Strain	***for3⁺ gfp-CHD***	***for3Δ INT41for3-mCherry gfp-CHD***	***for3Δ INT41tea1-cdc12-mCherry gfp-CHD***
Filament Growth ($\mu msec^{-1}$)	0.57 ± 0.09	0.59 ± 0.10	0.79 ± 0.13
Filament Shrinkage ($\mu msec^{-1}$)	0.77 ± 0.10	0.79 ± 0.17	0.83 ± 0.14
Filament Intensity (AU/μm^2)	-	141	107

Table 3.4. The dynamic properties of interphase actin cables nucleated by different formins. The filament growth and shrinkage rates and filament intensity were measured in wild type cells and cells expressing either For3-mCherry or Tea1-Cdc12-mCherry. Cables nucleated by Tea1-Cdc12-mCherry had a higher growth rate and a lower intensity than those nucleated by endogenous For3 or For3-mCherry. n=15 cables from upto 10 cells. Experiments were all carried out on the same day.

3.4 Formins determine which tropomyosin population is recruited to interphase actin filaments.

As Tea1-Cdc12 is able to nucleate actin cables, and that they have distinct physical properties from cables nucleated by For3, it was hypothesized that the composition of these actin cables could be different, specifically which population of Tm was on these cables. It has previously been shown that different the single *S.pombe* Tm Cdc8 is present in acetylated and unacetylated forms, and these forms associate with specific actin structures each nucleated by a different formin (Coulton & East 2010). Immunofluorescence experiments were carried out on cells expressing either Tea1-GFP, Tea1-For3-GFP or Tea1-Cdc12-GFP. The ability of Tea1-For3 and Tea1-Cdc12 to nucleate actin cables with Tm bound was confirmed by use of an anti-Tm antibody. As can be seen in figure 3.6 actin cables decorated with Tm were observed in *for3Δ* cells expressing either Tea1-For3-GFP or Tea1-Cdc12-GFP, whilst no Tm cables were seen when Tea1-GFP alone was expressed. In order to determine which population of Tm was on these cables, acetylation specific anti-Tm antibodies were used. When expressing Tea1-For3 actin cables were decorated with unacetylated Tm, as is the case with wild-type cells (Coulton & East 2010) whilst acetylated Tm is only seen at the CAR. In contrast, as figure 3.7 shows when expressing Tea1-Cdc12 acetylated Tm is seen recruited to both the CAR and actin cables, thus providing evidence that formins specify which population of Tm is recruited to actin cables within the cell.

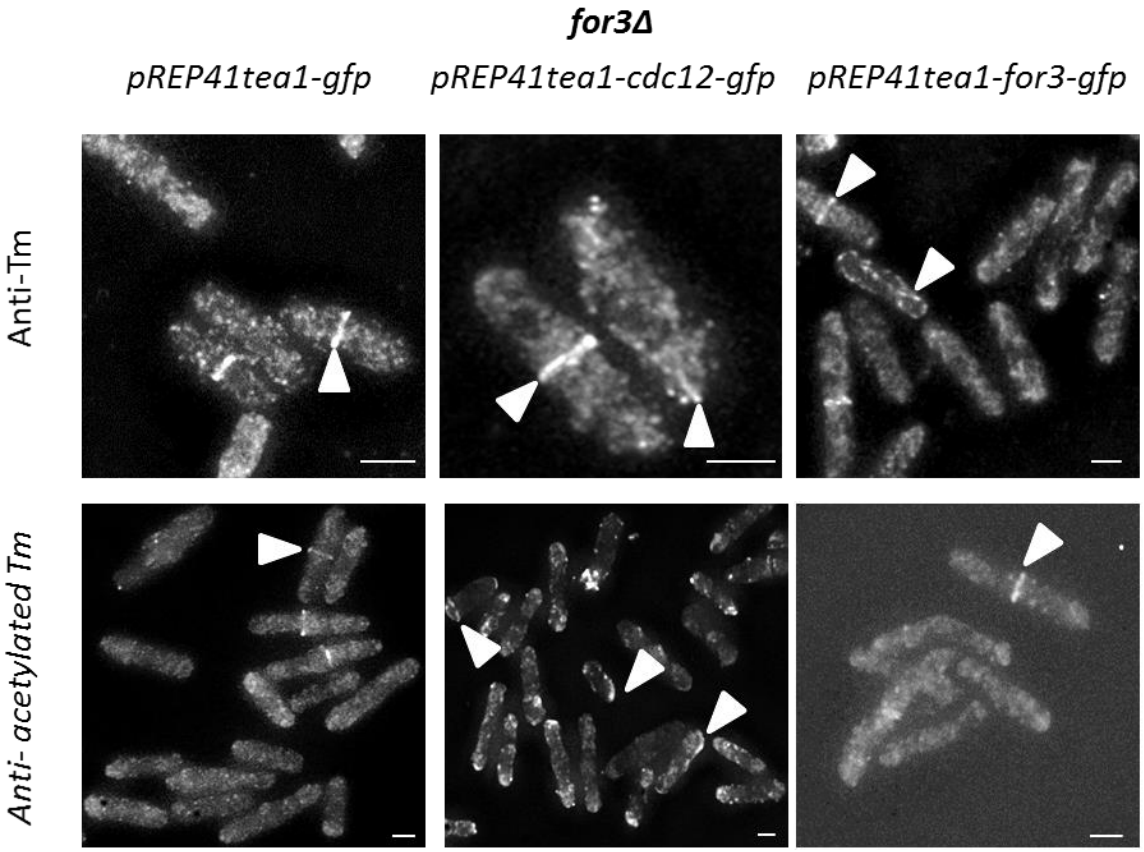

Figure 3.7. Immunofluorescence images of *for3Δ* cells expressing either Tea1-GFP, Tea1-Cdc12-GFP or Tea1-For3-GFP. Cells were probed with an antibody that binds to all Tm in the cell (upper row) or an acetylation specific antibody that only binds to acetylated Tm (lower row). Expression of either formin fusion resulted in the presence of actin filaments with Tm bound to them however acetylated Tm was only seen on interphase actin cables nucleated by Tea1-Cdc12. Scale bars 5 µm.

3.5 Formins Also Regulate the Interaction of Other Actin Binding Proteins with Actin

It has been shown that formins regulate the population of Tm that is recruited to actin cables, and the effect that this switch in Tm composition of the actin cable has on the recruitment of other ABP's to the actin cable was subsequently investigated. As has already been shown in figure 3.4 the type V myosin, Myo52 accumulates at cell poles and moves along actin cables when either For3 or Cdc12 is nucleating actin cables at the cell poles. However in *for3Δ cdc10-v50 myo52-mCherry* cells expressing only Tea1-GFP, Myo52-mCherry has no distinct localisation with signal dispersed throughout the cytoplasm. The speed of Myo52 movement was affected depending on which formin had nucleated the actin cables, with Myo52-mCherry moving along Tea1-Cdc12-GFP nucleated cables at 75% of the velocity of Myo52-mCherry movement along Tea1-For3 nucleated cables. Thus whilst Myo52 is able to move along actin cables containing either acetylated or unacetylated Tm, the regulation of this movement is affected.

Strain	Myo52 velocity (µm/sec)
myo52-tdTomato	0.56 ± 0.05
for3Δ myo52-tdTomato + pREP41tea1-for3-gfp	0.59 ± 0.05
for3Δ myo52-tdTomato + pREP41tea1-for3-gfp	0.44 ± 0.01

Table 3.5. Mean velcocities of Myo52-tdTomato in wild type cells and *for3Δ* cells expressing Tea1-For3-GFP or Tea1-Cdc12-GFP.

The localisation of 2 other ABP's, Adf1 (Cofilin) and Rng2 (IQGAP) was also investigated. Nucleation of actin cables by either formin had no effect on the localisation of Adf1-GFP, as shown in figure 3.8. However the localisation of Rng2 was disrupted, with an altered

localisation observed when cables were nucleated by Tea1-Cdc12-GFP. In wild type cells Rng2 localises exclusively to the CAR during mitosis (figure 3.8), however when Rng2-YFP localisation was observed in *for3Δ* cells expressing Tea1-Cdc12-GFP, Rng2 appeared to co-localise with Tea1-Cdc12-GFP foci at the cell poles (figure 3.8).

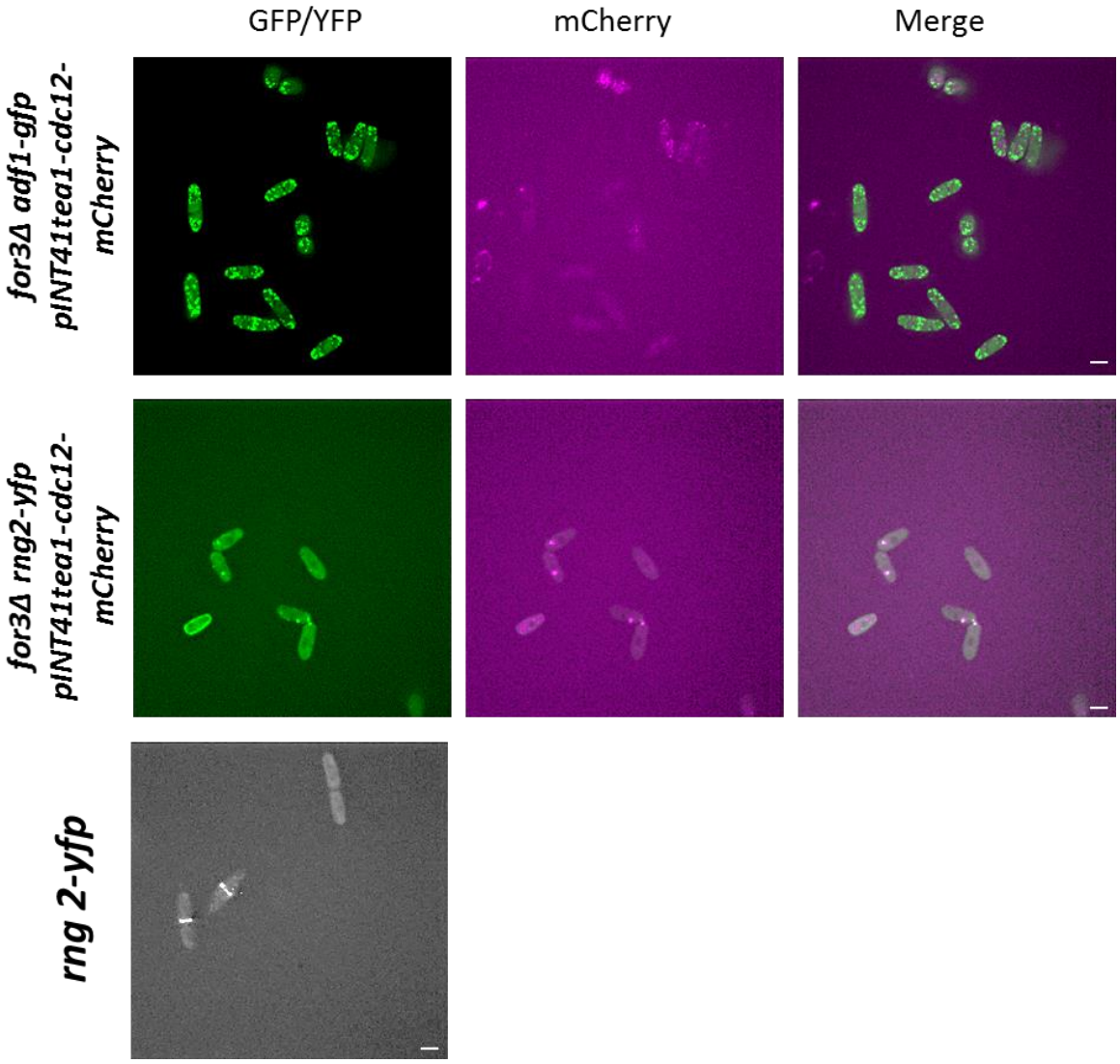

Figure 3.8. Maximum projection images (31 Z slices) of *for3Δ* cells expressing Tea1-Cdc12-mCherry and either Rng2YFP or Adf1-GFP and a Rng2-YFP strain alone. Tea1-Cdc12-mCherry is shown in magenta and Adf1-GFP or Rng2-YFP is shown in green. Expression of Tea1-Cdc12-mCherry results in the localisation of Rng2YFP being affected, with foci seen at the cell poles colocalising with Tea1-Cdc12-mCherry. Usually Rng2-YFP is only seen at the contractile ring of dividing cells. Scale bars 5 µm.

3.6 Fusion of Formins to a Portion of the Myo2 Tail Recruits Them to the CAR

After observing that Cdc12 was able to complement For3 interphase function, and alter the Tm composition of actin cables when localised to the poles of the cell, the function of formins in nucleating actin rings at the CAR was investigated. It has previously been shown that amino acid residues 1228-1526 in the carboxyl terminal of the tail region of the class II myosin, Myo2 (Myo2T) localise to the CAR (Mulvihill, Barretto & Hyams 2001). Therefore, similar to the Tea1 fusions previously described, fusions were generated in which For3 and Cdc12 were fused to the carboxyl terminus of the Myo2T in order to localise them to the CAR. These were again generated in both a multi-copy plasmid (*pREP41*) with a C-terminal -GFP tag and a construct allowing the integration of the gene with a C-terminal mCherry tag into the *leu1* locus of the *S. pombe* chromosome 1 (*pINT41*). These constructs are shown in figure 3.9 below.

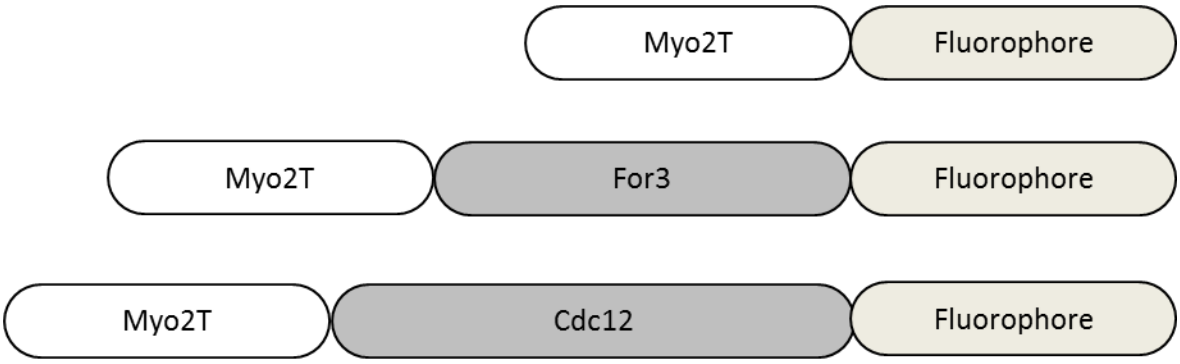

Figure 3.9. A cartoon representing fusion proteins used to localise formins to the contractile ring. The C-terminal half of the Myo2 tail (Myo2T) was fused to the N-terminus of the formin, either For3 or Cdc12 with a $(Gly\text{-}Ala)_5$ linker and a GFP tag was located at the C-terminus of the fusion protein.

The localisation of these constructs was examined in a temperature sensitive *cdc12-112* strain also expressing myo2-mCherry as a CAR marker, first at the permissive temperature. As can be seen in figure 3.10, Myo2T-GFP, Myo2T-For3-GFP, Myo2T-Cdc12-GFP and Cdc12-GFP all localised to the CAR of dividing cells, as shown by their co-localisation with Myo2-mCherry.

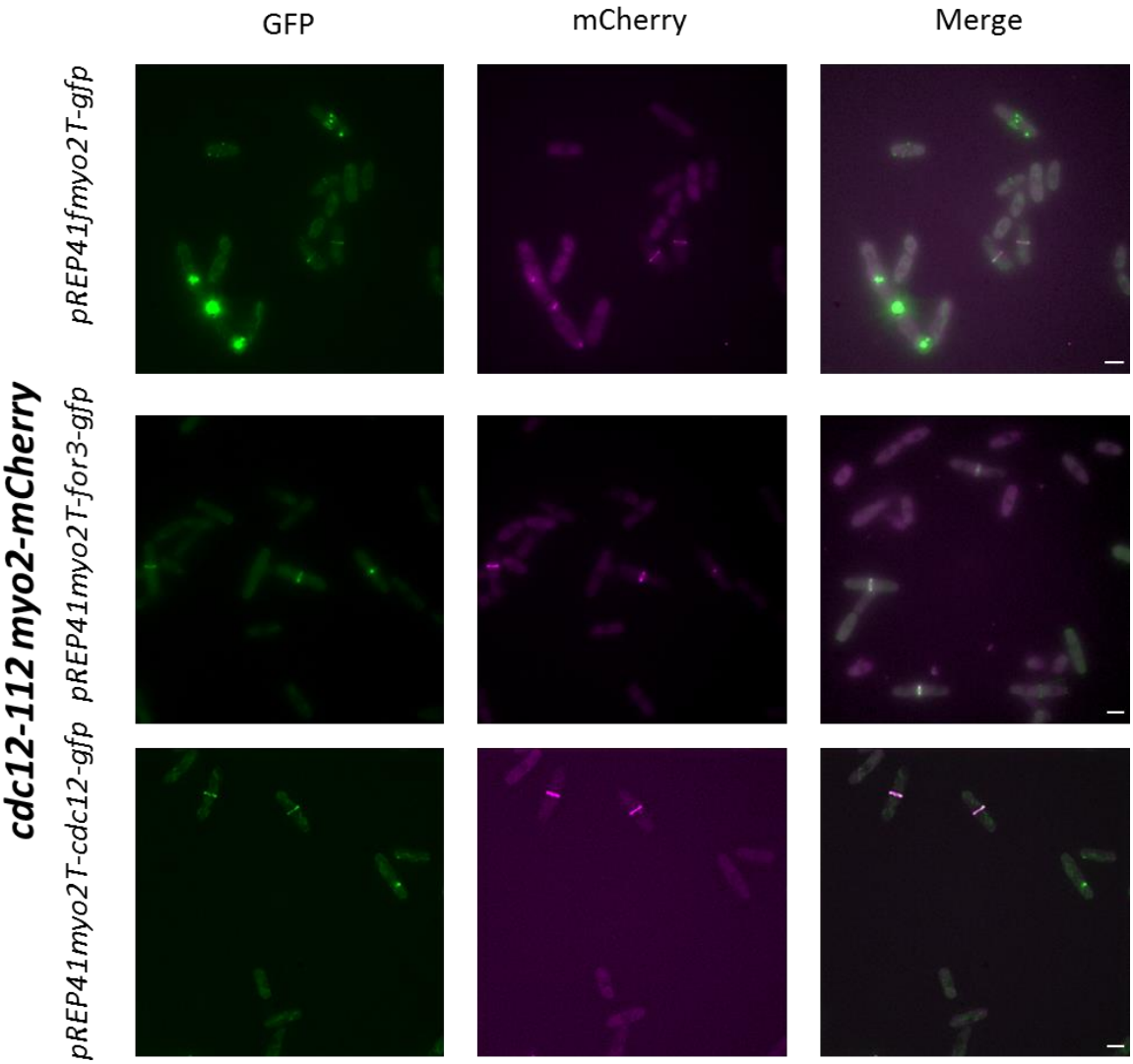

Figure 3.10. *cdc12-112 myo2-mCherry* cells expressing Myo2T-GFP, Myo2T-For3-GFP, Myo2T-Cdc12-GFP or Cdc12-GFP were grown at 25 °C and localisation of the formin fusions was examined. Myo2T-GFP, Myo2T-For3-GFP, Myo2T-Cdc12-GFP all localised to the centre of the cell and co-localised with Myo2-mCherry. Scale bars 5 µm.

3.7. Myo2T-For3 is Able to Complement Cdc12 Function

As the fusion of formins to the Myo2T was sufficient to localise them to the CAR, next the ability of a Myo2T-For3-GFP fusion to complement Cdc12 function was investigated. *cdc12-112 myo2-mCherry* cells expressing Myo2T-GFP, Myo2T-For3-GFP, Myo2T-Cdc12-GFP, Tea1-Cdc12-GFP and Cdc12-GFP were incubated at the restrictive temperature (36 °C) for 4 hours and then examined by live cell imaging whilst continuing to incubate the cells at 36 °C. Figure 3.11 shows that the strains expressing Myo2T-GFP alone showed no formation of contractile rings, with disorganised actin structures observed at the centre of the cell. Cdc12-GFP was able to fully rescue the *cdc12-112* phenotype, with many cells observed with fully formed CARs. In a small number of cells expressing Myo2T-For3 what appeared to be normally formed contractile rings were observed. Many other cells exhibited rings that appeared to either be forming incorrectly or forming and then falling apart, similar to the phenotype observed in a *naa25Δ* strain which lacks acetylated Tm (Skoumpla et al. 2007). When a contractile ring had formed correctly, constriction of the ring was observed, however the rate of constriction was lower than that observed in wild-type cells. Surprisingly Myo2T-Cdc12-GFP only resulted in partial rescue of the *cdc12-112* phenotype. Some cells contained what appeared to be fully formed contractile rings, whilst others had wispy actin structures at the centre of the cell (as shown by arrows in Figure 3.11).

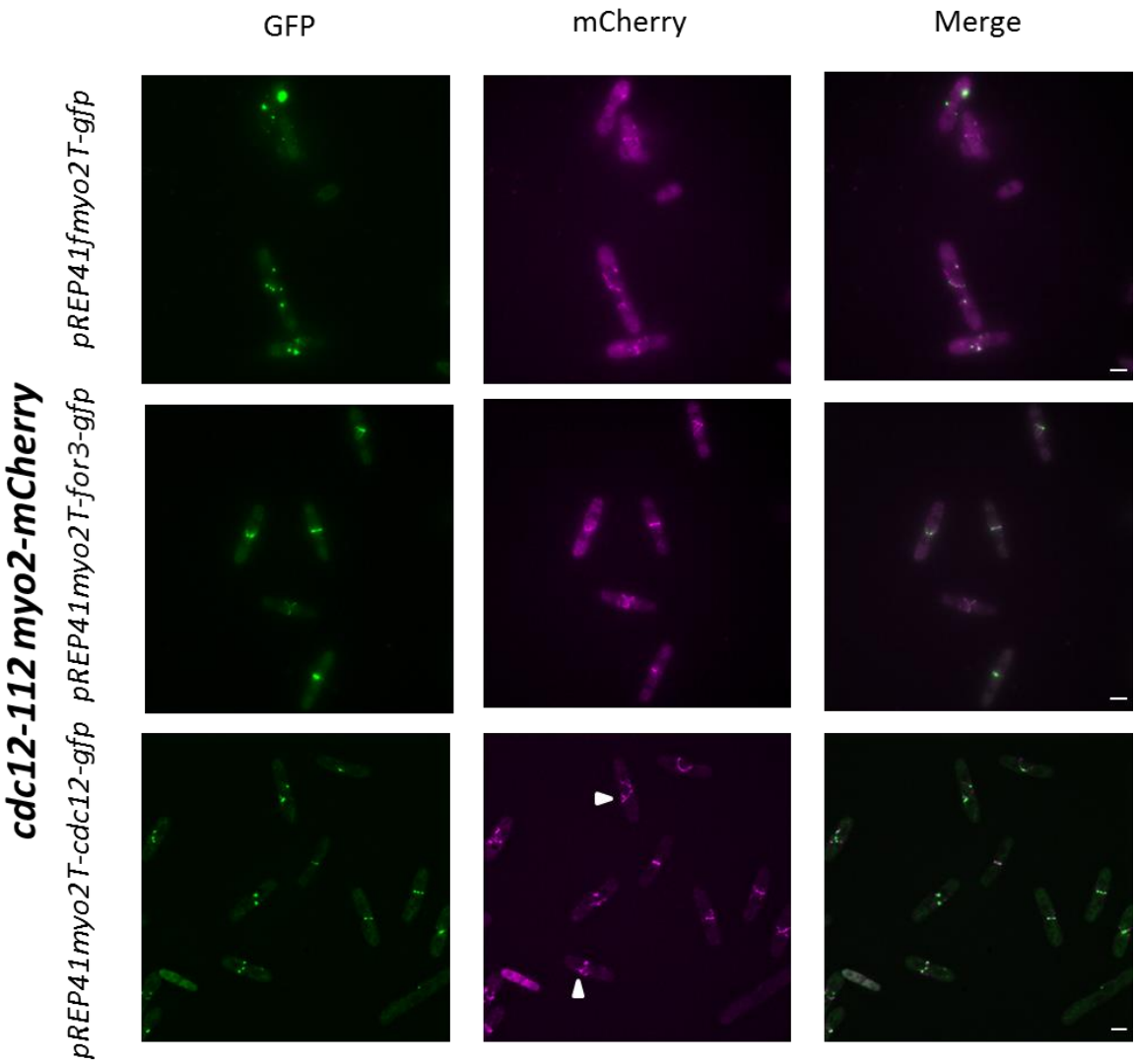

Figure 3.11. *cdc12-112myo2-mCherry* cells expressing Myo2T-GFP, Myo2T-For3-GFP, Myo2T-Cdc12-GFP or Cdc12-GFP were arrested at 36 °C for 4 hours and the localisation of the formins and the formation of Myo2-mCherry rings was examined. Cells expressing only Myo2T-GFP formed no rings, whilst Myo2T-For3-GFP and Myo2T-Cdc12-GFP partially rescued the *cdc12-112* mutation with some cells able to form contractile rings. Scale bars 5 µm.

To investigate the extent to which Myo2T-For3-GFP was able to rescue a *cdc12-112* mutant a growth curve was generated at the restrictive temperature with *cdc12-112* cells containing different formin constructs. As can be seen in figure 3.12 expression of Cdc12-GFP resulted in full rescue of the *cdc12-112,* whereas Myo2T-For3 only appeared to allow the cells to go through a small number of generations before the curve plateaus. Nevertheless, Myo2T-For3-GFP was able to rescue the *cdc12-112* mutant to a greater

degree than Myo2T-GFP alone, indicating that some functional CARs were formed when expressing Myo2T-For3-GFP.

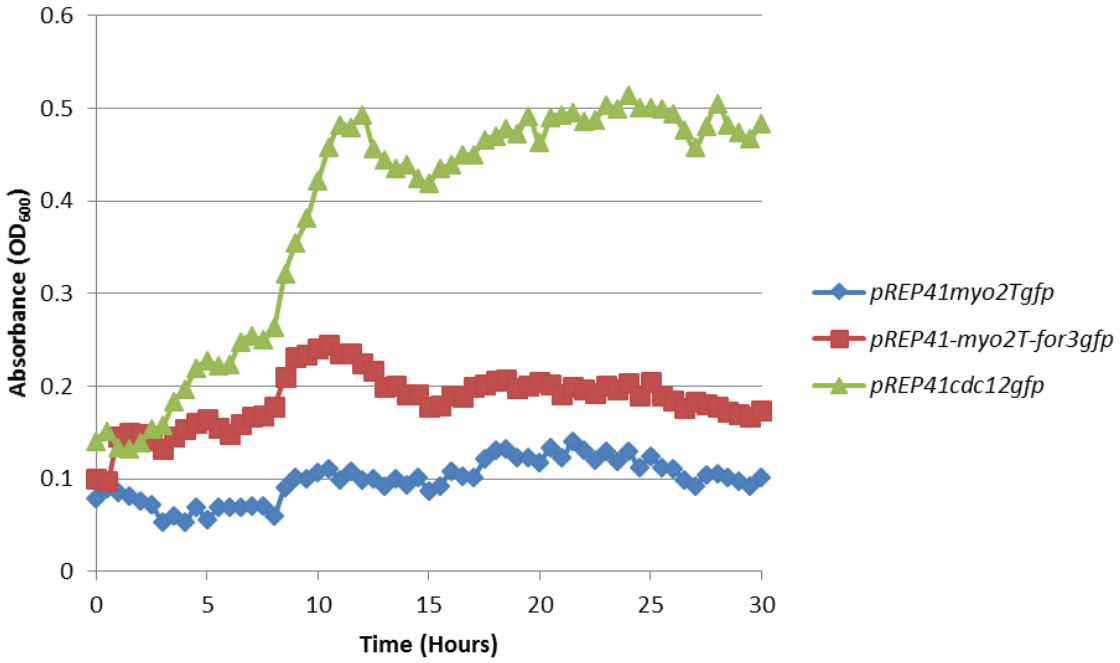

Figure.3.12. Growth curve of *cdc12-112myo2-mCherry* cells expressing formin proteins at 36 °C. Expression of Cdc12-GFP alone lead to a full rescue of the cdc12-112 growth defect, whilst expression of Myo2T-GFP resulted in no growth of the cells. Expression of Myo2T-For3-GFP lead to a partial rescue of the *cdc12-112* mutant, with the cells appearing to divide a small number of times before the curve plateaus.

As Myo2T-For3-GFP was able to partially rescue the temperature sensitive *cdc12-112* mutant, its ability to rescue the lethal *cdc12Δ* was investigated, however only Cdc12-GFP was able to rescue the *cdc12Δ.*

3.8. Formins Determine Which Form of Tropomyosin is Recruited to the CAR

Having seen that For3 is able to partially complement Cdc12 function when recruited to the CAR, and as Cdc12 can partially complement For3 function when localised to the cell poles, it was hypothesised that Tm composition of the CAR is regulated by formins in a similar manner. *cdc12-112 mts3-1* cells expressing either Cdc12-GFP or Myo2T-For3-GFP were arrested at the restrictive temperature for 4 hours before being fixed. Mts3 is a component of the 26S proteasome and a temperature sensitive mutant arrests the cells at the metaphase-anaphase transition, therefore the *mts3-1* temperature sensitive allele was combined with the *cdc12-112* to try increase the number of cells with CARs. First the presence of Tm on CARs was confirmed by anti-Tm immunofluorescence, with a small number of CARs observed when expressing Myo2T-For3-GFP and multiple CARs observed when expressing Cdc12-GFP (figure 3.13). The Tm composition of actin polymers within these CARs was determined by immunofluorescence using acetylation state specific anti-Tm antibodies as shown previously in figure 3.6. As can be seen in figure 3.13 when expressing Cdc12-GFP, only acetylated Tm is observed on the CAR, with unacetylated Tm found on interphase actin cables as is seen in wild type cells (Coulton & East 2010). However when cells express Myo2T-For3-GFP, unacetylated Tm associates with the CAR, a phenomenon which is never observed in either wild-type or *cdc12-112* cells expressing Cdc12-GFP (Figure 3.13). Consistent with this finding which suggests that For3 recruits only unacetylated Tm to actin structures, acetylated Tm was not seen associating with any CARs in *cdc12-112* cells expressing Myo2T-For3-GFP (Figure 3.13).

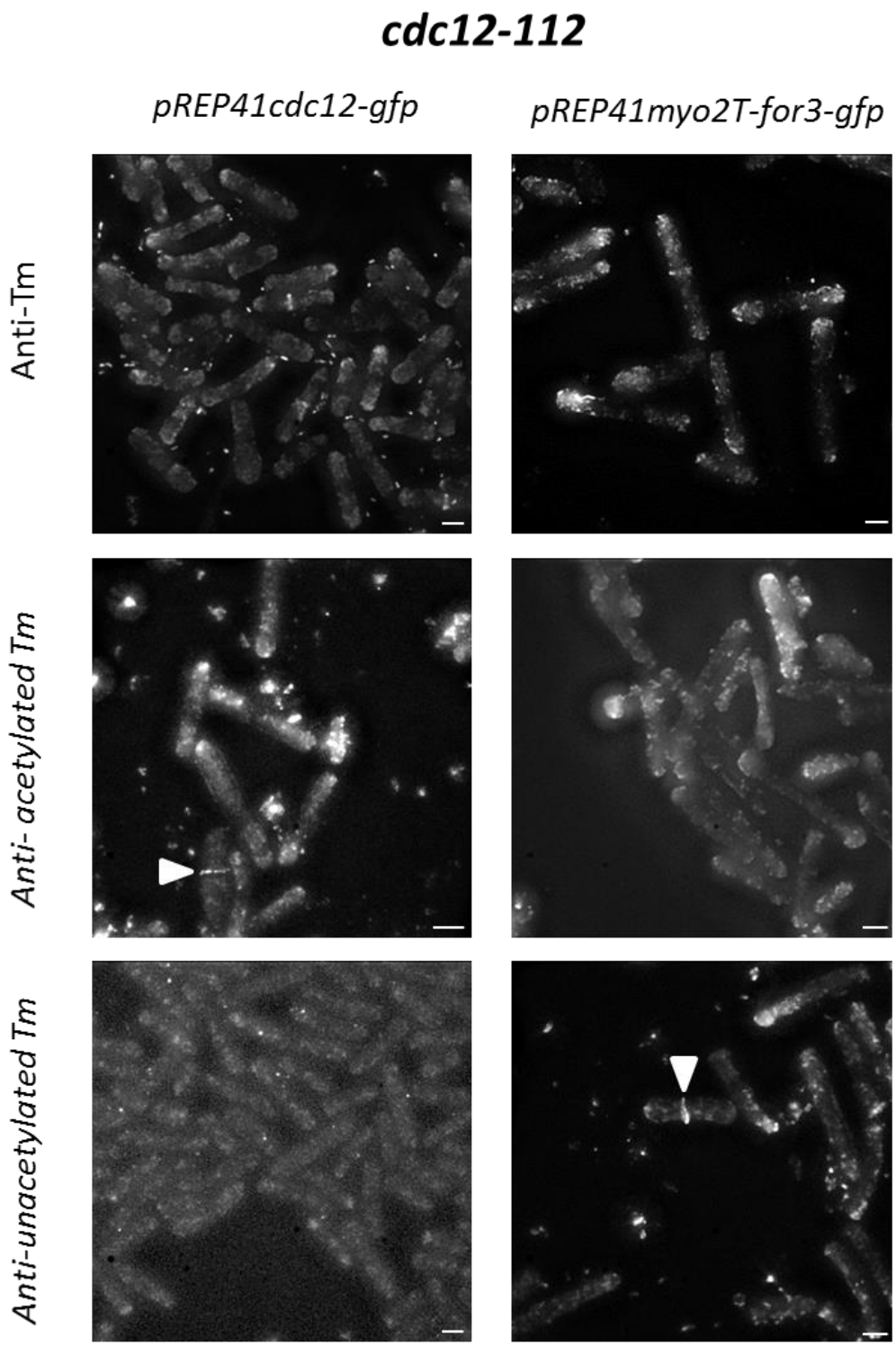

Figure.3.13. Immunofluorescence images of *cdc12-112 mts3-1* cells expressing either Cdc12-GFP of Myo2T-For3-GFP. Cells were probed with an antibody that binds to all Tm in the cell (upper row) or acetylation specific antibodies that only binds to acetylated Tm (middle row) or unacetylated Tm (lower row). Expression of Cdc12-GFP resulted in CARs containing only acetylated Tm being observed, whilst expression of Myo2T-For3-GFP resulted in CARs incorporating unacetylated Tm being seen. Scale bars 5 µm.

3.9. For3 is Functional at Any Location Within the Cell

Having seen that formin function is not restricted to a specific cellular location and that formins are responsible for recruiting different populations of tropomyosin to different actin structures within the cell, an additional experiment was carried out to determine if For3 could function if recruited to any location around the cell membrane and what effect this has on interphase actin cable formation. A construct allowing the integration of a Psy1-For3 fusion into the *leu1* locus of the *S. pombe* chromosome 1 was generated. Psy1 is a protein that localises to the cell membrane of cells in the vegetative growth cycle and in an attempt to recruit For3 to any location around the cell membrane, For3 was fused to Psy1 in the hope it would be recruited by Psy1 to the cell membrane. This construct was expressed in *for3ΔCHD-gfp* cells and as can be seen in figure 3.14, the expression of this Psy1-For3 fusion leads to increased nucleation of actin filaments from multiple points within the cell.

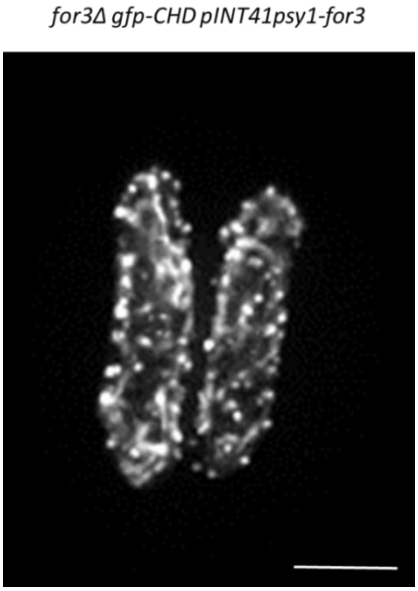

Figure 3.14. Maximum projection image (31 Z slices) of *for3Δ gfp-CHD* cells expressing the Psy1-For3 fusion. As can be seen expression of For3 around the entire cell membrane leads to an increase in the number of interphase actin cables, which are nucleated not only from the cell poles present in the cell. Scale bars 5 µm.

Following this the localisation of Myo52 and Tip1, components of the actin and microtubule cytoskeletons respectively was examined, however expression of Psy1-For3 had no observable effect on their localisation to the actin and microtubule cytoskeletons, as shown in figure 3.15.

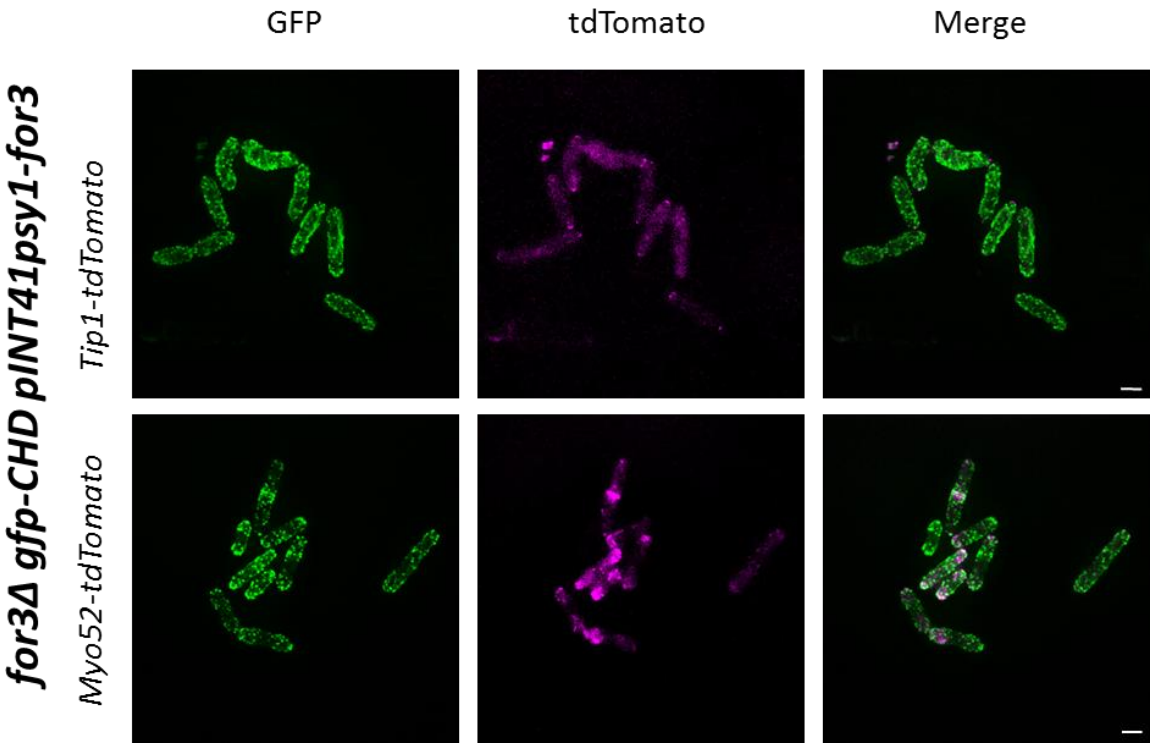

Figure 3.15. *for3Δ gfp-CHD* cells expressing Psy1-For3 and either Myo52tom or Tip1tom. Expression of Psy1-For3 leads to an increase in actin filament nucleation as described in figure 3.14 however the localisation of Myo52tom and Tip1tom is not affected. Images are a maximum projections of 31 Z slices. Scale bars 5 µm.

3.10. Summary

These data have shown that formin function is not restricted by cellular location or by which stage of the cell cycle cells are at. Recruiting the mitotic formin Cdc12 from the CAR to the cell poles of *for3Δ* cells still resulted in nucleation of interphase actin cables, demonstrating that Cdc12 actin nucleation activity is not restricted to its localisation to the CAR and that it can function at other points of the cell cycle than during mitosis. Similarly recruiting the interphase formin For3 to the CAR had a similar effect with For3 able to partially complement Cdc12 function in a *cdc12-112* strain at the restrictive temperature, again demonstrating that For3's function is not restricted to its cellular location at the cell poles and that it can function during mitosis as well as interphase. Further to this, it was seen that For3 function was not restricted to cellular locations that usually contain formin function (either For3 or Cdc12), as fusing For3 to Psy1 so that it localised to the entire cell membrane caused an increase in the numbers of actin cables which appeared to be nucleated from numerous points around the cell membrane. These data also demonstrate that it is the formins that determine which population of tropomyosin associates with specific actin structures. In wild type cells interphase cables nucleated by For3 associate with unacetylated tropomyosin and the CAR nucleated by Cdc12 associates with acetylated tropomyosin (Coulton & East 2010). However when the localisation of formins is altered such that For3 is at the CAR and Cdc12 is at the cell poles there is a switch in Tm population associating with the corresponding actin structures. Interphase cables nucleated by Cdc12 associate with acetylated Tm and the CAR nucleated by For3 contains unacetlyated Tm, phenomena which are never observed in wild type cells. This switch in Formin and Tm

population has subsequent effects on actin dynamics and the regulation of other actin binding proteins, as discussed later in chapter 6.

Chapter 4: The Regulation of Cell Polarity by the Actin and Microtubule Cytoskeletons

4.1. Introduction

The fission yeast cell grows only in length in a highly polarized manner (Mitchison & Nurse 1985) which is dependent on both the actin and microtubule cytoskeletons. Within both of these cytoskeletons there are a number of proteins with various functions that have been shown to be critical for regulating polarized growth of *S.pombe*. Many of these proteins are required for the establishment of a link between the two cytoskeletons in order to regulate the organization and dynamics of both, with a number of these proteins having been shown to be required for the localisation of other important polarity proteins.

In order to gain further understanding of how the proteins involved in polarity in fission yeast function, and how they interact with one another to tightly regulate the polarized growth of the cell the effect that deleting individual polarity proteins has upon the localization and abundance of each of the other polarity proteins was investigated. To do this a library of approximately 100 novel strains was generated (see Table 2.1) and the effect of individual gene deletions upon the localisation and intensity of the fluorescence signal of the polarity proteins when compared simultaneously to wild type cells was investigated.

4.2. Generation of Wild Type Control Strains

In order to be able to confidently conclude that any difference in GFP fluorescence is due to the gene deletion alone and not external factors such as media, or fluctuations in temperature, light source intensity, camera or acquisition settings, mix experiments were carried out. In this mix experiment a strain containing a polarity gene deletion and a different GFP tagged polarity protein was mounted onto a coverslip along with a strain containing the same GFP tagged polarity protein but with no gene deletion (hereby referred to as control cells). In order to differentiate between deletion and control cells, the control strains were generated so that they also possessed a tdTomato tag on the spindle pole body. Sid4 is a scaffold protein at the SPB, required for the localisation of components of the Septation Initiation Network (SIN) to the SPB during cell division, with no known role in the regulation of polarized growth of the cell (Chang & Gould 2000). Due to this it was decided that a Sid4-tdTomato allele would be used to differentiate control cells. Once generated, control strains containing each GFP tagged polarity protein and the Sid4-tdTomato were examined by fluorescence microscopy to ensure that the expected fluorescence and localisation patterns were observed. As shown in figure 4.1, the Sid4-tdTomato had no effect on the localisation of any of the polarity proteins. Bud6-GFP and For3-GFP both localised to the cell poles and also to the site of division. Mal3-GFP was observed on interphase microtubules and the mitotic spindle. All of the “Tea” proteins, Tea1-GFP, Tea2-GFP, Tea3-GFP and Tea4-GFP were observed at the cell poles, with Tea2-GFP also clearly seen on interphase microtubules and Tea3-GFP observed at the septum. Both Mod5-GFP and Tip1-GFP were present at the cell poles and the site of division, with

Tip1-GFP also observed on microtubules. Finally Myo52-GFP was seen at the cell poles, the site of division and moving along interphase actin cables.

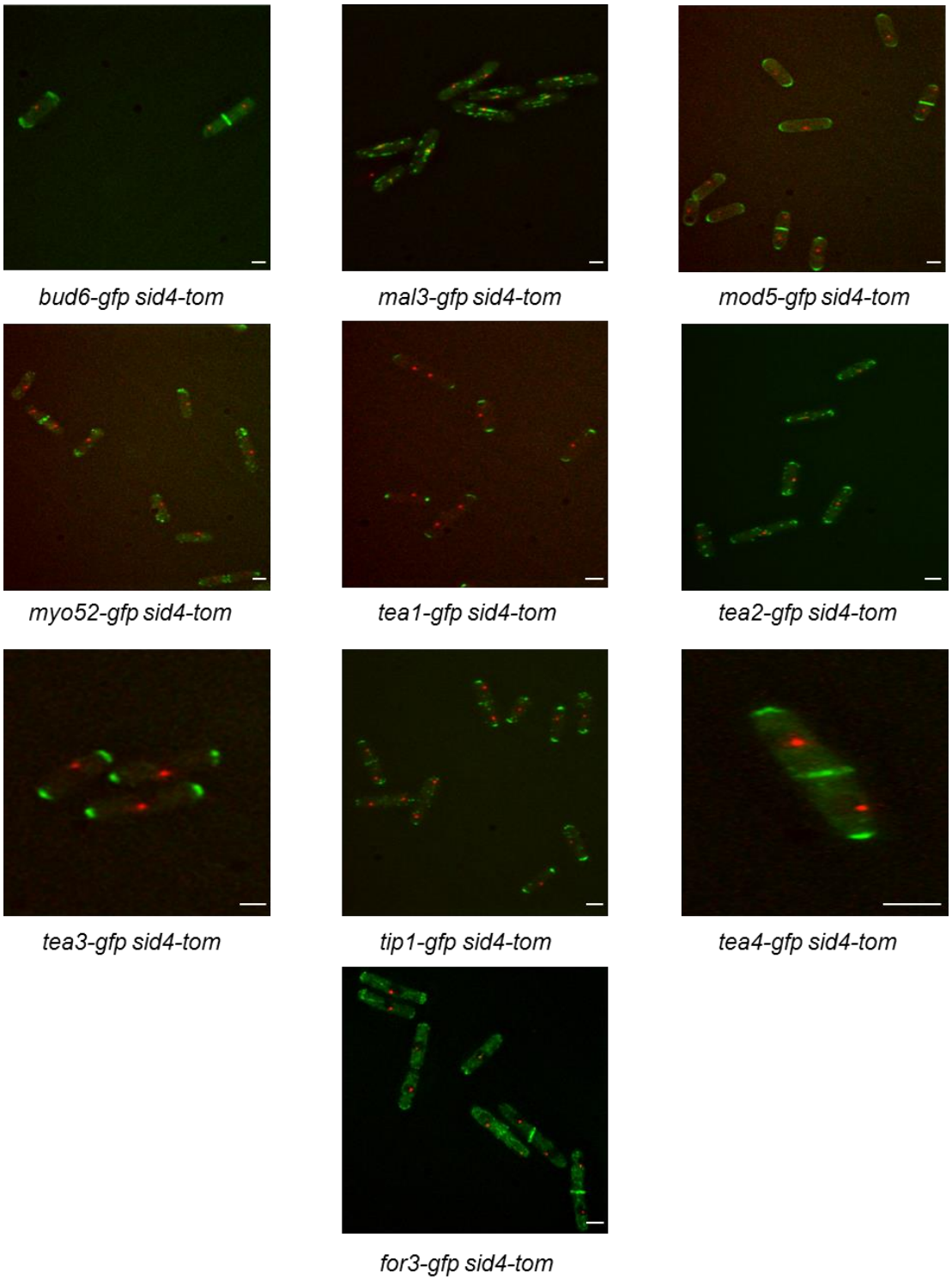

Figure.4.1. Maximum projection (31 Z slice) images of control strains used in the polarity study. Each polarity protein is tagged with GFP at the C terminus, and is coupled with a Sid4tdTomato, in order to distinguish between wild type cells and deletion cells. As can be seen, expression of Sid4tdTomato leads to no change in the localisation of polarity proteins.

4.3. Effect of Polarity Gene Deletions on Bud6-GFP

Bud6 is an actin associated protein involved in maintenance of cell polarity, regulation of the formin For3 and the initiation of NETO. Bud6 localizes to the cell tips in an actin dependent manner and also to the CAR (Martin, Rincon & Basu 2007; Glynn et al. 2001). It was expected that deletion of *for3* and *myo52* would reduce the levels of Bud6-GFP at the cell poles due to a lack of actin mediated transport. In addition deletion of "Tea" proteins could also have an effect as interactions between Bud6 and "Tea" proteins have previously been shown (Martin et al. 2005). The effect of deleting each of the genes encoding polarity proteins on the localisation and intensity of Bud6-GFP was investigated and the following results were found.

4.3.1. Gene Deletions Resulting in no Significant Changes in Intensity of Bud6-GFP

The deletion of *tea2* had no observable effect on the localisation of Bud6-GFP and both the average and maximum signal intensity was unaffected at either of the cell poles or in the cytoplasm.

4.3.2. Gene Deletions Resulting in Increases in the Intensity of Bud6-GFP at Cell Poles

Deletion of *for3* lead to an increase in Bud6-GFP signal within the cell particularly at the cell poles where there was a large increase in the amount of Bud6-GFP. As a result the average

signal intensity increased by 57% at End 1, 38% at End 2 and 26% in the cytoplasm. Similarly the maximum signal intensity increased by 153% at End 1, 76% at End 2 and 24% in the cytoplasm. Deletion of *gef1* had no clear observable effect on Bud6-GFP localisation, however differences were observed when looking at the signal intensity with a slight increase in Bud6-GFP levels at the cell poles and a decrease in the cytoplasm. The average signal intensity at End 1 increased by 16%, at End 2 there was no significant effect and in the cytoplasm there was a 13% decrease. The maximum signal intensity at End 1 increased by 25%, at End 2 by 23% and in the cytoplasm there was an 11% decrease. Deletion of *mal3* also resulted in no obvious change in Bud6-GFP localisation, but again changes were observed when examining the signal intensity, with an increase in Bud6-GFP levels at the cell poles. This was reflected by the average signal intensity at End 1 increasing by 21% whilst at End 2 and in the cytoplasm there was no significant change. However the maximum signal intensity increased at both ends of the cell, with a 27% increase observed at End 1 and a 19% increase observed at End 2 whilst no significant change was seen in the cytoplasm. Finally deletion of *tip1* appeared to result in a slight increase in Bud6-GFP levels at the cell poles. The average signal intensity was unaffected at both End 1 and End 2, whilst there was a 22% decrease in the cytoplasm. However when looking at the maximum signal intensity a 20% increase was observed at End 1 and a 23% increase was observed at End 2. Similar to the average signal intensity, a 15% decrease was observed in the cytoplasm.

4.3.3. Gene Deletions Resulting in Decreases in Intensity of Bud6-GFP at the Cell Poles

Deletion of *myo52* led to a reduction of Bud6-GFP in all areas of the cells, however it was also noted that the cells did not possess the typical short stubby phenotype of a *myo52Δ* strain, with cells instead being elongated. The average signal intensity showed no significant change at End 1, whilst at End 2 there was a 20% decrease and a 13% decrease was observed in the cytoplasm. The maximum signal intensity showed higher decreases, with a 20% decrease seen at End 1, 32% at End 2 and 19% in the cytoplasm. Deletion of *tea1* had no obvious effect on the localisation of Bud6-GFP, and this was shown by only small changes in the signal intensity which indicated a slight reduction in the accumulation of Bud6-GFP at the cell poles. There was a 12% decrease in average signal intensity at End 1 and a 13% decrease at End 2, whilst there was no significant change in the cytoplasm. This was repeated with the maximum signal intensity, with a 10% decrease observed at End 1 and 14% decrease at End 2, whilst again there was no significant change in the cytoplasm.

4.3.4. Gene Deletions Resulting in an Increase in Monopolar Intensity of Bud6-GFP

Deletion of *tea3* led to a more monopolar localisation of Bud6-GFP, which was supported by a decrease in Bud6-GFP signal at End 2 with a 10% decrease in average signal intensity and a 12% decrease in maximum signal intensity observed. Both the average and maximum signal intensity showed no significant change at End 1, whilst the cytoplasm had no significant change in average signal intensity, but a 10% increase in maximum signal

intensity. Deletion *tea4* also caused a slight increase in monopolar localisation of Bud6-GFP, whilst the average signal intensity was unaffected at either of the cell poles or in the cytoplasm, deletion of *tea4* did result in an 18% increase in maximum signal intensity at End 1 of the cell.

4.3.5. Gene Deletions Resulting in Changes in the Intensity of Bud6-GFP in the Cytoplasm

Deletion of *mod5* had a mixed effect on the localisation of Bud6-GFP, most cells appeared almost identical to wild type, whilst a small number had disrupted Bud6-GFP localisation, with Bud6-GFP failing to accumulate at the cell poles and accumulating as large clumps in the cytoplasm or along the side of the cell (shown by arrows, Fig 4.2). However as this only affected a small number of cells, both the average and maximum signal intensity were only affected in the cytoplasm, where the average signal intensity increased by 11% and the maximum signal intensity increased by 13%.

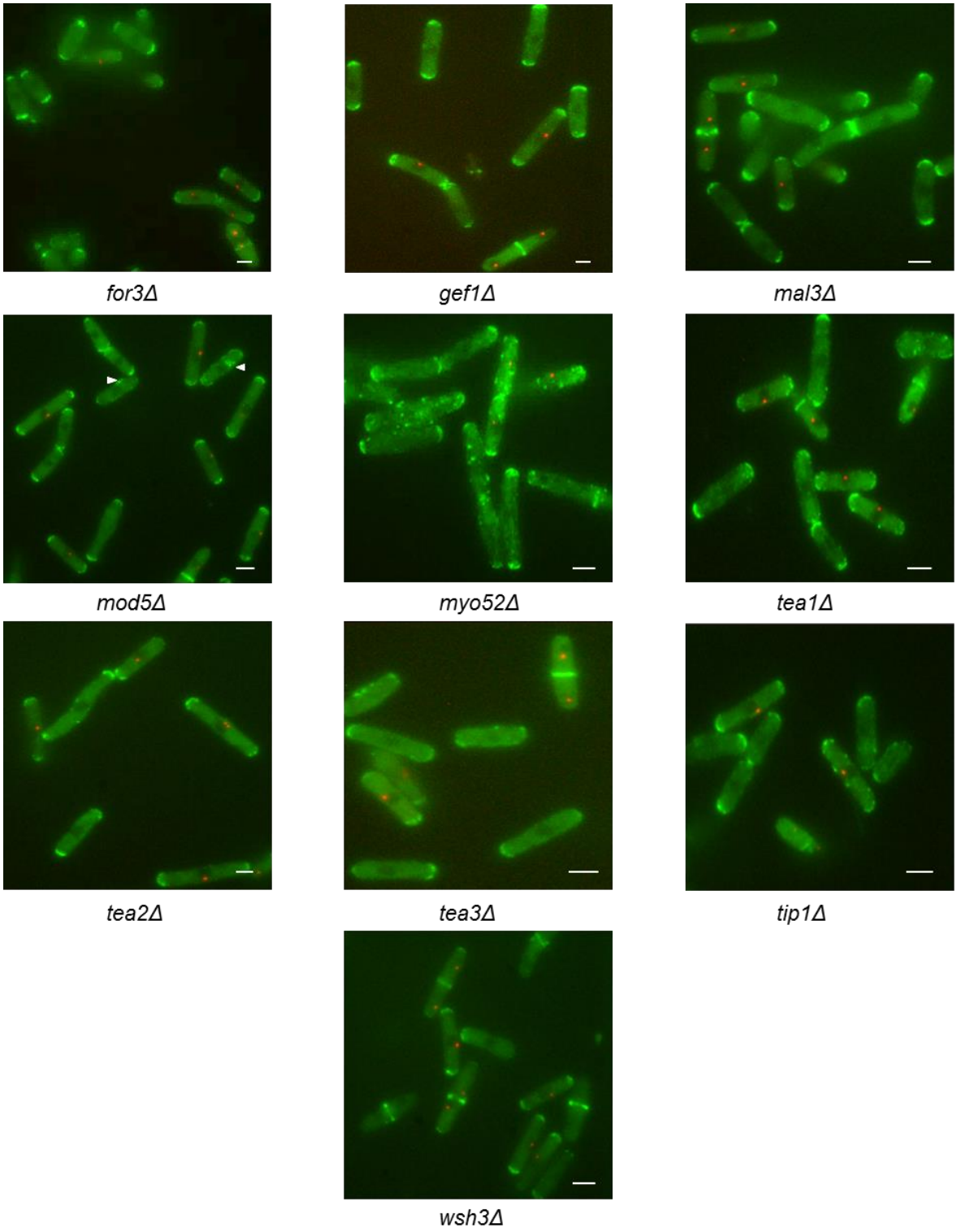

Figure 4.2. Images of cells containing Bud6-GFP and a deletion of one of the polarity genes (as labelled). Images are maximum projections of Z slices 5-25 of a 31 Z slice image. Scale bars 5 µm. n=80 cells.

	End1	End2	Cytoplasm
for3Δ	+57%	+38%	+26%
gef1Δ	+16%	-	-13%
mal3Δ	+21%	-	-
mod5Δ	-	-	+11%
myo52Δ	-	-20%	-13%
tea1Δ	-12%	-13%	-
tea2Δ	-	-	-
tea3Δ	-	-10%	-
tea4Δ	-	-	-
tip1Δ	-	-	-22%

Table 4.1. Changes in average signal intensity of Bud6-GFP relative to wild type cells following deletion of polarity genes.

	End1	End2	Cytoplasm
for3Δ	+153%	+76%	+24%
gef1Δ	+25%	+23%	-
mal3Δ	+27%	+19%	-
mod5Δ	-	-	13%
myo52Δ	-20%	-32%	-19%
tea1Δ	-10%	-14%	-
tea2Δ	-	-	-
tea3Δ	-	-12%	+10%
tea4Δ	-	-	+18%
tip1Δ	+20%	+23%	-15%

Table 4.2. Changes in maximum signal intensity of Bud6-GFP relative to wild type cells following deletion of polarity genes.

4.4. Effect of Polarity Gene Deletions on For3-GFP

The formin For3 is involved in the organization of the actin cytoskeleton during interphase, promoting proper cell polarity, symmetric cell division and is required for the formation of actin cables observed along the length of the cell during interphase, which the type V myosin Myo52 travels along in order to deliver various cargoes to diverse cellular locations (Feierbach & Chang 2001; Nakano 2002; Martin & Chang 2006). During interphase For3 localises to both tips of the cell, where it is associated with the actin patches. When the cell is in early mitosis For3 is seen as a medial spot in a similar fashion to Cdc12, which then progresses to a double ring in late mitosis however it does not associate with the CAR (Feierbach & Chang 2001). It was expected that deletion of *bud6* and certain "Tea" proteins may have an effect on the localisation of For3, due to the formation of multi-protein complexes at the cell tips (Martin et al. 2005). The effect of deleting each of the polarity genes on the localisation and intensity of For3-GFP was investigated and the following results were found.

4.4.1. Gene Deletions Resulting in no Significant Changes in Intensity of For3-GFP

Deletion of *tip1* had no significant effect on For3-GFP localisation, with no effect seen on the maximum or average signal intensity at End 1, End 2 or in the cytoplasm.

4.4.2. Gene Deletions Resulting in Increases in the Intensity of For3-GFP at Cell Poles

Deletion of *mal3* lead to an increase in the levels of For3-GFP at the cell poles, although it had very little effect on the average signal intensity, with only the cytoplasm showing a decrease of 15%. However there was more of an effect observed on the maximum signal intensity which reflected the increase in For3-GFP levels at the cell poles, with a 9% increase at End 1, a 15% increase at End 2 and similar to the average signal intensity, a 16% decrease in the cytoplasm. Deletion of *myo52* resulted in an increase in accumulation of For3-GFP at the cell poles. An effect at End 1 was seen in regards to average signal intensity where there was a 22% increase, whilst End 2 and the cytoplasm had no significant change. However, more of an effect was seen in the maximum signal intensity, where there was an 80% increase at End 1 and a 19% increase at End2, again no significant change was seen in the cytoplasm.

4.4.3. Gene Deletions Resulting in Decreases in the Intensity of For3-GFP at Cell Poles

Deletion of *bud6* lead to a reduction in the accumulation of For3-GFP at the cell poles. This was reflected by an 18% decrease at End 1 and a 16% decrease at End 2 in the average signal intensity. Similarly the maximum signal intensity was reduced at both ends, by 37% at End 1 and 27% at End 2. No significant effect was seen for both the average and maximum signal intensity in the cytoplasm.

4.4.4 Gene Deletions Resulting in Changes in the Intensity of For3-GFP in the Cytoplasm

Deletion of *gef1* had very little effect on the localisation of For3-GFP, with no significant change seen in both the average and maximum signal intensity at End 1 or End 2. However there was a slight decrease in the cytoplasm for both, with a 15% decrease in average signal intensity and a 14% decrease in maximum signal intensity.

4.4.5. Gene Deletions Resulting in an Increase in Monopolar Intensity of For3-GFP

Deletion of *mod5* appeared to result in a more monopolar localisation of For3-GFP. There was very little effect on the average signal intensity, with only End 2 showing a 13% decrease whilst both End 1 and the cytoplasm had no significant change. The maximum signal intensity was affected at both End 1 and End 2, with a 15% increase at End 1 and a 19% decrease at End 2, reflecting a more monopolar localisation of For3-GFP. Similar to the deletion of *mod5Δ,* deletion of *tea1* resulted in a more monopolar localisation of For3-GFP. The average intensity measurements did not show this particularly well, with only a 10% decrease in End 2 seen whilst End 1 and the cytoplasm had no significant change. The maximum signal intensity better showed the monopolar localisation, with a 14% increase at End 1, an 11% decrease at End 2 whilst again the cytoplasm showed no significant change. Deletion of *tea2* resulted in no obvious change in For3-GFP localisation however changes in signal intensity suggested a possible slight increase in For3-GFP levels at End 1 (again becoming slightly more monopolar). The average signal intensity were affected at

End 2 and the cytoplasm, with a 10% decrease observed at both, whilst End 1 had no significant change. The maximum signal intensity differed in that there was a 10% increase at End 1 and a 9% decrease in the cytoplasm, whilst there was no significant change at End 2. Deletion of *tea3* did not cause a large change in For3-GFP, however it did appear to lead to For3-GFP having a slightly more monopolar localisation. This was reflected in the intensity measurements in a different way to other deletions when there is a more monopolar localisation of For3-GFP, instead of an increase in signal at End 1 where no significant change was observed in either the average or maximum signal intensity, there was only a decrease in average and maximum signal intensity at End 2 and in the cytoplasm. The average signal intensity decreased by 16% at End 2 and 15% in the cytoplasm whilst the maximum signal intensity decreased by 14% at End 2 and 15% in the cytoplasm. Finally deletion of *tea4* again resulted in a more monopolar localisation of For3-GFP. This was reflected by increases of 10% and 27% at End 1 for the average and maximum signal intensity respectively and a 10% decrease in the average signal intensity at End 2. No significant changes were observed at in the cytoplasm or in the maximum signal intensity at End 2.

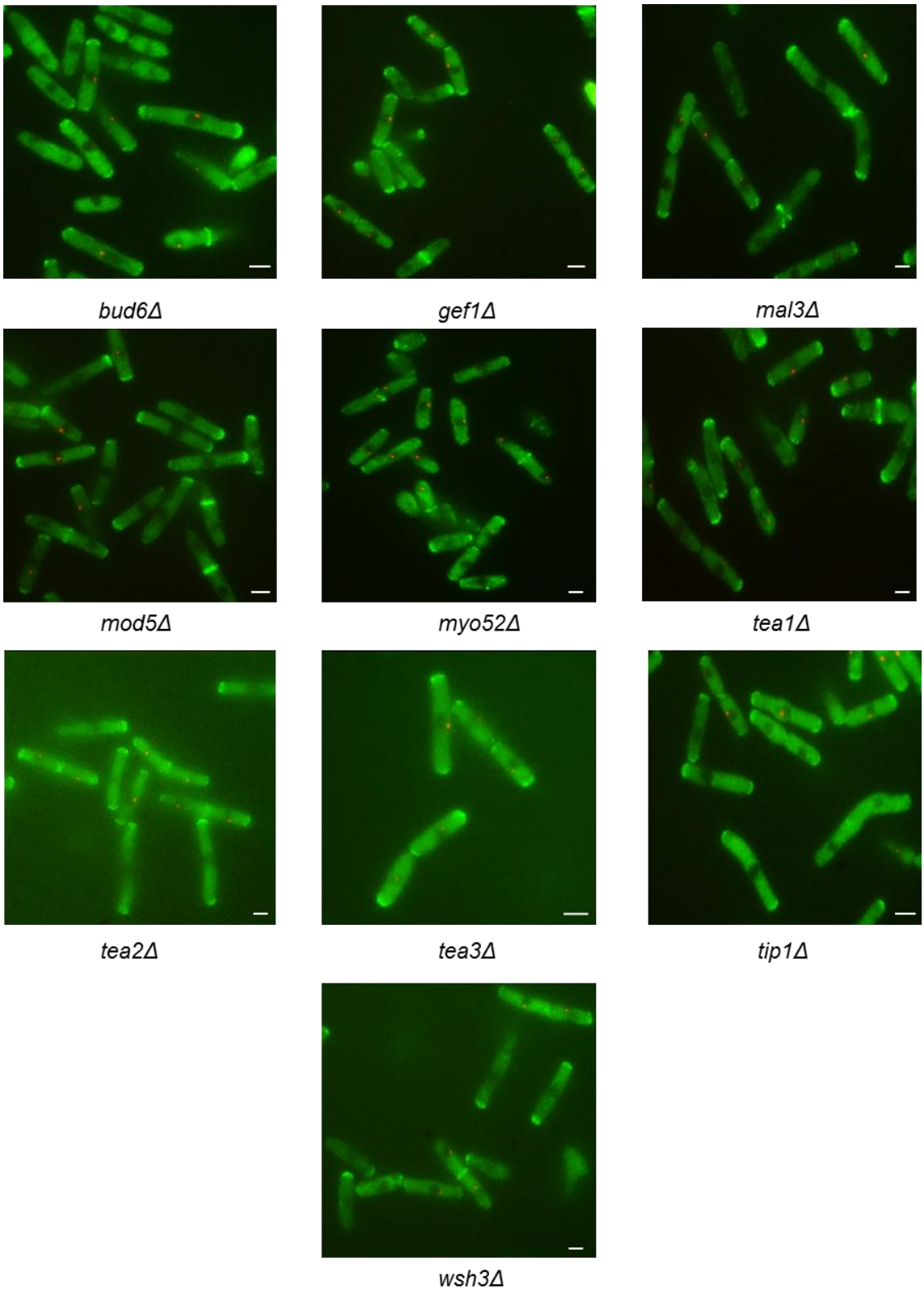

Figure 4.3. Images of cells containing For3-GFP and a deletion of one of the polarity genes (as labelled). Images are maximum projections of Z slices 5-25 of a 31 Z slice image. Scale bars 5 µm. n=80 cells.

	End1	End2	Cytoplasm
bud6Δ	-18%	-16%	-
gef1Δ	-	-	-15%
mal3Δ	-	-	-15%
mod5Δ	-	-13%	-
myo52Δ	+22%	-	-
tea1Δ	-	-10%	-
tea2Δ	-	-10%	-10%
tea3Δ	-	-16%	-15%
tea4Δ	+10%	-10%	-
tip1Δ	-	-	-

Table 4.3. Changes in average signal intensity of For3-GFP relative to wild type cells following deletion of polarity genes.

	End1	End2	Cytoplasm
bud6Δ	-37%	-27%	-
gef1Δ	-	-	-14%
mal3Δ	+9%	+15%	-16%
mod5Δ	+15%	-19%	-
myo52Δ	+80%	+19%	-
tea1Δ	+14%	-11%	-
tea2Δ	+10%	-	-9%
tea3Δ	-	-14%	-13%
tea4Δ	+27%	-	-
tip1Δ	-	-	-

Table 4.4. Changes in maximum signal intensity of For3-GFP relative to wild type cells following deletion of polarity genes.

4.5. Effect of Polarity Gene Deletions on Mal3-GFP

Mal3 is a microtubule associated protein, first identified in a screen undertaken to isolate proteins required for chromosome segregation in fission yeast (Polakova et al. 2014). Mal3 localizes to both cytoplasmic microtubules and the mitotic spindle, and faint localization to a central ring structure during anaphase also occurs (J D Beinhauer et al. 1997). As Mal3-GFP does not localise to the cell poles as other polarity proteins do the signal intensity was not measured, as it would be highly variable on microtubules due to the variation in microtubule structures in different cells. However the localisation of Mal3-GFP was observed when each of the other polarity proteins were deleted. Although deletion of polarity proteins can affect microtubule structures within the cell, Mal3-GFP was still able to interact with any microtubules present within the cell (figure 4.4).

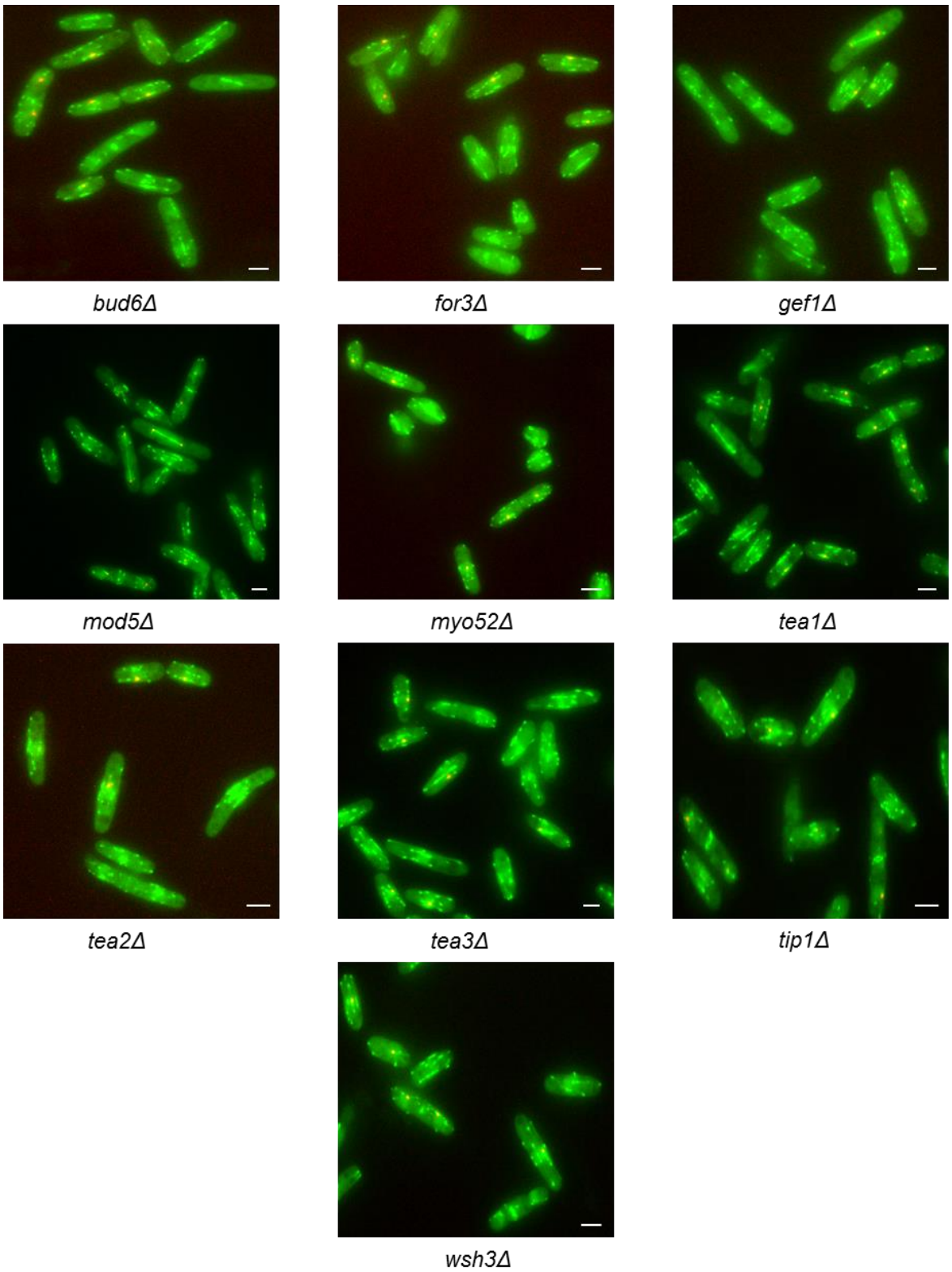

Figure 4.4. Images of cells containing Mal3-GFP and a deletion of one of the polarity genes (as labelled). Images are maximum projections of Z slices 5-25 of a 31 Z slice image. Scale bars 5 µm. n=80 cells.

4.6. Effect of polarity gene deletions on Mod5-GFP

Mod5 is a membrane associated protein that is involved in regulation of cell polarity via interactions with microtubules and Tea1 (Snaith & Sawin 2003). Mod5 localises to the ends of the fission yeast cell where it is involved in the anchoring of Tea1 at the ends of the cells (Snaith & Sawin 2003; Snaith et al. 2005; Bicho et al. 2010). The deletion of *tea1* was expected to reduce the accumulation of Mod5 at the cell poles, as shown previously (Snaith & Sawin 2003). In addition the deletion of other "Tea" proteins may have also had an effect. The effect of deleting each of the polarity genes on the localisation and intensity of Mod5-GFP was investigated and the following results were found.

4.6.1. Gene Deletions Resulting in no Significant Changes in Intensity of Mod5-GFP

Deletion of *tip1* had no significant effect on Mod5-GFP localisation, with no effect seen on the maximum or average signal intensity at End 1, End 2 or in the cytoplasm.

Deletion of *gef1* had no obviously noticeable effect on Mod5-GFP and this was reflected by only small changes in signal intensity, predominantly with a slight increase in signal in the cytoplasm observed where there was an increase of 13% and 20 % in the average and maximum signal intensity respectively. End 2 showed no significant changes, whilst End 1 showed an 8% decrease in the maximum signal intensity only. Deletion of *myo52* resulted in an unexpected cell morphology, with cells appearing elongated and slightly wider than wild type instead of short stubby cells usually observed in a *myo52Δ* strain as shown in figure 4.5. Aside from this unusual cell morphology, no clear effect on Mod5-GFP

localisation was observed and only small changes were observed in the signal intensity. A slight increase in localisation of Mod5-GFP to End 1 was observed, with the average signal intensity at End 1 increasing by 18% with End 2 and the cytoplasm showing no significant change. The maximum signal intensity showed no significant change at End 1 or in the cytoplasm, but there was a 9% decrease at End 2.

4.6.2. Gene Deletions Resulting in Increases in the Intensity of Mod5-GFP at Cell Poles

Deletion of *bud6* appeared to lead to an increase in the levels of Mod5-GFP throughout the cells. This was reflected by increases in signal intensity at all areas of the cell, where the average signal intensity increased by 42% at End 1 and End 2 and also increased by 56% in the cytoplasm. The maximum signal intensity were similar; End 1 had a 33% increase, End 2 a 27% increase and the cytoplasm a 61% increase. Deletion of *for3* had a similar effect to that of *bud6* with an overall increase of Mod5-GFP within the cells which was again reflected by increases in all signal intensity. The average signal intensity increased by 25% at End 1, 30% at End 2 and 29% in the cytoplasm. The maximum signal intensity increased by 21% at End 1, 29% at End 2 and 21% at in the cytoplasm. Deletion of *tea3* resulted in an increase in Mod5-GFP levels throughout the cell. This was shown by large increases to both the average and maximum signal intensity. The average signal intensity increased by 71% at End 1, 67% at End 2 and 81% in the cytoplasm. Similarly the maximum signal intensity increased by 43% at End 1, 41% at End 2 and 81% in the cytoplasm.

4.6.3. Gene Deletions Resulting in Decreases in the Intensity of Mod5-GFP at Cell Poles

Deletion of *mal3* lead to a large reduction in the accumulation of Mod5-GFP at the cell poles. This was best reflected in the maximum signal intensity, where a 28% decrease was observed at End 1, and a 31% decrease at End 2, whilst there was no significant change in the cytoplasm. The average signal intensity showed no significant change at End 1 or in the cytoplasm, whilst a 16% decrease was observed at End 2. Deletion of *tea1* lead to a reduced accumulation of Mod5-GFP at the cell poles with its localisation appearing almost completely uniform around the entire cell membrane. This was reflected by decreases in both the average and maximum signal intensity at End 1 and End 2. In the case of the average signal intensity there was a 14% decrease and End 1 and an 18% decrease at End 2, with no significant change observed in the cytoplasm. There was a greater decrease seen in regards to the maximum signal intensity, with a 39% decrease at End 1 and a 41% decrease at End 2, again there was no significant change in the cytoplasm. Deletion of *tea2* also resulted in less Mod5-GFP localising to the cell poles however the effect was not as severe as that of *tea1Δ* in that there was still a slight enrichment of Mod5-GFP at the cell poles compared to the rest of the cell membrane. This affect was best shown by the maximum signal intensity where there was a 29% decrease at End 1 and a 21% decrease at End 2, coupled with a 14% increase in the cytoplasm. The average signal intensity did not replicate this pattern, with no significant changes observed at End 1 or end 2, but there was again an increase in the cytoplasm, this time of 18%. Deletion of *tip1* lead to an increase in the cytoplasmic levels of Mod5-GFP. As can be seen in figure 4.5 this gave the appearance of a large decrease in the levels of Mod5-GFP at the cell ends, however there was only a

slight decrease. Due to the increased levels of cytoplasmic Mod5-GFP the average signal intensity showed a 42% increase at End 1, a 22% increase at End 2 and a 70% increase in the cytoplasm. The maximum signal intensity showed the slight reduction in Mod5-GFP at the cell poles, with an 11% decrease observed at End 1 and a 16% decrease at End 2, again there was an increase in the cytoplasm of 66%.

4.6.4. Gene Deletions Resulting in an Increase in Monopolar Intensity of Mod5-GFP

Deletion of *tea4* resulted in a more monopolar localisation of Mod5-GFP, whilst Mod5-GFP also appeared less uniformly distributed at the cell tips, with more individual foci observed (shown by arrows in figure 4.4). This resulted in decreases in the average signal intensity at End 2 and in the cytoplasm of 25% and 19% respectively, whilst there was no significant change at End 1. However there was a 49% increase in the maximum signal intensity at End 1, coupled with a 36% decrease at End 2 and an 11% decrease in the cytoplasm.

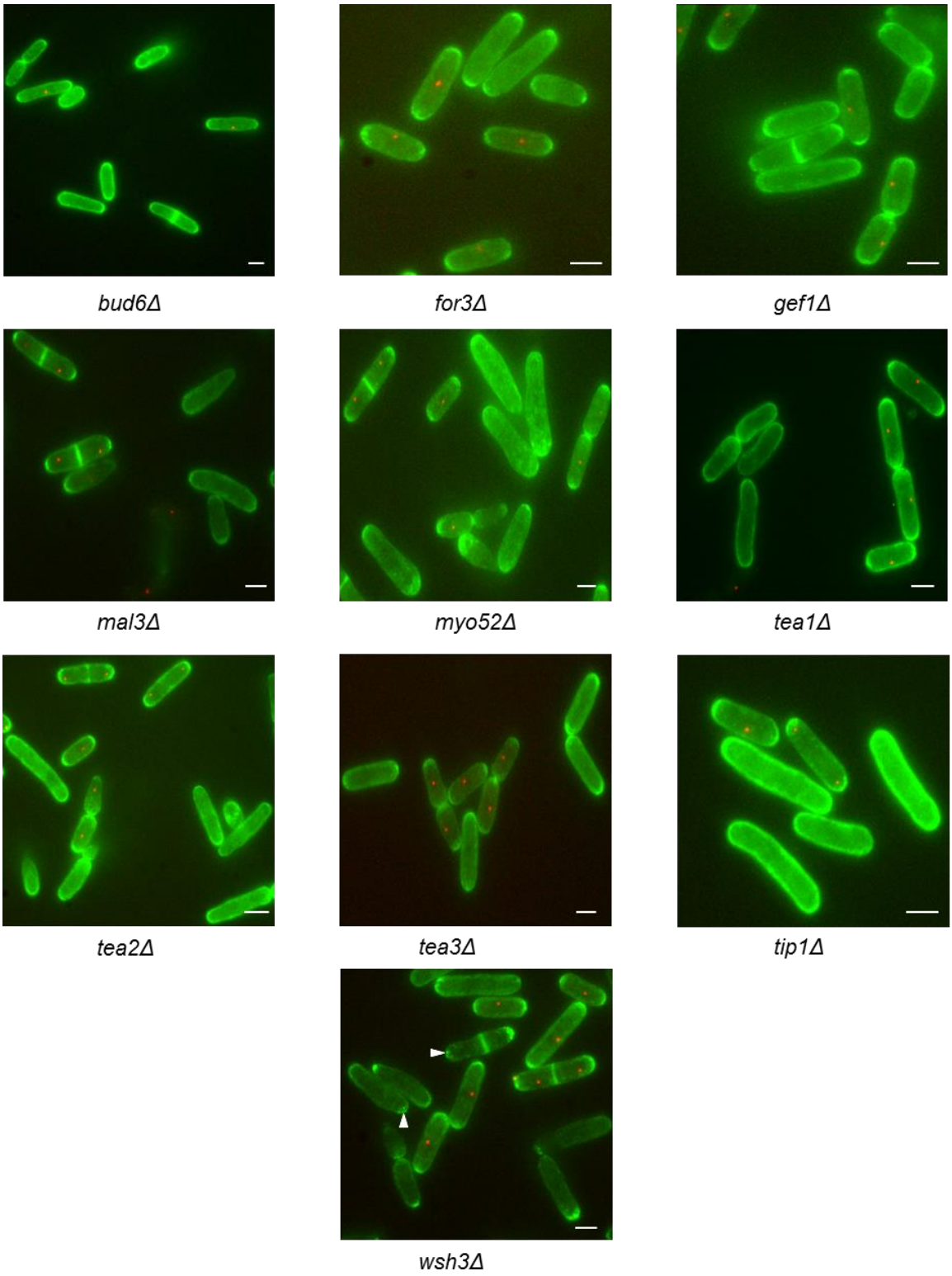

Figure.4.5. Images of cells containing Mod5-GFP and a deletion of one of the polarity genes (as labelled). Images are maximum projections of Z slices 5-25 of a 31 Z slice image. Scale bars 5 µm. n=80 cells.

	End1	End2	Cytoplasm
bud6Δ	+42%	+42%	+56%
for3Δ	+25%	+30%	+29%
gef1Δ	-	-	+13%
mal3Δ	-	-16%	-
myo52Δ	+18%	-	-
tea1Δ	-14%	-18%	-
tea2Δ	-	-	+18%
tea3Δ	+71%	+67%	+81%
tea4Δ	-	-25%	-19%
tip1Δ	+42%	+22%	+70%

Table 4.5. Changes in average signal intensity of Mod5-GFP relative to wild type cells following deletion of polarity genes.

	End1	End2	Cytoplasm
bud6Δ	+33%	+27%	+61%
for3Δ	+21%	+29%	+21%
gef1Δ	-8%	-	+20%
mal3Δ	-28%	-31%	-
myo52Δ	-	-9%	-
tea1Δ	-39%	-41%	-
tea2Δ	-29%	-21%	+14%
tea3Δ	+43%	+41%	+81%
tea4Δ	+49%	-36%	-11%
tip1Δ	-11%	-16%	+66%

Table 4.6. Changes in maximum signal intensity of Mod5-GFP relative to wild type cells following deletion of polarity genes.

4.7. Effect of polarity gene deletions on Myo52-GFP

Myo52 is a dimeric motor protein which "walks" along actin filaments and delivers cargoes to discrete cellular locations. Myo52 moves around the cell and accumulates at areas of cell growth (the tips) and at areas of cell wall deposition (site of division) (T Z Win et al. 2001). The localization of Myo52 is dependent upon actin, while loss of Myo52 leads to reduced cell polarity, with cells being rounder in shape. It was expected that the deletion of *for3* would abolish the accumulation of Myo52 at the cell poles, however the effects of other deletions were uncertain. The effect of deleting each of the polarity genes on the localisation and intensity of Myo52-GFP was investigated and the following results were found.

4.7.1. Gene Deletions Resulting in Increases in the Intensity of Myo52-GFP at Cell Poles

Deletion of *gef1* resulted in a slight increase in Myo52-GFP levels at the cell poles. This resulted in the average signal intensity decreasing by 13% in the cytoplasm, whilst there was no significant effect at End 1 or 2. The maximum signal intensity better showed this increase in Myo52-GFP at the poles, with a 17% increase at End 1 and 24% at End 2, whilst the cytoplasm had no significant change. Deletion of *mal3* also lead to an increase in Myo52-GFP accumulation at the cell poles, shown particularly well by the cell marked with an arrow in figure 4.6. There was no significant change in the average signal intensity, whilst there was an increase in the maximum signal intensity to reflect this effect. At End 1 there was a 13% increase, at End 2 a 30% increase and in the cytoplasm a 19% increase. Deletion

of *mod5* had no noticeable effect Myo52-GFP localisation, however when examining the signal intensity it seemed to result in a more bipolar localisation of Myo52-GFP shown by an increase in signal intensity at the End2. This was reflected by an 11% increase in the average signal intensity and a 24% increase in the maximum signal intensity. There were no significant changes at End 1 or in the cytoplasm. Deletion of *tea2* like *tea1Δ* caused an increase in Myo52-GFP levels at the cell poles, however this time Myo52-GFP localisation remained bi polar, as can be seen in figure 4.6. This was reflected by the average signal intensity increasing by 13% at End 1 and 10% at End 2, whilst the cytoplasm had no significant change. This pattern was repeated with the maximum signal intensity where there was a 10% increase at end 1, an 18% increase at End 2 and again no significant change in the cytoplasm. Deletion of *tip1* resulted in an increase in Myo52-GFP accumulation at the cell poles. This again was best reflected by the maximum signal intensity where there was a 29% increase at End 1, a 56% increase at End 2 and a 27% decrease in the cytoplasm. The average signal intensity showed an 11% increase at End 2 and a 31% decrease in the cytoplasm, whilst no significant change was seen at End 1. Finally deletion of *tea4* had no immediately obvious effect on Myo52-GFP localisation. There were no significant changes to the average signal intensity, whilst the maximum signal intensity increased by 17% at End 2 and 29% in the cytoplasm, whilst there was no significant change at End 1, perhaps indicating a slight increase in cellular levels of Myo52-GFP.

4.7.2. Gene Deletions Resulting in Decreases in the Intensity of Myo52-GFP at Cell Poles

Deletion of *bud6* resulted in a large reduction in Myo52-GFP accumulating at the cell poles, however there were still numerous motile foci observed throughout the cells. The average signal intensity decreased by 15% at End 1 and 10% at End 2, whilst there was no significant change in the cytoplasm. Similarly, the maximum signal intensity decreased by 24% at End 1 and 17% at End 2, whilst there was also a 21% increase in the cytoplasm. Deletion of *for3* showed a more severe effect, with no distinct Myo52-GFP localisation observed at the cell poles, with numerous non motile foci of Myo52-GFP observed, however they were of very low intensity. This was not well shown by the average signal intensity where there was a 13% increase at End 2 and a 46% increase in the cytoplasm, with no significant change seen at End 1. These increases at the ends were most likely due to the area of measurement also including a large area of cytoplasm which will have contained many Myo52-GFP foci. However the maximum signal intensity did better represent this loss of Myo52-GFP accumulation at the cell poles, with a 32% decrease observed at End 1, an 11% decrease at End 2 and a 77% increase in the cytoplasm.

4.7.3. Gene Deletions Resulting in an Increase in Monopolar Intensity of Myo52-GFP

Deletion of *tea1* resulted in an increase in the levels of Myo52-GFP in a much more monopolar fashion with large accumulations of Myo52-GFP observed at just one end of most cells. This was shown by a 42% increase in the average signal intensity at End 1 and a

59% increase in the maximum signal intensity at End 1. There was also a 15% increase in the maximum signal intensity at End 2, whilst there were no significant changes in the cytoplasm. Deletion of *tea3* had little effect on Myo52-GFP, there was possibly a slight increase in Myo52-GFP levels at one end of the cell. There were no significant changes to the average signal intensity or the maximum signal intensity at End 2 or in the cytoplasm. There was however a 10% increase in maximum signal intensity at End 1, reflecting this slight increase in Myo52-GFP levels.

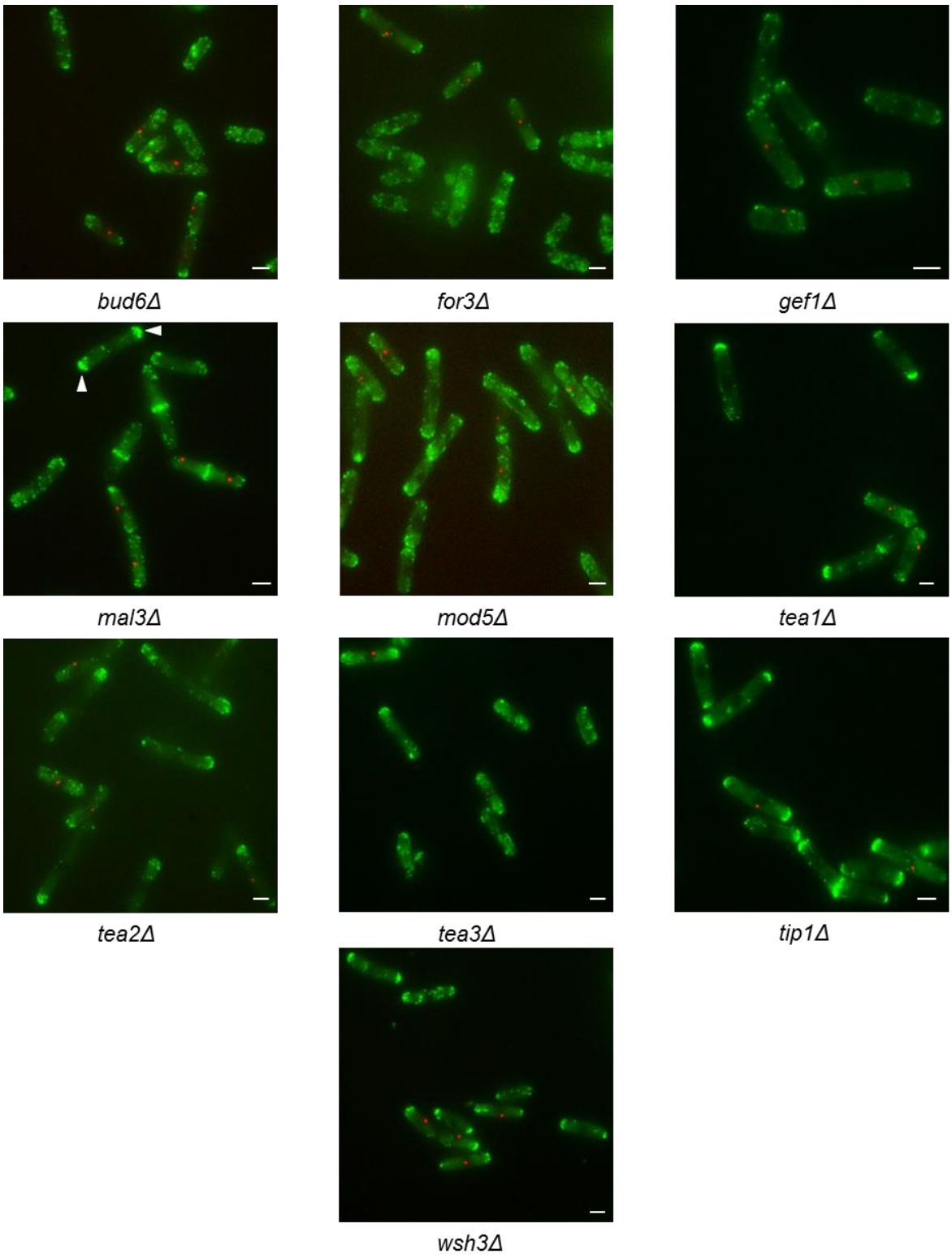

Figure 4.6. Images of cells containing Myo52-GFP and a deletion of one of the polarity genes (as labelled). Images are maximum projections of Z slices 5-25 of a 31 Z slice image. Scale bars 5 µm. n=80 cells.

	End1	End2	Cytoplasm
bud6Δ	-15%	-10%	-
for3Δ	-	+13%	+46%
gef1Δ	-	-	-13%
mal3Δ	-	-	-
mod5Δ	-	+11%	-
tea1Δ	+42%	-	-
tea2Δ	+13%	+10%	-
tea3Δ	-	-	-
tea4Δ	-	-	-
tip1Δ	-	+11%	-31%

Table 4.7. Changes in average signal intensity of Myo52-GFP relative to wild type cells following deletion of polarity genes.

	End1	End2	Cytoplasm
bud6Δ	-24%	-17%	+21%
for3Δ	-32%	-11%	+77%
gef1Δ	+17%	+24%	-
mal3Δ	+13%	+30%	+19%
mod5Δ	-	+24%	-
tea1Δ	+59%	+15%	-
tea2Δ	+10%	+18%	-
tea3Δ	+10%	-	-
tea4Δ	-	+17%	+29%
tip1Δ	+29%	+56%	-27%

Table 4.8. Changes in maximum signal intensity of Myo52-GFP relative to wild type cells following deletion of polarity genes.

4.8. Effect of Polarity Gene Deletions on Tea1-GFP

Tea1 is a cell end marker that localizes to the tips of the cell, both growing and non-growing in a microtubule dependent manner and directs growth machinery to these regions Tea1 also plays a role in regulating the microtubule cytoskeleton (Mata & Nurse 1997; Niccoli et al. 2003; Behrens & Nurse 2002). It was expected that the deletion of *mod5* would prevent the proper accumulation of Tea1 at the cell poles, as shown previously (Snaith & Sawin 2003), and that the deletion of other "Tea" proteins, especially *tea2* may also prevent Tea1 accumulation at the cell poles. The effect of deleting each of the polarity genes on the localisation and intensity of Tea1-GFP was investigated and the following results were found.

4.8.1. Gene Deletions Resulting in no Significant Changes in Intensity of Tea1-GFP

Deletion of *for3* caused no significant change to the localisation or intensity of Tea1-GFP.

4.8.2. Gene Deletions Resulting in Decreases in the Intensity of Tea1-GFP at Cell Poles

Deletion of *bud6* had little effect on the localisation of Tea1-GFP and only a few small changes were seen in the signal intensity. The average signal intensity decreased by 15% in the cytoplasm whilst there was no significant change at End 1 or 2. The maximum signal intensity decreased by 10% at End 2 and by 16% in the cytoplasm but there was no

significant change at End 1, suggesting possibly a slight reduction in Tea1-GFP levels within the cells. Deletion of *gef1* resulted in a decrease in Tea1-GFP levels at both cell ends and there also appeared to be less Tea1-GFP on microtubules in the cell. This resulted in the average signal intensity decreasing by 25% at End 1, 24% at End 2 and 45% in the cytoplasm. Similarly the maximum signal intensity decreased by 10% at End 1, 13% at End 2 and 53% in the cytoplasm. Deletion of *mal3* resulted in a large decrease in Tea1-GFP localisation to the cell poles and less Tea1-GFP was also observed on microtubules. Also, some cells appeared to be slightly elongated and in these longer cells Tea1-GFP appeared to accumulate on the cell membrane at the centre of these cells, as shown by the arrows in figure 4.7. This effect caused the average signal intensity to decrease by 40% at End 1, 36% at End 2 whilst there was a 49% increase in the cytoplasm. A similar pattern was observed with the maximum signal intensity, with a 66% decrease seen at End 1, a 46% decrease at End 2 and a 66% increase in the cytoplasm. Deletion of *mod5* resulted in Tea1-GFP not localising to the cell poles correctly. Occasionally small foci of Tea1-GFP were observed at the cell poles, but the usual uniform distribution of Tea1-GFP around the cell tip was not observed. In addition there appeared to be more cytoplasmic foci of Tea1-GFP. This in turn resulted in the average signal intensity decreasing by 53% at End 1, 23% at End 2 and increasing by 22% in the cytoplasm. The maximum signal intensity revealed a slightly different pattern, with a 45% decrease observed at End1, a 25% increase at End 2 and a 163% increase in the cytoplasm. Deletion of *myo52* resulted in a large decrease in the amount of Tea1-GFP localising to the cell poles. The average signal intensity decreased by 22% at End 1 and 19% and End2 whilst increasing 26% in the cytoplasm. The maximum signal intensity decreased by 32% at End 1, 38% at End 2 and by 13% in the cytoplasm.

Deletion of *tea2* exhibited a similar effect to that of myo52Δ, with less Tea1-GFP observed at the cell poles. The average signal intensity decreased by 37% at End 1, 62% at End 2 and 60% in the cytoplasm. Similarly the maximum signal intensity decreased by 75% at End 1, 73% at End 2 but increased by 45% in the cytoplasm. Deletion of *tip1* resulted in a large reduction in Tea1-GFP localisation to the cell poles. This was reflected by decreases in the average signal intensity of 26% at End 1 and 25% at End 2, whilst in the cytoplasm there was a 20% increase. Similarly with the maximum signal intensity there was a 75% decrease at End 1, a 68% decrease at End 2 and a 35% decrease in the cytoplasm.

4.8.3. Gene Deletions Resulting in an Increase in Monopolar Intensity of Tea1-GFP

Deletion of *tea3* resulted in the distribution of Tea1-GFP at the cell poles being different. Rather than having a uniform distribution around the cell tip, quite often a large single foci of Tea1-GFP was observed. Also often Tea1-GFP appeared to have a more monopolar localisation. This was reflected by the average signal intensity decreasing by 32% at End 1 and by 37% at End 2 and in the cytoplasm. The maximum signal intensity decreased by 11% at End 2 and by 36% in the cytoplasm, whilst there was no significant change at End 1. Finally deletion of *tea4* resulted in an increase in monopolar localisation of Tea1-GFP, and there often appeared to be slightly more Tea1-GFP at this single cell pole. The average signal intensity had no significant change at End 1, but decreased by 29% at End 2 and by 15% in the cytoplasm whilst the maximum signal intensity increased by 12% at End 1, whilst decreasing by 18% at End 2 and by 27% in the cytoplasm.

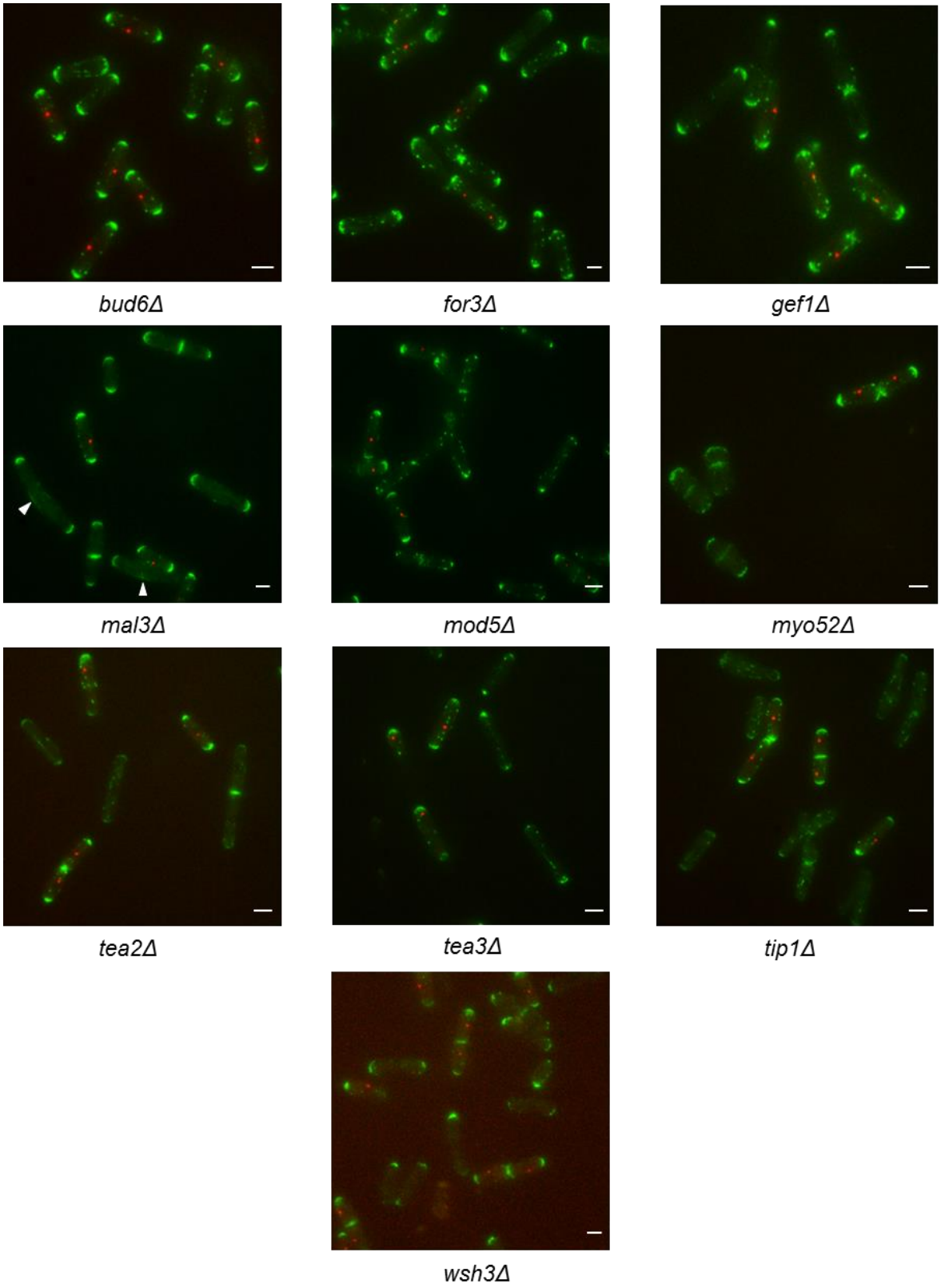

Figure 4.7. Images of cells containing Tea1-GFP and a deletion of one of the polarity genes (as labelled). Images are maximum projections of Z slices 5-25 of a 31 Z slice image. Scale bars 5 µm. n=80 cells.

	End1	End2	Cytoplasm
bud6Δ	-	-	-15%
for3Δ	-	-	-
gef1Δ	-25%	-24%	-45%
mal3Δ	-40%	-26%	+49%
mod5Δ	-53%	-23%	+22%
myo52Δ	-22%	-19%	+26%
tea2Δ	-62%	-60%	+22%
tea3Δ	-32%	-37%	-37%
tea4Δ	-	-29%	-15%
tip1Δ	-58%	-56%	-

Table 4.9. Changes in average signal intensity of Tea1-GFP relative to wild type cells following deletion of polarity genes.

	End1	End2	Cytoplasm
bud6Δ	-	-10%	-16%
for3Δ	-	-	-
gef1Δ	-10%	-13%	-53%
mal3Δ	-66%	-46%	+66%
mod5Δ	-45%	+24%	+163%
myo52Δ	-32%	-38%	-13%
tea2Δ	-75%	-73%	+45%
tea3Δ	-	-11%	-36%
tea4Δ	+12%	-18%	-73%
tip1Δ	-73%	-71%	-15%

Table 4.10. Changes in maximum signal intensity of Tea1-GFP relative to wild type cells following deletion of polarity genes.

4.9. Effect of Polarity Gene Deletions on Tea2-GFP

Tea2 is a kinesin-like protein required for the polarized growth of *S. pombe* (Browning et al. 2000). Similar to Tea1, Tea2 localizes to the ends of the cell and is also seen as cytoplasmic dots on microtubules, and this localization is microtubule dependent (Browning et al. 2000; Busch et al. 2004). It was expected that deletion of *mal3* would abolish Tea2 localisation at the cell poles, as shown previously (Browning & Hackney 2005b). The deletion of other "Tea" proteins was also expected to have an effect, due to improper targeting of microtubules to the cell poles. The effect of deleting each of the polarity genes on the localisation and intensity of Tea2-GFP was investigated and the following results were found.

4.9.1. Gene Deletions Resulting in Increases in the Intensity of Tea2-GFP at Cell Poles

Deletion of *for3* resulted in a large increase in Tea2-GFP localisation to the cell poles. This resulted in the average signal intensity increasing by 65% at End 1, 57% at End 2 and 10% in the cytoplasm. The maximum signal intensity showed a greater effect, with a 97% increase at End 1, 94% at end 2 and an 11% decrease in the cytoplasm. Deletion of *mod5* resulted in Tea2-GFP being less dispersed at the cell poles, with there often being only 1 individual foci at the cell pole, and a possible increase in Tea2-GFP foci on microtubules. However the intensity of these Tea2-GFP foci at the cell poles was increased. This was best shown by the maximum signal intensity where there was a 23% increase at End 1, an 18% increase at End 2 and a 33% increase in the cytoplasm. The average signal intensity were

largely unaffected, with no significant change observed at End 1 or in the cytoplasm, however there was a 13% decrease at End 2. Deletion of *myo52* appeared to result in a slight increase in Tea2-GFP levels within the cell, some cells also appeared to have more cytoplasmic foci of Tea2-GFP on microtubules. The average signal intensity increased by 34% at End 1, by 19% at End 2 and by 46% in the cytoplasm. The maximum signal intensity had a similar pattern with a 14% increase at End 1 and a 21% increase in the cytoplasm, however no significant change was observed at End 2. Deletion of *tea3* resulted in an increase in Tea2-GFP levels both at the cell poles and in the cytoplasm. This lead to the average signal intensity increasing by 28% at End 1, 14% at End 2 and 18% in the cytoplasm. Similarly the maximum signal intensity increased by 21% at End 1, 14% at End 2 and by 20% in the cytoplasm.

4.9.2. Gene Deletions Resulting in Decreases in the Intensity of Tea2-GFP at Cell Poles

Deletion of *bud6* did not have a noticeable effect on Tea2-GFP localisation, however when examining the signal intensity a slight decrease in Tea2-GFP localisation to the cell poles was observed. This was best seen in the maximum signal intensity where there was a 16% decrease at End 1 and a 13% decrease at End 2, whilst no significant change was observed in the cytoplasm. The average signal intensity exhibited no significant changes at End 1 or 2, but there was a 10% increase in the cytoplasm. Deletion of *tea1,* similar to *mod5Δ* resulted in Tea2-GFP being less dispersed at the cell poles, again with there often being only 1 individual foci at the cell pole, and a possible increase in Tea2-GFP foci on microtubules. However the intensity of these Tea2-GFP foci at the cell poles differed, being

less bright in a *tea1Δ.* This was again best shown by the maximum signal intensity where there were decreases of 31% at End 1, 24% at End 2 and an increase of 18% in the cytoplasm. The average signal intensity decreased by 19% at End 1 and increased by 18% in the cytoplasm, whilst no significant change was seen at End 2. Deletion of *mal3* lead to a very large decrease in the amounts of Tea2-GFP at the cell poles, and there was also a complete absence of Tea2-GFP foci on microtubules, this was shown by decreases in the maximum signal intensity of 64% at End 1, 60% at End 2 and 45% in the cytoplasm. This pattern was also observed in the average signal intensity with an 11% decrease observed at End 1, 14% at End 2 however there was a 15% increase in the cytoplasm. Deletion of *tip1* resulted in a complete loss of Tea2-GFP localisation to the cell poles or on microtubules with only cytoplasmic background signal observed. As a result the average signal intensity decreased by 26% at End 1 and by 25% at End 2, whilst there was a 20% increase in the cytoplasm. A much greater effect was seen with the maximum signal intensity, where there was a 75% decrease at End 1, a 68% decrease at End 2 and a 35% decrease in the cytoplasm.

4.9.3. Gene Deletions Resulting in Changes in the Intensity of Tea2-GFP in the Cytoplasm

Deletion of *gef1* appeared to reduce the levels of bright Tea2-GFP foci on microtubules in the cytoplasm with a 42% decrease in the maximum signal intensity observed, whilst no other significant changes were seen. Finally deletion of *tea4* resulted in a decrease in cytoplasmic levels of Tea2-GFP. The average signal intensity showed no significant change at End 1, End 2 or the cytoplasm, however the maximum signal intensity showed a 23% decrease in the cytoplasm whilst there was no significant change at End 1 or End 2.

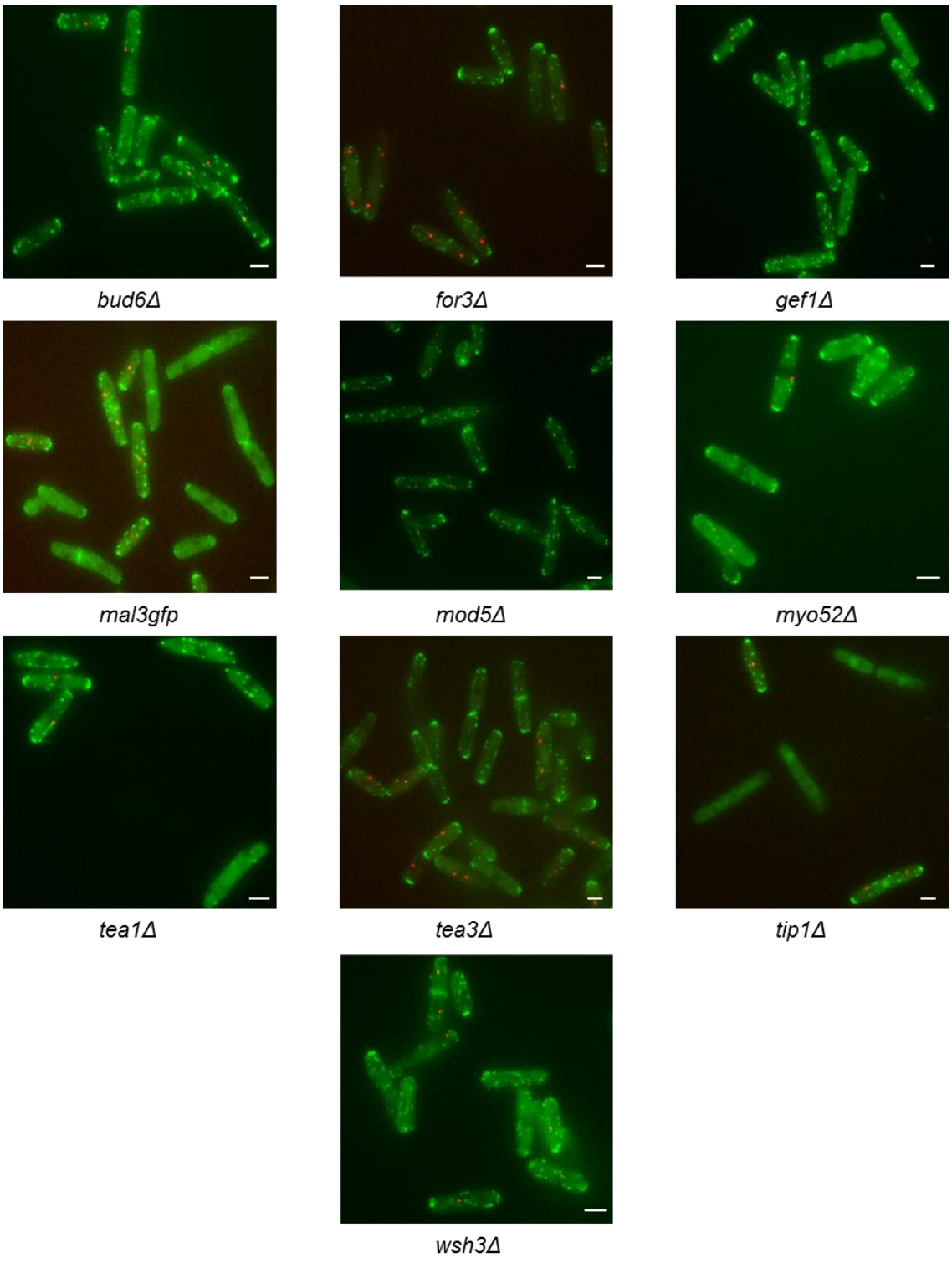

Figure 4.8. Images of cells containing Tea2-GFP and a deletion of one of the polarity genes (as labelled). Images are maximum projections of Z slices 5-25 of a 31 Z slice image. Scale bars 5 µm. n=80 cells.

	End1	End2	Cytoplasm
bud6Δ	-	-	+10%
for3Δ	+65%	+57%	+10%
gef1Δ	-	-	-
mal3Δ	-11%	-14%	+15%
mod5Δ	-	-13%	-
myo52Δ	+34%	+19%	+46%
tea1Δ	-19%	-	+18%
tea3Δ	+28%	+14%	+18%
tea4Δ	-	-	-
tip1Δ	-26%	-25%	+20%

Table 4.11. Changes in average signal intensity of Tea2-GFP relative to wild type cells following deletion of polarity genes.

	End1	End2	Cytoplasm
bud6Δ	-16%	-13%	-
for3Δ	+97%	+94%	-11%
gef1Δ	-	-	-42%
mal3Δ	-64%	-60%	-45%
mod5Δ	+23%	+18%	+33%
myo52Δ	+14%	-	+21%
tea1Δ	+20%	+21%	-14%
tea3Δ	+21%	+14%	+20%
tea4Δ	-	-	-23%
tip1Δ	-75%	-68%	-35%

Table 4.12. Changes in maximum signal intensity of Tea2-GFP relative to wild type cells following deletion of polarity genes.

4.10. Effect of Polarity Gene Deletions on Tea3-GFP

Tea3, similar to Tea1 is a cell end marker that localizes to both the growing and non-growing tips of the cells in a Tea1 and microtubule dependent manner (Arellano, Niccoli & Nurse 2002; Niccoli, Arellano & Nurse 2003). Tea3 is slightly enriched at the non-growing cell end where it has been shown to be required for NETO, resulting in the activation of growth at the previously non-growing end of the cell resulting in bipolarity (Arellano, Niccoli & Nurse 2002). It also localizes to the septum of dividing cells as a late event of cytokinesis, and is required for the correct positioning of the septum (Arellano, Niccoli & Nurse 2002). It was expected that deletion of "Tea" proteins would affect the accumulation of Tea3 at cell poles. In addition, the deletion of the actin associated proteins may have also had an effect, due to the interaction between Tea3 and actin associated proteins in stimulating NETO. The effect of deleting each of the polarity genes on the localisation and intensity of Tea3-GFP was investigated and the following results were found.

4.10.1. Gene Deletions Resulting in Increases in the Intensity of Tea3-GFP at Cell Poles

Deletion of *bud6* had no obvious effect on Tea3-GFP localisation however when examining the intensity it was observed that *bud6Δ* increased the levels of Tea3-GFP at the cell poles. This was reflected by increases in both the average and maximum signal intensity at Ends 1 and 2. The average signal intensity increased by 15% and 17% at End1 and 2 respectively, whilst there was an 18% decrease in the cytoplasm. The maximum signal intensity increased by 21% at End 1 and by 22% at End 2, but there was no significant change in the

cytoplasm. Deletion of *myo52* resulted in an increase in the levels of Tea3-GFP observed throughout the cell with both a brighter accumulation of Tea3-GFP at the cell poles and a higher level of cytoplasmic background. The average signal intensity increased by 43% at End 1, by 28% at End 2 and by 82% in the cytoplasm and similarly the maximum signal intensity increased by 42% at End 1,]17% at End 2 and by 62% in the cytoplasm. Deletion of *tea1* resulted in a slight increase in Tea3-GFP localisation to the cell poles. The average signal intensity increased by 13% at End 2 and decreased by 15% in the cytoplasm whilst there was no significant change at End 1. The maximum signal intensity increased by 20% at End 1 and by 21% at End 2 and again decreased by 14% in the cytoplasm.

4.10.2. Gene Deletions Resulting in Decreases in the Intensity of Tea3-GFP at Cell Poles

Deletion of *mal3* affected the way in which Tea3-GFP was distributed at the cell poles with Tea3-GFP being less uniformly distributed and instead appearing to be an accumulation of lots of very small foci as indicated by the arrows in figure 4.8. There also appeared to be slightly more Tea3-GFP foci in the cytoplasm. This caused no significant change to the average signal intensity at End 1 or 2, but there was a 21% increase in the cytoplasm. However the maximum signal intensity decreased by 32% at both End 1 and End 2, whilst again there was an increase in the cytoplasm, this time of 39%. Deletion of *mod5* resulted in a decrease in Tea3-GFP localisation to the cell poles. This was reflected by the average signal intensity decreasing by 28% at End 1 and 25% at End 2, whilst there was a 15% increase in the cytoplasm. Similarly the maximum signal intensity decreased by 14% at End 1 and 29% at End 2, whilst again there was an increase in the cytoplasm, this time of 24%.

Deletion of *tea2* resulted in a decrease of Tea3-GFP localisation to the cell poles, whilst there also appeared to be more speckles of Tea3-GFP within the cytoplasm as shown by arrows in figure 4.8. This resulted in the average signal intensity decreasing by 20% at End 1 and by 19% at End 2, whilst increasing by 17% in the cytoplasm. Similarly the maximum signal intensity decreased by 40% at End 1 and by 35% at End 2, whilst increasing by 45% in the cytoplasm.

4.10.3. Gene Deletions Resulting in Changes in the Intensity of Tea3-GFP in the Cytoplasm

Deletion of *for3* had little effect on the localisation of Tea3-GFP with only a decrease in cytoplasmic levels of Tea3-GFP observed. There were no significant changes in the average or maximum signal intensity at both End 1 and End 2, however there were decreases in the cytoplasm of 31% and 30% respectively. Deletion of *gef1* had a similar effect to that of *for3Δ* with only a slight decrease in cytoplasmic signal observed. Again there were no significant changes in the average or maximum signal intensity at both End 1 and End 2, however there were decreases in the cytoplasm of 21% and 15% respectively. Deletion of *tip1* had little effect on Tea3-GFP with the only noticeable effect being a slight reduction in cytoplasmic background signal. The average signal intensity showed no significant change at Ends 1 and 2, whilst there was a 23% decrease in the cytoplasm. The maximum signal intensity showed no significant change at End 2 or in the cytoplasm, whilst there was a 15% decrease at End 1.

4.10.4. Gene Deletions Resulting in an Increase in Monopolar Intensity of Tea3-GFP

Finally deletion of *tea4* resulted in a more monopolar localisation of Tea3-GFP with there being an increase in Tea3-GFP levels at this single cell pole. The average signal intensity increased by 48% at End 1 whilst decreasing by 18% and 19% at End 2 and in the cytoplasm respectively. Similarly the maximum signal intensity increased by 50% at End 1 however no significant change was observed at End 2 or in the cytoplasm.

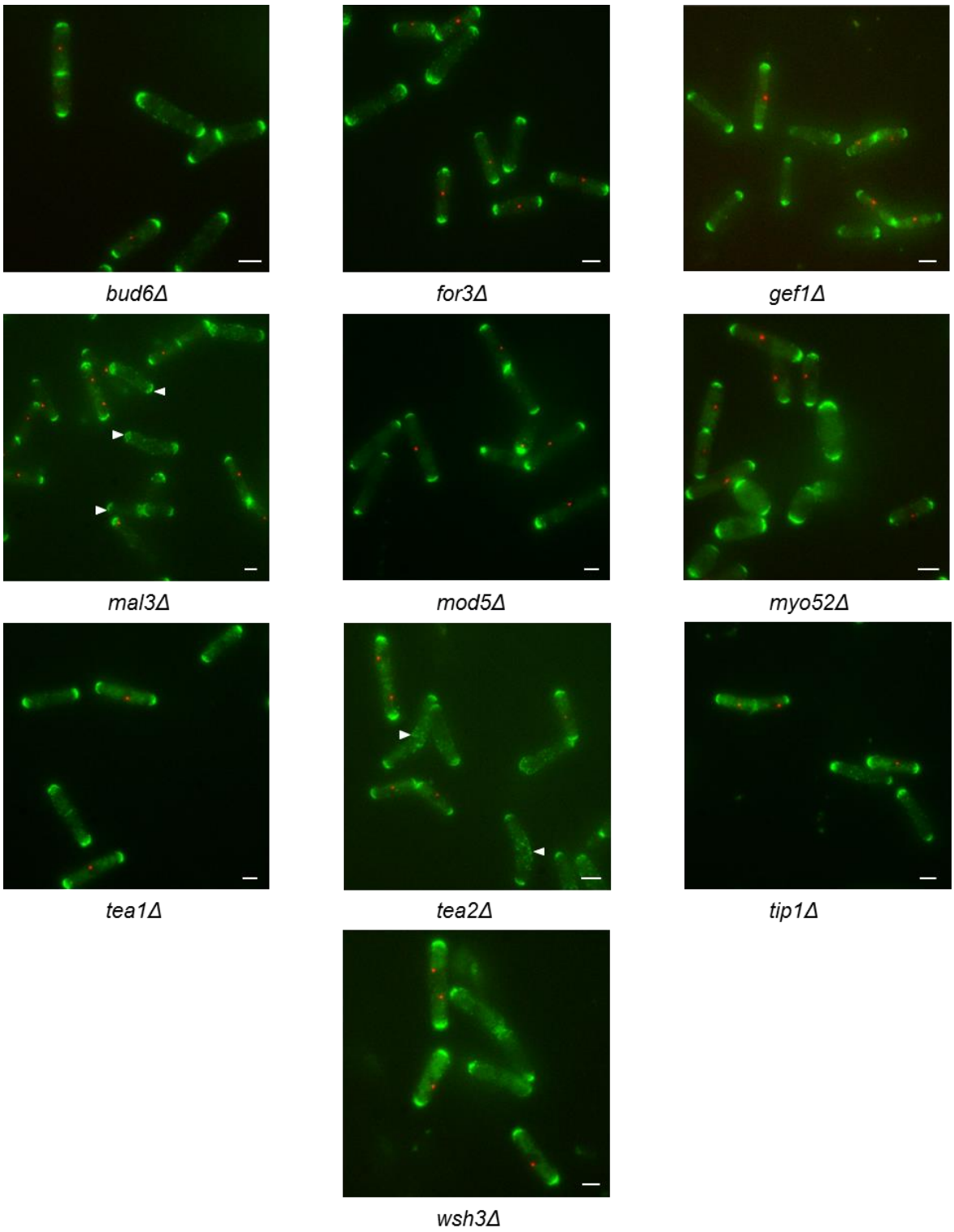

Figure 4.9. Images of cells containing Tea3-GFP and a deletion of one of the polarity genes (as labelled). Images are maximum projections of Z slices 5-25 of a 31 Z slice image. Scale bars 5 µm. n=80 cells.

	End1	End2	Cytoplasm
bud6Δ	+15%	+17%	-18%
for3Δ	-	-	-31%
gef1Δ	-	-	-21%
mal3Δ	-	-	+21%
mod5Δ	-28%	-25%	+15%
myo52Δ	+43%	+28%	+82%
tea1Δ	-	+13%	-15%
tea2Δ	-20%	-19%	+17%
tea4Δ	+20%	-18%	-19%
tip1Δ	-	-	-23%

Table 4.13. Changes in average signal intensity of Tea3-GFP relative to wild type cells following deletion of polarity genes.

	End1	End2	Cytoplasm
bud6Δ	+21%	+22%	-
for3Δ	-	-	-30%
gef1Δ	-	-	-15%
mal3Δ	-32%	-32%	+39%
mod5Δ	-14%	-29%	+24%
myo52Δ	+42%	+17%	+62%
tea1Δ	+20%	+21%	-14%
tea2Δ	-40%	-35%	+45%
tea4Δ	+50%	-	-
tip1Δ	-15%	-	-

Table 4.14. Changes in maximum signal intensity of Tea3-GFP relative to wild type cells following deletion of polarity genes.

4.11. Effect of Polarity Gene Deletions on Tea4-GFP

Tea4 is a cell polarity factor essential for the bipolar localization and function of structures containing Tea1 and For3 (Martin et al. 2005). It localizes to microtubule plus ends and the cell ends in a Tea1 dependent manner, where it is required for the localization of For3 at the cell tip, specifically during initiation of bipolar growth (NETO) (Tatebe et al. 2005; Martin et al. 2005). During NETO, formation of a protein complex that includes Tea1, Tea4 and For3 is necessary for the establishment of cell polarity and localized actin assembly at new cell ends (Tatebe et al. 2005; Martin et al. 2005). It was expected that deletion of "Tea" proteins would affect the accumulation of Tea4 at cell poles. In addition, the deletion of the actin associated proteins may have also had an effect, due to the interaction between Tea4 and actin associated proteins in stimulating NETO. The effect of deleting each of the polarity genes on the localisation and intensity of Tea4-GFP was investigated and the following results were found.

4.11.1. Gene Deletions Resulting in no Significant Changes in Intensity of Tea4-GFP

Deletion of *tea3* had no obvious effect on Tea4-GFP localisation. The only effect seen when examining signal intensity was a 10% decrease in the maximum signal intensity at End 2. The average signal intensity and the maximum signal intensity at End 1 and in the cytoplasm showed no significant changes. Deletion of *bud6* did not affect Tea4-GFP localisation, and there was no significant change in any of the average or maximum signal intensities.

4.11.2. Gene Deletions Resulting in Increases in the Intensity of Tea4-GFP at Cell Poles

Deletion of *myo52* resulted in higher levels of Tea4-GFP throughout the cell. This was reflected by increases in both the average and maximum signal intensity at all locations in the cell however the increase at the cell poles was especially noticeable. The average signal intensity increased by 65% at End 1 and 58% at End 2 and in the cytoplasm. The maximum signal intensity increased by 78% at End 1, 65% at End 2 and 59% in the cytoplasm.

4.11.3. Gene Deletions Resulting in Decreases in the Intensity of Tea4-GFP at Cell Poles

Deletion of *for3* resulted in a decrease in Tea4-GFP throughout the cells, though it still localised to the cell poles. The cells also did not possess a typical *for3Δ* phenotype, with the cells being long rather than slightly shorter and wider than wild type cells. The average signal intensity decreased by 31% at End 1, 34% at End 2 and 44% in the cytoplasm. Similarly the maximum signal intensity decreased by 35% at End 1, 37% at End 2 and 43% in the cytoplasm. Deletion of *mal3* almost completely abolished Tea4-GFP localisation to the cell poles, however it did still localise to the site of division. This resulted in the maximum signal intensity decreasing by 37% at End 1 and 58% at End 2, whilst there was no significant change in the cytoplasm. The average signal intensity decreased by 14% at End 2, but there was no significant change at End 1 or in the cytoplasm. Deletion of *tea1* resulted in a loss of Tea4-GFP localisation to the cell poles, with only cytoplasmic background signal

observed. The average signal intensity decreased by 14% at both End 1 and End 2 whilst there was no significant change in the cytoplasm. The maximum signal intensity decreased by 56% at End 1 and 50% at End 2 whilst again there was no significant change in the cytoplasm. Deletion of *tea2* had a similar effect. The average signal intensity only changed in the cytoplasm where there was a 10% increase. However the maximum signal intensity decreased by 46% at End 1 and 41% at End 2 whilst increasing by 11% in the cytoplasm. Finally deletion of *tip1* resulted in a decrease in the amount of Tea4-GFP localising to the cell poles. As a result the average signal intensity decreased by 15% at End 1 and 21% at End 2, whilst there was no significant change in the cytoplasm. Similarly the maximum signal intensity decreased by 47% at End 1 and 44% at End 2 whilst again no significant change was observed in the cytoplasm.

4.11.4. Gene Deletions Resulting in Changes in the Intensity of Tea4-GFP in the Cytoplasm

Deletion of *gef1* had no obvious effect on Tea4-GFP localisation. The average signal intensity increased by 19% at End 1 and in the cytoplasm and by 20% at End 2. The maximum signal intensity only increased by 17% in the cytoplasm whilst there was no significant change at End 1 or End 2. As only the cytoplasm showed an increase in maximum signal intensity, the increase in average signal intensity at End 1 and 2 was probably due to higher cytoplasmic levels in the measurement area rather than an actual increase in Tea4-GFP at the cell poles. Deletion of *mod5* resulted in Tea4-GFP being less dispersed around the curvature of the cell pole, instead more single foci were observed. There also appeared to be more Tea4-GFP on microtubules. The average signal intensity showed no significant

change at End 1 or 2 however there was a 15% increase in the cytoplasm. Similarly the maximum signal intensity increased by 42% in the cytoplasm, whilst again there was no significant change at End 1 or 2.

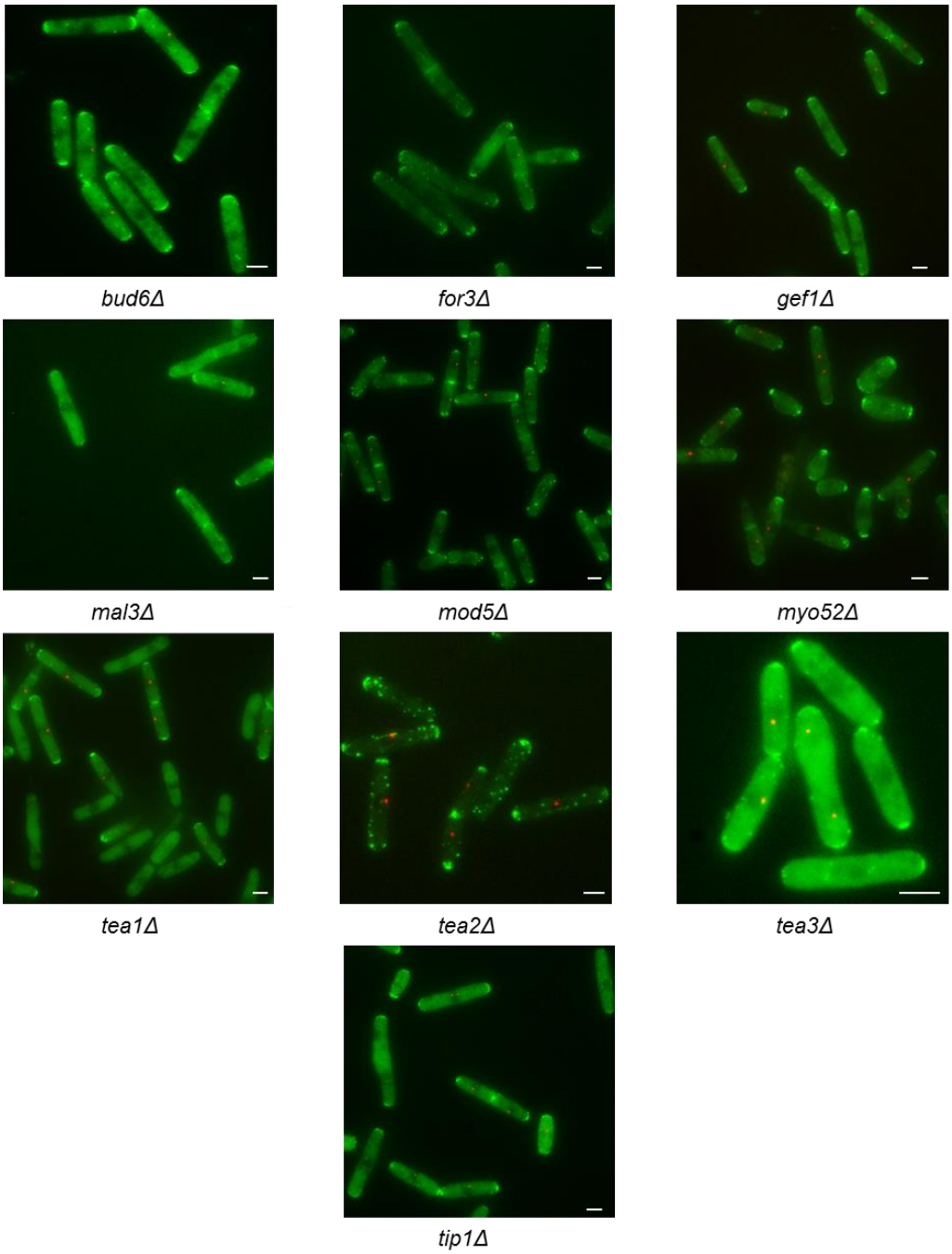

Figure.4.10. Images of cells containing Tea4GFP and a deletion of one of the polarity genes (as labelled). Images are maximum projections of 31 Z slices. Scale bars 5 µm. n=80 cells.

	End1	End2	Cytoplasm
bud6Δ	-	-	-
for3Δ	-31%	-34%	-44%
gef1Δ	+19%	+20%	+19%
mal3Δ	-	-14%	-
mod5Δ	-	-	+15%
myo52Δ	+65%	+58%	+58%
tea1Δ	-14%	-14%	-
tea2Δ	-	-	+10%
tea3Δ	-	-	-
tip1Δ	-15%	-21%	-

Table 4.15. Changes in average signal intensity of Tea4-GFP relative to wild type cells following deletion of polarity genes.

	End1	End2	Cytoplasm
bud6Δ	-	-	-
for3Δ	-35%	-37%	-43%
gef1Δ	-	-	+17%
mal3Δ	-37%	-42%	-
mod5Δ	-	-	+42%
myo52Δ	+78%	+65%	+59%
tea1Δ	-56%	-50%	-
tea2Δ	-46%	-41%	+11%
tea3Δ	-	-10%	-
tip1Δ	-47%	-44%	-

Table 4.16. Changes in maximum signal intensity of Tea4-GFP relative to wild type cells following deletion of polarity genes.

4.12. Effect of Polarity Gene Deletions on Tip1-gfp

Tip1 is a microtubule end factor that stabilizes and targets microtubules to the cell ends (Brunner & Nurse 2000). Tip1 is transported along microtubules to the tips by the Tea2 kinesin (Busch et al. 2004) where it delays microtubule catastrophe until the microtubules reach the membrane at the cell tips. Tip1 prevents catastrophe when growing microtubule tips reach other regions of the membrane, indicating that Tip1 can distinguish between the cell tips and other regions of the cell membrane (Busch & Brunner 2004). It was expected that deletion of *myo52* would result in an increase in Tip1 levels at the cell poles, as shown previously (Martín-García & Mulvihill 2009). It would be possible for deletion of *for3* to have a similar effect, due to a loss of Myo52 accumulation at the cell poles. Deletion of "Tea" proteins could also have an effect. The effect of deleting each of the polarity genes on the localisation and intensity of Tip1-GFP was investigated and the following results were found.

4.12.1. Gene Deletions Resulting in Increases in the Intensity of Tip1-GFP at Cell Poles

Deletion of *bud6* resulted in an increase in the levels of Tip1-GFP throughout the cells, particularly at the cell poles. The average signal intensity increased by 47% at End 1, 35% at End 2 and 23% in the cytoplasm. Similarly the maximum signal intensity increased by 18% at End 1, 23% at End 2 and 33% in the cytoplasm. Deletion of *myo52* lead to increased levels of Tip1-GFP throughout the cells, especially at the cell poles. The average signal intensity increased by 63% at End 1, 44% at End 2 and by 45% in the cytoplasm with similar

increases observed for the maximum signal intensity with an increase of 25% at both Ends 1 and 2 and of 18% in the cytoplasm. Deletion of *tea1* resulted in Tip1-GFP being prevented from properly accumulating at the cell poles, and there was the appearance of multiple bright foci in the cells, including at the cell poles. This was reflected by increases in average signal intensity of 22% at End 1, 12% at End 2 and 54% in the cytoplasm. Similarly the maximum signal intensity increased by 39% at End 1, 38% at End 2 and 103% in the cytoplasm. These increases at Ends 1 and 2 were most probably due to extremely bright individual foci at a cell pole. Deletion of *tea3* resulted in an increase in Tip1-GFP levels at the cell poles and brighter foci were observed in the cytoplasm on microtubules. This resulted in the average signal intensity increasing by 33% at End 1 and by 26% at End 2, with no significant change seen in the cytoplasm. The maximum signal intensity increased by 41% at End 1, 38% at End 2 and by 47% in the cytoplasm.

4.12.2. Gene Deletions Resulting in Decreases in the Intensity of Tip1-GFP at Cell Poles

Deletion of *for3* resulted in reduced levels of Tip1-GFP at the cell poles, and as had been observed with some other GFP tagged polarity proteins the cells were elongated rather than shorter than wild type cells. Due to the reduction in Tip1-GFP at the cell poles the average signal intensity decreased by 20% at End 1 and 15% at End 2, whilst there was no significant change in the cytoplasm. Similarly the maximum signal intensity decreased by 45% at both End 1 and End 2, with again no significant change observed in the cytoplasm. Deletion of *gef1* had little effect on Tip1-GFP, with only a slight reduction in Tip1-GFP signal at the cell poles observed. There were no significant changes in the average signal intensity,

whilst the maximum signal intensity decreased by 18% at End 1 and 19% at End 2, with no significant change observed in the cytoplasm. Deletion of *mal3* resulted in a large decrease in Tip1-GFP accumulation at the cell poles. The average signal intensity decreased by 31% at End 1 and 26% at End 2 whilst there was a 14% increase in the cytoplasm. The maximum signal intensities all decreased, with a 63% decrease observed at both End 1 and End 2, and a 35% decrease observed in the cytoplasm. Deletion of *tea2* also resulted in a dramatic decrease in Tip1-GFP levels in the cells, with no Tip1-GFP observed at the cell poles and only faint speckles seen on microtubules around the nuclei of cells (shown by arrow in figure 4.11). The average signal intensity decreased by 31% at End 1 and 20% at End 2 whilst increasing by 47% in the cytoplasm. The effect on maximum signal intensity was more severe with an 82% decrease observed at End 1, 78% at End 2 and 77% in the cytoplasm.

4.12.3. Gene Deletions Resulting in Changes in the Intensity of Tip1-GFP in the Cytoplasm

Deletion of *mod5* appeared to prevent Tip1-GFP from properly accumulating at the cell poles as was seen in a *tea1Δ*, which was coupled with the appearance of multiple bright foci in the cells, including at the cell poles. This lead to increases in the cytoplasmic signal intensity, however there was not much effect at the cell ends. The average signal intensity increased by 43% in the cytoplasm and decreased by 11% at End 1, however no significant change was observed at End 2. The maximum signal intensity showed a greater increase of 95% in the cytoplasm, but no significant change was seen at End 1 or 2.

4.12.4. Gene Deletions Resulting in an Increase in Monopolar Intensity of Tip1-GFP

Finally deletion of *tea4* resulted in a more monopolar localisation of Tip1-GFP where a large amount would accumulate at 1 cell pole and small individual foci were observed at the opposite cell pole. This was shown by increases in both the average and maximum signal intensity at End 1, by 48% and 38% respectively. No significant changes were observed at End 2 or in the cytoplasm.

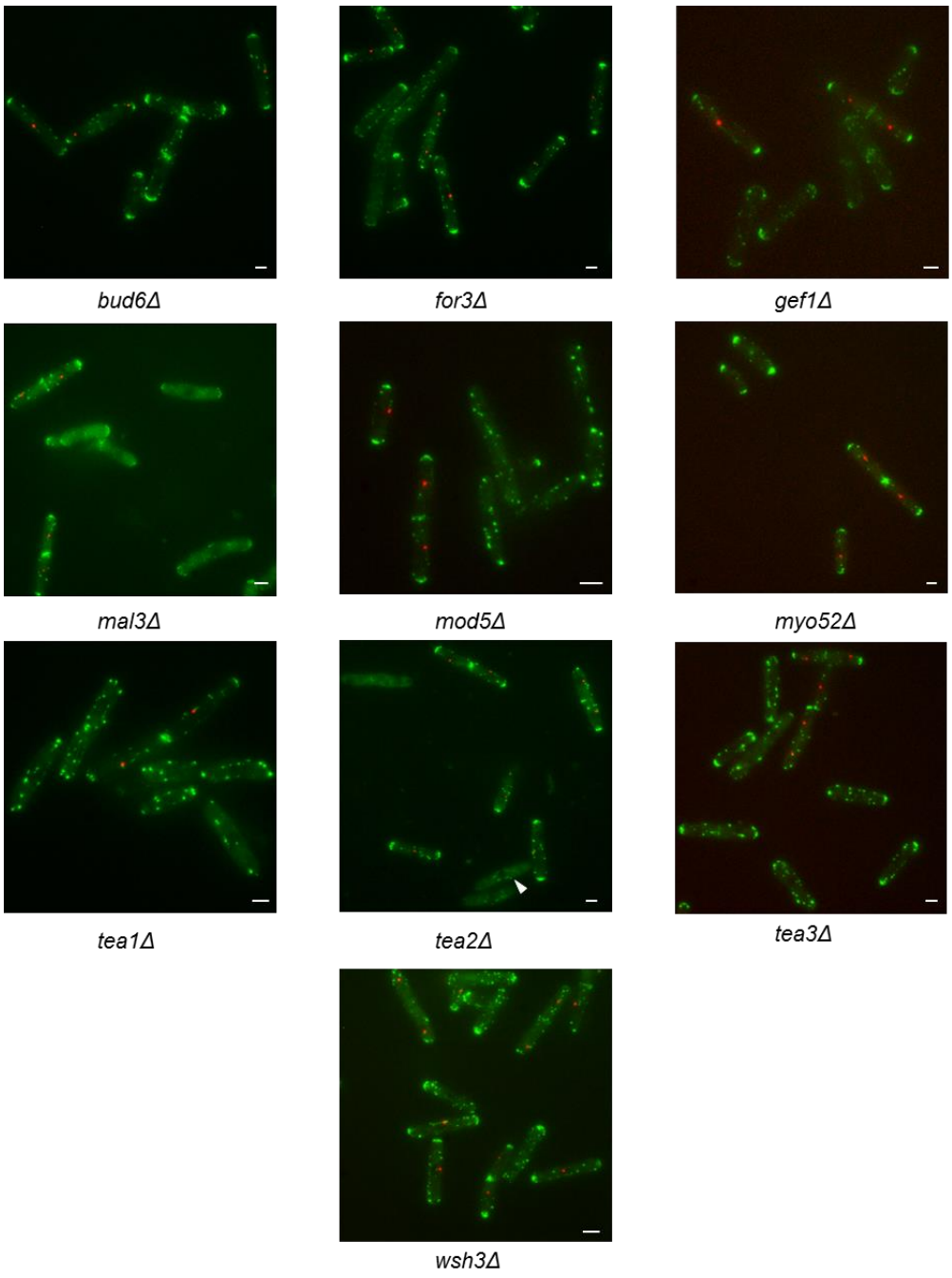

Figure 4.11. Images of cells containing Tip1-GFP and a deletion of one of the polarity genes (as labelled). Images are maximum projections of Z slices 5-25 of a 31 Z slice image. Scale bars 5 µm. n=80 cells.

	End1	End2	Cytoplasm
bud6Δ	+47%	+35%	+23%
for3Δ	-20%	-15%	-
gef1Δ	-	-	-
mal3Δ	-	-14%	-
mod5Δ	-11%	-	+43%
myo52Δ	+63%	+44%	+45%
tea1Δ	-14%	-14%	-
tea2Δ	-	-	+10%
tea3Δ	+33%	+26%	-
tea4Δ	+48%	-	-

Table 4.17. Changes in average signal intensity of Tip1-GFP relative to wild type cells following deletion of polarity genes.

	End1	End2	Cytoplasm
bud6Δ	+18%	+23%	+33%
for3Δ	-45%	-45%	-
gef1Δ	-18%	-19%	-
mal3Δ	-63%	-63%	-35%
mod5Δ	-	-	+98%
myo52Δ	+25%	+25%	+18%
tea1Δ	+39%	+38%	+103%
tea2Δ	-82%	-78%	-23%
tea3Δ	+41%	+38%	+47%
tea4Δ	+38%	-	-

Table 4.18. Changes in maximum signal intensity of Tip1-GFP relative to wild type cells following deletion of polarity genes.

4.13. Summary

These data have shown that the regulation of polarised growth in fission yeast is very complex, with a large number of proteins from both the actin and microtubule cytoskeletons playing key roles. These data suggest that the polarity proteins all have involvement in the transport, recruitment, tethering and turnover of each other most likely through the formation of multi protein complexes as suggested previously (Feierbach et al. 2004; Behrens & Nurse 2002; Bicho et al. 2010; Glynn et al. 2001; Martin et al. 2005), with deletions of one polarity protein often having a significant effect on the localisation and abundance of other proteins. The deletion of certain polarity proteins appeared to have more noticeable effects than others, with clear patterns observed when *myo52, mal3, tea2, tea3, tea4 and tip1* were deleted. Deletion of *myo52* resulted in an apparent increase in the levels of a large number of microtubule associated polarity proteins (Tea2, Tea3, Tea4, Tip1). It has previously been shown that Myo52 regulates ubiquitin-dependent degradation of Tip1 (Martín-García & Mulvihill 2009), so it may be that Myo52 also plays a similar role with other microtubule associated polarity proteins. Deletion of both *mal3* and *tea2* appeared to prevent the transport of microtubule associated polarity proteins to the cell poles, with the localisation of Mod5, Tea1, Tea3, Tea4, Tip1 all affected. As Tea2 is a kinesin it is probable that it transports these other polarity proteins along microtubules to the cell poles, so it's deletion would prevent this transport. Similarly Mal3 has previously been shown to regulate Tea2 function by recruiting it to the microtubule, with deletion of *mal3* abolishing Tea2 localisation to microtubules, leading to a similar effect on microtubule associated polarity proteins as a *tea2Δ.* Finally deletion of Tea3 and Tea4 both appeared to promote a more monopolar localisation of a large number of polarity proteins. Both Tea3

and Tea4 have been shown to play key roles in promoting NETO, with deletion of either resulting in cells growing in a monopolar fashion (Arellano, Niccoli & Nurse 2002; Martin et al. 2005; Tatebe et al. 2005). Therefore it is not surprising that their deletion leads to monopolar localisation of most polarity proteins.

Chapter 5: Investigation into the Function of the Class V Myosin Myo52

5.1. Introduction

The fission yeast type V myosin Myo52 plays a key role in the growth of the cell, transporting a diverse range of cargoes around the cell via actin cables. This myosin consists of three distinct regions, the cargo binding tail region, the neck region which contains binding sites for light chains and calmodulins and the head region which contains the ATPase motor activity of the protein. Previous studies have shown that Myo52 transport of cargoes along actin filaments can be re-directed onto microtubules by fusing the cargo binding tail region of Myo52 to the motor containing head region of the fission yeast kinesin Tea2 (Lo Presti & Martin 2011). In order to further understand Myo52 function and its interaction with actin cables that allow it to transport various cellular cargoes a similar set of experiments were proposed, in which the cargo binding Myo52 tail region would be fused to various Myosin heads from both *S. pombe* and *Drosophila melanogaster.* The Myo52 tail region (hereby referred to as Myo52T) was cloned into the fission yeast expression vector *pREP41* in conjunction with a C-terminal GFP tagging vector (Craven et al. 1998). This would allow the localisation and any movement of the myosin chimeras to be observed by fluorescence microscopy. The fission yeast Myo52 and Myo51 heads (Myo52H and Myo51H) as well as the *D. melanogaster* MyoV (Didum) and MyoVI (Jaguar) heads were then cloned into the subsequent *pREP41myo52T-gfp* vector. MyoVI is a unique myosin in that it moves towards the pointed end of the actin filament, unlike most other myosins which move towards the barbed end of the actin filament (Wells et al. 1999). This ability to move “backwards” along the actin filament is due to an additional 53 amino acid in the neck region, referred to as the inverter domain, which rotates the direction of the lever arm by 180° (Wells et al. 1999; Tsiavaliaris, Fujita-Becker & Manstein 2004; Ménétrey

et al. 2005). In order to fully examine the function of the MyoVI head in these chimeras the head was cloned into the *pREP41myo52T-gfp* vector both with and without the inverter domain. These constructs are shown in figure 5.1 below.

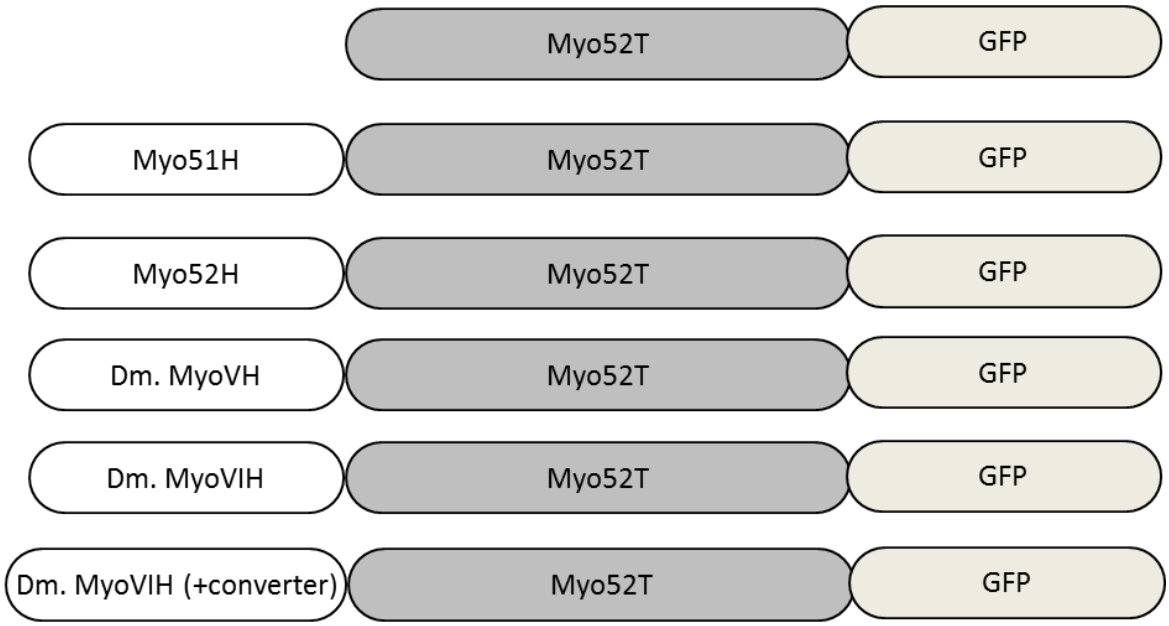

Figure 5.1. A cartoon representing chimera proteins used. The tail domain of fission yeast Myo52 with a -GFP tag located at the C-terminus. Different myosin head domains were placed before the Myo52T at the N-terminus of the chimera protein.

5.2. The Myosin Chimeras Cannot Complement Myo52 Function

In order to determine the functionality of the various myosin chimeras, a *myo52Δ* strain of *S. pombe* was transformed with plasmids containing each of the myosin chimera GFP fusions. The cells were first observed by light microscopy to examine the morphology of the cells. A *myo52Δ* strain exhibits a strong cell morphology defect in which the cells are much shorter than their usual ~14 µm average cell length, whilst also being much wider than the average 4 µm diameter of wild type cells. This leads to cells having a short, stubby appearance with some appearing to have lost all polarity and being an almost spherical shape. As can be seen in figure 5.2 only the expression of the Myo52H-Myo52T-GFP chimera, effectively restoring Myo52 function was able to rescue the *myo52Δ* phenotype, with the cells still having a short, stubby appearance when expressing any of the other chimeras.

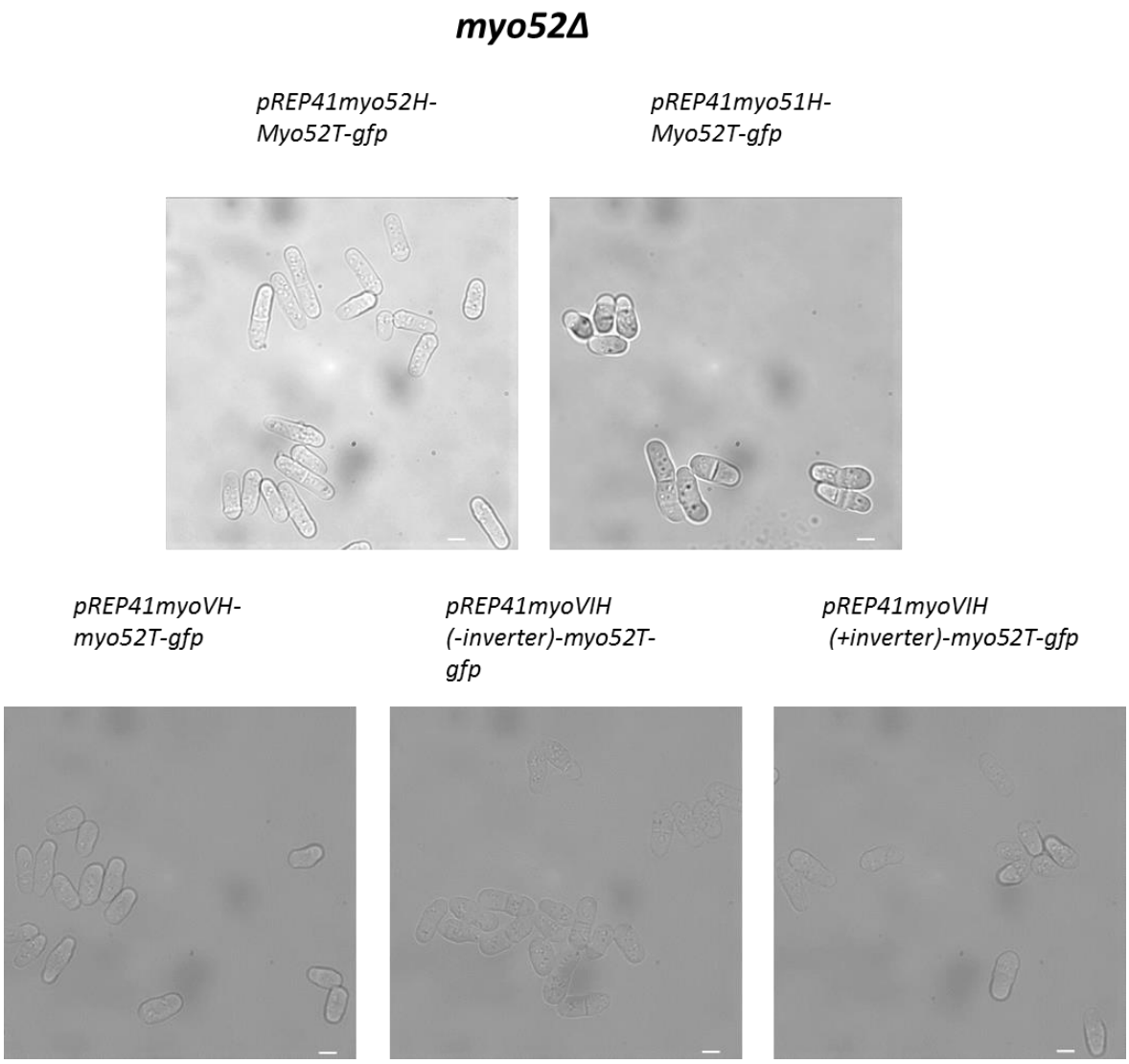

Figure 5.2. Phase images of *myo52Δ* cells expressing myosin chimeras. Only the chimera containing *S. pombe* Myo52H was able to rescue the *myo52Δ* phenotype, with the expression of all of the other chimeras still resulting in the cells being short and stubby. Scale bars 5 µm.

In order the further explore the functionality of the myosin chimeras and why they were unable to rescue the *myo52Δ* phenotype the cells were observed under the fluorescence microscope. Figure 5.3 shows that as expected the Myo52H-Myo52T-GFP chimera localised to the poles of the cells like wild type Myo52, and that it also moved around on actin cables. Both the Myo51H-Myo52T-GFP and MyoVH-Myo52T-GFP chimeras were seen to localise

to distinct foci throughout the cell, not at the cell tips but these foci were non-motile. Both MyoVIH-Myo52T-GFP chimeras (with and without the inverter domain) displayed varied localisation, with the construct containing the inverter domain having no discrete localisation and the construct without the inverter domain localising to discrete foci, however these were less intense than those observed for other chimeras.

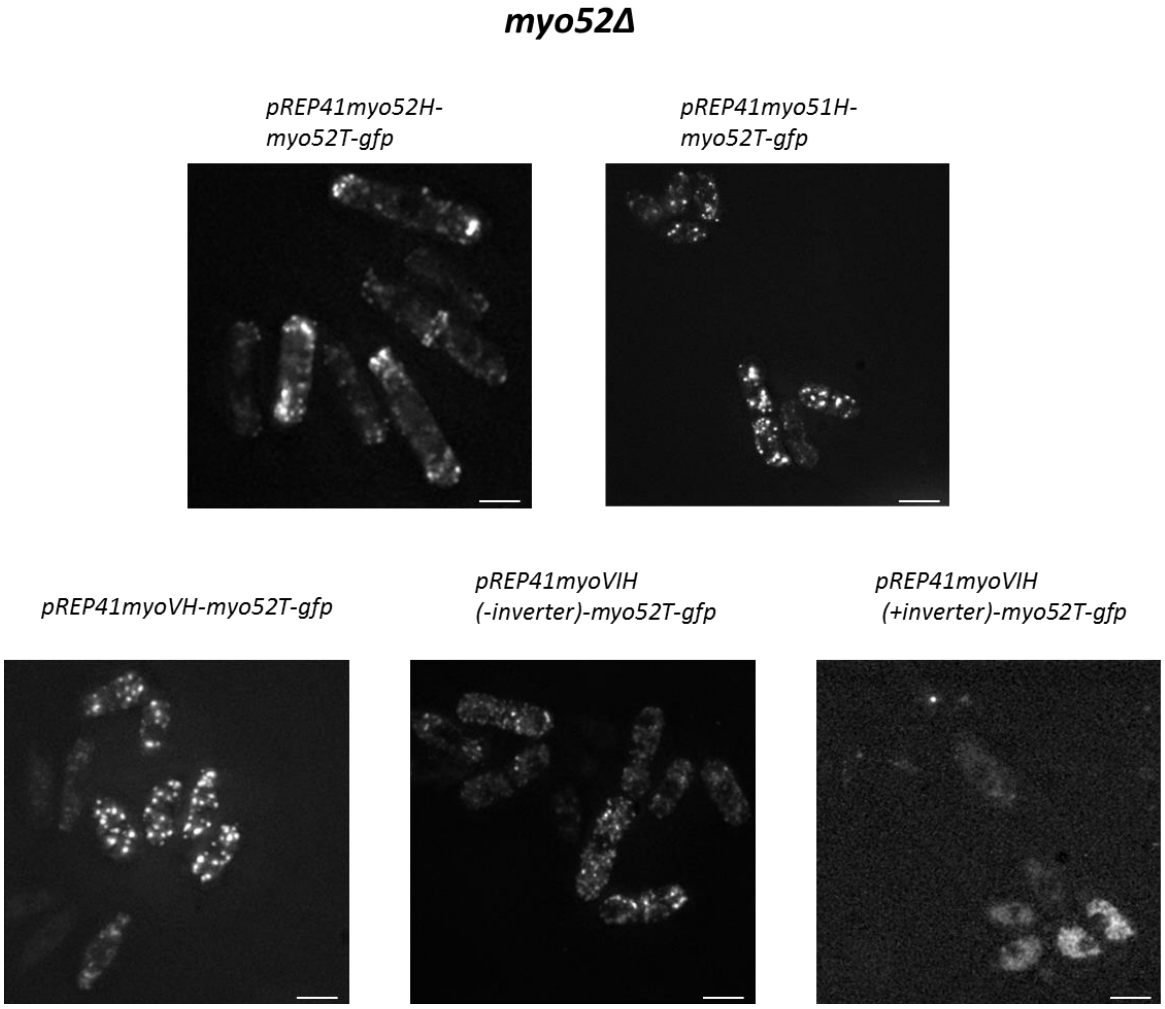

Figure 5.3. Maximum projection images (31 Z slice) of *myo52Δ* cells expressing myosin chimera proteins. The chimeras containing the *D. melanogaster* MyoVIH both with and without the inverter domain had little or no discrete localisation within the cells. The chimeras containing *S. pombe* Myo51H and *D. melanogaster* MyoVH localised to discrete non-motile foci distributed throughout the cell, whilst the chimera containing *S. pombe* Myo52H localised to the cell poles and moved around the cells. Scale bars 5 µm.

5.3. Chimeras Consisting of Other Class V Myosin Head Domains are Able to Interact with Endogenous Myo52

The function of the myosin chimeras was further investigated, in particular to understand why both the Myo51H-Myo52T-GFP and MyoVH-Myo52T-GFP chimeras localised to distinct foci, presumably on actin filaments in a *myo52Δ* strain, yet did not localise to the cell tips as Myo52 does. In order to examine this further a *myo52-tdTomato* strain was transformed with plasmids containing the myosin chimeras. The localisation of each of the chimeras was then examined again by fluorescence microscopy. Again the Myo52H-Myo52T-GFP chimera was found localising to cell tips whilst also moving around the cell. Both of the MyoVIH-Myo52T-GFP chimeras had the same localisation as that observed in the *myo52Δ* strain, with GFP signal dispersed throughout the cytoplasm. Interestingly, both the Myo51H-Myo52T-GFP and MyoVH-Myo52T-GFP chimeras had a different localisation to that observed in the *myo52Δ* strain, with both localising to the cell tips. Multi-wavelength analysis revealed that both of these chimeras co-localised with endogenous Myo52, suggesting that these chimeras were able to dimerise with Myo52-tdTomato via the coiled-coil region (Grallert et al. 2007) as shown in figure 5.4.

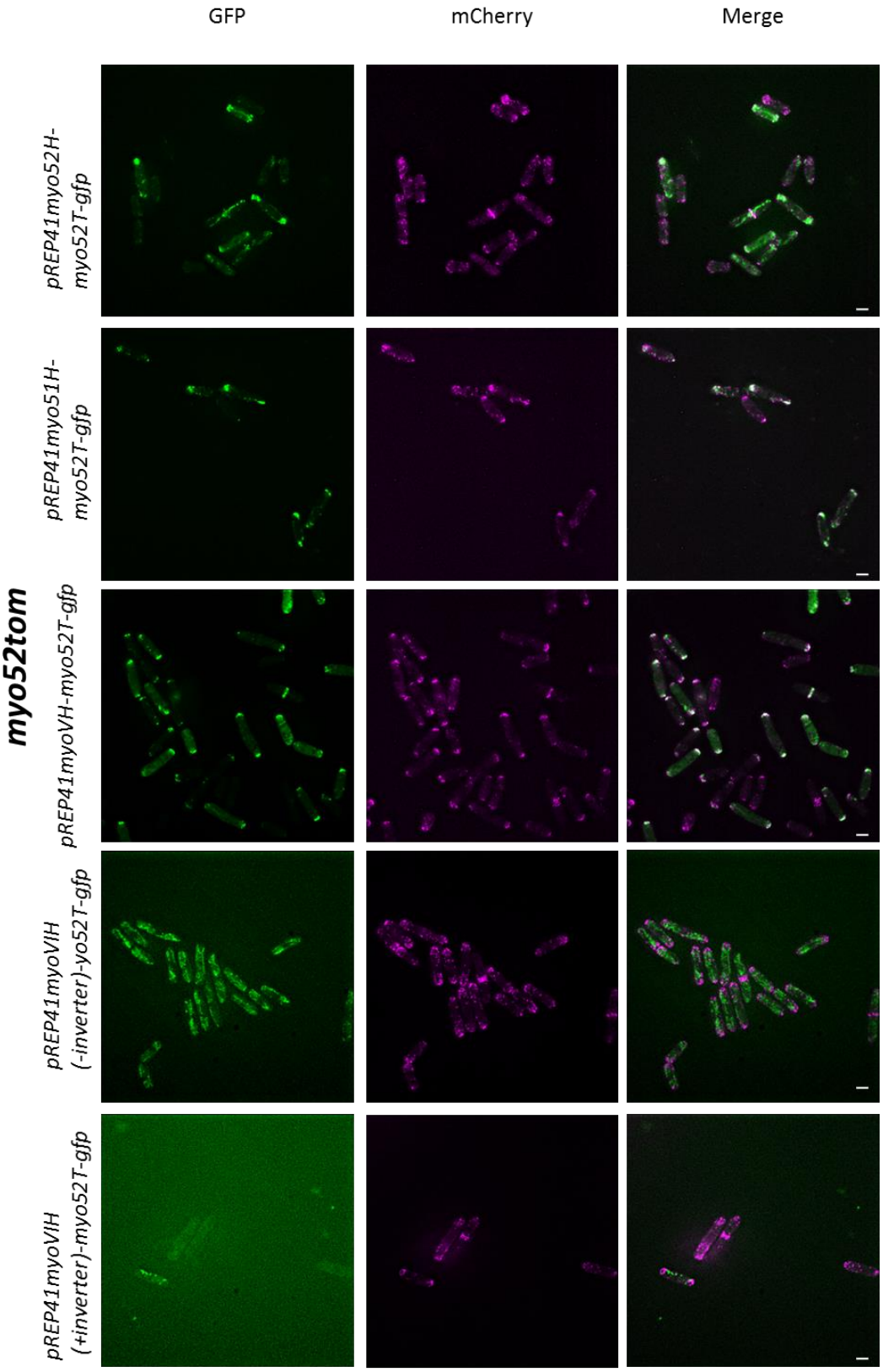

Figure 5.4. Maximum projection images (31 Z slice) of *myo52td-tdTomato* cells expressing the myosin chimeras. Chimeras containing the *S. pombe* Myo51H or Myo52H and the *D. melanogaster* MyoVH colocalised with Myo52td-tdTomato, whilst the chimeras containing *D. melanogaster* MyoVIH had no discrete localisation. Scale bars 5 µm.

In addition to this co-localisation of certain chimeras with the endogenous Myo52-tdTomato, foci were seen to be moving in a myosin V like manner in the cells, however chimeras containing Myo51H or MyovH appeared to move slower and over shorter distances, as shown in figure 5.5 below.

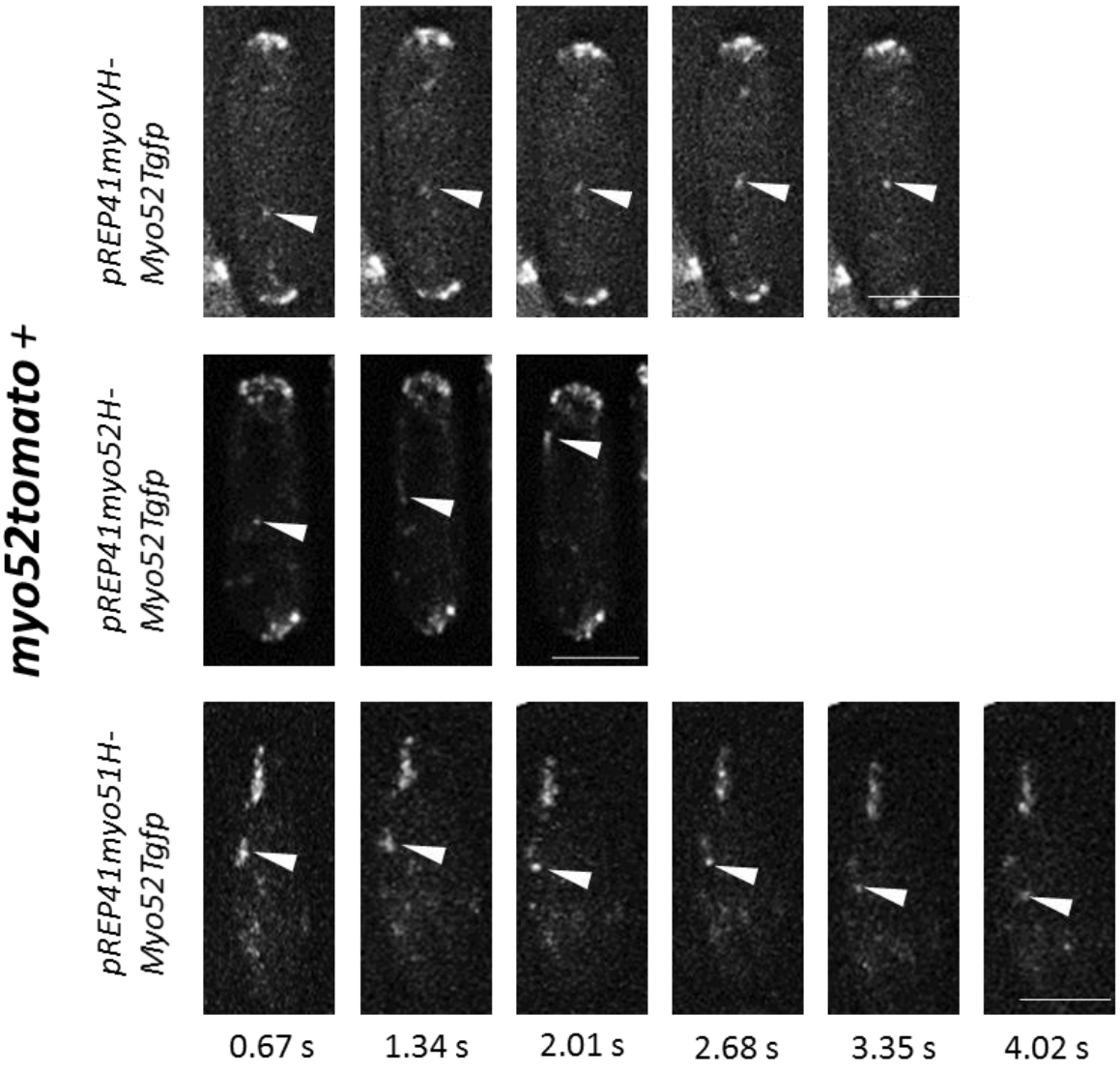

Figure 5.5. Maximum projection time points (13 Z slices) of *myo52-tdTomato* cells expressing chimeras containing either the *S. pombe* Myo52 or Myo52 head or the *D. melanogaster* MyoV head. The GFP signal of the myosin chimera is shown. Foci of all 3 chimeras are seen moving in the cell, however chimeras containing Myo51 or MyoV appear to move slower and over shorter distances. Images were taken at 0.67 second intervals. Scale bars 5 µm.

5.4. Summary

These data have shown that whilst chimeras containing the *S. pombe* Myo52Tail and different myosin heads can be generated and expressed in *S. pombe* they are not able to complement Myo52 function. Their expression does not result in a rescue of the *myo52Δ* phenotype and their localisation is random throughout the cells, with no movement observed. When expressed in *myo52-tdTomato* cells, chimeras containing a type V myosin head appeared to be able to dimerise with the endogenous Myo52 -tdTomato, resulting in the localisation of these chimeras to the cell poles and movement of foci was observed in these cells. However, chimeras containing either the *S. pombe* Myo51H or *D. melanogaster* MyoVH appeared to travel shorter distances within the cell and at much lower speeds than the chimera containing Myo52 (essentially wild-type Myo52). Chimeras expressing the *D. melanogaster* MyoVIH both with and without its inverter domain did not appear able to dimerise with the endogenous Myo52 in the same manner.

Chapter 6: Discussion

6.1: Regulation of the Actin Cytoskeleton by Formins.

Over the last 15-20 years our understanding of the actin cytoskeleton and how it is regulated has increased greatly, with the identification of key actin nucleators such as the Arp2/3 complex (Mullins, Heuser & Pollard 1998) and formins (Woychik et al. 1990; Castrillon & Wasserman 1994; Evangelista et al. 1997; Feierbach & Chang 2001; Chang, Drubin & Nurse 1997) being highly significant. Whilst the overall function of formins as actin nucleators has been identified, research is still ongoing to gain a thorough understanding of their function and how different formins are specialised to carry out a specific role. In fission yeast a recent study has shown that the 2 formins involved in the vegetative growth cycle, For3 and Cdc12 have distinct actin assembly properties (Scott, Neidt & Kovar 2011). This study has provided further information on the properties of these formins, as well as identifying a novel role in the organisation of the actin cytoskeleton.

6.1.1 Formin Function is not Restricted by Cellular Location or Cell Cycle Stage.

In this study the localisation of the formins For3 and Cdc12 was modified by fusing them to either the cell end marker Tea1 or a portion of the tail domain of the myosin motor Myo2. This had the effect of localising them to either the cell poles, or the CAR respectively. The function of these formin fusion proteins was then examined in strains lacking the relevant formin, for example the Tea1-Cdc12 fusion was examined in a *for3Δ* strain whilst a Myo2T-For3 fusion was examined in a temperature sensitive *cdc12-112* strain at the restrictive temperature. Both of these experiments revealed that by altering the localisation of these

formins they were able to almost completely (Tea1-Cdc12) or at least partially (Myo2T-For3) complement each other's function. A further experiment using a Psy1-For3 chimera to localise For3 to the plasma membrane around the entire cell also resulted in an increase in the number of interphase actin cables within cells. This suggests that the function of these formins is not restricted by their cellular location. Similarly, these findings suggest that the function of each formin is not cell cycle dependent. The primary role of For3 is to nucleate cytoplasmic actin cables during interphase, whilst Cdc12 is responsible for the nucleation of actin filaments for incorporation into the CAR during mitosis (Feierbach & Chang 2001; Kovar et al. 2003; Wu et al. 2006) however these experiments have shown that For3 is able to partially nucleate actin filaments for the CAR during mitosis, whilst similarly Cdc12 is able to nucleate interphase cables.

Intriguingly it has previously been reported that For3 usually adopts an autoinhibited state that is relieved through the binding of Cdc42 and Bud6 (Martin, Rincon & Basu 2007) however the ability of the Myo2T-For3 fusion to partially complement Cdc12 function is of interest as Cdc42 has not been shown to be present at the CAR. As shown in figure 1.22 Cdc42 is localised to the plasma membrane at the cell poles and at the septum, however the ability of the Myo2T-For3 fusion to facilitate the formation of the CAR in some *cdc12-112* cells potentially suggests two possibilities. The first is that whilst adopting the autoinhibited state For3 still retains a small amount of nucleating activity, and that its full activity is achieved once Cdc42 and Bud6 relieve the autoinhibited state. It would be interesting to see what effect altering the localisation of Cdc42 so that it is present at the site of CAR formation has on the efficiency of the Myo2T-For3 fusion, perhaps enhancing its ability to complement Cdc12 function. Alternatively it is possible that Cdc12 also adopts

an autoinhibited state which is relieved by a different regulatory mechanism, and that this is also able to relieve For3 autoinhibition in the Myo2T-For3 chimera, and this allows the partial rescue of the *cdc12-112* phenotyope.

6.1.2 Fusing Formins to Tea1 Bypasses NETO.

In order to further examine the roll of the cell cycle in the function of formin fusions, Tea1-For3 and Tea1-Cdc12 fusions were examined, as well as For3 alone in a *for3Δ myo52-mCherry cdc10-v50* temperature sensitive mutant. *cdc10-v50* cells arrest in the G1 stage of the fission yeast cell cycle, before NETO has occurred, and it was anticipated that at the restrictive temperature For3 localisation, and subsequently Myo52 localisation would be completely monopolar however instead a majority of the cells (58%) showed monopolar localisation of Myo52-mCherry whilst 42% exhibited bipolar localisation. This may be due to the level of For3-GFP expression form the *pREP41* plasmid (under the *nmt41* promoter) differing from endogenous levels of For3, the GFP tag on For3 having an effect or an incomplete arrest of the cells in G1 by the *cdc10-v50* allele. Despite this, when examining both the Tea1-For3 the majority of cells and Tea1-Cdc12 a large proportion of cells exhibited bipolar localisation of the formin fusion and Myo52. In the case of Tea1-For3 98% of cells exhibited bipolar localisation, whilst with Tea1-Cdc12 41% of cells exhibited bipolar localisation, 34% monopolar and in 24% of cells Tea1-Cdc12 localised to a bright dot at the centre of the cell, presumably as a result of Cdc12 dragging Tea1 to this location. These findings suggested that fusing the formins to Tea1 allowed cells to bypass NETO and the effect this has on growth rate and cell length was examined. It was shown that expression of the Tea1-For3 fusion resulted in a quicker growth rate of cells in addition to an increased

cell length, both presumably as a result of the cells growing in a bipolar manner throughout the entirety of interphase. This may have coincided with an increase in protein synthesis within the cell, brought about by changes in the actin and microtubule cytoskeletons affecting the transport of vesicles within the cell.

6.1.3. Formins Nucleate Actin Cables with Distinct Physical Properties

Previous studies have shown that For3 and Cdc12 possess different actin nucleating properties (Scott, Neidt & Kovar 2011). However, the properties of the subsequently nucleated actin filaments are less understood. In order to investigate this, the properties of actin cables nucleated by endogenous For3, For3-mCherry and Tea1-Cdc12-mCherry were examined. The properties were investigated using a GFP-calponin homology domain which binds to all actin structures within the cell, and the filament growth and shrinkage rates of interphase actin cables in addition to the fluorescence intensity of these cables were measured. Firstly, the growth and shrinkage rates between endogenous For3 and For3-mCherry were very similar, indicating that neither varying expression levels from the *nmt41* promoter or the mCherry tag had an effect on the actin nucleating properties of For3. However when examining filaments nucleated by Tea1-Cdc12 there were clear differences in both the filament growth rate and filament intensity. The filament growth rate increased by 39% whilst the filament intensity decreased by 25%. This correlates well with previous studies which have shown that Cdc12 is a much more efficient actin nucleator than For3 (Scott, Neidt & Kovar 2011), and also suggests that filaments nucleated by Cdc12 have fewer actin polymers bundled to form interphase cables. These differences in filament

activity may be as a result of interactions with different actin bundling proteins. Within fission yeast there are two main actin bundling proteins, Fimbrin and α-actinin (Ain1) found at the cell poles and the CAR respectively (Skau, Neidt & Kovar 2009). Whilst Fimbrin is responsible predominantly for the bundling of actin filaments in cortical actin patches and actin cables, Ain1 is responsible for bundling at the CAR. These localisations and roles correspond directly with the localisation of the Formins and the actin polymers they nucleate. Therefore filaments nucleated by Tea1-Cdc12 may have a lower signal intensity as the actin filaments are bundled by Ain1 rather than Fimbrin. This could be examined by looking at the localisation of Ain1 in cells expressing Tea1-Cdc12 to see if Ain1 is interacting with cables nucleated by Tea1-Cdc12.

6.1.4. Formins Regulate the Binding of Actin Binding Proteins to ABP's

Having seen that the formins nucleate actin cables with distinct physical properties, the ability of the formins to regulate the binding of ABP's to actin was examined, with particular attention paid to the fission yeast tropomyosin, Cdc8. Fission yeast contains only one tropomyosin; Cdc8, however it is present in the cell in both N-terminally acetylated and unacetylated forms. These two populations of Cdc8 have distinct localisation patterns, with acetylated Cdc8 only observed at the CAR and unacetylated Cdc8 observed on interphase actin cables (Coulton & East 2010). These localisations match the localisations of Cdc12 and For3, and this fact along with previous suggestions (Michelot & Drubin 2011; Gunning et al. 2005) prompted the question of whether the formins played a role in determining which form of Cdc8 associated with distinct actin polymers. This was investigated through the use of the previously described formin fusions and acetylation state specific anti-Tm antibodies, which revealed that altering the localisation of Cdc12 to the cell poles resulted in acetylated Cdc8 associating with interphase actin cables, and similarly, altering the localisation of For3 to the CAR resulted in unacetlyated Cdc8 associating with the CAR. Both of these observations have never been made in wild type cells providing clear evidence that it is the formins that determine which form of tropomyosin associates with specific actin structures. This form of tropomyosin "sorting" has never been presented before, and could be of significant interest in higher eukaryotes where different tropomyosin isoforms each are associated with different actin structures in different cell types (Gunning et al. 2005). The mechanism by which formins determine which population of Tm associates with an actin polymer remains unclear. One possibility is that there is room for tropomyosin to slot

into the sleeve that the FH2 domains form around the actin filament, associating with the actin filament as polymerisation occurs. Alternatively the Tm may interact with the actin filament after polymerisation occurs, with a defining "landmark" left on the filament by the formin which promotes the binding of a specific Tm isoform.

Subsequently the interactions of other ABPs with actin cables nucleated by Tea1-Cdc12 were examined. Whilst the localisation of Myo52 was unaffected, the speed of its movement along actin cables was approximately 25% slower when cables were expressed by Tea1-Cdc12. This suggests differences between acetylated and unacetylated Cdc8, specifically in how they regulate myosin interactions with actin. Acetylated Cdc8 is usually present at the CAR, where the Class II myosin Myo2 is involved in generating the required force for constriction of the CAR. However on interphase cables unacetylated Cdc8 does not have to withstand such higher forces, as Myo52 simply walks along the surface of the actin, exerting little force. This difference may explain the change in speed, with acetylated Cdc8 somehow affecting the way in which Myo52 interacts with actin. Subsequently the localisation of two other ABP's was examined in cells expressing Tea1-Cdc12. The cofilin, Adf1 was found to be unaffected however localisation of the IQGAP Rng2 was altered. Rng2 usually localises to the CAR, however in cells expressing Tea1-Cdc12, Rng2 was observed co-localising with Tea1-Cdc12 foci at cell poles. The fact that Rng2 was only observed at these foci, and not on interphase actin cables suggests that the change in localisation was due to a physical interaction with Cdc12, rather than a preference for actin polymers containing acetylated Cdc8.

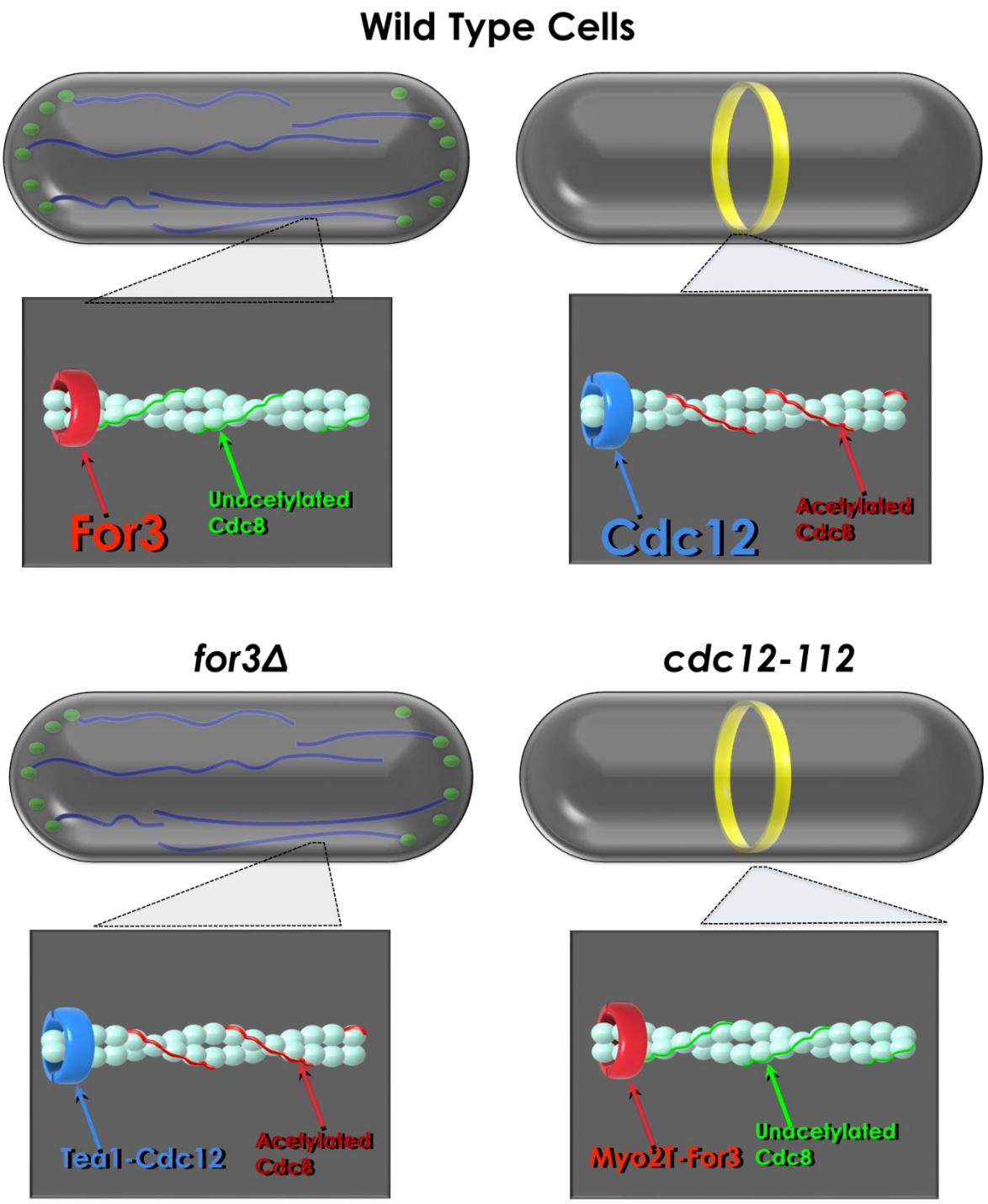

Figure 6.1. Cartoon to show how the distribution of acetylated and unacetylated Cdc8 is mediated by formins in wild type cells, and how this can be altered by the use of Tea1-Cdc12 and Myo2T-For3 fusions. Adapted from (East & Mulvihill 2011).

6.2. Regulation of Cell Polarity in Fission Yeast

In this study, the regulation of cell polarity by the actin and microtubule cytoskeletons was examined. Whilst many of the localisation dependencies observed have already been described in literature previously, a number of intriguing observations and patterns were observed. These are each discussed in the following sections.

6.2.1. Deletion of *myo52* Results in Increased Levels of Many "Tea" Proteins.

It has previously been observed that deletion of Myo52 results in increased levels of Tip1 within the cells. This was shown to be due to Myo52 playing a role in regulating the degradation of Tip1 via ubiquitin dependent proteolysis (Martín-García & Mulvihill 2009). Interestingly in this study it was observed that deletion of *myo52* also resulted in an increase in the levels of many other microtubule associated proteins, specifically Tea2, Tea3, and Tea4. There are several possible explanations for this observation. The first is that Myo52 may also play a role in mediating the degradation of these "Tea" proteins in a similar manner to its role in Tip1 degradation, therefore an absence of Myo52 would result in reduced degradation of these proteins. Alternatively the increase in levels of these "Tea" proteins may be a consequence of the increased Tip1 levels brought about by the *myo52Δ,* with a positive feedback loop driven by Tip1 levels resulting in increased levels of the other "Tea" proteins. Further evidence for Tip1 directly influencing the levels of other "Tea" proteins is that when looking in a *tip1Δ* strain, the levels of the "Tea" proteins are all significantly reduced. Despite most of the "Tea" proteins being at an increased level, it was

interesting that Tea1 levels were actually decreased in a *myo52Δ* strain, most noticeably at both cell poles. It has previously been shown that in a *myo52Δ* strain, in addition to increased Tip1 levels microtubule dynamics are also affected, with microtubules failing to undergo catastrophe when they reach the cell poles (Martín-García & Mulvihill 2009). As a result of this, it is possible that due to this failure of microtubules to undergo catastrophe Tea1 is prevented from disassociating from the microtubule at the cell pole. However if this was the case, an increase in cytoplasmic levels of Tea1 would be expected, rather than the decrease which was actually observed. Alternatively, the increased levels of other "Tea" proteins may have an effect on Tea1 levels, with a negative feedback loop driven by the levels of the "Tea" proteins decreasing Tea1 levels.

In order to further investigate this, the levels of the Tea proteins could be examined in a strain overexpressing Tip1, whilst Tea1 levels could also be examined in strains overexpressing other "Tea" proteins.

6.2.2. Deletion of *for3* does not Have the Same Effect as Deletion of *myo52*

As discussed in section 6.2.1, deletion of *myo52* resulted in up-regulation of many "Tea" proteins. It would be expected that deletion of *for3* may result in a similar observation, given that deletion of *for3* results in an absence of interphase actin cables within the cell (Feierbach & Chang 2001), which in turn disrupts the localisation of Myo52 to the cell poles. However, in this study the effects observed in a *for3Δ* strain did not mirror that observed in a *myo52Δ* strain. In some cases, the opposite was observed, with deletion of *for3* actually

resulting in a decrease in the levels of Tip1 and Tea4 at the cell poles, however an increase in Tea2 levels was still observed, and this effect was far greater than that observed in a *myo52Δ* strain. In addition, other conflicting observations were made, for example deletion of *for3* resulted in increases in the levels of Bud6 and Mod5 throughout the cells, whilst deletion of *myo52* resulted in a decrease in Bud6 levels, whilst Mod5 levels remained mostly unaffected. It is unclear why these differences between a *for3Δ* and *myo52Δ* occur, in a similar way in that it is unknown why deletion of *myo52* results in a much more disrupted cell morphology than deletion of *for3* does. Despite this large uncertainty, there is one possible explanation for the large increase in Bud6, and decrease in Tea4 levels at the cell poles. Bud6 and Tea4 play a key role in linking the actin and microtubule cytoskeletons, with Bud6 acting as a link between For3 and Tea4. The absence of For3, and subsequently inability to link the actin and microtubule cytoskeletons may be recognised by the cell, resulting in an increase in Bud6 and a decrease in Tea4 levels to try in an attempt to enhance the binding of Bud6 to For3.

In addition to these differences between the effects of deletion of *myo52* and *for3,* the deletion of each also has a contrasting effect on the localisation of the other. Deletion of *for3* results in a decreased accumulation of Myo52 at the cell poles. This can be explained by the lack of interphase actin cables within the cell, meaning there is no track present for Myo52 to move along towards the cell poles. However deletion of *myo52* resulted in an increase in For3 levels at the cell poles. A possible explanation is that the cells recognises that there is an absence of Myo52 at the cell poles, and in order to try and resolve this issue For3 is overexpressed, with the aim of increasing the number of actin cables.

6.2.3. Mal3 Plays a Key Role in the Regulation of Microtubule Associated Proteins

Deletion of *mal3*, resulted in a large reduction in the accumulation of all microtubule associated proteins (Tea1-4, Mod5, Tip1) at the cell poles. This disruption of the microtubule associated proteins is not surprising, given that *mal3Δ* cells display severe morphological defects such as curving and T shaped cells. Deletion of *mal3* is likely to prevent the accumulation of these proteins at the cell poles in a number of different ways. Mal3 has been shown to be a key regulator of microtubule dynamics, where it is responsible for both the initiation of microtubule growth, and prevents catastrophe at locations other than the cell poles (J.D. Beinhauer et al. 1997; Busch & Brunner 2004). Deletion of *mal3* results in cells possessing very short, and often faint cytoplasmic microtubules (J D Beinhauer et al. 1997). This disrupted microtubule cytoskeleton is likely to disrupt delivery of the microtubule associated proteins to the cell poles. In addition, Mal3 plays a role in regulating Tea2 activity, where it is responsible for stimulating its ATPase activity by recruiting it to microtubules. Deletion of *mal3* resulted in a total loss of Tea2 localisation to microtubules within the cell (Figure 4.8), and with Tea2 playing a role in delivering the microtubule associated proteins to the cell poles, this too would explain why *mal3* deletion greatly affects this. Further evidence for this is provided by the fact that deletion of Tea2 also results in a similar effect, with the localisation of all microtubule associated proteins to the cell poles being greatly reduced.

6.2.4. Deletion of Tea3 and Tea4 Results in an Increased Monopolar Distribution of Polarity Proteins

Previous research has shown that Tea3 and Tea4 play a key role in the initiation of New End Take Off (NETO) (Arellano, Niccoli & Nurse 2002; Tatebe et al. 2005; Martin et al. 2005). They are responsible for ensuring that components of the polarisome are directed to the non-growing end of the cell, and that bipolar growth is initiated. In this study it was observed that deletion of *tea3* resulted in a more monoplar localisation of Bud6, For3, Myo52, Tea1, and Tea4, either through an increase in intensity at End 1 of the cell or a decrease in intensity at End2. Similarly deletion of *tea4* resulted in a more monopolar localisation of all polarity proteins except Myo52 and Tea2. In proteins showing an increase in monopolar localisation, there was always an increase in intensity at End1, which was sometimes coupled with a decrease in intensity at End2. This finding of increased monopolar localisation of many polarity proteins in *tea3Δ* and *tea4Δ* strains is not surprising given the roles they play in the initiation of NETO. An absence of Tea3 would prevent the anchoring of Tea1 at the cell poles, which would subsequently prevent the recruitment of other "Tea" and microtubule associated proteins to the cell poles, including Tea4. A lack of Tea4 at the non-growing end, either due to the absence of Tea1 caused by *tea3Δ* or due to the deletion of *tea4* would prevent the recruitment of Bud6 and For3 to the non-growing end, subsequently preventing Myo52 localisation due to the absence of For3 nucleated actin cables. In addition to the increase in monopolar localisation of some proteins, deletion of *tea3* also appeared to upregulate the levels of Mod5, Tea2 and Tip1 at all locations in the cell. Deletion of Tea3 resulted in a decrease in Tea1 levels at End2, which would subsequently reduce the recruitment of other polarity proteins to the cell

pole. The increase in Mod5, Tea2 and Tip1 may come about as a mechanism in which the cell is trying to increase the accumulation of Tea1 at the cell pole to compensate for the absence of Tea3.

6.2.5. Deletion of *mod5* Results in an Increase in Cytoplasmic Signal of Polarity Proteins.

Mod5 plays a key role in the establishment of the polarisome at both poles of the cell, where it is responsible for the anchoring of Tea1 and Tea3 (Snaith & Sawin 2003; Snaith et al. 2005). Deletion of Mod5 resulted in an increase in the signal intensity of all polarity proteins except For3 and Myo52 in the cytoplasm. In addition there was a decrease in the signal intensity of Tea1 at End1 and of Tea3 at both End1 and End2. The increase in cytoplasmic may be as a result of the reduced anchoring of Tea1 and Tea3 at the cell poles. This would subsequently reduce the recruitment of other polarity proteins to the cell poles, resulting in an increase in cytoplasmic signal. The reduction in localisation of Tea1 and Tea3 to the cell poles matches previous findings (Snaith et al. 2005). All of the findings described in section 6.2 are demonstrated in figure 6.2 below.

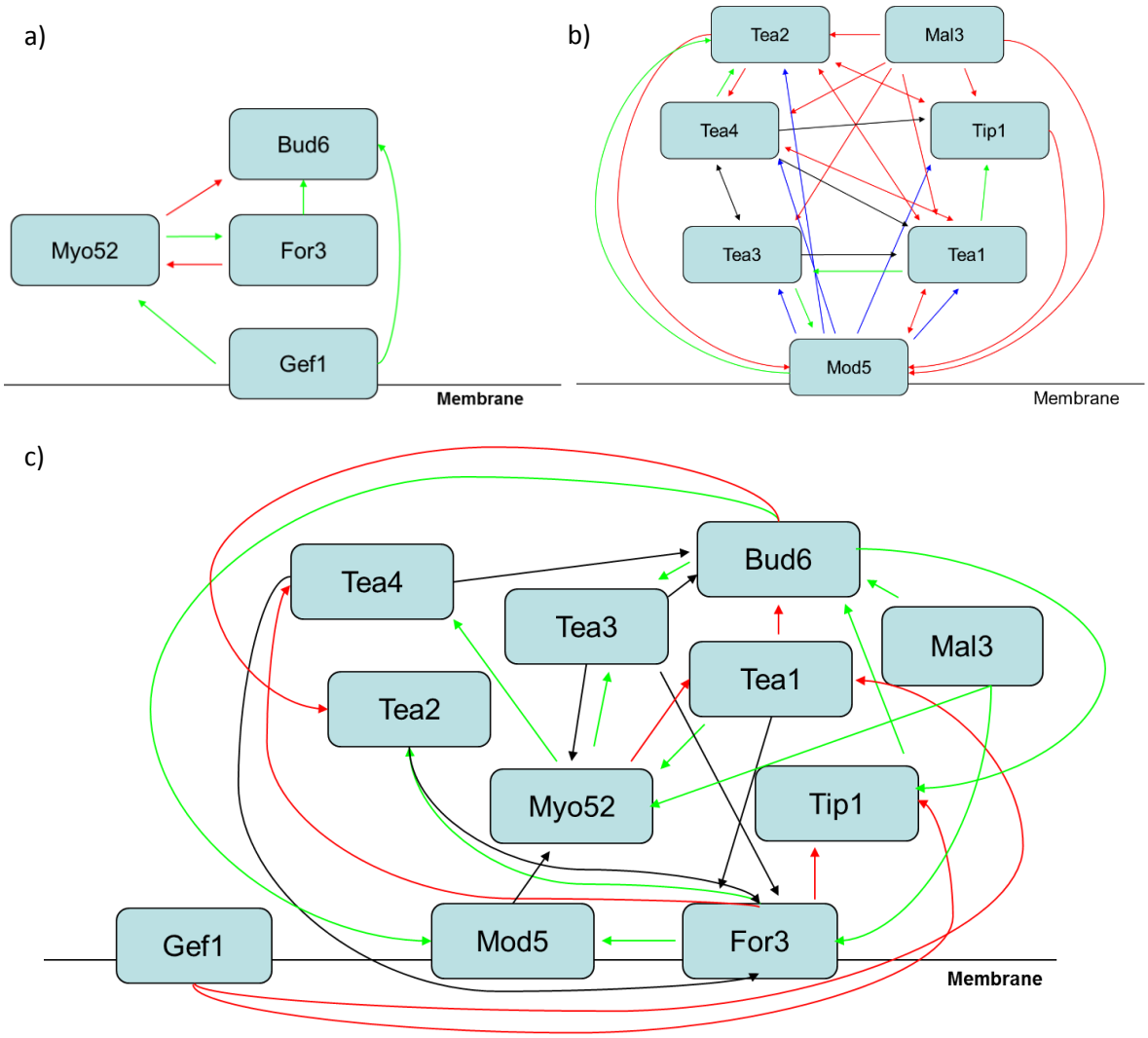

Figure 6.2. Schematics showing interactions/ regulatory mechanisms between members of the actin cytoskeleton (a) the microtubule cytoskeleton (b) and between members of both cytoskeletons (c). Arrows represent the effect of deleting the gene has on a protein the arrow points to. Green arrows represent an increase in protein levels at the cell poles, red arrows represent a decrease in protein levels at the cell poles, black arrows represent a more monopolar distribution of the protein and blue arrows represent an increase in cytoplasmic protein levels.

6.3. Investigation into the Function of the Type V Myosin Myo52

6.3.1. Chimeras Containing Other Myosin Head Domains Cannot Complement Myo52 Function

The fission yeast type V myosin Myo52 plays a key role in the growth of the cell, transporting a diverse range of cargoes around the cell via actin cables. This myosin consists of three distinct regions, the cargo binding tail region, the neck region which contains binding sites for light chains and calmodulins and the head region which contains the ATPase motor activity of the protein. In order to further understand Myo52 function and its interaction with actin cables that allow it to transport various cellular cargoes the cargo binding Myo52 tail region was fused to various myosin heads from both *S. pombe* and *Drosophila melanogaster.* Expression of constructs containing other class V myosin heads from both *S. pombe* and *D. melanogaster* as well as constructs containing the class VI myosin head from *D. melanogaster* did not rescue a *myo52Δ* phenotype. When examining this via fluorescence microscopy it was noted that none of these myosins localised to the cell poles as Myo52 does, nor were they motile. It was especially surprising that even replacing the Myo52 head domain with the head domain of Myo51, another class V myosin from fission yeast was not able to at least partially complement Myo52 function. There are several possible explanations for why these constructs were not able to complement Myo52 function. Firstly, only the head domain of the myosin was exchanged, the converter and neck domain (containing the light chain- binding IQ motifs) were those of Myo52, which possibly prevented the myosin heads from functioning. It would be very interesting

to repeat the study whilst also removing the Myo52 converter domain and neck and replacing them with those corresponding to the myosin head inserted. The converter and neck domains are involved in the generation of the power stroke, whereby they rotate/tilt relative to the catalytic core of the head, producing the power stroke (Jontes, Wilson-Kubalek & Milligan 1995; Dominguez et al. 1998; Houdusse & Cohen 1996; Corrie et al. 1999). If the Myo52 converter and neck domains are not compatible with the other myosin heads, this would explain why they are not functional.

Alternatively the way in which Myo52 interacts with actin may differ from that of the other myosins. *S. pombe* Myo51 is usually found at the CAR where it plays a role in the movement of actin filaments to facilitate assembly of the contractile ring (T.Z. Win et al. 2001; Wang et al. 2014). As has previously been described the CAR in fission yeast contains a different population of tropomyosin to that found on interphase actin cables, perhaps highlighting a regulatory mechanism that allows Myo51 to perform its function at the CAR, but not allow it to complement Myo52 function on interphase actin cables. This would be consistent with the finding that Myo52 moves 25% slower along actin cables containing acetylated tropomyosin, demonstrating that the tropomyosin composition of actin cables does impact myosin function. Another possibility is that Myo51 possess different physical properties that allow in to carry out its function in arranging actin filaments into the CAR, which prevent it from being able to move along interphase actin cables in a processive manner. In the case of Myosin V and Myosin VI from *D. melanogaster,* tropomyosin could again play a role in their interaction with actin cables, or differences in actin between the two organisms could prevent them from complementing Myo52 function.

6.3.2. Alternative Type V Myosin Heads From Both *S. pombe* and *D. melanogaster* are Able to Dimerise with Endogenous Myo52 and are Motile.

Although none of the myosin chimeras were able to complement Myo52 function in a *myo52Δ* strain, chimeras containing either the head domain of Myo51 or the *D. melanogaster* MyoV were able to dimerise with endogenous Myo52 in a *myo52-tdTomato* strain. This resulted in the chimeras localising to the cell poles and appearing to move along actin cables. However, as can be seen in figure 5.5 it the movement exhibited by these two chimeras compared to wild type Myo52 appeared to be both much shorter in length and also at a much lower velocity, however this was not quantified. The most likely explanation for this limited movement is that although the chimera protein is able to dimerise with endogenous Myo52, it is not functional, supported by the fact that none of the chimeras could complement Myo52 function. It is likely that the localisation and movement observed are as a result of the activity of the endogenous Myo52, perhaps moving along actin cables and dragging the inactive myosin chimera along with it. The two chimeras containing *D. melanogaster* MyoVI (with and without the inverter domain) were not able to dimerise with endogenous Myo52, suggesting that it is not the inverter domain of MyoVI preventing dimerization. It is surprising that dimerization was not possible, given that the tail region of the chimera was identical to that of endogenous Myo52, which would be expected to be sufficient for dimerization to occur. However it has previously been shown that dimerization of Myosin VI is regulated by mechanisms in addition to the presence of a coiled coil motif within the tail domain. Studies have shown that cargo biding also plays a key role in the dimerization of Myosin VI (Yu et al. 2009), and the potential absence of

Myosin VI cargoes in fission yeast may explain why dimerization does not occur. In addition this finding that the MyoVI head containing chimeras cannot dimerise with Myo52 suggests that the head domain of Myosin VI may play a role in its cargo dependent dimerization.

6.4. Summary

In this thesis, it has been shown that formins play a key role in the regulation of the actin cytoskeleton, determining which isoform of tropomyosin interacts with specific actin structures. In addition it has been shown that the two formins involved in vegetative growth of *S. pombe* are able to complement each other's function, and nucleate actin filaments with distinct physical properties. In addition a large volume of new data, highlighting key interactions and apparent regulatory pathways in the establishment and regulation of cell polarity has been generated. This, in addition to further experiments, should allow for a far more complete picture of the regulation of cell polarity in *S. pombe* to be established.

References

Arai, R. & Mabuchi, I., 2002. F-actin ring formation and the role of F-actin cables in the fission yeast Schizosaccharomyces pombe. *Journal of Cell Ccience*, 115, pp.887–898.

Arellano, M., Niccoli, T. & Nurse, P., 2002. Tea3p is a cell end marker activating polarized growth in Schizosaccharomyces pombe. *Current biology*, 12, pp.751–56.

Arnesen, T., Van Damme, P., Polevoda, B., Helsens, K., Evjenth, R., Colaert, N., Varhaug, J.E., Vandekerckhove, J., Lillehaug, J.R., Sherman, F. & Gevaert, K., 2009. Proteomics analyses reveal the evolutionary conservation and divergence of N-terminal acetyltransferases from yeast and humans. *Proceedings of the National Academy of Sciences of the United States of America*, 106, pp.8157–62.

Aschenbrenner, L., Lee, T. & Hasson, T., 2003. Myo6 facilitates the translocation of endocytic vesicles from cell peripheries. *Molecular biology of the cell*, 14(7), pp.2728–2743.

Assémat, E., Bazellières, E., Pallesi-Pocachard, E., Le Bivic, A. & Massey-Harroche, D., 2008. Polarity complex proteins. *Biochimica et Biophysica Acta - Biomembranes*, 1778(3), pp.614–630.

Attanapola, S.L., Alexander, C.J. & Mulvihill, D.P., 2009. Ste20-kinase-dependent TEDS-site phosphorylation modulates the dynamic localisation and endocytic function of the fission yeast class I myosin, Myo1. *Journal of Cell Science*, 122, pp.3856–61.

Avraham, K.B., Hasson, T., Steel, K.P., Kingsley, D.M., Russell, L.B., Mooseker, M.S., Copeland, N.G. & Jenkins, N.A., 1995. The mouse Snell's waltzer deafness gene encodes an unconventional myosin required for structural integrity of inner ear hair cells. *Nature Genetics*, 11, pp.369–375.

Ayscough, K., Hajibagheri, N.M., Watson, R. & Warren, G., 1993. Stacking of Golgi cisternae in Schizosaccharomyces pombe requires intact microtubules. *Journal of Cell Science*, 106, pp.1227–1237.

Bähler, J. & Nurse, P., 2001. Fission yeast pom1p kinase activity is cell cycle regulated and essential for cellular symmetry during growth and division. *EMBO Journal*, 20, pp.1064–1073.

Bähler, J. & Pringle, J.R., 1998. Pom1p, a fission yeast protein kinase that provides positional information for both polarized growth and cytokinesis. *Genes & Development*, 12, pp.1356–1370.

Bahloul, A., Chevreux, G., Wells, A.L., Martin, D., Nolt, J., Yang, Z., Chen, L.-Q., Potier, N., Van Dorsselaer, A., Rosenfeld, S., Houdusse, A. & Sweeney, H.L., 2004. The unique

insert in myosin VI is a structural calcium-calmodulin binding site. *Proceedings of the National Academy of Sciences of the United States of America*, 101, pp.4787–4792.

Bailey, K., 1946. Tropomyosin: a New Asymmetric Protein Component of Muscle. *Nature*, 157, pp.368–369.

Balasubramanian, M.K., Helfman, D.M. & Hemmingsen, S.M., 1992. A new tropomyosin essential for cytokinesis in the fission yeast S. pombe. *Nature*, 360, pp.84–87.

Baum, J., Papenfuss, A.T., Baum, B., Speed, T.P. & Cowman, A.F., 2006. Regulation of apicomplexan actin-based motility. *Nature reviews. Microbiology*, 4, pp.621–628.

Bear, J.E., Rawls, J.F. & Iii, C.L.S., 1998. SCAR, a WASP-related Protein, Isolated as a Suppressor of Receptor Defects in Late. *The Journal Of Cell Biology*, 142, pp.1325–1335.

Behrens, R. & Nurse, P., 2002a. Roles of fission yeast tea1p in the localization of polarity factors and in organizing the microtubular cytoskeleton. *The Journal of Cell Biology*, 157, pp.783–93.

Behrens, R. & Nurse, P., 2002b. Roles of fission yeast tea1p in the localization of polarity factors and in organizing the microtubular cytoskeleton. *The Journal of Cell Biology*, 157, pp.783–93.

Beinhauer, J.D., Hagan, I.M., Hegemann, J.H. & Fleig, U., 1997. Mal3, the fission yeast homologue of the human APC-interacting protein EB-1 is required for microtubule integrity and the maintenance of cell form. *The Journal of Cell Biology*, 139, pp.717–728.

Beinhauer, J.D., Hagan, I.M., Hegemann, J.H. & Fleig, U., 1997. Mal3, the fission yeast homologue of the human APC-interacting protein EB-1 is required for microtubule integrity and the maintenance of cell form. *The Journal of Cell Biology*, 139, pp.717–28.

Benton, R. & St Johnston, D., 2003. Drosophila PAR-1 and 14-3-3 inhibit Bazooka/PAR-3 to establish complementary cortical domains in polarized cells. *Cell*, 115, pp.691–704.

Bezanilla, M., Wilson, J.M. & Pollard, T.D., 2000. Fission yeast myosin-II isoforms assemble into contractile rings at distinct times during mitosis. *Current Biology*, 10, pp.397–400.

Bharadwaj, S., Hitchcock-DeGregori, S., Thorburn, A. & Prasad, G.L., 2004. N terminus is essential for tropomyosin functions: N-terminal modification disrupts stress fiber organization and abolishes anti-oncogenic effects of tropomyosin-1. *The Journal of Biological Chemistry*, 279, pp.14039–48.

Bicho, C.C., Kelly, D. a, Snaith, H. a, Goryachev, A.B. & Sawin, K.E., 2010a. A catalytic role for Mod5 in the formation of the Tea1 cell polarity landmark. *Current Biology*, 20, pp.1752–7.

Bicho, C.C., Kelly, D. a, Snaith, H. a, Goryachev, A.B. & Sawin, K.E., 2010b. A catalytic role for Mod5 in the formation of the Tea1 cell polarity landmark. *Current Biology*, 20, pp.1752–7.

Bilder, D., Li, M. & Perrimon, N., 2000. Cooperative regulation of cell polarity and growth by Drosophila tumor suppressors. *Science*, 289, pp.113–116.

Bilder, D., Schober, M. & Perrimon, N., 2003. Integrated activity of PDZ protein complexes regulates epithelial polarity. *Nature Cell Biology*, 5, pp.53–58.

De Boer, P., Crossley, R. & Rothfield, L., 1992. The essential bacterial cell-division protein FtsZ is a GTPase. *Nature*, 359, pp.254–256.

Bork, P., Sander, C. & Valencia, A., 1992. An ATPase domain common to prokaryotic cell cycle proteins, sugar kinases, actin, and hsp70 heat shock proteins. *Proceedings of the National Academy of Sciences of the United States of America*, 89, pp.7290–4.

Bornens, M., 2002. Centrosome composition and microtubule anchoring mechanisms. *Current Opinion in Cell Biology*, 14, pp.25–34.

Brown, J.H., Kim, K.H., Jun, G., Greenfield, N.J., Dominguez, R., Volkmann, N., Hitchcock-DeGregori, S.E. & Cohen, C., 2001. Deciphering the design of the tropomyosin molecule. *Proceedings of the National Academy of Sciences of the United States of America*, 98, pp.8496–501.

Browning, H., Hackney, D. & Nurse, P., 2003. Targeted movement of cell end factors in fission yeast. *Nature Cell Biology*, 5, pp.812–818.

Browning, H. & Hackney, D.D., 2005a. The EB1 homolog Mal3 stimulates the ATPase of the kinesin Tea2 by recruiting it to the microtubule. *The Journal of Biological Chemistry*, 280, pp.12299–12304.

Browning, H. & Hackney, D.D., 2005b. The EB1 homolog Mal3 stimulates the ATPase of the kinesin Tea2 by recruiting it to the microtubule. *The Journal of Biological Chemistry*, 280, pp.12299–304.

Browning, H., Hayles, J., Mata, J., Aveline, L., Nurse, P. & McIntosh, J.R., 2000a. Tea2p is a kinesin-like protein required to generate polarized growth in fission yeast. *The Journal of Cell Biology*, 151, pp.15–28.

Browning, H., Hayles, J., Mata, J., Aveline, L., Nurse, P. & McIntosh, J.R., 2000b. Tea2p is a kinesin-like protein required to generate polarized growth in fission yeast. *The Journal of Cell Biology*, 151, pp.15–28.

Brunner, D. & Nurse, P., 2000. CLIP170-like tip1p spatially organizes microtubular dynamics in fission yeast. *Cell*, 102, pp.695–704.

Bryant, D.M. & Mostov, K.E., 2008. From cells to organs: building polarized tissue. *Nature Reviews. Molecular Cell Biology*, 9, pp.887–901.

Burgess, S., Walker, M., Wang, F., Sellers, J.R., White, H.D., Knight, P.J. & Trinick, J., 2002. The prepower stroke conformation of myosin V. *The Journal of Cell Biology*, 159, pp.983–991.

Busch, K. & Brunner, D., 2004. The microtubule plus end-tracking proteins mal3p and tip1p cooperate for cell-end targeting of interphase microtubules. *Current Biology*, 14, pp.548–559.

Busch, K.E., Hayles, J., Nurse, P. & Brunner, D., 2004. Tea2p kinesin is involved in spatial microtubule organization by transporting tip1p on microtubules. *Developmental Cell*, 6, pp.831–43.

Buss, F., Arden, S.D., Lindsay, M., Luzio, J.P. & Kendrick-Jones, J., 2001. Myosin VI isoform localized to clathrin-coated vesicles with a role in clathrin-mediated endocytosis. *EMBO Journal*, 20, pp.3676–3684.

Buss, F., Luzio, J.P. & Kendrick-Jones, J., 2001. Myosin VI, a new force in clathrin mediated endocytosis. *FEBS Letters*, 508, pp.295–299.

La Carbona, S., Le Goff, C. & Le Goff, X., 2006. Fission yeast cytoskeletons and cell polarity factors: connecting at the cortex. *Biology of the Cell*, 98, pp.619–31.

Carlsson, L., Nyström, L.E., Sundkvist, I., Markey, F. & Lindberg, U., 1977. Actin polymerizability is influenced by profilin, a low molecular weight protein in non muscle cells. *Journal of Molecular Biology*, 115(3), pp.465–483.

Carminati, J.L. & Stearns, T., 1997. Microtubules Orient the Mitotic Spindle in Yeast through Dynein-dependent Interactions with the Cell Cortex. *The Journal Of Cell Biology*, 138, pp.629–641.

Casella, J.F., Maack, D.J. & Lin, S., 1986. Purification and initial characterization of a protein from skeletal muscle that caps the barbed ends of actin filaments. *The Journal of Biological Chemistry*, 261, pp.10915–10921.

Castrillon, D.H. & Wasserman, S. a, 1994. Diaphanous is required for cytokinesis in Drosophila and shares domains of similarity with the products of the limb deformity gene. *Development*, 120, pp.3367–77.

Cereijido, M., Contreras, R.G. & Shoshani, L., 2004. Cell adhesion, polarity, and epithelia in the dawn of metazoans. *Physiological Reviews*, 84, pp.1229–1262.

Chang, E.C., Barr, M., Wang, Y., Jung, V., Xu, H.P. & Wigler, M.H., 1994. Cooperative interaction of S. pombe proteins required for mating and morphogenesis. *Cell*, 79, pp.131–141.

Chang, F., Drubin, D. & Nurse, P., 1997. Cdc12P, a Protein Required for Cytokinesis in Fission Yeast, Is a Component of the Cell Division Ring and Interacts With Profilin. *The Journal of Cell Biology*, 137, pp.169–82.

Chang, F. & Martin, S.G., 2009. Shaping fission yeast with microtubules. *Cold Spring Harbor Perspectives in Biology*, 1, p.a001347.

Chang, L. & Gould, K.L., 2000. Sid4p is required to localize components of the septation initiation pathway to the spindle pole body in fission yeast. *Proceedings of the National Academy of Sciences of the United States of America*, 97, pp.5249–5254.

Cheeseman, I.M. & Desai, A., 2008. Molecular architecture of the kinetochore-microtubule interface. *Nature Reviews. Molecular Cell Biology*, 9, pp.33–46.

Cheney, R.E., O'Shea, M.K., Heuser, J.E., Coelho, M. V, Wolenski, J.S., Espreafico, E.M., Forscher, P., Larson, R.E. & Mooseker, M.S., 1993. Brain myosin-V is a two-headed unconventional myosin with motor activity. *Cell*, 75, pp.13–23.

Coffman, V.C., Nile, A.H., Lee, I.-J., Liu, H. & Wu, J.-Q., 2009. Roles of formin nodes and myosin motor activity in Mid1p-dependent contractile-ring assembly during fission yeast cytokinesis. *Molecular Biology of the Cell*, 20, pp.5195–5210.

Coll, P.M., Rincon, S.A., Izquierdo, R.A. & Perez, P., 2007. Hob3p, the fission yeast ortholog of human BIN3, localizes Cdc42p to the division site and regulates cytokinesis. *The EMBO journal*, 26, pp.1865–1877.

Coll, P.M., Trillo, Y., Ametzazurra, A. & Perez, P., 2003. Gef1p , a New Guanine Nucleotide Exchange Factor for Cdc42p , Regulates Polarity in Schizosaccharomyces pombe. *Molecular Biology of the Cell*, 14, pp.313–323.

Corrie, J.E., Brandmeier, B.D., Ferguson, R.E., Trentham, D.R., Kendrick-Jones, J., Hopkins, S.C., van der Heide, U. a, Goldman, Y.E., Sabido-David, C., Dale, R.E., Criddle, S. & Irving, M., 1999. Dynamic measurement of myosin light-chain-domain tilt and twist in muscle contraction. *Nature*, 400, pp.425–30.

Coulton, A. & East, D., 2010. The recruitment of acetylated and unacetylated tropomyosin to distinct actin polymers permits the discrete regulation of specific myosins in fission yeast. *Journal of Cell Science*, 123, pp.3235–3243.

Cramer, L.P., 2000. Myosin VI: roles for a minus end-directed actin motor in cells. *The Journal of Cell Biology*, 150, pp.F121–6.

Craven, R.A., Griffiths, D.J.F., Sheldrick, K.S., Randall, R.E., Hagan, I.M. & Carr, A.M., 1998. Vectors for the expression of tagged proteins in Schizosaccharomyces pombe. *Gene*, 221, pp.59–68.

Crick, F.H.C., 1953. The packing of α-helices: simple coiled-coils. *Acta Crystallographica*, 6, pp.689–697.

Das, M., Wiley, D.J., Chen, X., Shah, K. & Verde, F., 2009. The Conserved NDR Kinase Orb6 Controls Polarized Cell Growth by Spatial Regulation of the Small GTPase Cdc42. *Current Biology*, 19, pp.1314–1319.

Das, M., Wiley, D.J., Medina, S., Vincent, H.A., Larrea, M., Oriolo, A. & Verde, F., 2007. Regulation of cell diameter, For3p localization, and cell symmetry by fission yeast Rho-GAP Rga4p. *Molecular Biology of the Cell*, 18, pp.2090–2101.

Derry, J.M., Ochs, H.D. & Francke, U., 1994. Isolation of a novel gene mutated in Wiskott-Aldrich syndrome. *Cell*, 78, pp.635–644.

Dominguez, R., Freyzon, Y., Trybus, K.M. & Cohen, C., 1998. Crystal structure of a vertebrate smooth muscle myosin motor domain and its complex with the essential light chain: visualization of the pre-power stroke state. *Cell*, 94, pp.559–71.

Drees, B., Brown, C., Barrell, B.G. & Bretscher, A., 1995. Tropomyosin is essential in yeast, yet the TPM1 and TPM2 products perform distinct functions. *The Journal of Cell Biology*, 128, pp.383–92.

Drubin, D.G. & Nelson, W.J., 1996. Origins of Cell Polarity. *Cell*, 84, pp.335–344.

East, D. a & Mulvihill, D.P., 2011. Regulation and function of the fission yeast myosins. *Journal of Cell Science*, 124, pp.1383–90.

Erickson, H.P., 1995. FtsZ , a Prokaryotic Homolog of Tubulin? *Cell*, 80, pp.367–370.

Etienne-Manneville, S. & Hall, A., 2002. Rho GTPases in cell biology. *Nature*, 420, pp.629–635.

Evangelista, M., Blundell, K., Longtine, M.S., Chow, C.J., Adames, N., Pringle, J.R., Peter, M. & Boone, C., 1997. Bni1p, a yeast formin linking cdc42p and the actin cytoskeleton during polarized morphogenesis. *Science*, 276, pp.118–122.

Evangelista, M., Zigmond, S. & Boone, C., 2003. Formins: signaling effectors for assembly and polarization of actin filaments. *Journal of Cell Science*, 116, pp.2603–11.

Feierbach, B. & Chang, F., 2001. Roles of the fission yeast formin for3p in cell polarity, actin cable formation and symmetric cell division. *Current Biology*, 11, pp.1656–65.

Feierbach, B., Verde, F. & Chang, F., 2004. Regulation of a formin complex by the microtubule plus end protein tea1p. *The Journal of Cell Biology*, 165(5), pp.697–707.

Fürst, D., Osborn, M., Nave, R. & Weber, K., 1988. The organization of titin filaments in the half-sarcomere revealed by monoclonal antibodies in immunoelectron microscopy: a map of ten nonrepetitive epitopes starting. *The Journal of Cell Biology*, 106, pp.1563–1572.

Gassama-Diagne, A. & Payrastre, B., 2009. Phosphoinositide Signaling Pathways. Promising Role as Builders of Epithelial Cell Polarity. *International Review of Cell and Molecular Biology*, 273, pp.313–343.

Gassama-Diagne, A., Yu, W., ter Beest, M., Martin-Belmonte, F., Kierbel, A., Engel, J. & Mostov, K., 2006. Phosphatidylinositol-3,4,5-trisphosphate regulates the formation of the basolateral plasma membrane in epithelial cells. *Nature Cell Biology*, 8, pp.963–970.

Gee, M. & Vallee, R., 1998. The role of the dynein stalk in cytoplasmic and flagellar motility. *European Biophysics Journal*, 27, pp.466–73.

Geeves, M.A. & Holmes, K.C., 1999. Structural mechanism of muscle contraction. *Annual Review of Biochemistry*, 68, pp.687–728.

Glynn, J.M., Lustig, R.J., Berlin, A. & Chang, F., 2001. Role of bud6p and tea1p in the interaction between actin and microtubules for the establishment of cell polarity in fission yeast. *Current Biology*, 11, pp.836–45.

Goldstein, B. & Macara, I.G., 2007. The PAR Proteins: Fundamental Players in Animal Cell Polarization. *Developmental Cell*, 13, pp.609–622.

Goode, B.L. & Eck, M.J., 2007. Mechanism and function of formins in the control of actin assembly. *Annual review of biochemistry*, 76, pp.593–627.

Grallert, A., Martín-García, R., Bagley, S. & Mulvihill, D.P., 2007. In vivo movement of the type V myosin Myo52 requires dimerisation but is independent of the neck domain. *Journal of Cell Science*, 120, pp.4093–8.

Greenfield, N., 1994. The effect of N-terminal acetylation on the structure of an N-terminal tropomyosin peptide and αα-tropomyosin. *Protein Science*, 3, pp.402–410.

Gunning, P.W., Schevzov, G., Kee, A.J. & Hardeman, E.C., 2005. Tropomyosin isoforms: divining rods for actin cytoskeleton function. *Trends in Cell Biology*, 15, pp.333–41.

Hachet, O. & Simanis, V., 2008. Mid1p/anillin and the septation initiation network orchestrate contractile ring assembly for cytokinesis. *Genes & Development*, 22, pp.3205–16.

Hagan, I. & Yanagida, M., 1997. Evidence for cell cycle-specific, spindle pole body-mediated, nuclear positioning in the fission yeast Schizosaccharomyces pombe. *Journal of Cell Science*, 110, pp.1851–1866.

Hagan, I. & Yanagida, M., 1995. The product of the spindle formation gene sad1+ associates with the fission yeast spindle pole body and is essential for viability. *The Journal of Cell Biology*, 129, pp.1033–1047.

Hagan, I.M., 1998. The fission yeast microtubule cytoskeleton. *Journal of Cell Science*, 111, pp.1603–12.

Hagan, I.M. & Hyams, J.S., 1996. Forces acting on the fission yeast anaphase spindle. *Cell Motility and the Cytoskeleton*, 34, pp.69–75.

Hagan, I.M. & Hyams, J.S., 1988. The use of cell division cycle mutants to investigate the control of microtubule distribution in the fission yeast Schizosaccharomyces pombe. *Journal of Cell Science*, 89, pp.343–357.

Hammer, J.A. & Sellers, J.R., 2011. Walking to work: roles for class V myosins as cargo transporters. *Nature Reviews Molecular Cell Biology*, 13, pp.13–26.

Hanukoglu, I. & Fuchs, E., 1982. The cDNA sequence of a human epidermal keratin: divergence of sequence but conservation of structure among intermediate filament proteins. *Cell*, 31, pp.243–52.

Hirata, D., Kishimoto, N., Suda, M., Sogabe, Y., Nakagawa, S., Yoshida, Y., Sakai, K., Mizunuma, M., Miyakawa, T., Ishiguro, J. & Toda, T., 2002. Fission yeast Mor2/Cps12, a protein similar to Drosophila Furry, is essential for cell morphogenesis and its mutation induces Wee1-dependent G(2) delay. *The EMBO Journal*, 21, pp.4863–74.

Hirokawa, N., 1998. Kinesin and dynein superfamily proteins and the mechanism of organelle transport. *Science*, 279, pp.519–526.

Hirota, K. & Tanaka, K., 2003. Gef1p and Scd1p, the Two GDP-GTP exchange factors for Cdc42p, form a ring structure that shrinks during cytokinesis in Schizosaccharomyces pombe. *Molecular Biology of the Cell*, 14, pp.3617–3627.

Hitchcock-DeGregori, S.E. & Singh, A., 2010. What makes tropomyosin an actin binding protein? A perspective. *Journal of Structural Biology*, 170, pp.319–24.

Höök, P. & Vallee, R.B., 2006. The dynein family at a glance. *Journal of Cell Science*, 119, pp.4369–71.

Horio, T., Uzawa, S., Jung, M.K., Oakley, B.R., Tanaka, K. & Yanagida, M., 1991. The fission yeast gamma-tubulin is essential for mitosis and is localized at microtubule organizing centers. *Journal of Cell Science*, 99, pp.693–700.

Hou, M., Wiley, D., Verde, F. & McCollum, D., 2003. Mob2p interacts with the protein kinase Orb6p to promote coordination of cell polarity with cell cycle progression. *Journal of Cell Science*, 116, pp.125–135.

Houdusse, A. & Cohen, C., 1996. Structure of the regulatory domain of scallop myosin at 2 A resolution: implications for regulation. *Structure*, 4, pp.21–32.

Huang, J., Huang, Y., Yu, H., Subramanian, D., Padmanabhan, A., Thadani, R., Tao, Y., Tang, X., Wedlich-Soldner, R. & Balasubramanian, M.K., 2012. Nonmedially assembled F-actin cables incorporate into the actomyosin ring in fission yeast. *The Journal of Cell Biology*, 199, pp.831–47.

Huang, Y., Yan, H. & Balasubramanian, M.K., 2008. Assembly of normal actomyosin rings in the absence of Mid1p and cortical nodes in fission yeast. *The Journal of Cell Biology*, 183, pp.979–988.

Huckaba, T.M., Lipkin, T. & Pon, L. a, 2006. Roles of type II myosin and a tropomyosin isoform in retrograde actin flow in budding yeast. *The Journal of Cell Biology*, 175, pp.957–69.

Hunt, T. & Murray, A., 1993. *The Cell Cycle, an introduction*,

Huxley, A.F. & Niedergerke, R., 1954. Structural Changes in Muscle During Contraction: Interference Microscopy of Living Muscle Fibres. *Nature*, 173, pp.971–973.

Huxley, H. & Hanson, J., 1954. Changes in the cross-striations of muscle during contraction and stretch and their structural interpretation. *Nature*, 173, pp.973–976.

Huxley, H.E., 1973. Structural Changes in Actin and Myosin Containing Filaments During Contraction. *Cold Spring Harbor Symposia on Quantitative Biology*, 37, pp.361–376.

Iden, S. & Collard, J.G., 2008. Crosstalk between small GTPases and polarity proteins in cell polarization. *Nature Reviews. Molecular Cell Biology*, 9, pp.846–859.

Ishikawa, H., Bischoff, R. & Holtzer, H., 1968. Mitosis and intermediate-sized filaments in developing skeletal muscle. *The Journal of Cell Biology*, 38, pp.538–55.

Ishikawa, K., Catlett, N.L., Novak, J.L., Tang, F., Nau, J.J. & Weisman, L.S., 2003. Identification of an organelle-specific myosin V receptor. *The Journal of Cell Biology*, 160, pp.887–897.

Jackson, J.R., Patrick, D.R., Dar, M.M. & Huang, P.S., 2007. Targeted anti-mitotic therapies: can we improve on tubulin agents? *Nature Reviews. Cancer*, 7, pp.107–117.

Jaffe, A.B. & Hall, A., 2005. Rho GTPases: biochemistry and biology. *Annual Review of Cell and Developmental Biology*, 21, pp.247–269.

Jin, H. & Amberg, D.C., 2001. Fission yeast Aip3p (spAip3p) is required for an alternative actin-directed polarity program. *Molecular biology of the cell*, 12(5), pp.1275–91.

Jontes, J.D., Wilson-Kubalek, E.M. & Milligan, R.A., 1995. A 32 degree tail swing in brush border myosin I on ADP release. *Nature*, 378, pp.751–753.

Kamasaki, T., Osumi, M. & Mabuchi, I., 2007. Three-dimensional arrangement of F-actin in the contractile ring of fission yeast. *The Journal of Cell Biology*, 178, pp.765–71.

Kanai, M., Kume, K., Miyahara, K., Sakai, K., Nakamura, K., Leonhard, K., Wiley, D.J., Verde, F., Toda, T. & Hirata, D., 2005. Fission yeast MO25 protein is localized at SPB and septum and is essential for cell morphogenesis. *The EMBO Journal*, 24, pp.3012–3025.

Karagiannis, J. & Bimbó, A., 2005. The Nuclear Kinase Lsk1p Positively Regulates the Septation Initiation Network and Promotes the Successful Completion of Cytokinesis in Response to Perturbation of the Actomyosin Ring in Schizosaccharomyces pombe □. *Molecular Biology of the Cell*, 16, pp.358–371.

Kawashima, S.A., Takemoto, A., Nurse, P. & Kapoor, T.M., 2012. Analyzing fission yeast multidrug resistance mechanisms to develop a genetically tractable model system for chemical biology. *Chemistry and Biology*, 19(7), pp.893–901.

Kemphues, K.J., Priess, J.R., Morton, D.G. & Cheng, N.S., 1988. Identification of genes required for cytoplasmic localization in early C. elegans embryos. *Cell*, 52, pp.311–320.

Kim, H., Yang, P., Catanuto, P., Verde, F., Lai, H., Du, H., Chang, F. & Marcus, S., 2003. The kelch repeat protein, Tea1, is a potential substrate target of the p21-activated kinase, Shk1, in the fission yeast, Schizosaccharomyces pombe. *The Journal of Biological Chemistry*, 278, pp.30074–30082.

Kovács, M., Wang, F., Hu, A., Zhang, Y. & Sellers, J.R., 2003. Functional divergence of human cytoplasmic myosin II: kinetic characterization of the non-muscle IIA isoform. *The Journal of Biological chemistry*, 278, pp.38132–38140.

Kovar, D.R., 2006. Cell Polarity: Formin on the Move. *Current biology*, 16, pp.R536–8.

Kovar, D.R., Harris, E.S., Mahaffy, R., Higgs, H.N. & Pollard, T.D., 2006. Control of the Assembly of ATP- and ADP-Actin by Formins and Profilin. *Cell*, 1, pp.423–435.

Kovar, D.R., Kuhn, J.R., Tichy, A.L. & Pollard, T.D., 2003. The fission yeast cytokinesis formin Cdc12p is a barbed end actin filament capping protein gated by profilin. *The Journal of Cell Biology*, 161, pp.875–87.

Kovar, D.R., Sirotkin, V. & Lord, M., 2011. Three's company: The fission yeast actin cytoskeleton. *Trends in Cell Biology*, 21, pp.177–187.

Krendel, M. & Mooseker, M.S., 2005. Myosins: tails (and heads) of functional diversity. *Physiology*, 20, pp.239–51.

Kurahashi, H., Imai, Y. & Yamamoto, M., 2002. Tropomyosin is required for the cell fusion process during conjugation in fission yeast. *Genes to Cells*, 7(4), pp.375–84.

Kwon, S. & Schnapp, B.J., 2001. RNA localization: SHEdding light on the RNA-motor linkage. *Current Biology*, 11, pp.R166–168.

De La Cruz, E.M. & Ostap, E.M., 2004. Relating biochemistry and function in the myosin superfamily. *Current Opinion in Cell Biology*, 16, pp.61–7.

Langford, G.M., 2002. Myosin-V, a versatile motor for short-range vesicle transport. *Traffic*, 3, pp.859–865.

Leonhard, K. & Nurse, P., 2005. Ste20/GCK kinase Nak1/Orb3 polarizes the actin cytoskeleton in fission yeast during the cell cycle. *Journal of Cell Science*, 118, pp.1033–1044.

Leupold, U., 1958. Studies on recombination in Schizosaccharomyces pombe. *Cold Spring Harbor Symposia on Quantitative Biology*, 23, pp.161–170.

Lister, I., Schmitz, S., Walker, M., Trinick, J., Buss, F., Veigel, C. & Kendrick-Jones, J., 2004. A monomeric myosin VI with a large working stroke. *The EMBO Journal*, 23, pp.1729–1738.

Liu, H. & Bretscher, A., 1992. Characterization of TPM1 disrupted yeast cells indicates an involvement of tropomyosin in directed vesicular transport. *The Journal of Cell Biology*, 118, pp.285–99.

Lodish, H., Berk, A., Zipursky, S., Matsudaira, P., Baltimore, D. & J, D., 2000. Intermediate Filaments. In *Molecular Cell Biology, 4th edition*. p. Section 19.6.

Loo, T.-H. & Balasubramanian, M., 2008. Schizosaccharomyces pombe Pak-related protein, Pak1p/Orb2p, phosphorylates myosin regulatory light chain to inhibit cytokinesis. *The Journal of Cell Biology*, 183, pp.785–93.

Lord, M., Laves, E. & Pollard, T.D., 2005. Cytokinesis depends on the motor domains of myosin-II in fission yeast but not in budding yeast. *Molecular Biology of the Cell*, 16, pp.5346–5355.

MA, H. & Spudich, J.A., 2012. The myosin superfamily at a glance. *Journal of Cell Science*, 125, pp.1627–1632.

Machesky, L.M. & Insall, R.H., 1999. Scar1 and the related Wiskott-Aldrich syndrome protein, WASP, regulate the actin cytoskeleton through the Arp2/3 complex. *Current Biology*, 8, pp.1347–56.

Marston, S.B. & Taylor, E.W., 1980. Comparison of the myosin and actomyosin ATPase mechanisms of the four types of vertebrate muscles. *Journal of Molecular Biology*, 139, pp.573–600.

Martin, D.J. & Rubenstein, P.A., 1987. Alternate pathways for removal of the class II actin initiator methionine. *Journal of Biological Chemistry*, 262(13), pp.6350–6356.

Martin, S., McDonald, W., Yates, J. & Chang, F., 2005. Tea4p links microtubule plus ends with the formin for3p in the establishment of cell polarity. *Developmental Cell*, 8, pp.479–91.

Martin, S., Rincon, S. & Basu, R., 2007. Regulation of the formin for3p by cdc42p and bud6p. *Molecular Biology of the Cell*, 18, pp.4155– 4167.

Martin, S.G. & Berthelot-Grosjean, M., 2009. Polar gradients of the DYRK-family kinase Pom1 couple cell length with the cell cycle. *Nature*, 459, pp.852–6.

Martin, S.G. & Chang, F., 2003. Cell Polarity : A New Mod (e) of Anchoring Microtubules play a central role in the establishment. *Science*, 13, pp.711–713.

Martin, S.G. & Chang, F., 2006. Dynamics of the Formin For3p in Actin Cable Assembly. *Current Biology*, 2, pp.1161–1170.

Martin-Belmonte, F., Gassama, A., Datta, A., Yu, W., Rescher, U., Gerke, V. & Mostov, K., 2007. PTEN-Mediated Apical Segregation of Phosphoinositides Controls Epithelial Morphogenesis through Cdc42. *Cell*, 128, pp.383–397.

Martín-García, R. & Mulvihill, D.P., 2009. Myosin V spatially regulates microtubule dynamics and promotes the ubiquitin-dependent degradation of the fission yeast CLIP-170 homologue, Tip1. *Journal of Cell Science*, 122, pp.3862–72.

Mata, J. & Nurse, P., 1997. Tea1 and the Microtubular Cytoskeleton Are Important for Generating Global Spatial Order Within the Fission Yeast Cell. *Cell*, 89, pp.939–49.

May, K.M., Watts, F.Z., Jones, N. & Hyams, J.S., 1997. Type II myosin involved in cytokinesis in the fission yeast, Schizosaccharomyces pombe. *Cell Motility and the Cytoskeleton*, 38, pp.385–396.

McKillop, D.F. & Geeves, M.A., 1993. Regulation of the interaction between actin and myosin subfragment 1: evidence for three states of the thin filament. *Biophysical Journal*, 65, pp.693–701.

Mehta, a D., Rock, R.S., Rief, M., Spudich, J. a, Mooseker, M.S. & Cheney, R.E., 1999. Myosin-V is a processive actin-based motor. *Nature*, 400, pp.590–3.

Mendoza, M., Redemann, S. & Brunner, D., 2005. The fission yeast MO25 protein functions in polar growth and cell separation. *European Journal of Cell Biology*, 84, pp.915–926.

Ménétrey, J., Bahloul, A., Wells, A.L., Yengo, C.M., Morris, C.A., Sweeney, H.L. & Houdusse, A., 2005. The structure of the myosin VI motor reveals the mechanism of directionality reversal. *Nature*, 435, pp.779–785.

Michelot, A. & Drubin, D.G., 2011. Building distinct actin filament networks in a common cytoplasm. *Current Biology*, 21, pp.R560–9.

Miller, P. & Johnson, D., 1994. Cdc42p GTPase Is Involved in Controlling Polarized Cell Growth in Schizosaccharomyces pombe. *Molecular and Cellular Biology*, 14, pp.1075–83.

Mitchison, J.M., 1957. The growth of single cells. I. Schizosaccharomyces pombe. *Experimental Cell Research*, 13, pp.244–262.

Mitchison, J.M. & Nurse, P., 1985. Growth in cell length in the fission yeast Schizosaccharomyces pombe. *Journal of Cell Science*, 75, pp.357–76.

Mitchison, T. & Kirschner, M., 1984. Dynamic instability of microtubule growth. *Nature*, 312, pp.237–242.

Monteiro, P.B., Lataros, R.C. & Ferro, J.A., 1994. Functional a-Tropomyosin Produced in Escherichia coli. *Journal of Biological Chemistry*, 269, pp.10461–10466.

Moreno, S., Klar, A. & Nurse, P., 1991. Molecular genetic analysis of fission yeast Schizosaccharomyces pombe. *Methods in Enzymology*, 194, pp.795–823.

Moseley, J.B. & Goode, B.L., 2005. Differential activities and regulation of Saccharomyces cerevisiae formin proteins Bni1 and Bnr1 by Bud6. *The Journal of Biological Chemistry*, 280, pp.28023–28033.

Moseley, J.B., Mayeux, A., Paoletti, A. & Nurse, P., 2009. A spatial gradient coordinates cell size and mitotic entry in fission yeast. *Nature*, 459, pp.857–60.

Motegi, F., Arai, R. & Mabuchi, I., 2001. Identification of two type V myosins in fission yeast, one of which functions in polarized cell growth and moves rapidly in the cell. *Molecular Biology of the Cell*, 12, pp.1367–80.

Muller, J., Oma, Y., Vallar, L., Friederich, E., Poch, O. & Winsor, B., 2005. Sequence and comparative genomic analysis of actin-related proteins. *Molecular Biology of the Cell*, 16, pp.5736–5748.

Mullins, R.D., Heuser, J. a & Pollard, T.D., 1998. The interaction of Arp2/3 complex with actin: nucleation, high affinity pointed end capping, and formation of branching networks of filaments. *Proceedings of the National Academy of Sciences of the United States of America*, 95, pp.6181–6.

Mulvihill, D.P., Barretto, C. & Hyams, J.S., 2001. Localization of fission yeast type II myosin, Myo2, to the cytokinetic actin ring is regulated by phosphorylation of a C-terminal coiled-coil domain and requires a functional septation initiation network. *Molecular Biology of the Cell*, 12, pp.4044–53.

Mulvihill, D.P., Edwards, S.R. & Hyams, J.S., 2006. A critical role for the type V Myosin, Myo52, in septum deposition and cell fission during cytokinesis in Schizosaccharomyces pombe. *Cell Motility and the Cytoskeleton*, 63(3), pp.149–161.

Mulvihill, D.P. & Hyams, J.S., 2003. Role of the two type II myosins, Myo2 and Myp2, in cytokinetic actomyosin ring formation and function in fission yeast. *Cell Motility and the Cytoskeleton*, 54, pp.208–216.

Nakano, K., 2002. The small GTPase Rho3 and the diaphanous/formin For3 function in polarized cell growth in fission yeast. *Journal of Cell Science*, 115, pp.4629–4639.

Nakano, K. & Mabuchi, I., 2006. Actin-depolymerizing protein Adf1 is required for formation and maintenance of the contractile ring during cytokinesis in fission yeast. *Molecular Biology of the Cell*, 17, pp.1933–1945.

Nakano, K., Mutoh, T. & Mabuchi, I., 2001. Characterization of GTPase-activating proteins for the function of the Rho-family small GTPases in the fission yeast Schizosaccharomyces pombe. *Genes to Cells*, 6, pp.1031–1042.

Niccoli, T., Arellano, M. & Nurse, P., 2003. Role of Tea1p, Tea3p and Pom1p in the determination of cell ends in Schizosaccharomyces pombe. *Yeast*, 20, pp.1349–58.

Nobes, C.D. & Hall, A., 1995. Rho, rac, and cdc42 GTPases regulate the assembly of multimolecular focal complexes associated with actin stress fibers, lamellipodia, and filopodia. *Cell*, 81, pp.53–62.

Odronitz, F. & Kollmar, M., 2007. Drawing the tree of eukaryotic life based on the analysis of 2,269 manually annotated myosins from 328 species. *Genome biology*, 8, p.R196.

Ohtsuki, I., Masaki, T., Nonomura, Y. & Ebashi, S., 1967. Periodic distribution of troponin along the thin filament. *Journal of Biochemistry*, 61, pp.817–819.

Okten, Z., Churchman, L.S., Rock, R.S. & Spudich, J. a, 2004. Myosin VI walks hand-over-hand along actin. *Nature Structural & Molecular Biology*, 11, pp.884–7.

Otomo, T., Tomchick, D.R., Otomo, C., Panchal, S.C., Machius, M. & Rosen, M.K., 2005. Structural basis of actin filament nucleation and processive capping by a formin homology 2 domain. *Nature*, 433, pp.488–494.

Di Paolo, G. & De Camilli, P., 2006. Phosphoinositides in cell regulation and membrane dynamics. *Nature*, 443, pp.651–657.

Pardo, M. & Nurse, P., 2003. Equatorial retention of the contractile actin ring by microtubules during cytokinesis. *Science*, 300, pp.1569–1574.

Park, H.O., Bi, E., Pringle, J.R. & Herskowitz, I., 1997. Two active states of the Ras-related Bud1/Rsr1 protein bind to different effectors to determine yeast cell polarity. *Proceedings of the National Academy of Sciences of the United States of America*, 94, pp.4463–8.

Paschal, B.M., Shpetner, H.S. & Vallee, R.B., 1987. MAP 1C is a microtubule-activated ATPase which translocates microtubules in vitro and has dynein-like properties. *The Journal of Cell Biology*, 105, pp.1273–82.

Pece, S., Chiariello, M., Murga, C. & Gutkind, J.S., 1999. Activation of the Protein Kinase Akt/PKB by the Formation of E-cadherin-mediated Cell-Cell Junctions: Evidence for the association of phosphatidylinositol 3-kinase with the E-cadherin adhesion complex. *Journal of Biological Chemistry*, 274, pp.19347–19351.

Pereira, G. & Schiebel, E., 1997. Centrosome-microtubule nucleation. *Journal of Cell Science*, 110, pp.295–300.

Perrin, B.J. & Ervasti, J.M., 2010. The actin gene family: Function follows isoform. *Cytoskeleton*, 67, pp.630–634.

Perry, S. V, 2001. Vertebrate tropomyosin: distribution, properties and function. *Journal of muscle research and cell motility*, 22, pp.5–49.

Petersen, J., Nielsen, O., Egel, R. & Hagan, I.M., 1998. F-actin distribution and function during sexual differentiation in Schizosaccharomyces pombe. *Journal of Cell Science*, 111 (, pp.867–876.

Pierre, P., Scheel, J., Rickard, J.E. & Kreis, T.E., 1992. CLIP-170 links endocytic vesicles to microtubules. *Cell*, 70, pp.887–900.

Plotnikov, S. V, Millard, A.C., Campagnola, P.J. & Mohler, W. a, 2006. Characterization of the myosin-based source for second-harmonic generation from muscle sarcomeres. *Biophysical Journal*, 90, pp.693–703.

Polakova, S., Benko, Z., Zhang, L. & Gregan, J., 2014. Mal3, the Schizosaccharomyces pombe homolog of EB1, is required for karyogamy and for promoting oscillatory nuclear movement during meiosis. *Cell Cycle*, 13, pp.72–7.

Polevoda, B., Arnesen, T. & Sherman, F., 2009. A synopsis of eukaryotic N α -terminal acetyltransferases : nomenclature , subunits and substrates. *BMC Proceedings*, 3, p.S2.

Polevoda, B., Cardillo, T.S., Doyle, T.C., Bedi, G.S. & Sherman, F., 2003. Nat3p and Mdm20p are required for function of yeast NatB Nalpha-terminal acetyltransferase

and of actin and tropomyosin. *The Journal of Biological Chemistry*, 278, pp.30686–97.

Polevoda, B. & Sherman, F., 2003a. Composition and function of the eukaryotic N-terminal acetyltransferase subunits. *Biochemical and Biophysical Research Communications*, 308, pp.1–11.

Polevoda, B. & Sherman, F., 2000. Nalpha -terminal acetylation of eukaryotic proteins. *The Journal of Biological Chemistry*, 275, pp.36479–82.

Polevoda, B. & Sherman, F., 2003b. N-terminal Acetyltransferases and Sequence Requirements for N-terminal Acetylation of Eukaryotic Proteins. , 2836(02), pp.595–622.

Pollard, T.D., 1986. Rate constants for the reactions of ATP- and ADP-actin with the ends of actin filaments. *The Journal of Cell Biology*, 103, pp.2747–54.

Pollard, T.D., 2007. Regulation of actin filament assembly by Arp2/3 complex and formins. *Annual Review of Biophysics and Biomolecular Structure*, 36, pp.451–77.

Pollard, T.D., Blanchoin, L. & Mullins, R.D., 2001. Actin dynamics. *Journal of cell science*, 114(Pt 1), pp.3–4.

Pollard, T.D. & Borisy, G.G., 2003. Cellular motility driven by assembly and disassembly of actin filaments. *Cell*, 112, pp.453–465.

Pollard, T.D. & Cooper, J. a, 2009. Actin, a central player in cell shape and movement. *Science*, 326, pp.1208–12.

Pollard, T.D. & Korn, E.D., 1973. Acanthamoeba myosin. I. Isolation from Acanthamoeba castellanii of an enzyme similar to muscle myosin. *The Journal of Biological Chemistry*, 248, pp.4682–4690.

Poole, K.J. V, Lorenz, M., Evans, G., Rosenbaum, G., Pirani, A., Craig, R., Tobacman, L.S., Lehman, W. & Holmes, K.C., 2006. A comparison of muscle thin filament models obtained from electron microscopy reconstructions and low-angle X-ray fibre diagrams from non-overlap muscle. *Journal of Structural Biology*, 155, pp.273–84.

Lo Presti, L. & Martin, S.G., 2011. Shaping fission yeast cells by rerouting actin-based transport on microtubules. *Current Biology*, 21(24), pp.2064–2069.

Pring, M., Weber, A. & Bubb, M.R., 1992. Profilin-actin complexes directly elongate actin filaments at the barbed end. *Biochemistry*, 31, pp.1827–1836.

Pruyne, D., Evangelista, M., Yang, C., Bi, E., Zigmond, S., Bretscher, A. & Boone, C., 2002. Role of formins in actin assembly: nucleation and barbed-end association. *Science*, 297, pp.612–615.

Qin, Y., Meisen, W.H., Hao, Y. & Macara, I.G., 2010. Tuba, a Cdc42 GEF, is required for polarized spindle orientation during epithelial cyst formation. *The Journal of Cell Biology*, 189(4), pp.661–669.

Reck-Peterson, S.L., Provance, D.W., Mooseker, M.S. & Mercer, J.A., 2000. Class V myosins. *Biochimica et Biophysica Acta - Molecular Cell Research*, 1496, pp.36–51.

Rock, R.S., Rice, S.E., Wells, A.L., Purcell, T.J., Spudich, J.A. & Sweeney, H.L., 2001. Myosin VI is a processive motor with a large step size. *Proceedings of the National Academy of Sciences of the United States of America*, 98, pp.13655–13659.

Rodriguez-Boulan, E. & Macara, I.G., 2014. Organization and execution of the epithelial polarity programme. *Nature Reviews. Molecular Cell Biology*, 15(4), pp.225–42.

Romero, S., Le Clainche, C., Didry, D., Egile, C., Pantaloni, D. & Carlier, M.F., 2004. Formin is a processive motor that requires profilin to accelerate actin assembly and associated ATP hydrolysis. *Cell*, 119, pp.419–429.

Sawin, K.E. & Nurse, P., 1998. Regulation of cell polarity by microtubules in fission yeast. *The Journal of Cell Biology*, 142, pp.457–71.

Schafer, D.A., Jennings, P.B. & Cooper, J.A., 1996. Dynamics of capping protein and actin assembly in vitro: uncapping barbed ends by polyphosphoinositides. *The Journal of Cell Biology*, 135, pp.169–179.

Scott, B.J., Neidt, E.M. & Kovar, D.R., 2011. The functionally distinct fission yeast formins have specific actin-assembly properties. *Molecular Biology of the Cell*, 22, pp.3826–39.

Shaw, S.L., Yeh, E., Maddox, P., Salmon, E.D. & Bloom, K., 1997. Astral microtubule dynamics in yeast: a microtubule-based searching mechanism for spindle orientation and nuclear migration into the bud. *The Journal of Cell Biology*, 139, pp.985–994.

Singer, J.M. & Shaw, J.M., 2003. Mdm20 protein functions with Nat3 protein to acetylate Tpm1 protein and regulate tropomyosin – actin interactions in budding yeast. *Proceedings of the National Academy of Sciences of the United States of America*, 100, pp.7644–9.

Skau, C.T., Neidt, E.M. & Kovar, D.R., 2009. Role of tropomyosin in formin-mediated contractile ring assembly in fission yeast. *Molecular Biology of the Cell*, 20(8), p.2160.

Skoumpla, K., Coulton, A.T., Lehman, W., Geeves, M. a & Mulvihill, D.P., 2007. Acetylation regulates tropomyosin function in the fission yeast Schizosaccharomyces pombe. *Journal of Cell Science*, 120, pp.1635–45.

Smith, D. a & Geeves, M. a, 1995. Strain-dependent cross-bridge cycle for muscle. *Biophysical Journal*, 69, pp.524–37.

Smith, D. a, Maytum, R. & Geeves, M. a, 2003. Cooperative regulation of myosin-actin interactions by a continuous flexible chain I: actin-tropomyosin systems. *Biophysical Journal*, 84, pp.3155–67.

Snaith, H. a, Samejima, I. & Sawin, K.E., 2005. Multistep and multimode cortical anchoring of tea1p at cell tips in fission yeast. *The EMBO Journal*, 24, pp.3690–9.

Snaith, H. & Sawin, K.E., 2003. Fission yeast mod5p regulates polarized growth through anchoring of tea1p at cell tips. *Nature*, 573(1954), pp.647–651.

Snaith, H. & Sawin, K.E., 2005. Tea for three: control of fission yeast polarity. *Nature cell biology*, 7(5), pp.450–451.

Stafford, W.F., Walker, M.L., Trinick, J.A. & Coluccio, L.M., 2005. Mammalian class I myosin, Myo1b, is monomeric and cross-links actin filaments as determined by hydrodynamic studies and electron microscopy. *Biophysical Journal*, 88(1), pp.384–391.

Stark, B.C., Sladewski, T.E., Pollard, L.W. & Lord, M., 2010. Tropomyosin and myosin-II cellular levels promote actomyosin ring assembly in fission yeast. *Molecular Biology of the Cell*, 21, pp.989–1000.

Stearns, T., Evans, L. & Kirschner, M., 1991. Gamma-tubulin is a highly conserved component of the centrosome. *Cell*, 65, pp.825–836.

Steuer, E., Wordeman, L. & Schroer, T., 1990. Localization of cytoplasmic dynein to mitotic spindles and kinetochores. *Nature*, 345, pp.266–268.

Stone, D. & Smillie, L.B., 1978. The amino acid sequence of rabbit skeletal alpha-tropomyosin. The NH2-terminal half and complete sequence. *The Journal of Biological Chemistry*, 253, pp.1137–1148.

Summers, K. & Kirschner, M.W., 1979. Characteristics of the polar assembly and disassembly of microtubules observed in vitro by darkfield light microscopy. *The Journal of Cell Biology*, 83, pp.205–17.

Takaine, M., Numata, O. & Nakano, K., 2009. Fission yeast IQGAP arranges actin filaments into the cytokinetic contractile ring. *The EMBO Journal*, 28, pp.3117–31.

Takeda, T. & Chang, F., 2005. Role of fission yeast myosin I in organization of sterol-rich membrane domains. *Current Biology*, 15, pp.1331–1336.

Tatebe, H., Shimada, K., Uzawa, S., Morigasaki, S. & Shiozaki, K., 2005. Wsh3/Tea4 is a novel cell-end factor essential for bipolar distribution of Tea1 and protects cell polarity under environmental stress in S. pombe. *Current Biology*, 15, pp.1006–15.

Tepass, U., 1996. Crumbs, a component of the apical membrane, is required for zonula adherens formation in primary epithelia of Drosophila. *Developmental Biology*, 177, pp.217–225.

Tepass, U. & Knust, E., 1993. Crumbs and stardust act in a genetic pathway that controls the organization of epithelia in Drosophila melanogaster. *Developmental Biology*, 159, pp.311–326.

Toda, T., Umesono, K., Hirata, A. & Yanagida, M., 1983. Cold-sensitive nuclear division arrest mutants of the fission yeast Schizosaccharomyces pombe. *Journal of Molecular Biology*, 168, pp.251–270.

Trotta, P., Dreizen, P. & Stracher, A., 1968. Studies on subfragment-I, a biologically active fragment of myosin. *Proceedings of the National Academy of Sciences of the United States of America*, 200, pp.659–666.

Tsiavaliaris, G., Fujita-Becker, S. & Manstein, D.J., 2004. Molecular engineering of a backwards-moving myosin motor. *Nature*, 427, pp.558–561.

Tyska, M.J. & Mooseker, M.S., 2003. Myosin-V motility: these levers were made for walking. *Trends in Cell Biology*, 13, pp.447–51.

Umesono, K., Toda, T., Hayashi, S. & Yanagida, M., 1983. Cell division cycle genes nda2 and nda3 of the fission yeast Schizosaccharomyces pombe control microtubular organization and sensitivity to anti-mitotic benzimidazole compounds. *Journal of Molecular Biology*, 168, pp.271–284.

Vaisberg, E. & Koonce, M., 1993. Cytoplasmic dynein plays a role in mammalian mitotic spindle formation. *The Journal of Cell Biology*, 123, pp.849–58.

Vale, R.D., 2003. The molecular motor toolbox for intracellular transport. *Cell*, 112, pp.467–480.

Vale, R.D., Reese, T.S. & Sheetz, M.P., 1985. Identification of a novel force-generating protein, kinesin, involved in microtubule-based motility. *Cell*, 42, pp.39–50.

Vavylonis, D., Wu, J.-Q., Hao, S., O'Shaughnessy, B. & Pollard, T.D., 2008. Assembly mechanism of the contractile ring for cytokinesis by fission yeast. *Science*, 319, pp.97–100.

Verde, F., Mata, J. & Nurse, P., 1995. Fission yeast cell morphogenesis: identification of new genes and analysis of their role during the cell cycle. *The Journal of Cell Biology*, 131, pp.1529–1538.

Verde, F., Wiley, D.J. & Nurse, P., 1998. Fission yeast orb6, a ser/thr protein kinase related to mammalian rho kinase and myotonic dystrophy kinase, is required for maintenance of cell polarity and coordinates cell morphogenesis with the cell cycle.

Proceedings of the National Academy of Sciences of the United States of America, 95, pp.7526–31.

Vibert, P., Craig, R. & Lehman, W., 1997. Steric-model for activation of muscle thin filaments. *Journal of Molecular Biology*, 266, pp.8–14.

Wacker, I.U., Rickard, J.E., De Mey, J.R. & Kreis, T.E., 1992. Accumulation of a microtubule-binding protein, pp170, at desmosomal plaques. *The Journal of Cell Biology*, 117, pp.813–824.

Walker, M.L., Burgess, S.A., Sellers, J.R., Wang, F., Hammer, J.A., Trinick, J. & Knight, P.J., 2000. Two-headed binding of a processive myosin to F-actin. *Nature*, 405, pp.804–807.

Wallar, B. & Alberts, A., 2003. The formins: active scaffolds that remodel the cytoskeleton. *Trends in Cell Biology*, 13, pp.435–446.

Wang, N., Lo Presti, L., Zhu, Y.-H., Kang, M., Wu, Z., Martin, S.G. & Wu, J.-Q., 2014. The novel proteins Rng8 and Rng9 regulate the myosin-V Myo51 during fission yeast cytokinesis. *The Journal of Cell Biology*, 205, pp.357–75.

Warshaw, D.M., Kennedy, G.G., Work, S.S., Krementsova, E.B., Beck, S. & Trybus, K.M., 2005. Differential labeling of myosin V heads with quantum dots allows direct visualization of hand-over-hand processivity. *Biophysical Journal*, 88, pp.L30–2.

Wegner, A., 1976. Head to tail polymerization of actin. *Journal of Molecular Biology*, 108(1), pp.139–50.

Weisenberg, R.C., 1972. Microtubule formation in vitro in solutions containing low calcium concentrations. *Science*, 177, pp.1104–1105.

Weisenberg, R.C., Deery, W.J. & Dickinson, P.J., 1976. Tubulin-nucleotide interactions during the polymerization and depolymerization of microtubules. *Biochemistry*, 15, pp.4248–54.

Wells, A.L., Lin, A.W., Chen, L.Q., Safer, D., Cain, S.M., Hasson, T., Carragher, B.O., Milligan, R.A. & Sweeney, H.L., 1999. Myosin VI is an actin-based motor that moves backwards. *Nature*, 401, pp.505–508.

Whitby, F.G. & Phillips, G.N., 2000. Crystal Structure of Tropomyosin at 7 A Resolution. *Cell*, 59, pp.49–59.

Wickstead, B. & Gull, K., 2011. The evolution of the cytoskeleton. *The Journal of Cell Biology*, 194, pp.513–25.

Win, T.Z., Gachet, Y., Mulvihill, D.P., May, K.M. & Hyams, J.S., 2001. Two type V myosins with non-overlapping functions in the fission yeast Schizosaccharomyces pombe:

Myo52 is concerned with growth polarity and cytokinesis, Myo51 is a component of the cytokinetic actin ring. *Journal of Cell Science*, 114(1), p.69.

Win, T.Z., Gachet, Y., Mulvihill, D.P., May, K.M. & Hyams, J.S., 2001. Two type V myosins with non-overlapping functions in the fission yeast Schizosaccharomyces pombe: Myo52 is concerned with growth polarity and cytokinesis, Myo51 is a component of the cytokinetic actin ring. *Journal of Cell Science*, 114(Pt 1), pp.69–79.

Wood, V. et al., 2002. The genome sequence of Schizosaccharomyces pombe. *Nature*, 415, pp.871–880.

Woychik, R.P., Maas, R.L., Zeller, R., Vogt, T.F. & Leder, P., 1990. "Formins": proteins deduced from the alternative transcripts of the limb deformity gene. *Nature*, 346, pp.850–853.

Wu, J.-Q., Bähler, J. & Pringle, J.R., 2001. Roles of a Fimbrin and an α-Actinin-like Protein in Fission Yeast Cell Polarization and Cytokinesis G. R. Fink, ed. *Molecular Biology of the Cell*, 12, pp.1061–1077.

Wu, J.-Q., Sirotkin, V., Kovar, D.R., Lord, M., Beltzner, C.C., Kuhn, J.R. & Pollard, T.D., 2006. Assembly of the cytokinetic contractile ring from a broad band of nodes in fission yeast. *The Journal of cell biology*, 174(3), pp.391–402.

Yaffe, M.P., Harata, D., Verde, F., Eddison, M., Toda, T. & Nurse, P., 1996. Microtubules mediate mitochondrial distribution in fission yeast. *Proceedings of the National Academy of Sciences of the United States of America*, 93, pp.11664–11668.

Yamanaka, T., Horikoshi, Y., Suzuki, A., Sugiyama, Y., Kitamura, K., Maniwa, R., Nagai, Y., Yamashita, A., Hirose, T., Ishikawa, H. & Ohno, S., 2001. PAR-6 regulates aPKC activity in a novel way and mediates cell-cell contact-induces formation of the epithelial junctional complex. *Genes to Cells*, 6, pp.721–731.

Yanagida, M., 1987. Yeast tubulin genes. *Microbiological Sciences*, 4, pp.115–118.

Yang, P., Qyang, Y., Bartholomeusz, G., Zhou, X. & Marcus, S., 2003. The novel Rho GTPase-activating protein family protein, Rga8, provides a potential link between Cdc42/p21-activated kinase and Rho signaling pathways in the fission yeast, Schizosaccharomyces pombe. *The Journal of Biological Chemistry*, 278, pp.48821–48830.

Yildiz, A., Tomishige, M., Vale, R.D. & Selvin, P.R., 2004. Kinesin walks hand-over-hand. *Science*, 303, pp.676–8.

Yu, C., Feng, W., Wei, Z., Miyanoiri, Y., Wen, W., Zhao, Y. & Zhang, M., 2009. Myosin VI Undergoes Cargo-Mediated Dimerization. *Cell*, 138, pp.537–548.